Order Number 9303411

Solute redistribution during freezing of sands saturated with saline solution

Matava, Timothy, Ph.D.

University of Alaska Fairbanks, 1991

U·M·I
300 N. Zeeb Rd.
Ann Arbor, MI 48106

SOLUTE REDISTRIBUTION DURING FREEZING OF SANDS SATURATED WITH SALINE SOLUTION

A

THESIS

Presented to the Faculty

of the University of Alaska Fairbanks

in Partial Fulfillment of the Requirements

for the Degree of

DOCTOR OF PHILOSOPHY

By

Timothy Matava, B.S., M.S.

Fairbanks, Alaska

May 1991

Solute Redistribution During Freezing of Sands Saturated with Saline Solution

By

Timothy Matava

RECOMMENDED:

Advisory Committee Chair

Department Head

APPROVED:

Dean, College of Natural Sciences

Dean of the Graduate School

5/1/91

Date

Abstract

Columns of saturated saline sands were frozen under hydrostatic conditions with constant surface and base temperatures. Nine freezing tests were conducted using a silica sand with a permeability of about 10^{-11} m^2 and salinities that ranged from 1 to 100 ppt but were generally near 35 ppt. Surface temperatures were generally 3 to 5 °C colder than the freezing temperature of the solution and base temperatures were generally 0.5 °C warmer.

A 4 to 10 day long period preceded the onset of convection and redistribution of the solute. The increased freezing rate due to the solute, the effects of brine expulsion and a small amount of water movement independent of the salt were measured during this period. Movement of water to the column surface was not associated with either vapor transport or salt sieving. The interface between the solid and liquid was a vertically diffuse interface rather than a sharp ice–bonded interface.

Convection of the pore fluid occurred throughout the entire column. Pore fluid velocities were estimated to be on the order of 0.1 to 0.3 $\frac{m}{day}$ and do not exceed 1.4 $\frac{m}{day}$. Convection consisted of pore fluid in one half of the column moving down and pore fluid in the other half moving up and was associated with radial asymmetries in salinity, water content and ice–bonding. The effects of convection could be measured in the salinity profiles, but not in profiles of water content or temperature. A stability analysis showed the unstable density gradient in the partially frozen region was not sufficient to lead to convection. It was tentatively concluded that convection resulted from dense brine in the partially frozen region overlying less dense brine in the thawed region. Methods for estimating the final salinity profiles were not satisfactory since the BPS theory could not be applied to the experimental results and a stability theory for the pore fluid could not be developed which matched the experimental results. Application of these results to field situations is limited because of the restricted horizontal and vertical length scales. However, solute redistribution by convection is probably limited to freezing soils with large solute concentrations and large permeabilities.

Contents

List of Figures

List of Tables

Acknowledgements

This thesis could not have been completed without the help and aide of my thesis advisory committee. Tom Osterkamp acted as advisor for the thesis and made major contributions to the quality of the thesis and research. The committee members, which included Joan Gosink, Dan Hawkins, Joe Niebauer, Walt Tape and Willy Weeks, took time from their busy schedules to review, edit and contribute to this manuscript. Additionally, Gary Gislason and Keith Echelmeyer acted as readers and attended the defense in the absence of two of the regular members who were conducting field work in Antartica. Joe Niebauer was kind enough to join the committee on the retirement of Dan Hawkins. His flexibility in agreeing to join the committee at such a late date and his comments on the thesis are appreciated.

During the last year and a half I have been a recipient of a Graduate Resource Fellowship from the Office of Graduate Studies at the University of Alaska Fairbanks. This fellowship provided a large degree of flexibility in the research and has allowed me the opportunity to complete the thesis without delay. Research support during the first part of this study was obtained through U.S.G.S. contract 14-08-0001-G1305, National Science Foundation contract DPP8312026 and Army Research Office contract DAAL03-89-K-0106.

Throughout my years as a graduate student I have been lucky enough to receive continuous support and kindness from my family and friends. My sister Kate Doran, her husband Tim Doran and their two daughters Claire and Bridget Doran have been especially kind and generous with their gifts of perspective, encouragement, and lively conversation which was usually accompanied by a delicious meal. The Petersen family has also provided a generous amount of hospitality and kindness over the years. I certainly have enjoyed their friendship and have thoroughly enjoyed the time I was lucky enough to spend with John, Becky, Richard, Grace and Ida.

Finally, it is with pleasure that I acknowledge the hospitality and friendship of Howard and Enid Cutler. Like my family, they have provided perspective, encouragement and lively conversation which, for my good fortune, was also very often accompanied by a delicious meal. Through their kindness, generosity and wisdom they have presented themselves as the very best of role models.

Chapter 1

Introduction and Literature Review

1.1 Introduction

The flow of solutes in soils has been the subject of increasing scientific interest in recent years due to the potential effects of solutes on the biological, chemical and physical processes occurring within soils. Phenomena associated with solute movement in soils during freezing have been investigated because of their effects on agricultural production, mechanical properties of soils, and environmental conditions in soils which may lead to the concentration of solutes to potentially hazardous levels. Agricultural interest in solute movement has resulted from a need to understand the fate of solutes which have been either applied or accumulate in soils that freeze annually. Freezing induced movement of fertilizers applied to soils and solutes that accumulate in the root zone as a result of irrigation are of interest because they strongly affect crop yields. Engineers designing offshore structures in the U.S. and Canadian Arctic have been interested in the mechanical properties of thawed, frozen and partially frozen soils. Fill material used for offshore gravel islands and causeways is typically saturated with seawater and the potential redistribution of solutes as the fill material freezes affects the strength of the material and the structure. Subsea pipelines which may be used in the future to transport oil onshore from wells located in the Beaufort or Chukchi Seas are a potential heat source which could degrade subsea permafrost and decrease the mechanical strength of the soil surrounding the pipeline. Environmental interest in the distribution of solutes in freezing and thawing soils has resulted from a

need to understand the fate of de-icing salts applied to roadways, salts applied to roadway and railroad beds to mitigate the effects of frost heave, and herbicides applied to rights of way along roads, railroads, and powerlines. Chemicals used in each of these situations all require repeated applications to remain effective.

Agricultural, engineering and environmental interests all have a need to understand the fate of solutes in soils that freeze annually; however, relatively little theoretical or experimental research has been conducted in this area. Research into the factors affecting the distribution of solutes in soils that freeze annually has been directed towards obtaining an understanding of the influence of potentials which develop during freezing on the distribution of solutes. Potentials which may affect the distribution of solutes during freezing include: matric, osmotic, chemical, surface (which includes mineral grain curvature), electrical and gravitational potentials. The influence of these potentials on the distribution of solutes during freezing is unclear, but research suggests that the important parameters are grain size, degree of saturation, solute concentration and freezing rate (Kay and Perfect 1988).

The present level of understanding suggests that the grain size and degree of saturation within the soil during freezing may affect the distribution of solutes in three general ways. First, during freezing in saturated coarse–grained soils, experimental results suggest that solutes are concentrated by freezing and are affected by the gravitational potential such that relatively dense pore fluid in the partially frozen soil displaces less dense solutions in the thawed soil (Mahar, et al. 1983, Wilson 1983, Baker 1987, Baker and Osterkamp 1988, Baker and Osterkamp 1989). In this case, convection of the pore fluid dilutes solution in the partially frozen upper portion of the soil and increases the concentration of solutes in solution within the thawed, lower, portion of the soil. Second, during freezing in fine–grained, saturated, frost susceptible soils, solutes appear to migrate to the freezing front during ice lense formation and soil heaving (Kay and Groenevelt 1983, Konrad 1989). In this case, solutes are drawn with solution in the thawed portion of the soil to the freezing front; however, the potential or potentials which develop during freezing that lead to this movement are unclear. Third, in freezing unsaturated soils, water appears to move to the cold side of the soil in response to a chemical potential gradient which develops due to the temperature gradient in the soil and phase relations between brine and ice (Hoekstra 1966, Cary and

Mayland 1972, Oliphant, et al. 1983, Wuttig 1988). It would appear that in this case the presence of solutes in the soil could actually increase the flux of material to the cold side of the soil by increasing the amount of liquid water within the soil. However, this hypothesis has not been clearly proven either experimentally or theoretically. To summarize these three cases, the effects of solutes on a naturally freezing soil may be to increase the solute concentration under the partially frozen layer or near the base of the active layer, or to increase the solute concentration near the middle of the freezing active layer. Finally, during freezing in saturated coarse-grained soils, the solute concentration changes, however, the gravimetric water content remains essentially constant. In unsaturated or frost susceptible soils, both the solute concentration and gravimetric water content change during freezing.

The movement of solutes in soils containing ice can occur because the soil is only partially frozen and is still permeable to flow, but at a much reduced level. Numerous measurements have been made of the permeability of partially frozen fine-grained soils that contain no added dissolved solutes (Perfect and Williams 1980, Oliphant, et al. 1983, Horiguchi and Miller 1983, Yoneyama, et al. 1983, Black 1990). These results show that hydraulic conductivity decreases several orders of magnitude between 0 °C and -1 °C. At temperatures below -1 °C the hydraulic conductivity is relatively constant (Kay and Perfect 1988). Black (1990) notes that no measurements have been published reporting the permeability of partially frozen fine or coarse-grained soils which contain dissolved solutes.

In an effort to increase the level of understanding associated with the movement of solutes in freezing soils, a laboratory investigation was initiated to study phenomena associated with gravitationally induced movement of the pore fluid during freezing. This study involved freezing a coarse-grained soil (composed of a medium to fine-grained silica sand) saturated with NaCl solutions of known initial concentration. The purpose of this thesis is to present and interpret the results of these experiments. The remainder of this chapter will present a review of the literature pertaining to the effects of freezing on the distribution of solutes in metals, in ice and in coarse-grained soils; the chapter ends with a statement of the research objectives of the thesis. Subsequent chapters will present material which will include: design of the laboratory apparatus in which the experiments were conducted; methods used in the laboratory investigation; results of the laboratory

investigation; interpretation of the experimental results; summary of conclusions and suggested areas of additional research.

1.2 Literature Review

In fine–grained soils significant amounts of unfrozen water may exist at temperatures below the freezing point of the pore fluid (Oliphant, et al. 1983). Surface potentials on the mineral grains in fine–grained soils alter the freezing properties of the pore fluid resulting in the unfrozen water. However, surface potentials are reduced when the pore fluid contains dissolved solutes. For example, an investigation conducted with swelling clays, one of the most frost susceptible types of soils, saturated with saline solution to $\approx$ 5 ppt showed that the phase relations were modified more by the presence of dissolved salts in the pore fluid than by the mineral grains (Yong, et al. 1978). If the phase relations in the most frost susceptible of soils containing solute concentrations of 5 ppt were modified more by the presence of solutes than by the mineral grains, then coarse–grained soils saturated with saline solution of seawater concentrations should be negligibly affected by surface potentials and the phase relations for a saline solution may be applied to the soil. Further, desalinization of the partially frozen coarse–grained soil saturated with saline solution may be similar to the desalinization of a freezing saline solution, sea ice for example. The purpose of this section is to review the literature on the processes leading to the redistribution of solutes during the solidification of metals, of ice grown from a saline solution, and then to review results from investigations involved with freezing coarse–grained soils saturated with saline solution.

1.2.1 Solute Redistribution and Heat Flow During the Solidification of Metals

Solidification of many substances involves the formation of a relatively pure solid from a relatively impure solution. Solidification of such a two component system, a lead tin melt or NaCl dissolved in water for example, is referred to as binary solidification (Flemings 1974) and results in the formation of two phases, solid and liquid phases, each with a concentration fixed by the temperature of the system.

Solutes rejected from the solid during its formation are expelled to the liquid at a solid–liquid interface. This interface may be planar, in which the solid contacts the liquid at a sharp front, or diffuse, in which the transition from a solid to a liquid occurs over a large distance perpendicular to the interface growth direction. Conditions which cause the planar solid–liquid interface to change to a diffuse one have been shown to be due to a small amount of supercooling of the liquid in front of the interface (Rutters and Chalmers 1953). This type of supercooling has been termed constitutional supercooling and occurs because the diffusivity of heat is several orders of magnitude greater than the molecular diffusivity of the solution. The large difference between the diffusivity of heat and solutes leads to the development of a small region in front of a planar solid–liquid interface that is supercooled and morphologically unstable to perturbations of the solid extending into the liquid, Figure 1.1. Conditions that lead to constitutional supercooling of the melt in front of the solid–liquid interface results in the transition from a planar to a cellular to a dendritic and ultimately to a globulitic interface that contains both solid and liquid (Viskanta 1988). The stability criterion for an interface to remain planar during solidification has been presented in detail by Flemings (1974) for metals and by Weeks and Ackley (1982) for sea ice.

BPS theory (Burton, Prim and Schlichter 1953, 1953a) was developed as a method of calculating the amount of impurity incorporated within a solidifying material based on the ratio of impurity concentration on either side of the interface (defined as the effective distribution coefficient) and the velocity of the interface. The basis for BPS theory is that the flux of solute rejected into the liquid at the moving solid–liquid interface is balanced by the flux of solute that diffuses from this interface into the bulk liquid. A balance between the fluxes into and out of the interface results in the formation of a boundary layer with greater solute concentration than the solid and remaining bulk liquid in front of the solid–liquid interface. The interface velocity is assumed to be constant and once solutes become incorporated into the solid they are assumed to remain in the solid. With BPS theory, knowledge of the interface growth velocity and an experimentally determined relation between the distribution coefficient and the freezing rate allows the solute concentration in the solid to be calculated.

The assumptions used to formulate the BPS theory are no longer valid at a

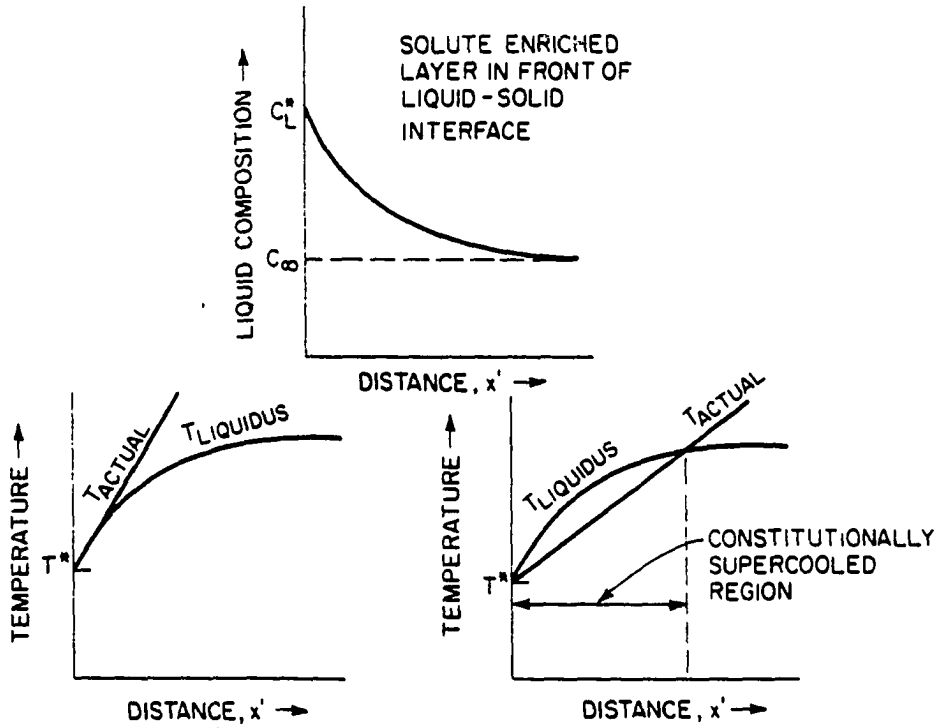

Figure 1.1: A schematic representation of the process that leads to the formation of a constitutionally supercooled layer in front of a solid–liquid interface, from Flemings (1974). The first figure shows the solute enriched region in front of the solid–liquid interface that results from the rejection of solutes from the liquid to the solid. The second figure is a stable interface because the freezing temperature of the solution is less than the solution temperature. The third figure is an unstable interface because the freezing temperature of the solution is greater than the solution temperature. A combination of a small temperature gradient and a small molecular diffusivity leads to the interface becoming constitutionally supercooled and unstable.

diffuse solid–liquid interface. Solute redistribution in the diffuse region is referred to as macrosegregation and occurs as a result of convection within the partially solidified region (Flemings 1974). Macrosegregation is a term used to describe solute redistribution at a diffuse solid–liquid interface and takes into account convection within the bulk liquid as well as convection within the partially solidified region. Techniques to determine the mode of convection within castings during solidification mainly involve numerical solutions and these analyses suggest that the mode of convection in the partially solidified region may be different than the modes in the bulk liquid (Chen and Chen 1988). Analytical techniques to deter-

mine the final solute concentration in the metal by taking into account convection within the system are not available. Numerical techniques to determine the final solute concentration in the metal have only recently been developed (Maples and Poirer 1984, Voller, et al. 1989).

Convection within the partially solidified region results not only in the redistribution of solutes during solidification, but also in an increased heat transfer within the system. If the velocity of convecting fluid becomes large, then temperature fluctuations develop in the partially solidified region which result in the formation of bands of solute enriched regions within the material that are perpendicular to the direction of heat flow (Flemings 1974). In these situations, convection in the partially solidified region can lead to local remelting and the formation of isolated channels, or *freckles*, which are the last material to solidify and are of eutectic concentrations (Flemings 1974, Glicksman, et al. 1986).

1.2.2 Brine Movement in Ice Grown from a Saline Solution

Solidification of a two component saline solution of NaCl with concentrations less than 233.1 ppt and at constant pressure results in phases of brine and essentially pure ice (Heiss and Kuhajek 1983). If the brine and ice are contained in a vessel which maintains the initial mass of the system, lowering the temperature of the vessel will reduce the fraction of brine (while increasing its concentration) and increase the fraction of pure ice until the eutectic temperature is reached. The eutectic temperature of NaCl dissolved in water is -21.12 °C (Heiss and Kuhajek 1983). If the vessel containing the saline solution is cooled under ideal conditions such that the heat flow is in the vertical direction and slow one directional freezing occurs, then pure ice forms in which solutes are rejected from the ice into the liquid at a sharp solid–liquid interface. Continued freezing increases the concentration of the remaining brine which further depresses the freezing point of the remaining solution. In practice, however, virtually any commonly observed growth situation involving a salt solution results in the interface becoming unstable early during its growth leading to cellular growth and the formation of a diffuse solid–liquid interface (Weeks and Ackley 1982). Solute redistribution by convection results in large amounts of brine becoming incorporated within the ice. The brine subsequently drains from the partially frozen region (any region above the eutectic

temperature) leading to a decrease in the overall salinity, or bulk salinity of the ice.

Weeks and Lofgren (1967) and Cox and Weeks (1975) recognized the similarity between the solidification of metals and the freezing of seawater. They used concepts associated with constitutional supercooling to characterize the morphological stability of an ice interface to perturbations from the ice extending into the liquid region. Nakawo and Sinha (1981) showed that salinity profiles in first year sea ice could be expressed in a form which results from the BPS theory. They concluded that by specifying only the ice growth velocity the bulk salinity of first year sea ice could be determined. The ice growth velocity was measured at the top of the dendritic layer where the ice layers began to bridge (Cox and Weeks 1975).

Laboratory measurements of growing NaCl ice (Weeks and Lofgren 1967) and field measurements of sea ice (Cox and Weeks 1975) have documented that sea ice incorporates large amounts of brine between crystals during its growth and that it rapidly desalinates to solute concentrations that are several percent of the initial solute concentration. Laboratory investigations into the mechanisms leading to the rapid desalinization of the ice have shown that a process referred to as brine drainage is responsible for the observed desalinization of the ice (Cox and Weeks 1975). These authors describe brine drainage as a process that results when colder, dense, saline brine within the ice sheet drains into warmer, less saline, and less dense fluid below the ice. They also have shown that solutes move within the ice sheet without a change in solvent concentration (water content). It was observed that brine drained from the ice and it appears that solution from some other less saline region took its place.

The experimental results of Cox and Weeks (1975) showed that a convective process, which they called brine drainage, was responsible for the desalinization of sea ice; however, their results did not provide insight into the dynamics of the motion leading to the desalinization. In laboratory studies of salt ice grown between closely spaced plexiglass sheets Eide and Martin (1975), and Niedrauer and Martin (1979) investigated the movement of brine within the cellular or dendritic region near the base of growing salt ice. Observations of brine drainage features made during both of these studies indicated that brine drainage channels seperated fingers of solution which extended from the fluid underneath the ice up into the ice.

Detailed observations of these features during their initial growth were presented by Niedrauer and Martin (1979). Their observations showed that the fingers have a width scale of ≈1 centimeter and are separated by brine drainage channels that have a width scale of ≈1 millimeter. Observations in each of these studies have indicated that the fingers continued moving up into the ice until the dye, used to trace the fingers, became too dilute to clearly observe their movement.

The laboratory study of Niedrauer and Martin (1979) also measured the flux of brine from the drainage channels in the growing ice and compared their measurements with calculations of the flux from the growing ice due to brine expulsion[1]. Their results indicated that under the most favorable circumstances the calculated flux of material exiting the brine channels during ice growth was less than 3% of the measured flux. The remaining 97% of the flux of brine from the drainage channels they associated with convection throughout the partially frozen ice. Convection within the ice is presumably associated with their observation of fingers of brine moving up into the ice from below.

1.2.2.1 Summary of Solute Movement in Ice Grown from a Saline Solution

In summary, the formation of a cellular or dendritic structure and the incorporation of large amounts of brine within ice grown from a saline solution may be understood in terms of constitutional supercooling, a phenomenon in which fluid immediately in front of a solid–liquid interface is supercooled a slight amount causing it to become unstable to perturbations in the interface. The instability in the interface leads to the formation of a cellular or dendritic interface in which large quantities of brine become incorporated within the ice. Brine incorporated within the ice during its formation drains from the ice, mixing with less dense fluid below the dendritic or cellular layer. Immediately above the cellular region, brine has been observed to drain from the ice through a phenomenon referred to as brine drainage. Dense brine draining from this region is replaced by less dense brine from lower, less saline, regions. These observations are consistent with observations of solidification at a diffuse interface in metals. Finally, it has been shown

[1]The density difference between brine and ice leads to a small amount of brine movement within the partially frozen ice during solidification. The movement of brine from a solidifying ice sheet due to this density difference is termed brine expulsion.

that by measuring the growth velocity of first year sea ice immediately above the cellular region, the salinity of the ice may be determined using the results of the BPS theory. BPS theory is developed under the assumption of a balance between the flux of solutes into the interface by rejection and the diffusion of these solutes from the interface. Application of BPS theory to the desalinization of sea ice does not match observations made during the growth of sea ice which suggests that phenomena associated with macrosegregation may be important in the desalinization of sea ice; however, the BPS theory seems to predict the bulk salinity of sea ice reasonably well.

1.2.3 Solute Movement and Heat Flow in Freezing Coarse–Grained Saline Soils

The presence of solutes within the pore fluid of a freezing soil complicates methods used to calculate freezing rates and physical properties of the soil because the pore fluid does not change phase at a constant temperature but over a range of temperatures. Convection of solutes within the thawed and partially frozen soil further complicates efforts to model the heat transfer and mechanical properties of the soil because both depend on the phase relations; the phase relations depend on the bulk salinity of the soil which is affected by convection (Wilson 1983). Previous investigations into the effects of solutes on freezing soils have concentrated on determining the effects of solutes on the heat transfer and the conditions which lead to solute movement in the soils. The purpose of this section is to review the experimental and theoretical literature pertaining to the effects of solutes on the heat transfer during freezing in coarse–grained soils and the effects of freezing on the distribution of solutes in the soil. This section will be divided into two parts, the first part will review the experimental studies and the second part will review the theoretical studies.

1.2.3.1 Experimental Studies

Wilson (1983) and Mahar, et al. (1983) presented results of a laboratory investigation on the effects of solutes on the heat transfer that occurred during freezing in a saturated coarse–grained soil obtained from Prudhoe Bay, Alaska. The laboratory investigation of Wilson (1983) consisted of freezing columns (dia.=0.42

length=0.71 m) of coarse-grained soils saturated with saline solution ranging in concentration from 0 ppt to 82 ppt. Seventeen freezing tests were conducted on a soil that ranged from a gravelly sand to a sandy gravel with a mass average particle diameter of 4.7×10^{-3} m. Freezing conditions were such that freezing took place from the top down under approximate Neumann conditions[2] using surface temperatures between -2 and -9.4 °C. Each column was frozen over a period of several days. Freezing conditions resulted in temperature gradients near the interface that ranged from 1 to 30 $\frac{°C}{m}$. Permeability of the soil was not measured at any time during this investigation.

Bulk salinity profiles were measured at the start and at the end of each freezing experiment to determine the change in solute concentration during freezing. Results of these measurements indicated that freezing resulted in an increase in solution concentration at the base of the column and a decrease in solution concentration in the partially frozen region of the column. In general, the amount of redistribution increased as the surface temperature was decreased with the maximum bulk salinity change of between 17 and 40% of the initial salinity. The minimum bulk salinity occurred several centimeters above the ice-bonded interface. Bulk salinity in the frozen portion of the column was greater than the initial bulk salinity at a distance of 60 to 80% of the maximum freeze depth (determined by bonding and visual inspection for ice crystals). Gravimetric water content of the frozen or thawed soil were not measured during this investigation.

Observations of the partially frozen column at the end of a freezing experiment indicated, in general, that the ice-bonded interface was a diffuse interface much like diffuse interfaces observed during the solidification of metals and sea ice. The diffuse interface was a zone of soil which was not bonded by ice, but which was often observed to contain ice crystals (Wilson 1983). Freezing test summaries described this diffuse interface as a transition interface between mechanically bonded soil and thermodynamically thawed soil extending over a distance of up to 8×10^{-2} m and often containing visible ice crystals.

Wilson's results indicate that the solid-liquid interface moved up to 300%

[2]Approximate Neumann boundary conditions consist of constant initial, base and surface temperatures each of which may be different; however, for freezing $T_{surf} < T_{base} \leq T_{init}$. The approximation is due to the finite length of the column, classic Neumann boundary conditions assume a half-space and no lateral heat conduction.

faster for a given set of freezing conditions when the the pore fluid contained solutes initially at 16 ppt than when the pore fluid was distilled water. Wilson (1983) concluded from the investigation that efforts to model soil freezing using standard finite difference techniques were unsuccessful because the model did not take into account the effects of a continuous phase change and distributed latent heat nor changes in the bulk salinity with time. Wilson (1983) suggested that diffusion of solutes from the partially frozen region to the thawed region was a contributing mechanism to the redistribution of solutes since solution in the partially frozen region of the column was more concentrated than near the base. Mahar, et al. (1983) interpreted Wilson's bulk salinity profiles to be a result of brine drainage during freezing in a manner similar to the processes that occur during the formation of sea ice.

A laboratory investigation on a soil similar to the type used by Wilson (1983) was conducted on a soil saturated with saline solution to determine the latent heat of fusion in the soil (Vinson and Jahn 1985). The soil used in this investigation was obtained from Prudhoe Bay, Alaska and was classified as either a gravelly sand or a sandy gravel with less than 2% fines (percent passing the No. 200 sieve). It was saturated with seawater solutions of three different concentrations, 15, 30 and 50 ppt, in three separate tests. The relationship between freezing temperature and salinity, and between the latent heat and temperature were calculated using relations given by Ono (1975) and Assur (1958) for seawater. Thermal resistance of the cell was calculated by testing the soil saturated with distilled water. Each of the tests on the soil containing saline solution was conducted on a thawing soil which had been rapidly frozen prior to the test. This procedure was followed to avoid potential complications due to supercooling the pore fluid which could occur during a freezing test.

Results of the study by Vinson and Jahn (1985) were used to calculate the latent heat as a function of temperature and the total latent heat between the minimum test temperature (typically -14 °C) and the freezing temperature of the solution. A comparison between the amount of latent heat released as a function of temperature and the theoretical curve (Ono 1975) suggests the two agree to within a few percent. A comparison between the theoretical and measured latent heat released between temperatures of -14 °C and the freezing temperature of

the solution showed that the measured latent heat matched to within 4.5%, 0.9% and 0.1% of theoretical value at salinities of 15, 30 and 50 ppt respectively. In each case the measured value was less than the theoretical value. Changes in the distribution of solutes due to freezing were not measured. Consequently, the effects of solute movement on the amount of latent heat released could not be measured or estimated. Results from this investigation suggest that application of freezing relations derived for seawater solutions may be directly applied to the coarse–grained soil tested. It may also be concluded that these results indicate that surface potentials on the mineral grains tested in this study had minimal effects on the latent heat released during freezing.

A laboratory investigation into the effects of freezing on the distribution of solutes in sand filled columns saturated with NaCl solution and frozen at constant rates was performed by Baker (1987). Subsequent reports and interpretation of these results have been presented by Baker and Osterkamp (1988), Baker and Osterkamp (1989) and Baker, et al. (1990). In these tests the sand used was a medium to fine–grained silica sand sieved to pass the 30 but not the 60 sieve. Freezing took place from the top down at constant rates that ranged from $1.2\text{x}10^{-8}$ to $2.2\text{x}10^{-7}$ $\frac{\text{m}}{\text{s}}$ by pulling columns (dia.=$6.03\text{x}10^{-2}$ m, length=0.42 m) from a glycol bath at -0.6 °C into a refrigerator at -14 °C. Six columns were mounted in the apparatus to be frozen with the first column removed after approximately 3–10 days of freezing (depending on the freezing rate) and approximately equally spaced intervals thereafter. A feature of this freezing apparatus was that the temperature gradient near the interface ranged from 79 to 120 $\frac{^{\circ}\text{C}}{\text{m}}$.

Results of this investigation were, in general, similar to the salt redistribution results obtained by Wilson (1983). However, the experimental apparatus used by Baker (1987) allowed for the measurement of the redistribution of solutes as a function of time. Baker (1987) showed that the amount of solute redistribution was inversely proportional to the freezing rate and the amount of redistribution increased with time (see Table 3.3 and Figure 3.10 of Baker 1987). Baker (1987) neglected the time–dependency of his data, which is particularly evident at the start of freezing, and used results from the BPS theory to describe the exclusion of solutes from the growing ice to the liquid ahead of the ice interface. A boundary layer region in front of the moving ice–bonded interface of high solute concen-

tration, predicted by the BPS theory, which could also indicate the formation of horizontal bands of solutes was not observed on a sampling scale of 1 centimeter. Baker (1987) performed a special freeze test in which small conductivity cells were placed within a column to determine if a boundary layer enriched in solutes formed ahead of the downward moving ice–bonded interface. Results of this test showed that a boundary layer could not detected to within the $5x10^{-4}$ m resolution of the the conductivity cells.

Baker's results also showed that solutes were redistributed in the partially frozen region some distance behind the ice–bonded interface. Baker (1987) (see Figure 3.8 of Baker 1987) shows that up to 40% of the redistribution of the solute occurred behind the ice–bonded interface. Baker (1987) also shows that approximately 10 to 20% of the solute redistribution occurred further than several centimeters behind the ice–bonded interface. His results generally show that redistribution of solutes occurred without a corresponding decrease in gravimetric water content (except near the surface and the ice–bonded interface where they sometimes change up to several percent), an indication that convection was occurring in the partially frozen region. Baker (1987) hypothesized that convection in the partially frozen portion of the sand occurred in a manner similar to the processes leading to the desalinization of sea ice.

Since movement of brine in Baker's experiments was time dependant and occurred by way of convection through the interface, applicability of the the BPS theory to this experiment is questionable. Time variations in the distribution coefficient at constant growth rates (see Table 3.3 in Baker 1987), may be interpreted to show that at least one or more physical processes which vary through time are as important as the freezing velocity in describing the redistribution of solutes in his experiment. Further investigation of his results showed that during a freezing experiment the temperature gradient at the interface increased in time from 79 to 120 $\frac{^{\circ}C}{m}$ and the cooling rate at the interface decreased from $5.8x10^{-6}$ to $2.7x10^{-6}$ $\frac{^{\circ}C}{s}$ (see Figure 3.7 in Baker 1987).

Baker (1987) and Baker, et al. (1990) showed that the resulting bulk salinity profiles could not result from brine expulsion during freezing. By adapting the model presented by Cox and Weeks (1975) to determine the amount of brine expulsion that could be expected during freezing to the partially frozen columns, it was shown that brine expulsion could account for only a small portion of the

observed solute redistribution. This conclusion was similar to the conclusion made by Cox and Weeks (1975) for laboratory grown NaCl ice.

In a separate set of laboratory experiments Baker (1987) and Baker and Osterkamp (1988,1989) investigated the type of convection that led to solute movement in the columns. The laboratory experiments consisted of filling a portion of either a sand column or plexiglass chamber with sand saturated with a dyed saline solution and the remainder with sand saturated with either clear distilled water or a clear saline solution of different concentration, typically 35 ppt less than the dyed solution. In virtually every case in which the more saline solution overlaid less saline solution, the two layers mixed with fingers of dense saline solution displacing the solution below and fingers of less saline solution displacing the solution above. Convection due to viscous fingering generally occurred with pore fluid on one side of the cell or column moving down and pore fluid on the opposite side moving up. Baker (1987) applied these observations and the results of a stability criterion developed for unstable density gradients in a porous media (Wooding 1959) to show that solutes excluded from the solid–liquid interface due to ice formation could be advected away from the interface. Baker (1987) referred to these fingers as salt fingers and tentatively concluded this type of convection was occurring in the freezing columns. Salt fingering was only tentatively concluded to lead to the redistribution of solutes in freezing saline soils because the density gradients in the freezing soils are substantially less than 35 ppt step changes in concentration used in the salt fingering experiments and because salt fingers have never been observed in a partially solidified system containing ice, brine and soil. It should be noted, however, that fingers have been observed during the growth of ice from sodium chloride solutions (Niedrauer and Martin, 1979) and during thawing experiments in which sand containing frozen, dyed, fresh water overlain by sand containing thawed saline solution was allowed to thaw (Baker 1987).

Chamberlain (1983) investigated the effects of saline pore fluid on the rate and amount of frost heave that occurred while soils saturated with seawater solution were frozen. The distribution of solutes within the soils were measured before and after freezing several columns of fine-grained soil and one of a silty sand. The column of silty sand consisted of a Dartmouth Sand saturated with a 35.7 ppt seawater solution. The sand contained 40% silts by weight and 1% clay in a

column 18 centimeters in length. Freezing took place from the top down in three stages: the first stage lasted 70 hours and resulted in 11 centimeters of the sample being frozen with an interface gradient of 25 $\frac{°C}{m}$; the second stage lasted 100 hours and resulted in an additional 2 centimeters of the sample being frozen under a substantially reduced interface gradient; the third stage lasted 10 hours and the remaining 5 centimeters of the sample was frozen.

Results of this test showed that the Dartmouth Sand heaved 2 centimeters during freezing. However, the final bulk salinity profile was qualitatively similar to profiles presented by Wilson (1983) and Baker (1987). The minimum bulk salinity occurred at a depth of 7 centimeters or only 53% of the freeze depth at the end of stage 2 freezing. During freezing the bottom portion of the column was dessicated and water migrated to the middle portion of the column which resulted in the sample heaving. Horizontal bands of solutes were hypothesized but not observed. However, bands were believed to be occurring on a scale much smaller than the sampling interval.

1.2.3.2 Theoretical Studies

Theoretical studies pertaining to the redistribution of solutes in freezing soils have applied results of BPS theory developed during the solidification of metals to soils. Hallet (1978) showed that most of the typical freezing rates observed in soils resulted in the the region ahead of the interface becoming constitutionally supercooled. He also suggested that the ice would nucleate ahead of the constitutionally supercooled region to produce alternating layers of solute enriched zones parallel to the isotherms in the soil. Multiple bands of solute enriched zones were envisioned as this process repeated itself. He suggested this mechanism as a way to produce the frozen fringes that Miller, et al. (1975) and Aguirre–Puente and Fremond (1976) suggest are important to the development of ice lenses in soils. Solute banding occurs in metals during solidification when the growth conditions are similar to the conditions described by Hallet (1978). However, in metals such banding is usually associated with changes in the growth velocity of the interface and has not been associated with nucleation of ice ahead of the constitutionally supercooled layer (Flemings 1974).

Several investigators have accepted Hallet's banding hypothesis and attempted

to predict the concentration of solutes in bands forming in soils (Kay and Groenevelt 1983). Their research suggests that the concentration of solutes in the band can be up to 80 times greater than the initial solute concentration. Other investigators have attempted to measure areas of increased concentration that could be associated with banding at the solid–liquid interface (Chamberlain 1983, Baker 1987). Their measurements involved measuring the concentration of solute in both the solid and in the liquid ahead of the solid–liquid interface. Their results did not indicate the presence of zones of enriched solute concentration on a length scale that was at least $\approx 5\text{x}10^{-3}$ m (Baker 1987).

In contrast to the predominance of experimental studies involving the redistribution of solutes during freezing, most research into the conduction of heat during solidification has involved theoretical studies. Such phase change solutions are non–linear in the absorption or liberation of heat at the phase change interface; consequently few complete analytical solutions exist. Solutions that do exist are one–dimensional particular solutions to the imposed boundary conditions (Lunardini 1988). Theoretical studies of heat conduction during a change in state that are of concern for this research are those that take into account the phase change at a planar interface and the phase change at a diffuse interface. Neumann (c. 1860) is credited with obtaining the first solution to the conduction of heat during a phase change (Carslaw and Jaeger 1959). Neumann's solution involves seeking solutions to the heat conduction equation for a two layered solution of ice overlying water with all the latent heat from freezing liberated at a planar interface between the layers. Boundary conditions for this problem consist of constant initial temperature, constant temperature as $x \rightarrow \infty$ and a constant surface freezing temperature applied at $t = 0$. The phase change boundary condition is satisfied by specifying the interface location as a function of time to be $\propto t^{\frac{1}{2}}$.

Cho and Sunderland (1969) presented an analytical result in which freezing occurs over a range of temperatures between a solidus and liquidus temperature which are taken to be constant during freezing. This solution considers the latent heat of fusion to be released uniformly between the solidus and liquidus. However, for situations involving the solidification of saline solutions, most of the latent heat is released near the liquidus temperature. The phase change boundary condition was satisfied using the same techniques as used by Neumann. Application of such a solution to the solidification of ice containing saline solution is not practical

because the latent heat released is not distributed uniformly between the solidus and liquidus temperatures and temperatures which are less than the solidus temperature of salt ice (< -21.12 °C) are not routinely encountered.

Osterkamp (1987) presented an analytical solution to the phase change problem that takes into account the distributed latent heat present at a diffuse interface. This solution consisted of constructing a series of layers, evenly spaced in temperature, which have constant temperature boundaries. Within each of these layers the distributed latent heat associated with the phase change is assumed to be constant and incorporated within the heat capacity to form an effective diffusivity. A solution for each layer is obtained in a manner similar to Neumann's method; however, the phase change boundary condition is greatly simplified by incorporating the latent heat into the heat capacity. An effective heat capacity for each layer reduces the heat conduction–phase change solution problem to a series of heat conduction problems each with constant thermal properties in a given layer, constant temperature boundaries and continuous heat flux at each boundary. Increasing the number of layers decreases the temperature difference for each layer which makes the solution a more accurate representation of the distributed latent heat released during freezing.

A comparison between the solution of the 2 layer phase change problem solved by Neumann and the n layer solution to the phase change problem solved by Osterkamp (1987) gives insight into the differences in the heat conduction associated with a planar and diffuse interface. Osterkamp (1987) compared cases for the situation in which a one–dimensional coarse–grained soil saturated with saline solution of seawater concentrations was frozen without any solute redistribution during freezing. These results showed that for given freezing conditions the diffuse interface moved 34% further than the two dimensional planar interface over a 10 year period. At shorter times the percentage difference in depth of propagation between the two solutions increases. Differences in the interface growth rate are due to the distributed latent heat released during solidification and the rate of propagation of a temperature disturbance instead of a phase boundary through the soil.

A comparison between the two layer solution and the n layer solution also highlights the effect of the phase change over a range of temperatures, due to the presence of the solutes, on the heat conduction. The presence of solutes cannot

be taken into account with the 2 layer solution, therefore, all of the latent heat is released at the solid–liquid interface. The n layer solution, however, can take into account the presence of solutes through the distributed latent heat. Distribution of the latent heat between the freezing temperature of the bulk solution and the eutectic temperature shows that the solutes affect the brine volume throughout the partially frozen region. However, this effect is not uniform between 0 °C and the eutectic temperature. Curvature associated with the phase diagram for NaCl is zero at 8.9 ppt and negative at greater salinities. For a solute concentration less than about 9 ppt the effect on the freezing relations is small and they affect the conduction of heat mainly near the freezing point. For a solute concentration greater than about 9 ppt the effect on the freezing relations is large and increases with initial solute concentration. In this case, the solute affects the conduction of heat between the freezing temperature and the eutectic temperature. The conclusion that may be drawn from the shape of the NaCl phase diagram and a comparison the 2 layer solution to the n layer solution is that the solutes affect the flow of heat during freezing and that these effects increase with solute concentration. It is clear that the flow of heat depends on the solute concentration, or that the heat flow is coupled to the concentration of solutes in the soil.

1.2.3.3 Summary of Solute Movement and Heat Flow During Freezing in Coarse–Grained Saline Soils

Wilson (1983) showed that coarse–grained soils from Prudhoe Bay, Alaska which had been saturated with saline solution and unidirectionally frozen led to the transport of solutes from the partially frozen portion of the column to the thawed portion of the column. A process similar to brine drainage was thought to occur during freezing and was suggested as a mechanism to explain the redistribution of 17 to 40% of the solutes over a distance of several tens of centimeters in a several day period. The presence of a diffuse interface was noted in virtually every freezing experiment in which the soil was saturated with a saline solution.

Vinson and Jahn (1985) performed freezing experiments on a coarse–grained soil obtained from Prudhoe Bay, Alaska to determine if the mineral grains of the soil had a measurable effect on the latent heat of freezing. Their results suggest that, for a soil with a mass average particle diameter of 4.7×10^{-3} m and less than

2% fines, mineral grains have a negligible effect on the quantity of latent heat between the freezing temperature and -14 °C for seawater salinities of 15, 30, and 50 ppt. Their study showed that the latent released as a function of temperature compared favorably to the theory developed for seawater suggesting that the phase relations for seawater may be directly applied to determine the phase relations of coarse–grained soils at temperatures below the freezing point of the solution.

Baker (1987) approached the problem of solute movement in freezing columns of medium to fine–grained sand using methods analogous to those which have been applied to explain and quantify the desalinization of sea ice. It was concluded that the redistribution of solutes in the soil columns due to freezing was by a mechanism similar to gravity drainage and that the results could be interpreted with BPS theory when time variations in the data were neglected. Bulk salinity profiles obtained during freezing suggest that a mechanism similar to brine drainage was responsible for the movement of brine within the partially frozen region during freezing. Salt fingering was suggested as the form of convection leading to the movement of brine that had been excluded from the solid–liquid interface; however, fingers were not observed in the freezing soil columns. Salt fingers have been directly observed in laboratory experiments in thawed sand saturated with solutions of two different salinities, one of which had been colored with a dye. They also have been observed during laboratory experiments in which dye was injected underneath growing salt ice. Baker's results showed that the solid–liquid interface was a diffuse interface rather than a planar interface (Baker 1987).

Theoretical studies hypothesized that similar processes that occur during the solidification of metals occur during the freezing of soils (Hallet 1978). These processes include the development of a boundary layer of enriched solute concentration in front of the solid–liquid interface which is subject to the same stability conditions as a planar interface and the formation of solute bands in front of the solid–liquid interface. However, the hypothesis proposed for the formation of banding in soils is quite different from that observed in metals.

Solutions to the heat conduction equation for planar and diffuse solid–liquid interfaces are available (Carslaw and Jaeger 1959, Osterkamp 1987). These solutions suggest that the mechanisms leading to heat conduction and propagation of the phase boundary are quite different depending on the morphology of the interface and that the presence of solutes within the soil solution implies a coupling

between solute concentration and heat flow in the soil. These heat conduction solutions do not consider solute redistribution. Analytic solutions to coupled heat and solute convection equations are not available.

1.3 Summary of Solute Redistribution During a Change in Phase

Processes that occur during the solidification of metals suggests that constitutional supercooling may be used to predict the onset of a diffuse interface in metals. If the interface is stable and planar, BPS theory has been shown to work well in predicting the concentration of solute in the solid and the redistribution of solutes. If the interface is diffuse, redistribution of solutes occurs by convection and the processes leading to convection are best understood in terms of the fluid dynamic instabilities that develop during solidification.

In sea ice research it has been generally accepted that constitutional supercooling results in a transition of the solid–liquid interface from a planar interface to a diffuse interface and that redistribution of solutes is due to convection throughout the partially frozen and thawed solution. Application of BPS theory to calculate the redistribution of solutes works well, but the theory does not match the observations made during ice growth. These results suggest that at some level the desalinization of sea ice is controlled by diffusive processes, or the convection that occurs may be such that it can be modeled with an effective diffusion coefficient which is much greater than the molecular diffusion coefficient.

Several experimental investigations on coarse–grained soils saturated with saline solution and frozen have shown that the interface is diffuse which leads to the incorporation of a large amount of brine within the soil which is redistributed by convection in the partially frozen region (Wilson 1983, Chamberlain 1983, Baker 1987). The form of convection in the partially frozen region has been suggested to occur by a fingering mechanism (Baker 1987, Baker and Osterkamp 1989) but has not been clearly demonstrated. Further, the mechanisms which control the onset of convection have not been clearly demonstrated. Neglecting the time dependency in his data, Baker (1987) applied results of the BPS theory to show that solute movement in freezing coarse–grained soils may be controlled by diffusive phenomena at the interface between the solid and liquid. Time variations in his

data, which cannot be accounted for with the BPS theory, and the presence of convection within the partially frozen region suggest that at least one or more physical processes which vary through time are as important as the freezing velocity in describing the redistribution of solutes in soils. Baker's experiments do not provide any insight into the factors that lead to the time variations in his data.

1.4 Dissertation Objective

The objective of this dissertation is to investigate the fluid dynamic instability that leads to convection and the redistribution of solutes during freezing. The redistribution of solutes during freezing by a convective mechanism was first suggested in the interpretation of Wilson's experiment by Mahar, et al. (1983) and quantified by Baker (1987). who showed that a gravity drainage phenomenon similar to the phenomenon that leads to the desalinization of sea ice led to the redistribution of solutes in the freezing soils. In this dissertation, the redistribution of solutes will be considered using earlier hypotheses that the fluid dynamic instability which develops during freezing leads to convection and the redistribution of solutes from the partially frozen region to the thawed region. Previous research which is based on interface stability and the presence of diffusion controlled redistribution, BPS theory, may be used to predict the final salinity profiles; however, the theory used to estimate the profiles and the observations of the processes that lead to the solute redistribution are contradictory. The purpose of this thesis is to directly address topics which pertain to the form of solute movement in the partially frozen region. These topics include developing a stability criterion for the fluid in the partially frozen portion of the sand, determining the velocity of the convecting fluid as the solutes are redistributed, and estimating the magnitude of redistribution that occurs during freezing of fine-grained sand saturated with saline solution. These topics will be discussed in reference to experimental data obtained from a series of laboratory experiments in which columns of medium to fine-grained sand saturated with saline solution with concentrations of 1, 35 and 100 ppt were frozen from the top down under conditions commonly encountered in the Arctic.

Chapter 2

Experimental Methods

2.1 Introduction

A major emphasis of this research was to develop a soil freezing apparatus capable of monitoring the distribution of a solute in freezing soils. The soils range from fine–grained frost susceptible soils that draw fluid to the interface during freezing to coarse–grained soils that expel fluid from the interface during freezing. The purpose of this chapter is to present material that relates to the design, construction and operation of the freezing apparatus in relation to its use on medium to fine–grained sands. The second section presents a review of experimental methods which have been used in investigations of solute movement in freezing experiments involving sodium chloride solutions. The third section presents a detailed description of the freezing apparatus including its physical dimensions. The fourth section presents details associated with preparation and operation of the apparatus.

2.2 Literature Review

Methods available to monitor the distribution of a solute during solidification may be classified as destructive or non–destructive and are presented in detail by Page, et al. (1982). Destructive methods are all similar in that they rely on solidification of one or more samples which are removed at different times during solidification to be analysed. Examples of destructive techniques include: measuring the electrical conductivity of a melted sample; titration of a portion of a melted sample; a direct measurement of concentration of the solidified sample with an electron microprobe. Non–destructive methods monitor the distribution of impurities remotely during

solidification. Examples of non-destructive techniques include: doping the solute with a radioactive tracer and monitoring its movement through time; removing a small amount of liquid from a partially frozen portion of the sample and measuring the change in concentration through time; placing electrical conductivity cells in the sample and measuring through time changes in conductivity which may be related to changes in concentration; using time domain reflectometry probes to determine solute concentration (Loon, et al. 1990).

Several of these techniques have been applied to measure the redistribution of soluble salts during the freezing of ionic solutions. Cox and Weeks (1975) monitored the distribution of a solute in growing sea ice by measuring the concentration of ^{22}Na with a scintillation detector. Their tests were conducted with a constant hydrostatic head during freezing and the solution was frozen under conditions that approximated Neumann boundary conditions (Carslaw and Jaeger 1959) to produce a growth rate that was proportional to $t^{-\frac{1}{2}}$. Wilson (1983) investigated the effects of solutes within the pore fluid on the heat transfer that occurred during the freezing of a large column (dia.=0.46 m) of soil. Wilson's tests were also conducted with a constant hydrostatic head and the soil was frozen under conditions that approximated Neumann boundary conditions (Wilson 1983). Baker (1987) investigated the effects of freezing on the distribution of a solute by freezing columns which were periodically removed during freezing, sectioned, then analyzed to determine the bulk salinity of each section. Bulk salinity measurements on each section of a column were used to construct a profile of bulk salinity for the column. Baker (1987) used the bulk salinity profiles obtained during freezing to monitor the solute redistribution that occurred during freezing. These tests were conducted at constant freezing rates and it appears that the hydrostatic head may not have been constant during freezing. In situ measurements of solute concentration during freezing were made by Loon, et al. (1990) using time domain reflectometry.

Each of the aforementioned experimental methods have advantages and disadvantages as methods to monitor the redistribution of solutes as soils freeze. For example, doping the salt solution with a radioactive tracer similar to that used by Cox and Weeks (1975) could be an excellent investigative method in soils, however, the soil grains could act as scattering sources for emitted radiation which may result in lost resolution. Drawing solution from the column to measure its concentration using methods similar to those of Wilson (1983) could also work

well, but experience has shown that even a small degree of undersaturation of the soil, which would occur when liquid is removed from the column, may significantly alter the transport processes that occur during freezing. Removing columns from a freezing apparatus using a method similar to the method used by Baker (1987) relies on the assumption that each column, and the processes occurring in each column are similar both spatially and temporally. Tests with conductivity cells show that they do not operate well in partially frozen environments, implying that conductivity cells placed within a saturated soil could only be used in the thawed portion of the column. Time domain reflectometry probes have recently been successfully used to measure the bulk electrical conductivity in partially frozen soil (Loon, et al. 1990), however, the results obtained from TDR probes indicate an average over the length and up to several diameters of the probe (Zegelin, et al. 1989, K. Kawasaki pers. comm. 1990).

2.3 Design and Construction of the Freezing Apparatus

Based on the design of each of the experiments discussed in the previous section, a combination of the principles used in earlier experiments were incorporated into the design and construction of the freezing apparatus built for this investigation. The principle used by Baker (1987) of freezing several sand columns which were periodically removed during freezing to be sectioned and analyzed was used because of its high degree of precision in the measurement of bulk salinity. The principle used by Cox and Weeks (1975) and Wilson (1983) of freezing from the top down, with a constant hydraulic head, under conditions that approximated those that occur naturally was used because the effects of a variable interface growth rate on the magnitude of solute redistribution could be investigated. A combination of these features resulted in a freezing apparatus which consisted of an insulated, sand filled box that contained seven vertical sand columns which rest on a heated radiator. Adjacent to the sand box was a heated chamber which contained the expansion reservoirs for each column and for the sand box used to maintain the hydraulic head during freezing. Figure 2.1 is a schematic cross section of the freezing apparatus and Figure 2.2 is a schematic plan view of the freezing apparatus. Figure 2.3 is a schematic description of the radiator and manifold used

in the freezing apparatus. Both the sand box and heated chamber were located in an environmental chamber. The purpose of this section is to present, in detail, the physical construction of the freezing apparatus. This section includes the physical dimensions and construction details of the freezing apparatus as well as the theoretical considerations used to determine various aspects of the apparatus design.

2.3.1 Environmental Chamber

The freezing apparatus was located in an environmental chamber so that the conditions which lead to freezing of the sand could be accurately controlled. The environmental chamber was a 1.8 m x 3.0 m x 2.5 m high room which utilized a Watlow 1500 PID Controller to operate a Barber-Coleman Freon 12/hot gas valve. The PID controller was tuned for minimum deviation from set point temperatures which were approximately ± 0.3 °C during normal operation. Tuning the controller for minimum deviation in the set point temperature resulted in a loss of temperature control for rapid temperature changes such as those encountered during initial start up of the system or after an approximately twice daily $\approx$ 5–10 minute automatic system shutdown to melt frozen condensate on the chambers evaporator coils. Precision in temperature ramping capabilities between set points was not affected by tuning the controller for minimum set point deviations as long as the ramping rate was not too large ($\leq 8\text{x}10^{-3}\ \frac{°C}{s}$). Rapid temperature changes, such as those that resulted from a defrost cycle, resulted in deviations of up to 5 °C from which the system recovered after approximately one hour.

2.3.2 Sand Filled Box Construction

The sand filled box consisted of the 0.216 m^3 cubic box that contained the sand and sand columns which rest on a radiator to control the temperature at the base of the box. The sand box was constructed of $9.5\text{x}10^{-3}$ m thick PVC sheets held in place with metal bands and strengthened with two sets of iron channel placed horizontally around the box. Corners of the sand box were sealed with a small amount of Dow Corning 732 Silicone RTV. Insulation, 0.1 m thick extruded polystyrene, placed around the sides of the box was also held in place with metal bands.

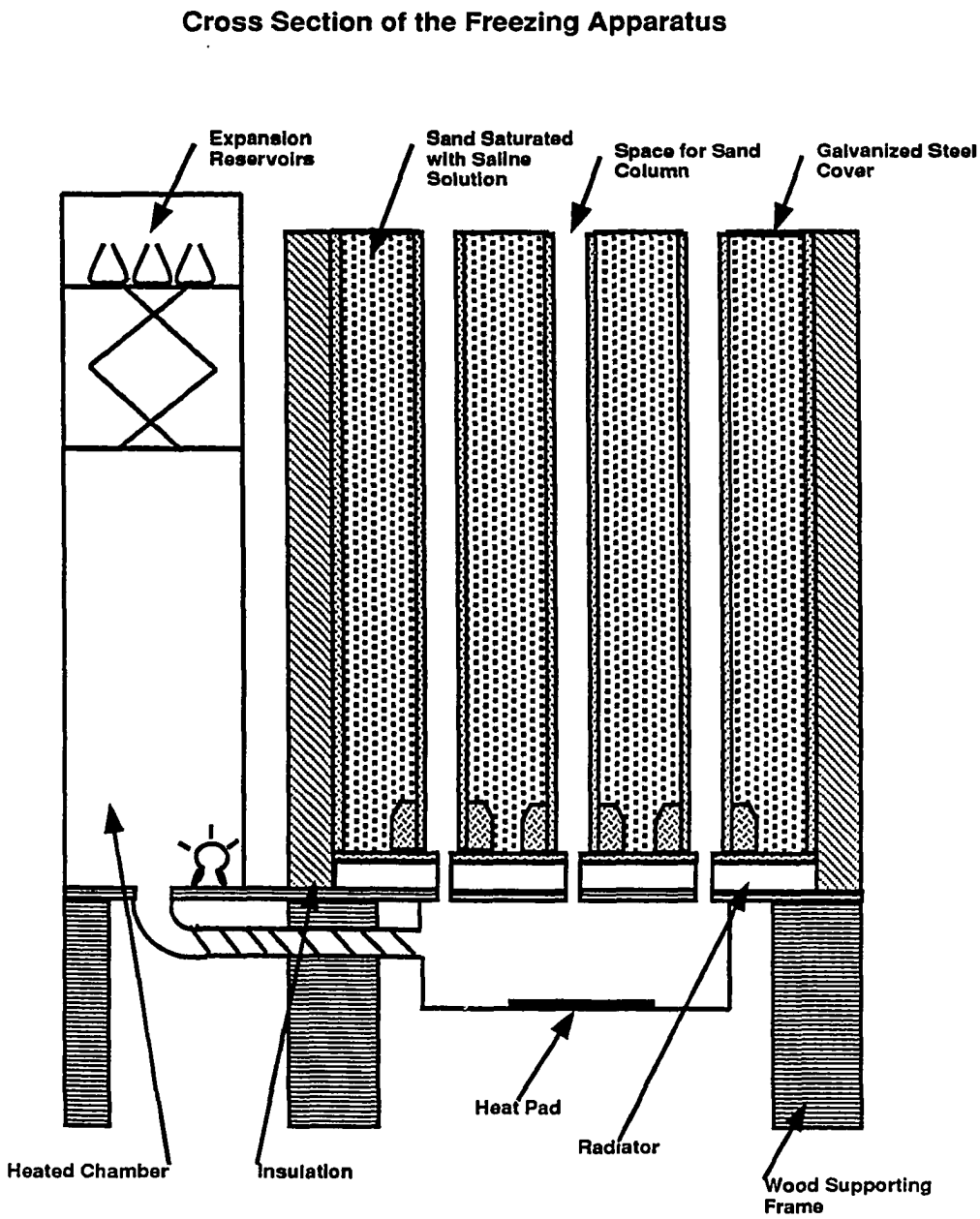

Figure 2.1: A schematic cross section of the freezing apparatus showing the insulated sand box, radiator, heated chamber for the expansion reservoirs and frame for the apparatus. The sand columns have not been included in this drawing to improve the clarity of the figure. However, sand columns are placed in the unshaded region in the sand filled box. Beneath the supporting frame is the heated passageway which connects the base of the columns with the expansion reservoirs.

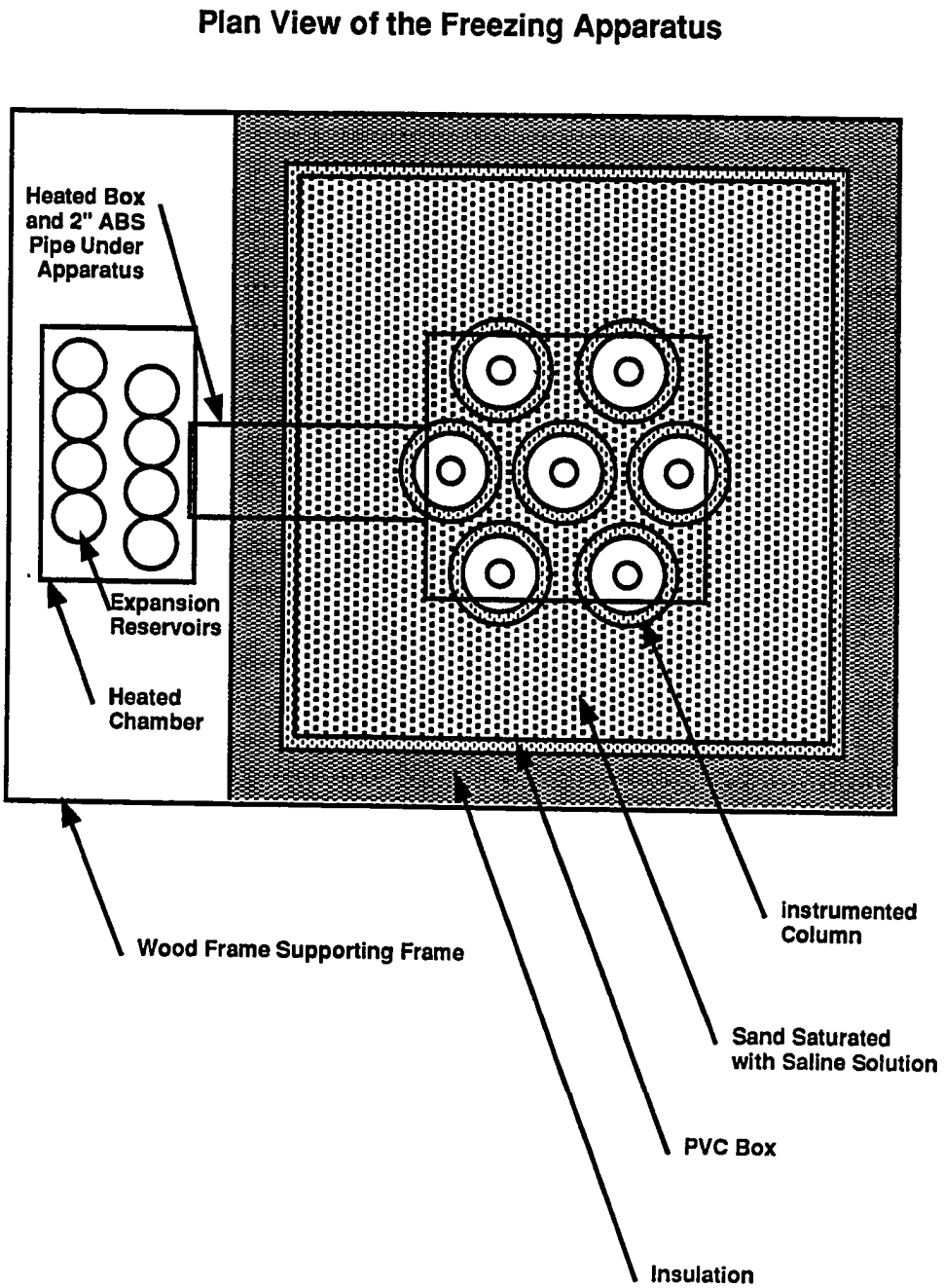

Figure 2.2: A schematic plan view of the freezing apparatus shown in Figure 2.1.

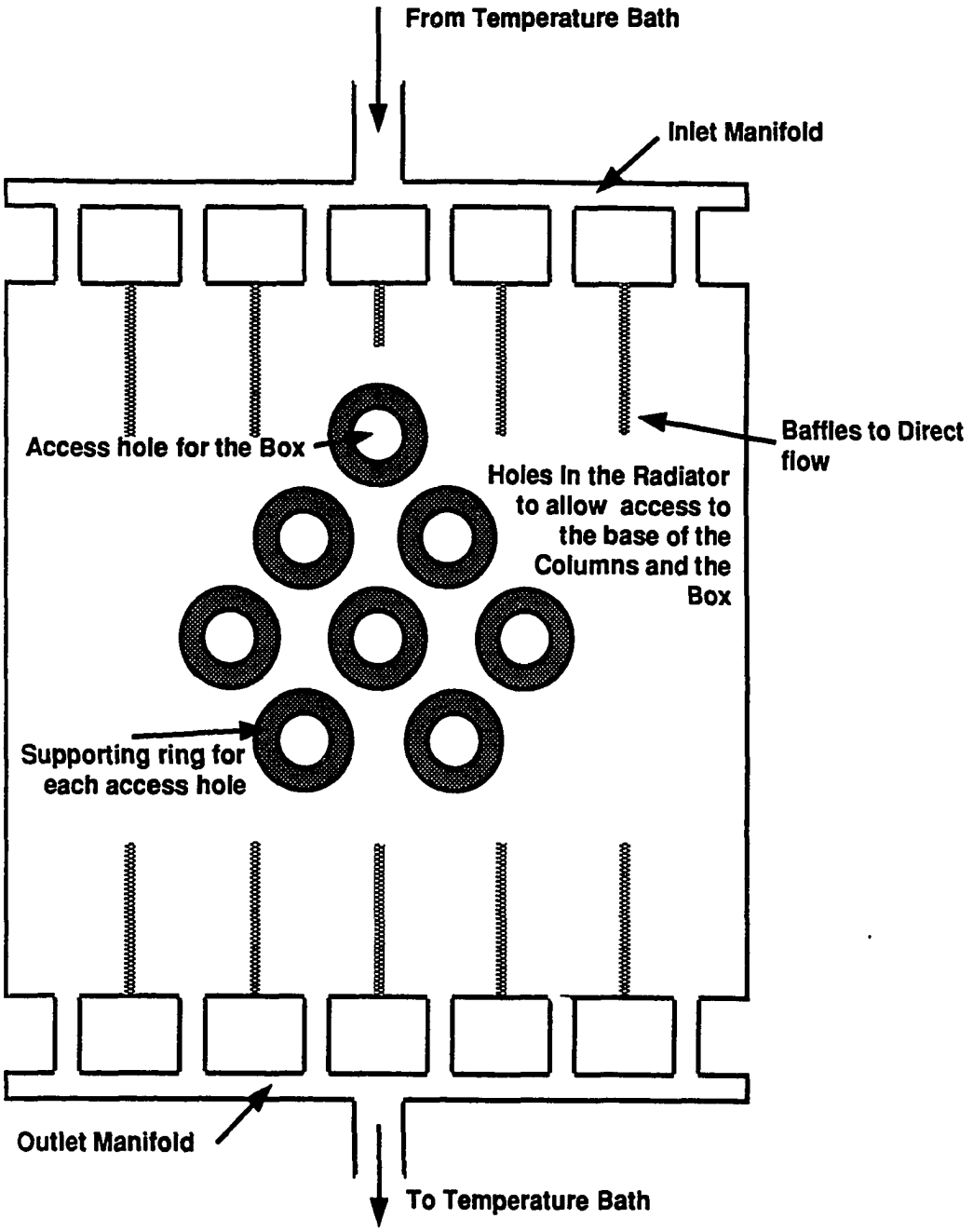

Figure 2.3: A schematic plan view of the radiator used to control the temperature at the base of the freezing apparatus. Glycol from a Forma Scientific temperature bath is distributed and collected through the inlet and outlet manifolds. Baffles within the radiator helped to channel the flow through the radiator. The eight vertical holes through the radiator are passageways for tubes connected to the base of sand box and the seven sand columns.

During freezing it was important that the freezing interface across the sand box be as horizontal and planar as possible so that the conditions which led to freezing in each column were similar. A horizontal freezing interface implies that the conduction of heat was one dimensional which was an important condition for avoiding the potential complications associated with two dimensional heat conduction. The purpose of the sand around the columns was to reduce the horizontal temperature gradients in the vicinity of the columns. To determine the horizontal dimensions of the freezing apparatus and the thickness of insulation required to produce a horizontal interface in the vicinity of the columns, a two dimensional finite difference program to numerically solve the heat conduction equation was developed for the sand box. This model employed an explicit enthalpy method (Voller and Cross 1981) to calculate the position of a downward moving freezing interface in a coarse-grained sand saturated with pure water. A $1x10^{-2}$ m node size was used in the model; consequently, the sand was treated as a homogenous unit neglecting the effects of the PVC sidewalls or sleeves since each of these features were less than $1x10^{-2}$ m in horizontal extent. Boundary conditions for this model included: a constant initial temperature, constant temperature at the base of the apparatus, constant surface temperature on the top and sides of the freezing apparatus and a constant phase change, or freezing temperature. The interface location calculated with this model was considered smooth and horizontal if the 0 °C isotherm deviated by less than 10^{-2} m across the apparatus during the freezing of the top 0.3 m of sand. Results from this model indicated that a cubic box 0.6 m on a side and insulated with 0.1 m of polystyrene insulation would be more than adequate to produce a horizontal interface in the region of the columns.

The seven vertical tubes that sleeved the sand columns were arranged in a hexagonal pattern about the middle of the box and were attached to the base of the sand box so that the sand columns could removed during freezing. Each sleeve was constructed of schedule 40, 3 inch nominal (I.D.=8.94 $x10^{-2}$ m, O.D.=1.02 $x10^{-1}$ m) PVC tubes that were threaded on one end to screw into a schedule 80, 3 inch pipe coupling mounted on the base of the box. Each schedule 80 coupling was mounted on the base of the apparatus with six brass countersink machine screws tapped into the coupling. A seal between the base of the box and the coupling was made with Dow Corning 732 Silicone RTV. The length of the PVC sleeve, when attached to the coupling, was 0.60 m. A seal between the sleeve and the

coupling was made by coating the threads of the sleeve with Whitlam Black Magic Industrial Grade Pipe Thread Compound.

Sand columns were constructed to fit into the PVC sleeves so that periodically during freezing each could be removed from the freezing apparatus without disrupting the other columns or the sand box. Figure 2.4 is a schematic drawing of the construction of a column and shows the location of an expansion reservoir in relation to the top of a column. Sand columns were constructed of Tenite Butyrate tubing 8.890×10^{-2} m in diameter. Convection in the annulus between the sand column and PVC sleeve was avoided or significantly reduced because of the tight fit between the sleeve and the sand column. The thickness of the annulus between the two cylinders was only 2.5×10^{-4} m and also the unevenness of the of the diameter of both the PVC and Tenite Butyrate tubing resulted in the tight fit.

Each sand column was sealed on both ends to contain the sand and pore fluid solution within the column while the sand was saturated and during freezing. The bottom was sealed with an aluminum plate 1.91×10^{-2} m thick with an outside diameter machined to be 2.5×10^{-4} m larger than the inside diameter of the Tenite Butyrate tubing. It was sealed and held in place with a small amount of Dow Corning 732 Silicone RTV. The top was sealed with an aluminum plate 6.3×10^{-3} m thick with an outside diameter machined to be 3.2×10^{-4} m smaller than the inside diameter of the Tenite Butyrate tubing. It too was sealed and held in place with a small amount of silicone RTV. The top seal was loose so that if the sand heaved during freezing the top seal would break rather than the bottom one. Both top and bottom aluminum plates on each column were center drilled and tapped to accept a $\frac{1}{8}$ inch pipe thread to male serrated hose fitting which facilitated filling the columns with fluid. Both top and bottom aluminum plates were fitted with bronze sintered filter elements to retain sand within the column as fluid passed through it during filling and during freezing.

Two thermistors were imbedded in the base plate of the instrumented column at a known spacing to measure the heat flux through the base of the column. These thermistors were calibrated similarly to the other thermistors used in this investigation, see Section 2.3.3. The two thermistors were placed in holes drilled with a #45 drill so that they were positioned halfway between the center and edge of the plate. They were separated by a vertical distance of 6.14×10^{-3} m (center

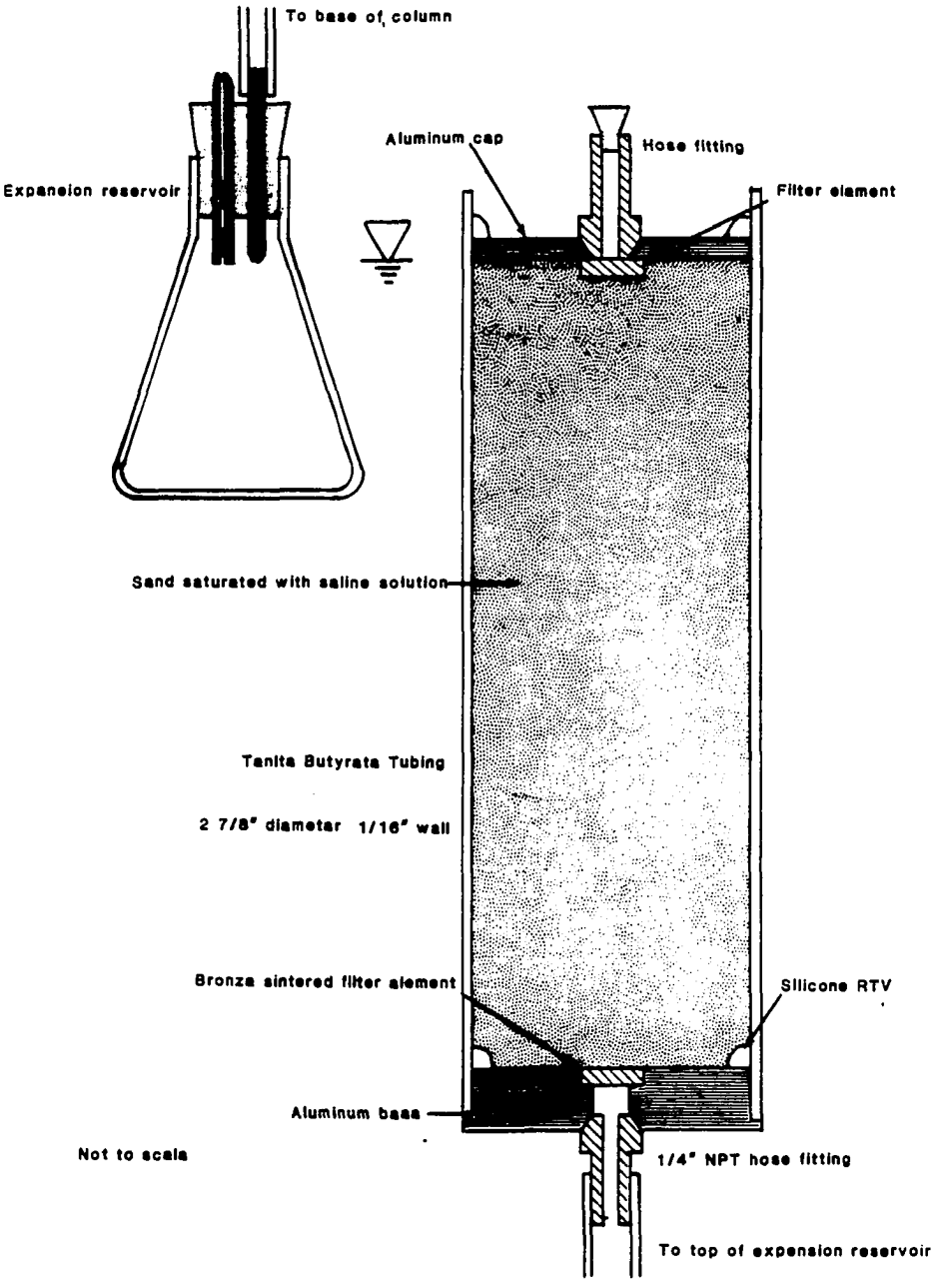

Figure 2.4: A schematic view of the sand columns used in the freezing experiments. Sand columns were placed in the sand box to freeze, Figure 2.1, and were periodically removed during freezing to monitor the distribution of the solute in the column. During freezing, the top of the column was capped and the base was connected to the expansion reservoir. Freezing took place with the top of the column level with the drip mark on the expansion reservoir.

to center distance) and were placed such that they were approximately halfway between the top and bottom of the plate. The aluminum plate was composed of Alcoa 6061-T6 alloy which has a thermal conductivity of 167 $\frac{W}{m°C}$ (Alcoa 1960).

Temperature control at the base of the sand box was achieved by placing the sand box on a heated radiator. The radiator consisted of two 0.6 m x 0.6 m aluminum plates separated by $2.5x10^{-2}$ m with glycol circulated between the plates. Five holes on two opposite sides of the radiator were connected to manifolds which distributed and collected fluid pumped from a Forma Scientific bath (model 2161) located outside the environmental chamber. The level of the bath was positioned to be at the level of the radiator to reduce head loss in the pump and thereby increase flow through the radiator. Flow rate through the radiator was $\approx 1.5x10^{-3}$ $\frac{m^3}{s}$ and was channeled within the radiator by vertical baffles that extended 0.1 m from the sides containing inlet and outlet ports into the middle of the radiator. Tests to determine the temperature variation at the surface of the radiator, prior to placing the sand box on it, showed that temperature differences were no greater than 0.1 °C (measured with an instrument having a resolution of 0.1 °C). Eight vertical sealed holes through the radiator allowed access to the bottom of each of the seven columns and a drainage port at the base of the sand box.

The heated chamber adjacent to the sand box contained the sand column expansion reservoirs. The heated chamber was a 0.3 m x 0.3 m x 0.77 m high plywood box insulated on the four vertical sides with $2.5x10^{-2}$ m of compressed styrofoam bead insulation and was heated with a 60 W light bulb at the base. Expansion reservoirs were mounted on an adjustable base so that their height could be adjusted to be level with the top of the sand columns at the start of the experiment. The height of the expansion reservoirs was kept constant after the start of the freezing experiment.

Sand columns and the sand box were connected with their expansion reservoirs by tubes routed through a 2 inch ABS pipe that connected the base of the heated chamber with a heated box attached to the bottom of the frame supporting the radiator and sand box. The 2 inch ABS pipe was wrapped with heat tape and insulated. The heated box was heated with a 75 W silicone heating pad glued to a 0.1 m x 0.1 m aluminum plate for a heat sink. Tygon tubing, $3.2x10^{-3}$ m in diameter, was used to connect the expansion supply reservoirs with the base of

the sand columns and sand box.

2.3.3 Measurement of Temperature Within the Freezing Apparatus

Measurements of the temperature field within the sand box were used to monitor freezing and to determine the uniformity of freezing conditions for the sand columns. Temperature measurements to monitor freezing were made with a string of thermistors placed next to one of the columns, the instrumented column, which were logged every half hour. Temperature measurements to determine the uniformity of the freezing conditions in the freezing apparatus were made by lowering a thermistor into any one of seven liquid filled stainless steel tubes adjacent to each of the columns. A temperature profile was measured next to a column prior to its removal from the freezing apparatus. All thermistor measurements were made with a Hewlett Packard data acquisition system which consisted of an HP 85 controller, an HP9836 voltmeter and multiplexer and an HP 82901 $5\frac{1}{4}$ inch dual disk drive. Resistances of the thermistors (Fenwall GB35P2 Glass Thermistor Probes–nominal resistance of 5000 ohms at 25 °C) were measured using a two wire configuration. Each thermistor was calibrated with the data acquisition unit in mercury and gallium triple-point cells and a water ice point cell. Results of the calibration were used to fit the thermistor resistances and temperatures to the Steinhart equation (Steinhart and Hart 1968). All resistance measurements were converted to temperature prior to storing them on disk.

Sensors at the instrumented column consisted of 28 thermistors placed such that a vertical temperature profile starting from above the top of the column to the base of the sand box could be obtained. One thermistor was located at $5\text{x}10^{-2}$ m above the column surface and another at the surface of the column. Twenty–four thermistors were mounted on a thin piece of PVC which was inserted between the column and the sleeve in a gap made by cutting away a section of the sleeve and resealing it with another piece of PVC that overlapped the outer surface of the sleeve. The two remaining thermistors were placed in the aluminum base at the bottom of the column and were used to measure the heat flux through the base of the column, see Section 2.3.2. Spacing of thermistors attached to the piece of PVC and the thermistors mounted in the aluminum plate were measured to

within 10^{-4} m, see Appendix D for these results.

The sensor lowered into the liquid filled stainless steel tubes consisted of a thermistor mounted on a thin stainless steel tube marked such that the probe could be lowered through the sand box in $\approx 2x10^{-2}$ m increments to obtain a vertical temperature profile. Appendix D presents the location of the marks on the probe; spacings were measured to within 10^{-4} m. Inside diameter of the liquid filled stainless steel tube was $3.8x10^{-3}$ m, its length was 0.61 m and it was filled with Dow Corning 200, a 5 centistoke non–conducting silicone fluid, to decrease equilibration time of the probe. The probe consisted of a 0.61 m stainless steel tube, $3.4x10^{-3}$ m in diameter, with a thermistor sensor mounted on one end in a protective aluminum guard. Equilibration of the sensor was assumed when the resistance value changed by no more than 1 ohm ($\approx$ 0.001 °C) in 7.5 seconds.

2.4 Preparation and Operation of the Freezing Apparatus

Preparation of the freezing apparatus includes the details associated with producing a constant salinity within the sand in the box and preparing seven sand columns for freezing. Operation of freezing apparatus includes the details associated with equilibrating the sand box to an initial temperature prior to the start of the experiment, starting the freezing experiment and the methods used to monitor freezing during the experiment.

2.4.1 Preparation of the Freezing Apparatus

Prior to performing a freezing test, sand in the sand box was drained of solution and saturated with a new solution of the type to be used in the test. This solution was recirculated through the sand box until the salinity became constant with depth. Sand columns were prepared for the test in a manner that produced as constant physical properties and degree of saturation as possible between the seven columns. The initial bulk salinity in the columns was such that it matched the bulk salinity in the box to within 0.2 ppt.

2.4.1.1 Preparation of the Sand Box

Freezing could have redistributed solution in the sand box in a manner similar to the redistribution that occurred in the sand columns. Therefore, it was necessary to take steps to obtain a constant sand solution salinity within the sand box after every test. In preparation for a freezing experiment, solution in the sand box from the previous test was syphoned from the box and discarded. The sand was then saturated with $\approx 7.5 \times 10^{-2}$ m^3 of new solution which was circulated from the bottom to the top of the box. Mixing of the sand solution continued until vertical salinity variations were less than 5% as measured by drawing solution from the sand box at 5×10^{-2} m intervals and measuring the salinity of the solution. It was necessary to circulate the new solution through the box 2 to 3 times. Solution was added from the bottom of the box in a manner similar to the techniques used to saturate the sand columns (discussed in the next part of this section) except that vacuum was not applied. Filling the box from the bottom and circulating fluid to the top also helped to displace air bubbles in the sand to the surface. Draining and filling the sand box was facilitated with a sintered filter element in each of the four lower corners of the box. These filter elements were attached to clear plastic tubing which extended through the top of the box at the corners and were were left in the apparatus during freezing. After the box was filled and saturated with solution, a piece of 20 gauge galvanized steel with a white surface and holes drilled in it so that it could fit over the sleeves was placed on top of the apparatus to reduce evaporation from the sand. The edge of the galvanized steel cover and the PVC wall of the box were covered with duct tape to further reduce evaporation. Salt solution for the sand box was made using Morton Canning and Pickling Salt which is an evaporated granulated salt, 99.9% NaCl (E. Kuhajek, written comm. 1989). Distilled water was used to prepare this solution.

2.4.1.2 Preparation of the Sand Columns

When preparing sand columns for the freezing apparatus it was important that the physical properties of a sand column be both known and as similar as possible to the other six columns. Critical properties for these tests were, permeability, bulk density, and gravimetric water content. Accurate permeability measurements could not be made on each sand column; the permeability was measured on several

samples of sand in a permeameter prior to the start of this investigation. Since permeability and water content of a given material depends on the packing, or density of the material, preparation of the sand columns involved reproducing the physical properties of the sand used in the permeability measurements (see Appendix C and ASTM Test D2434-68 A Standard Test Method For Permeability of Granular Soils).

Sand columns were constructed by glueing an aluminum plate into the base of a 0.62 m section of Tenite Butyrate tubing with a small amount of Dow Corning 732 Silicone RTV. The silicone cured for at least one day before the seal was tested for leaks and the column filled with sand. Sand columns were filled with Granusil 30 by adding $\approx$ 0.2 kg of dry sand then lightly tamping it with a weight using the same methods used when packing the sand for the permeability tests, Appendix C. This packing technique was repeated until the column was packed with material to a height of several millimeters less than 0.60 m, then the top of the column was covered with an aluminum cap which was siliconed in place. The mass of the sand used to fill the column as well as the height of the column were recorded to determine the initial dry bulk density of the sand.

Sand columns were saturated with salt solution 24 hours after the top aluminum cap had been siliconed in place. Each column was saturated in a manner similar to the methods outlined in ASTM D2434-68. As specified in the ASTM test, the sand and soil solution were held under a vaccum of at least 0.40 m of Hg for at least 20 minutes prior to filling. The sand columns were filled under a vacuum of at least 0.30 m of Hg. It took $\approx$ 20 minutes to fill a column. For reasons not well understood, it was necessary to add to each column 1 to $2x10^{-6}$ m^3 of salt solution over a period of several days prior to the experiment to insure that the sand was saturated. The mass of the solution added to the tygon tubing and column were recorded to determine the initial physical parameters and to perform a salt balance on the column after it was sectioned.

Salt solution for the columns was made with reagent grade NaCl and distilled water. Samples of NaCl were weighed before and after being dried in an oven for 24 hours to determine the component of absorbed water in the NaCl. These measurements indicated that absorbed water accounted for less than 0.2% by weight of the NaCl; consequently, the hydrated weight of the NaCl was not considered when preparing the solutions. A salt solution was prepared at least 24 hours prior

to saturating the columns.

Sand columns were loaded into the sand box after they had been saturated with solution. A small amount of silicone thermal grease was applied to the bottom of each column prior to inserting it into a PVC sleeve to insure good thermal contact between it and the base of the box. The tube connected to the base of the column was routed to the heated chamber adjacent to the sand box and connected with the expansion reservoir.

2.4.2 Operation of the Freezing Apparatus

Operation of the freezing apparatus included equilibrating the sand box and columns to the initial temperature, initiating a freezing experiment and monitoring freezing while the experiment was in progress. The remainder of this section will present the details associated with these three phases of operation.

2.4.2.1 Equilibration of the Freezing apparatus

The purpose of the equilibration period was to lower the temperature of the material within the sand box to within $\approx$0.5 °C of the freezing point of the pore fluid solution. In principle, equilibration was accomplished by lowering the temperature within the environmental chamber and the radiator to the desired temperature and waiting for the vertical temperature profile in the middle region of the sand box to become constant to within 0.1 °C. In practice, equilibration was difficult because the coarse analog adjustment on the Forma Scientific bath required many fine adjustments to attain the desired radiator temperature. It usually took approximately 1 week for the freezing apparatus to equilibrate to the desired initial temperature.

2.4.2.2 Start of a Freezing Experiment

An experiment was initiated when the temperature of the environmental chamber was lowered to a set point temperature which was below the freezing temperature of the sand solution. The temperature was typically lowered to the set point for the experiment in less than 15 minutes. The environmental chamber linearly ramped to the specified temperature, but since this time was a fraction of an hour over an experiment which lasted hundreds of hours, the temperature change was

considered a step change. The freezing experiment was considered to have begun when the temperature in the environmental chamber first began to change toward the freezing set point.

Supercooling the sand solution within the sand filled box and the sand columns was avoided by nucleating ice at the surface of the freezing apparatus with liquid nitrogen. During the time that the temperature within environmental chamber was cooling to the set point, approximately $5x10^{-4}$ m^3 of liquid nitrogen was poured over the surface of the sand box and the sand columns. Care was taken to make certain that some of the liquid nitrogen came in contact with the sand in the sand box (recall that the top of the sand box was covered with sheet metal), and that some of the liquid nitrogen was poured on the columns. Evidence that supercooling was avoided with this technique was observed when the sand in the box was probed with a knife and determined to be ice–bonded and when the small, transparent solution filled tube extending from the top of the column was observed to contain ice.

2.4.2.3 Monitoring the Freezing Experiment

The environmental chamber, temperature data acquisition unit[1] and Forma Scientific Bath were essentially self–operating while a freezing test was being performed. However, over the weeks that it took to perform a freezing test slight adjustments were performed to keep the experiment running well. This section will present details associated with adjustments made during the freezing experiments.

When the chamber temperature was reduced to the colder temperatures, for example -12 °C, the temperature of the glycol circulated through the aluminum radiator at the base of the sand box would slowly decrease during the experiment as fluid circulated through the radiator cooled. Since the pore fluid at the base of the box was within a few tenths of a degree of freezing, it was necessary to increase the bath temperature slightly to keep this solution from freezing. These adjustments were less than 0.2 °C and were not made until absolutely necessary. Adjustments in the radiator temperature were recorded by a thermistor located at the base of the instrumented column which was logged every half hour with the

[1]See Appendix E for the details of associated with the operation of the data acquisition unit and a program listing.

data acquisition system.

When experiments were performed at warmer surface temperatures, for example -5 °C, the expansion chamber for the sand box did not operate correctly. During these experiments it was observed that solution was expelled through the surface of the sand box rather than the base even though the tube connecting the base of the box to the reservoir was observed to be ice–free. Since the surface temperature was such that the maximum amount of ice present in the sand was less than 50% of the pore space, it appears that expulsion of brine through the surface required a smaller pressure than expelling the fluid through the tube connecting the base of the sand box with the expansion reservoir. Since the columns were capped, this problem was not encountered and the reservoirs appeared to work well in each of the freezing experiments.

Fluid expelled to the surface of the sand box, as described in the previous paragraph, evaporated into air contained within the environmental chamber. A portion of this water vapor became deposited on the refrigerant evaporation coils within the environmental chamber. At least once and sometimes twice a day the environmental chamber would shut down to allow electrical heating elements to defrost the evaporator coils. Each defrost cycle took $\approx$ 5–10 minutes during which time the temperature within the chamber would steadily rise to a maximum deviation of $\approx +5$ °C from the set point. When the defrost cycle was completed and the system restarted, it would overshoot the set point temperature by a maximum of ≈ -5 °C. It took the system approximately an hour to completely recover from the temperature change that occurred during a defrost cycle. Between defrost cycles the temperature response of the chamber would decrease slightly through time due to persons entering and leaving the environmental chamber. The change in temperature response was probably due to an increase in the thermal resistance at the evaporator coils caused by frost accumulating on them.

2.5 Salt Fingering Experiment

Experiments have been performed to view and measure the mixing that occurs due to salt fingering when a layer of Granusil 30 saturated with a saline solution was placed over a layer of Granusil 30 saturated with a saline solution of a smaller concentration. Baker (1987) and Baker and Osterkamp (1988) performed a de-

tailed set of these salt fingering experiments in a salt fingering cell built by Baker (1987) for concentration differences of 35 ppt. A separate salt fingering experiment was performed in this investigation to determine if viscous fingers would form in thawed Granusil 30 at density differences that approach those encountered in the freezing experiments and to produce a time lapse video of the early stages of finger growth. The details of this experiment were similar to those presented by Baker (1987) and Baker and Osterkamp (1988). Briefly, the lower half of the salt finger cell constructed by Baker (1987) was filled with Granusil 30 silica sand saturated with a 5 ppt saline solution dyed with Rhodamine B indigo dye. The upper half of the cell was filled with Granusil 30 saturated with distilled water that did not contain dye. The cell was left in the position of less dense pore fluid solution overlying dense pore fluid solution overnight before it was inverted. After it was inverted, filming with a time lapse video camera began. The cell was kept at room temperature during the experiment.

2.6 Summary

A major emphasis of this research was to develop a freezing apparatus that was capable of freezing sands saturated with saline solution under a hydrostatic stress at temperatures that approximated temperatures during freezing of the active layer. After a review of the methods available to monitor the distribution of solutes in a freezing sand, the general principles developed and used by Baker (1987) were considered the most practical for these experiments. This technique consisted of monitoring the distribution of a solute by freezing a number of columns in the freezing apparatus and then, periodically during freezing, removing one of the columns, sectioning it and analyzing each section to determine its bulk salinity and gravimetric water content. A comparison in the change in bulk salinity for each column allowed the redistribution of the solute during freezing to be monitored through time. The freezing apparatus consisted of a sand filled box which was open on the top and insulated on the sides. The sand box was mounted on a heated radiator and a heated chamber adjacent to the sand box contained expansion reservoirs for each of the columns and for the sand box. Within the sand box there were seven vertical tubes that sleeved the sand columns used in the freezing tests. The heated chamber contained eight reservoirs which were attached to the base of

each column, with the eighth attached to the base of the sand box. Preparation of the freezing apparatus for a freezing test involved preparing seven columns in a uniform manner with known initial properties. Packing the sand columns and saturating them with saline solution closely followed the guidelines set forth in ASTM D2434–68, Standard Test Method For Permeability of Granular Soils (Constant Head). After equilibrating, freezing within the sand box was initiated by simultaneously lowering the temperature within the environmental chamber to the freezing temperature and pouring a small amount of liquid nitrogen over the surface of the apparatus to nucleate ice and avoid supercooling within the sand. The temperature field during freezing was monitored by measuring a string of 28 thermistors located next to one of the columns and by measuring the vertical temperature profiles in a series of seven stainless steel tubes at various locations in the freezing apparatus. Finally, a separate experiment, similar to the experiment performed by Baker (1987) and Baker and Osterkamp (1989), was performed to determine if viscous fingers would form in saturated Granusil 30 with an unstable density gradient that approached those encountered in the freezing experiments conducted in this investigation.

Chapter 3

Analytical Methods

3.1 Introduction

Profiles of bulk salinity and gravimetric water content were the principle indicators of the redistribution of the solute and solvent during freezing in columns of sand saturated with saline solution. Profiles of these two parameters were measured during freezing by periodically removing a column from the freezing apparatus, horizontally sectioning the column and analyzing each section for bulk salinity and gravimetric water content. A profile of temperature obtained prior to removing the column from the freezing apparatus was used to calculate equilibrium values of brine salinity and density in the partially frozen portion of the column. Profiles of brine salinity and density were combined with the profile of bulk salinity to calculate a profile of unfrozen brine volume within the column. The purpose of this chapter is to present details associated with removing a column from the freezing apparatus, sectioning the column and analyzing each section to determine profiles of bulk salinity, gravimetric water content, brine salinity and density, and volumetric brine content. The second section presents details associated with removing a column from the freezing apparatus, sectioning it, and analyzing each section to determine its length, its mass before and after drying, and the electrical conductivity of the diluted pore fluid. The third section presents details associated with reducing the data from the analysis to determine the bulk salinity and water content of each section and profiles for each column. The final section presents details and methods used to determine the equilibrium unfrozen solution parameters within the column at the time it was removed from the freezing apparatus.

3.2 Laboratory Analysis

Freezing conditions just prior to the time a column was removed from the freezing apparatus were measured with respect to both the instrumented column and the column to be removed. Freezing conditions in the instrumented column were measured by recording the time when the column was removed from the apparatus in that the instrumented column was logged every half hour. Freezing conditions in the column to be removed were measured by lowering a thermistor into the stainless steel tube adjacent to the column to measure the vertical temperature profile. A comparison between the two temperature profiles allowed variations in the freezing conditions across the apparatus to be measured.

Removal of a sand column from the freezing apparatus took place after the vertical temperature profile next to the column was measured. The column was removed by disconnecting the tube from the base of the column to the reservoir at the reservoir, plugging the free end of the tube, and then pulling the column and tube through the top of the freezing apparatus. Another column containing dry sand, at the temperature of the environmental chamber, was placed in the empty sleeve to reduce the temperature disturbance associated with removing the sand column from the freezing apparatus. The column was taken from the environmental chamber to be sectioned with a bandsaw and the reservoir was taken from the heated chamber to measure both the mass of fluid expelled from the freezing column and the salinity of the fluid.

The column was sectioned from the top down while held in a vertical position to minimize brine drainage and the loss of fluid during cutting. A Sears Craftsmen 10 inch bandsaw mounted horizontally was used to section the columns. Each section was probed with a knife to determine the degree of bondedness of the section at the time it was cut. Cut sections were placed in numbered, pre–weighed sample jars. The last sample jar contained fluid from both the tube that connected the base of the column with the reservoir as well as fluid from the reservoir. Elapsed time between when the column was removed from the freezing apparatus, sectioned and when the jars containing the sections were weighed was usually 15 minutes or less. Information on bondedness as well as any other pertinent information or observations were verbally recorded on a tape recorder while the column was sectioned. Later, this information was transcribed to paper.

After weighing the sample jars which contained the sectioned column, the sleeve of Tenite Butyrate tubing containing each section was removed from each sample jar, rinsed with distilled water (which drained back into the sample jar) and allowed to dry in order that the mass and length of each sleeve could be measured. Sample jars were then placed in a drying oven for 24 hours at 110 °C and then cooled until their temperature was close to room temperature before they were weighed to determine the dry weight of the section. All mass measurements were made with a Mettler P1500 digital balance that had an accuracy and repeatability of $1x10^{-5}$ kg.

Electrical conductivity measurements to determine the bulk salinity of each section were made after the dried sections had been rewetted with distilled water and allowed to stand for up to 24 hours. Rewetting of the dried sample involved adding a measured amount of distilled water, M_{SW}, to the sample in an $\approx$ 2:1 ratio, distilled water:dried sand (Kay and Groenevelt 1983, Baker 1987) which were then capped. Capped sample jars were gently shaken after the distilled water was added, then allowed to stand for several hours before they were vigorously shaken by hand and allowed to stand for another 12 to 24 hours before the solution was measured to determine its electrical conductivity.

Electrical conductivity measurements were made of the diluted pore fluid solution with a Beckmann Conductivity Bridge, Model RC-19, and a Beckmann Pipet Conductivity Cell, model G-20. Both cell and bridge were calibrated as a unit over the full range of conductivities used in these tests to determine the cell constant for the conductivity cell with the conductivity bridge. Electrical conductivity calibrations and normal laboratory measurements were conducted following procedures outlined in ASTM Test D1125–82, Standard Test Methods for Electrical Conductivity and Resistivity of Water. Temperature measurements of the solution were made with a calibrated epoxy bead thermistor that had been placed through the top bulb in the conductivity cell at a level $\approx$1 centimeter above the top platinum plate. Resistance of this thermistor was measured with an HP 3465B DVM and was made at the same time as a conductivity measurement and was accurate to $\pm$0.2 °C. The bridge was balanced for both resistance and capacitance for each measurement and both values were recorded. Conductivity measurements were made starting from the top section, which was typically the lowest reading, and ending with the bottom section, typically the highest reading. The pipet

cell was rinsed with the solution to be measured three times before the electrical conductivity of the solution was measured.

3.3 Data Reduction

Measurements of the section length, electrical conductivity and the mass of the section before and after drying were used to calculate the bulk salinity and water content of each section. These measurements and calculations were stored on the hard disk of a VAX mainframe computer, and backed up on a 9 track magnetic tape formated for VMS Backup. Bulk salinity and gravimetric water content were calculated using a Fortran 77 program written for this experiment. Normally water content calculations are straightforward, however, the presence of salt within the pore fluid requires that the definition be explicitly presented to avoid ambiguity. The purpose of this section is to define salinity and gravimetric water content and to present methods used to calculate each of these parameters from data obtained in the laboratory analysis.

3.3.1 Bulk Salinity

The ratio of salt mass to brine mass in a solution is defined as the salinity, S, of the solution,

$$S(\text{ppt}) = 1000\frac{M_S}{M_{brine}} = 1000\frac{M_S}{M_S + M_W} \tag{3.1}$$

where M_W is the mass of the water, and M_S is the mass of the salt in solution. Salinity is a gravimetric measure of the salt concentration which is expressed as parts per thousand (ppt). Pore fluid salinity within the sand column was determined by measuring the electrical conductivity and temperature of the pore fluid in each section after it had been diluted with a known amount of distilled water. The temperature of the diluted solution was used to correct the measured conductivity to an equivalent value at 25 °C. Salinity of the diluted pore fluid was determined from the conductivity of the solution at 25 °C. Finally, the salinity of the diluted pore fluid was converted to the *in situ* salinity of the pore fluid at the time the column was sectioned. The pore fluid salinity calculated from these measurements was the thawed pore fluid salinity, or bulk salinity, S_B, of the solution. The purpose of this section is to explain in detail the methods used to

determine profiles of bulk salinity for each section in a column. These methods were first developed for seawater and were later applied to soils saturated with a NaCl solution by Baker (1987) and Baker (1987a).

Temperature corrections in NaCl solutions were made to correct the electrical conductivity to an equivalent conductivity at 25 °C by using a correction factor that was scaled to the difference between the measured temperature and 25 °C. A standard temperature of 25 °C (instead of 20 °C) was chosen since conductivity measurements typically were made near this temperature. The temperature correction factor, CF, to produce the equivalent conductivity at 25° was determined from the conductivity ratio

$$R_m = \frac{C(S_D,T)}{C(35,20)} = \frac{C(S_D,T)}{5.0700\text{x}10^{-3}\ \frac{\text{S}}{\text{m}}} \tag{3.2}$$

where $C(S_D,T)$ is the measured electrical conductivity of the diluted solution with an unknown salinity S_D and measured temperature T, and $C(35,20)$ is the electrical conductivity of a standard solution. Electrical conductivity is expressed in units of $\frac{\text{Siemens}}{\text{meter}} = \frac{\text{S}}{\text{m}}$ where S=$\frac{1}{\text{ohm}}$.

The temperature correction factor is a relation between the conductivity values of standard solutions at 20, and 25 °C and for salinity values that range from 0 to $\approx$ 247 ppt. CF has units of $\frac{\%}{^\circ\text{C}}$, and is expressed as a polynomial relation of R_m which was calculated using equation 3.2,

$$CF = \sum_{i=0}^{N} a_i (R_m)^i. \tag{3.3}$$

The values of a_i are presented in Table 3.1.

For a CF, the corresponding change in conductivity, ΔC, was calculated using

$$\Delta C = CF\left(\frac{C(S_D,T)\Delta T}{100}\right), \tag{3.4}$$

where ΔT is the difference between 25 °C and the measured temperature. The corrected conductivity is

$$C(S_D,25) = C(S_D,T) + \Delta C. \tag{3.5}$$

Finally, the corrected electrical conductivity was used to form the ratio R_{25}, where R_{25} is defined as

$$R_{25} = \frac{C(S_D,25)}{C(34.33,25)} = \frac{C(S_D,25)}{5.50176\text{x}10^{-3}\ \frac{\text{S}}{\text{m}}} \tag{3.6}$$

Table 3.1: Coefficients of the polynomial used to make temperature corrections to the electrical conductivity data such that an equivalent conductivity at 25 °C is determined.

	$0 \leq R_m < .7327$	$.7327 \leq R_m < 4.3695$
i	a_i	a_i
0	3.7461606	3.5714511
1	-1.1114586x10^{+1}	-9.0476802
2	2.4407970x10^{+1}	2.1547232x10^{+1}
3	-1.6991629x10^{+1}	-2.6031192x10^{+1}
4	–	1.7501440x10^{+1}
5	–	-6.8214558
6	–	1.5347021
7	–	-1.8520938x10^{-1}
8	–	9.2957738x10^{-3}

where the salinity of the diluted solution, S_D, is a polynomial expression in terms of R_{25},

$$S_D(\text{ppt}) = \sum_{i=0}^{N} b_i (R_{25})^i. \tag{3.7}$$

The coefficients, b_i, are presented in Table 3.2.

Table 3.2: Coefficients to the polynomial that relates the conductivity ratio at 25 °C, R_{25}, to the salinity of the solution.

	$.5362 \leq R_{25} < 3.5741$	$3.5741 \leq R_{25} < 4.4933$
i	b_i	b_i
0	-8.3858476x10^{-1}	-5.1988526x10^{+1}
1	3.3046262x10^{+1}	1.6388787x10^{+2}
2	1.4589501	-1.2431695x10^{+2}
3	1.0155453	5.7933311x10^{+1}
4	-3.8626444x10^{-1}	-1.2573977x10^{+1}
5	6.5810021x10^{-2}	1.0599801

Bulk pore fluid bulk salinity, S_B, was determined from the diluted salinity, S_D, by calculating the mass of the salt, M_S, in the section using the mass of distilled water added to the dried section, M_{SW}, and the definition of salinity, equation 3.1, to obtain

$$M_S = \frac{S_D M_{SW}}{1000 - S_D}. \tag{3.8}$$

Once the mass of the salt is calculated from equation 3.8, the mass of pure water in the section when it was cut, M_W, calculated as the change in mass before and after drying, was used to calculate the bulk salinity of the section using equation 3.1.

3.3.2 Gravimetric Water Content

The ratio of water mass to sand mass is defined as the gravimetric water content,

$$W_B(\%) = 100\frac{M_W}{M_{SL}} \tag{3.9}$$

where M_W is the mass of the water and M_{SL} is mass of the dry sand with the mass of the salt removed. Mass of the water, M_W is calculated from the decrease in the mass of the sample jar from drying.

3.3.3 Physical Properties of the Unfrozen Solution

Sodium chloride dissolved in pure water forms an ionic solution that, when cooled sufficiently, solidifies as a binary mixture of brine and pure ice for initial concentrations less than 233.1 ppt (Heiss and Kuhajek 1983). If the system of brine and ice are in equilibrium, then specifying the temperature of the system determines the salinity of brine in contact with the ice regardless of the bulk salinity of the system. The remainder of this section will present the details associated with determining the salinity and density of brine in contact with ice and to show how these parameters are used to calculate the volumetric brine content of a partially frozen salt solution.

Brine salinity, S_b, in contact with ice increases as the temperature of the solution decreases because salt rejected from the ice is expelled into the brine. Baker (1987) fit data presented by Weast (1976) which related the salinity of sodium chloride solutions to the equilibrium freezing point of the solution to determine brine salinity as a function of temperature. The expressions presented by Baker (1987) are polynomials over two salinity and temperature ranges, and have the form,

$$S_b = \sum_{i=0}^{N} c_i (T_F)^i \tag{3.10}$$

Table 3.3: Coefficients for the polynomial which relates equilibrium freezing temperature to solution salinity.

	$0 \leq T_F < -1.79$ °C	$-1.79 \leq T_F < -20.667$ °C
i	c_i	c_i
0	-3.5922089x10^{-2}	-7.3124826x10^{-1}
1	-1.6830587x10^{+1}	-1.7889927x10^{+1}
2	2.2433665x10^{-1}	-4.1168058x10^{-1}
3	1.4280893x10^{-1}	-3.2115794x10^{-3}
4	-	4.6955195x10^{-5}

where T_F is the phase equilibrium temperature of the solution. The coefficients, c_i, are presented in Table 3.3.

Since S_b increases as the temperature of an equilibrium mixture of brine and ice is decreased, the density of the brine, ρ_b, also increases with decreasing temperature. Zubov (1963) showed that the density of seawater brine in equilibrium with ice is related to the salinity by

$$\rho_b \left(\frac{\text{kg}}{\text{m}^3} \right) = 1000.0 + 0.8 S_b(\text{ppt}). \tag{3.11}$$

Equation 3.11 has been used to determine the density of NaCl solutions because of the similarity of seawater and NaCl solutions of seawater concentrations (Cox and Weeks 1975, Baker 1987, J. Johnson pers. comm. 1989).

Cooling of a mixture of brine and ice in which equilibrium between the two phases is maintained results in changes in the brine salinity, and density which may be calculated based only on the temperature of the solution. If the mixture is in a closed system, then the mass salt within the system will remain constant with temperature. Weeks (1962) used these principles to show that the unfrozen volumetric brine content, ν_b(ppt), may be expressed as

$$\nu_b(\text{ppt}) = 1000 \frac{V_b}{V_b + V_i} = 1000 \frac{\frac{S_i}{S_b \rho_b}}{\frac{S_i}{S_b \rho_b} + (1 - \frac{S_i}{S_b}) \frac{1}{\rho_i}} \approx 1000 \frac{S_i}{S_b} \tag{3.12}$$

where V_i and V_b refer to the absolute volume of ice and brine, S_i and S_b refer to the bulk salinity and brine salinity of a solution and ρ_i and ρ_b refer to the density of the ice and brine of a solution. Baker (1987) defined a similar relation for soils

$$V_U(\text{ppt}) = 1000 \frac{V_B}{V_B + V_I} = 1000 \frac{\frac{S_B}{S_U \rho_U}}{\frac{S_B}{S_U \rho_U} + (1 - \frac{S_B}{S_U}) \frac{1}{\rho_i}} \approx 1000 \frac{S_B}{S_U} \tag{3.13}$$

where V_I and V_B refer to the absolute volume of ice and brine, S_B and S_U refer to the bulk soil solution salinity and unfrozen soil solution salinity and ρ_U refers to the density of the brine in soil solution. The density of the pure ice that forms is a function of temperature and may be presented by a polynomial expression of the form (Osterkamp and Walker 1987)

$$\rho_i = \sum_{i=0}^{N} d_i(T)^i. \tag{3.14}$$

The coefficients, d_i are presented in Table 3.4

Table 3.4: Coefficients for the polynomial which relates density of ice to temperature.

i	d_i
0	916.88
1	-0.16805
2	-4.57x10^{-4}

For a bulk salinity of 35 ppt the approximation on the right hand side of equations 3.12 and 3.13 is accurate to better than 10% for brine volumes greater than 500 ppt.

Baker (1987) assumed the mineral grains on the soil did not alter the freezing relations from those derived for the liquid. This assumption leads to the assumption that $S_b = S_U$, $\rho_b = \rho_U$ and $\nu_b = V_U$ or the equivalency of equations 3.12 and 3.13 for $S_i = S_B$. A similar assumption will be used in this thesis (see section 1.2.3.1 for a justification of this assumption).

3.4 Summary

To summarize, prior to removing a column from the freezing apparatus, temperature profiles at the instrumented column and at the column to be removed were measured. Immediately after a column was removed from the freezing apparatus it was sectioned. The laboratory analysis of each section involved measuring the electrical conductivity of diluted pore fluid in each section and conducting a series of mass measurements which were used to determine the bulk salinity and gravimetric water content of the sections. Results from the analysis on each section

of a column were used to construct profiles of bulk salinity and gravimetric water content of the columns. Temperature measurements at the time columns were removed from the freezing apparatus were used with the bulk salinity profiles to determine profiles of salinity and density of brine in equilibrium with ice in the pore space for each column. Profiles of bulk salinity, S_B, brine salinity, S_U, and brine density, ρ_U, were used to calculate profiles of the volumetric unfrozen water content, V_U, for each column at the time it was removed from the freezing apparatus. Data obtained from each of the columns were combined to monitor the distribution of the solute during freezing and to interpret the results of the freezing experiment.

Chapter 4

Results

4.1 Introduction

This research investigated the effects of freezing on the distribution of a solute within sand which had been saturated with a saline solution prior to freezing. Freezing conditions were controlled by freezing the sands under approximate Neumann boundary conditions (Carslaw and Jaeger 1959) using a constant soil type and uniform initial soil solution salinity. Variations in the surface and base temperatures or the initial salinity between each freezing test allowed the effects of freezing rate, temperature gradient, cooling rate and bulk salinity on solute movement to be investigated. The purpose of this chapter is to present the results of the 9 freezing tests conducted in the freezing apparatus constructed for this investigation. The second section of this chapter presents a description of the sand used in the freezing tests and a summary of the freezing conditions for each test. The third section presents a complete set of results and observations from the freezing tests with special emphasis placed on Freezing Test 6.

4.2 Soil Description and Freezing Test Summary

The rate at which a soil freezes depends on the thermal properties of the soil and on the imposed temperature boundary conditions. The rate at which a solute moves in a soil depends on the physical properties of the soil, the permeability for example, and concentration gradients. In this research, a sand of known and relatively uniform mineralogy was used so that the thermal and physical properties of the sand could be held as constant as possible between experiments.

The purpose of this section is to describe the sand used in these tests and the temperature boundary conditions for each test.

4.2.1 Soil Description

Each freezing test was performed using a silica sand marketed under the trade name Granusil 30 by the Unimin Corporation of Emmett, Idaho. Granusil 30 is principally used in sandblasting applications; consequently, it is manufactured to be relatively clean and uniform in size. A sieve analysis and a visual inspection of a representative sample were used to describe this material.

The sieve analysis was performed on a 0.8 kg sample of the Granusil 30 which was obtained from twelve, 45 kg bags of the material which had been intermixed. Six U.S. Standard sieves that ranged in size from #12 to #140 were stacked in order of increasing mesh size to sieve the sample. A tray at the bottom of the stack of sieves was used to contain any material passing the #140 sieve. The sample was sieved in $\approx$ 0.2 kg increments. Results of the sieve analysis are shown in Table 4.1 and Figure 4.1 and indicate that the mass average particle size of the sample of Granusil 30 was 5.5×10^{-4} m and that $\approx$ 50% of the sand, by mass, had a particle diameter which was between 4.8×10^{-4} and 9.5×10^{-4} m.

Table 4.1: Results of a sieve analysis on a uniform sample of Granusil 30 silica sand.

Sieve No.	Mesh Size $\times 10^{-5}$ m	Mass Retained $\times 10^{-3}$ kg
12	1.680	0
30	0.596	300.1
40	0.420	395.4
50	0.297	92.5
70	0.210	14.5
140	0.105	1.2
tray	<.105	trace

The visual inspection of the sand was completed following ASTM Test D2488-84, A Standard Practice for Description and Verification of Soils (Visual and Manual Procedure). Results of the visual inspection indicated that $\approx$ 75% of Granusil 30 was medium-grained sand and $\approx$ 25% was fine-grained sand. This inspection also showed that Granusil 30 was principally composed of quartz; however,

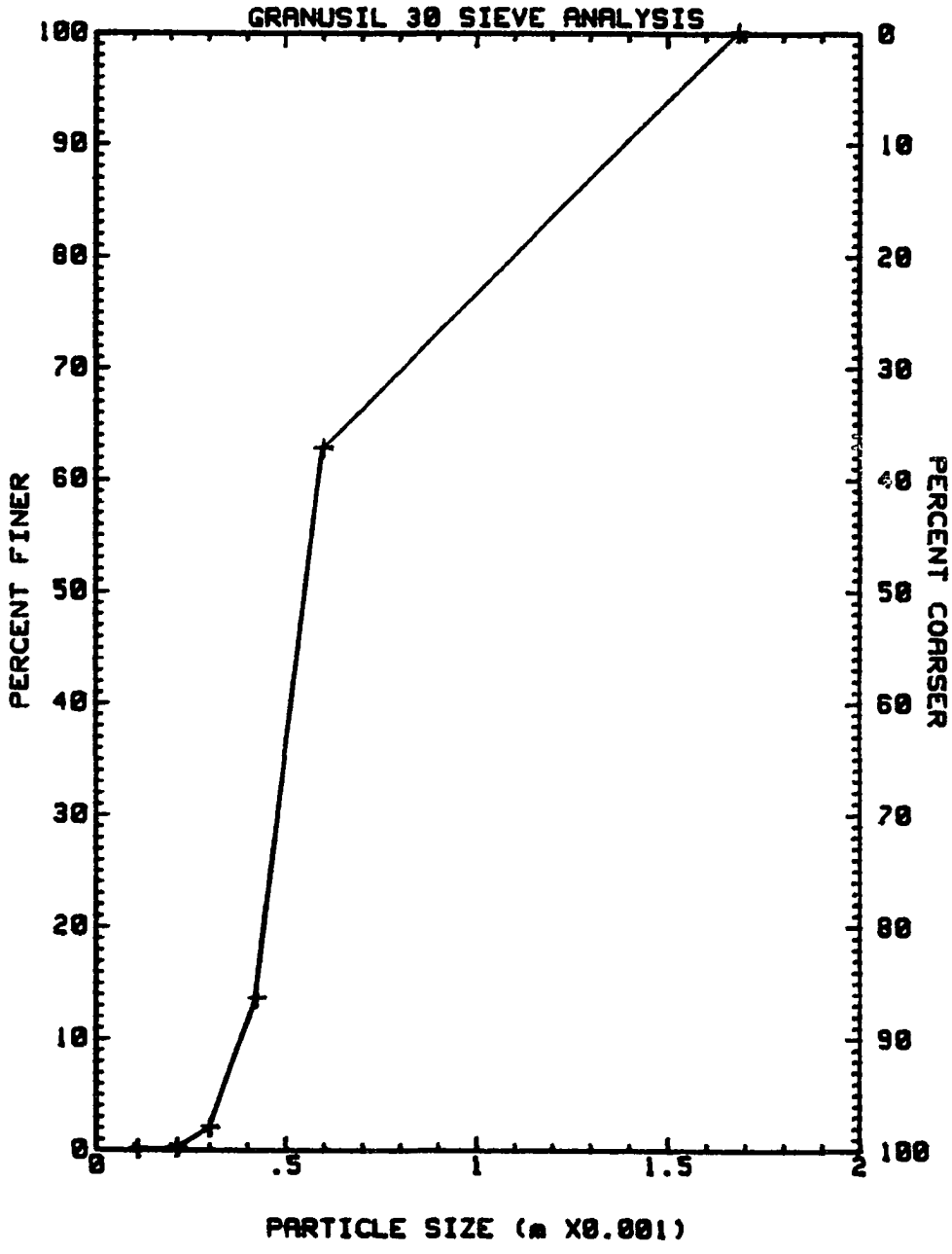

Figure 4.1: Results from sieving approximately 0.8 kg of Granusil 30, a silica sand used in all 9 freezing tests.

a small amount of plagioclase feldspar and muscovite mica were present. Quartz grains were angular but neither flute nor elongate. Feldspar grains were angular to subangular and slightly elongate. Mica grains were elongate and flat.

4.2.2 Freezing Test Summary

Nine freezing tests were conducted with Granusil 30 silica sand which had been packed into sand columns to a known initial dry density and saturated with a NaCl solution of known initial concentration. The purpose of this section is to present the physical properties of the soil used in the freezing tests and then to summarize the freezing tests.

Table 4.2 summarizes each freezing test in terms of the the initial sand and solution parameters, the temperature conditions and the purpose of each test. The initial bulk salinity was determined by measuring the salinity of the solution used to saturate the column. Temperature conditions which led to freezing consist of the surface temperature, measured at the top of the instrumented column, the base temperature, measured in the aluminum plate at the base of the instrumented column, and the initial temperature, measured throughout the column with the thermistor string prior to initiating freezing. Dry density at the start of freezing was calculated from the mass of sand packed into the column of a measured volume. Additionally, the initial porosity was calculated to range from 39 to 41% assuming a specific gravity of the sand to be 2630 $\frac{kg}{m^3}$ (Lunardini 1981), the permeability was measured to range from $7x10^{-11}$ to $1x10^{-10}$ m^2, and the saturated water content was estimated to range from 27 to 28%.

4.3 Experimental Results and Discussion

Measurements on sand columns that were removed from the freezing apparatus at different times during freezing resulted in values of bulk salinity and water content for each section of the column. Values for each section were used to compile profiles of the two parameters for the entire column. Temperature profiles, both at the instrumented column and adjacent to the column to be removed, were measured prior to removing a column from the sand box. Bulk salinity and temperature profiles were used to construct equilibrium profiles of brine salinity, density, and

unfrozen volumetric brine content within the column at the time it was removed from the sand box. The purpose of this section is to present these results for the 9 freezing tests with special reference in the discussion to Test 6. The first part of this section will present the measured profiles: bulk salinity, water content and temperature. The second part will present the calculated profiles: brine salinity, brine density, and volumetric brine content; however, these will be presented only for Test 6. Appendix B and Table 4.3 present the results of an analysis to determine the uncertainty in each of the measured and calculated profiles discussed in this chapter.

Table 4.2: A summary of the nine freezing tests performed in this investigation. The column information provides particular details on the way each of the seven columns in a test were frozen; hydrostatic implies that the surface of the column was closed and the base was open and connected to the expansion reservoir. The pore fluid stress in these columns was hydrostatic.

Test #	Initial Salinity (ppt)	Dry Density ($\frac{kg}{m^3}$)	$T_{surface}$ (°C)	T_{base} (°C)	T_{init} (°C)	Mechanism Investigated	Column Information
5	34.8	1410	-6.5	-1.5	-1.3	Initial freezing test.	All hydrostatic.
6	34.8	1510	-4.5	-1.5	-1.3	The effects of large freezing rates.	All hydrostatic.
7	35.2	1550	-5.4	-1.5	-1.5	Confirm long time transient prior to the start of convection.	1.071 days frozen uncapped, 6.125 and 8.132 days unsaturated. The remaining columns were hydrostatic.
8	35.4	1540	-5.8	-1.4	–	Confirm long time transient prior to the start of convection.	All hydrostatic.
9	35.0	1550	-12.6	+0.8	+1.0	Effects of a cold surface temperature on convection.	All hydrostatic.
10	34.0	1570	-4.4	-1.9	-1.5	Effects of rapid freezing on time transient prior to the start of convection.	0.876 and 7.153 days were frozen with the base plugged and the surface open. The remaining columns were hydrostatic.
11	36.3	–	-4.4	+0.3	+0.5	Effects of a large temperature gradient on the onset of convection.	3.990, 6.927 and 9.968 days were frozen with the base plugged and the surface open. The remaining columns were hydrostatic.
12	109	1560	-9.3	-6.1	-5.8	Effects of a large initial salinity on the redistribution of solutes.	All hydrostatic.
13	1.3	1560	-3.5	+0.5	+0.5	Effects of a small salinity on the redistribution of solutes.	All hydrostatic.

Table 4.3: Summary of the estimates of the random and systematic uncertainty associated with the measured and calculated parameters in Test 6. These results are generally applicable to the remaining 8 freezing tests.

Parameter		Uncertainty	
		Random	Systematic
Bulk Salinity	S_B(ppt)	0.5	0.3
Water Content	W_B(%)	0.6	2.
Temperature	T(°C)	0.01	0.1
Brine Salinity	S_U(ppt)	0.17	1.7
Brine Density	$\rho_U \left(\frac{\text{kg}}{\text{m}^3}\right)$	0.14	1.4
Volumetric Brine Content	V_U(ppt)	14	56

4.3.1 Measured Results

Measured profiles of bulk salinity and water content for a sand column were produced by combining results obtained from the measurements on each section of a column after it was sectioned (Section 3.3 for methods). Temperature profiles resulted from resistance measurements made of the thermistor string at the instrumented column (Section 2.5) within ± 15 minutes of the time the column was removed from the freezing apparatus.

Figures 4.2 through 4.28 show profiles of bulk salinity, water content and temperature in each of the columns for each of the 9 freezing tests. The legend on each figure shows the time since the beginning of the experiment, in decimal days, when each column was removed from the freezing apparatus. Each profile has the location of the ice–bearing/ice–free interface, or alternatively, the thermodynamic interface[1] marked adjacent to the profile. In general, the depth of the ice–bearing interface increases with time, however, Figures 4.5 thru 4.7 indicate that variations do occur from column to column in a given test. Apparent discrepancies associated with the position of the ice–bearing interface appear to be associated with the presence or absence of convection in the column.

While each column was sectioned, two other interfaces were recorded which have not been presented in Figures 4.2 thru 4.28 for reasons of clarity, but are presented in the test summary. The first interface, the interface nearest the surface of the column, where the bondedness of the sand grains decreased significantly, was located by probing each section with a knife while the column was cut. This interface was termed the transition interface. The second interface, where the sand grains were no longer bonded by ice, was also located by probing each section with a knife. This interface was termed the ice–bonded interface. The precision of the location of these two interfaces is reflected by the method used to determine their position. Observations indicate that the region between the transition interface and the ice–bonded interface became progressively less well bonded with depth with the sand grains becoming progressively more bonded by ice towards the center

[1]The location from the top of the column at which the brine salinity (calculated from the *in situ* temperature) is less than the measured bulk salinity is defined as the thermodynamically thawed interface or ice–bearing interface. Brine salinity was calculated using equation 3.10.

of the column. Radial changes in the degree of bondedness between the transition and ice–bonded interfaces were not always symmetric. Often one side would be slightly softer than the opposite side of the column. Below the top transition interface and the ice–bonded interface was the ice–bearing interface. Ice–bonded and ice–bearing interfaces were usually separated by more than a centimeter.

Summary of Freezing Test 5

- Test Purpose
  1. This test was to determine the effects of a variable freezing rate on the distribution of the solute in the sand.
- Notes
  1. Each of the seven columns were capped at the surface, open at the base and frozen under hydrostatic conditions.
  2. Fluid mass in the reservoir was not measured prior to the start of freezing.

Column Number	Date Removed	Mass Fluid ($kgx10^{-3}$)	Interface Location(m)		
			Transition	Ice–Bonded	Thermodynamic
4	0.985	–	0.04	0.09	–
7	2.926	–	0.11	0.17	–
2	7.962	–	–	0.28	0.31
3	10.974	–	0.26	0.33	0.36
5	13.125	–	0.29	0.34	0.39
6	14.878	–	0.35	0.38	0.41
1	16.708	–	0.36	0.40	0.48

- Results
  1. Results of this first test suggest that convection continues until the end of the experiment.
  2. The procedure used to determine the bulk salinity profiles in the first two columns sectioned yielded erroneous results. This mistake did not allow the effects of rapid freezing on the distribution of the solute to be determined.
  3. The dry density of the columns used in this first test was significantly less than the dry density used in the remaining tests.
  4. Convection of the pore fluid only affected the profiles of bulk salinity.
  5. An analog pressure gauge installed at the surface of the instrumented column did not indicate any surface pressures at the surface of the column greater than atmospheric during freezing.

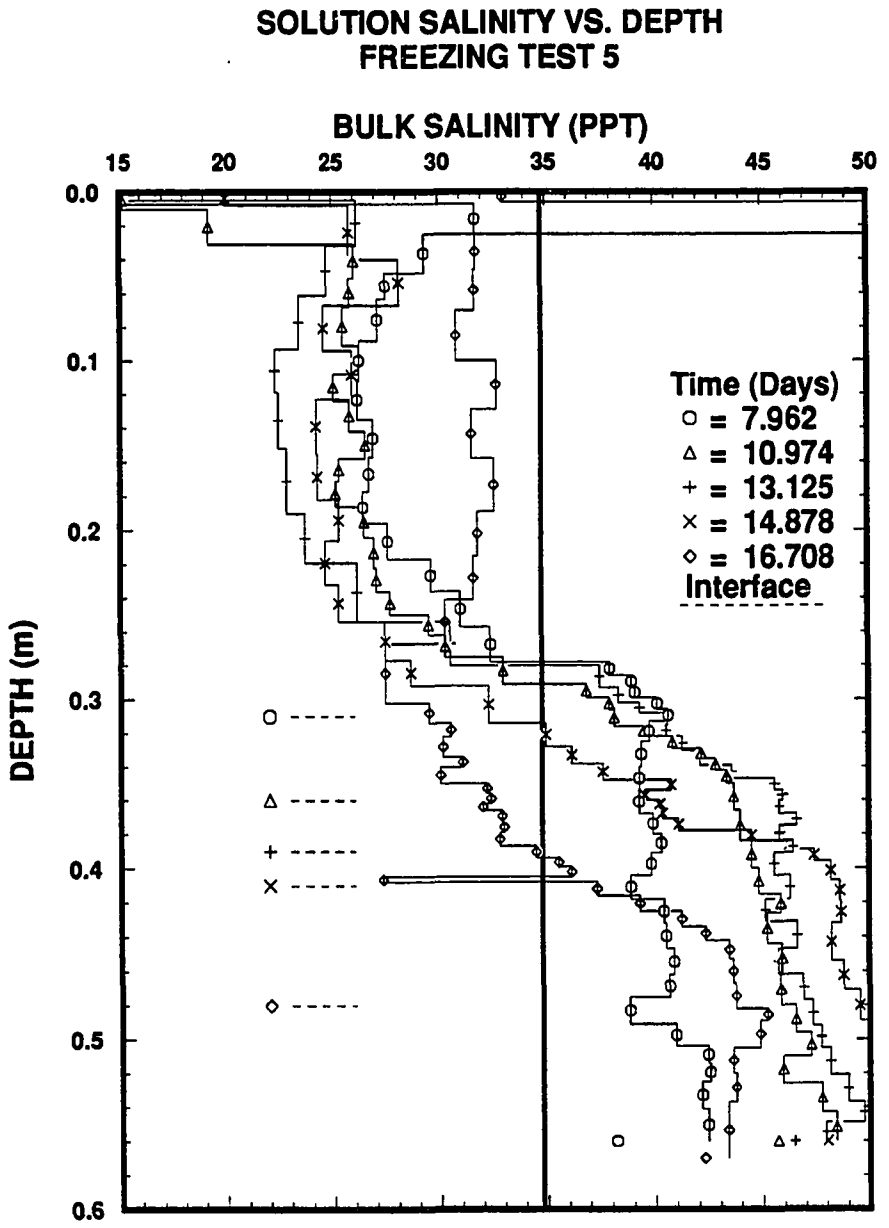

Figure 4.2: Bulk salinity profiles measured in each column during Test 5. The legend shows the time, in decimal days, when each column was removed from the freezing apparatus. The horizontal dashed line and symbol indicates the position of the ice–bearing interface at the time a column was removed from the freezing apparatus. The first data point at the surface of several profiles extended beyond the scale of the figure. At the time these columns were removed, the surface bulk salinity values were the following: 2.926 days 19.3 ppt, 7.962 days 13.2 ppt, 10.974 days 15.2 ppt, 13.125 days 11.6 ppt.

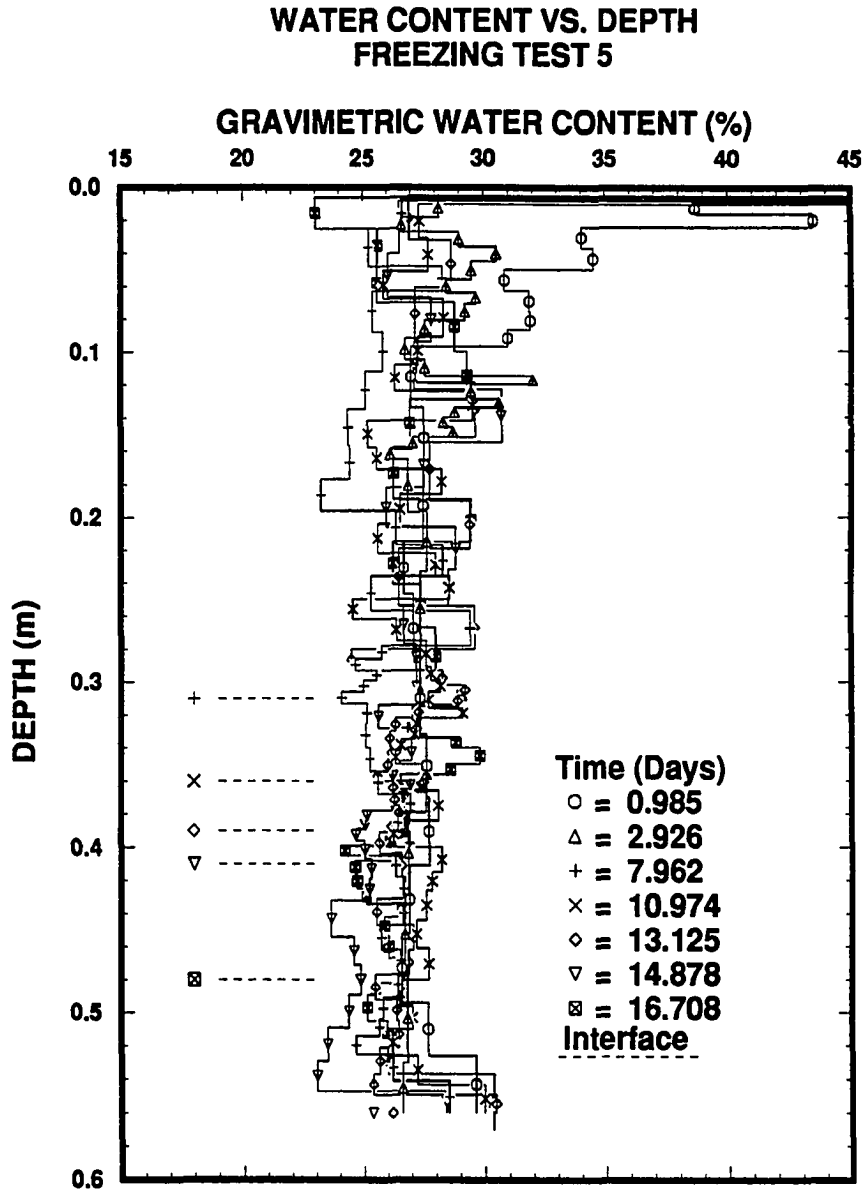

Figure 4.3: Water Content profiles measured in each column during Test 5. The first data point at the surface of several profiles extended beyond the scale of the figure. At the time these columns were removed, the surface water content values were the following: 0.985 days 194.4%, 2.926 days 55.3%, 7.962 days 177.1%, 10.974 days 171.6%, 13.125 days 186.8%, 14.878 days 85.6%, 16.708 days 110.7%.

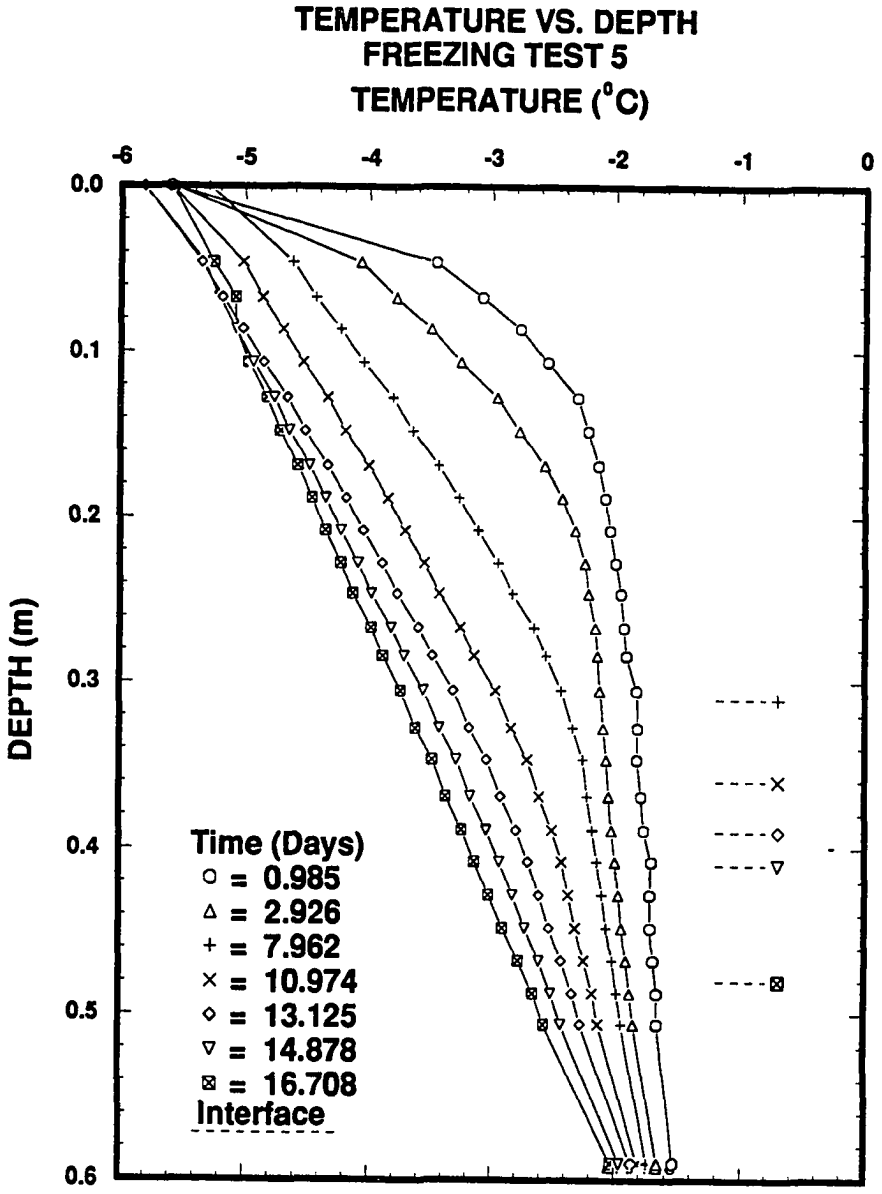

Figure 4.4: Temperature profiles measured during Test 5 at the time the columns were removed from the freezing apparatus. Temperature profiles were measured at the instrumented column.

Summary of Freezing Test 6

- Test Purpose
  1. This test was to determine the effects of rapid freezing on the distribution of the solute in the sand. This test was to obtain data that was not obtained in Test 5. A smaller surface temperature decrease at the start of freezing allowed these data to be obtained.
- Notes
  1. Each of the seven columns were capped at the surface, open at the base and frozen under hydrostatic conditions.
  2. After the sixth column was removed, 10 days after freezing began, the surface temperature was increased to -2 °C.

Column Number	Date Removed	Mass Fluid ($kgx10^{-3}$)	Interface Location(m)		
			Transition	Ice-Bonded	Thermodynamic
7	0.997	3.17	0.07	0.11	0.24
2	2.087	7.29	0.11	0.17	0.32
3	4.000	8.43	–	–	–
5	4.132	13.39	0.17	0.24	0.32
4	9.028	16.63	0.20	0.27	0.38
6	10.021	19.66	0.24	0.31	0.31
1	14.000	17.64	0.14	0.31	0.31

- Results
  1. This test showed that convection of the pore fluid was preceded by a transient period of approximately 4 days in which nearly 100% of the solute was incorporated within the partially frozen sand.
  2. Only the bulk salinity profiles were affected by convection of the pore fluid.
  3. An analog pressure gauge installed at the surface of the instrumented column did not indicate pressures at the surface of the column greater than atmospheric during freezing.
  4. The third column removed on the fourth day of freezing was split along its axis to observe features associated with the interface. Only the frozen sections were analyzed.
  5. The column removed after 9.028 days of freezing did not exhibit features which can be associated with convection, however, columns removed prior to and after this column indicate that they are affected by convection. The depth to the ice–bearing interface in this column was greatest of all the columns in this test.

6. The location of the ice–bearing interface appears to decrease between the period when the sixth and seventh columns were removed. The location of the ice–bearing interface is less in the column removed after 14.000 days of freezing than in the column removed after 9.028 days of freezing. After 10.021 days of freezing the surface temperature of the column was increased to -2 °C.

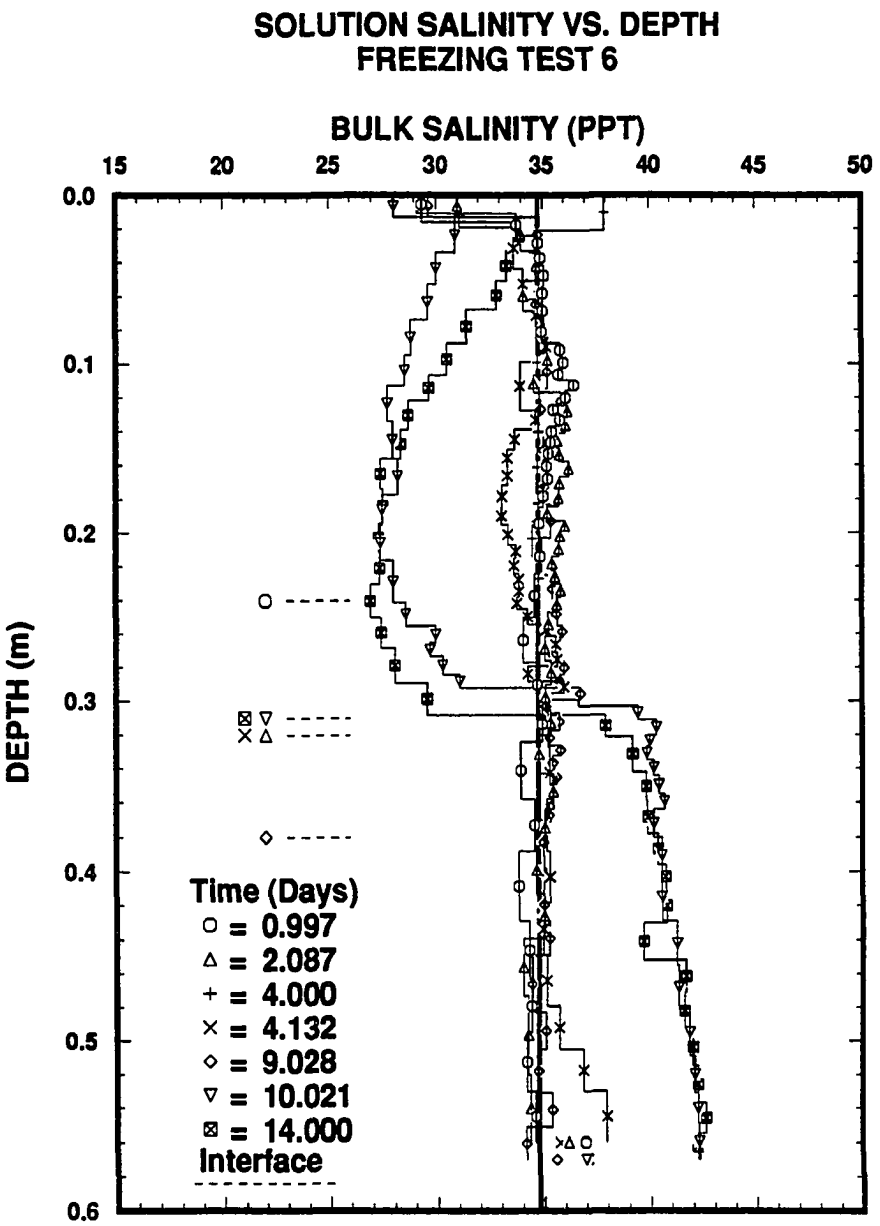

Figure 4.5: Bulk salinity profiles measured in each column during Test 6. The legend shows the time, in decimal days, when each column was removed from the freezing apparatus. The horizontal dashed line and symbol indicates the position of the ice–bearing interface at the time a column was removed from the freezing apparatus.

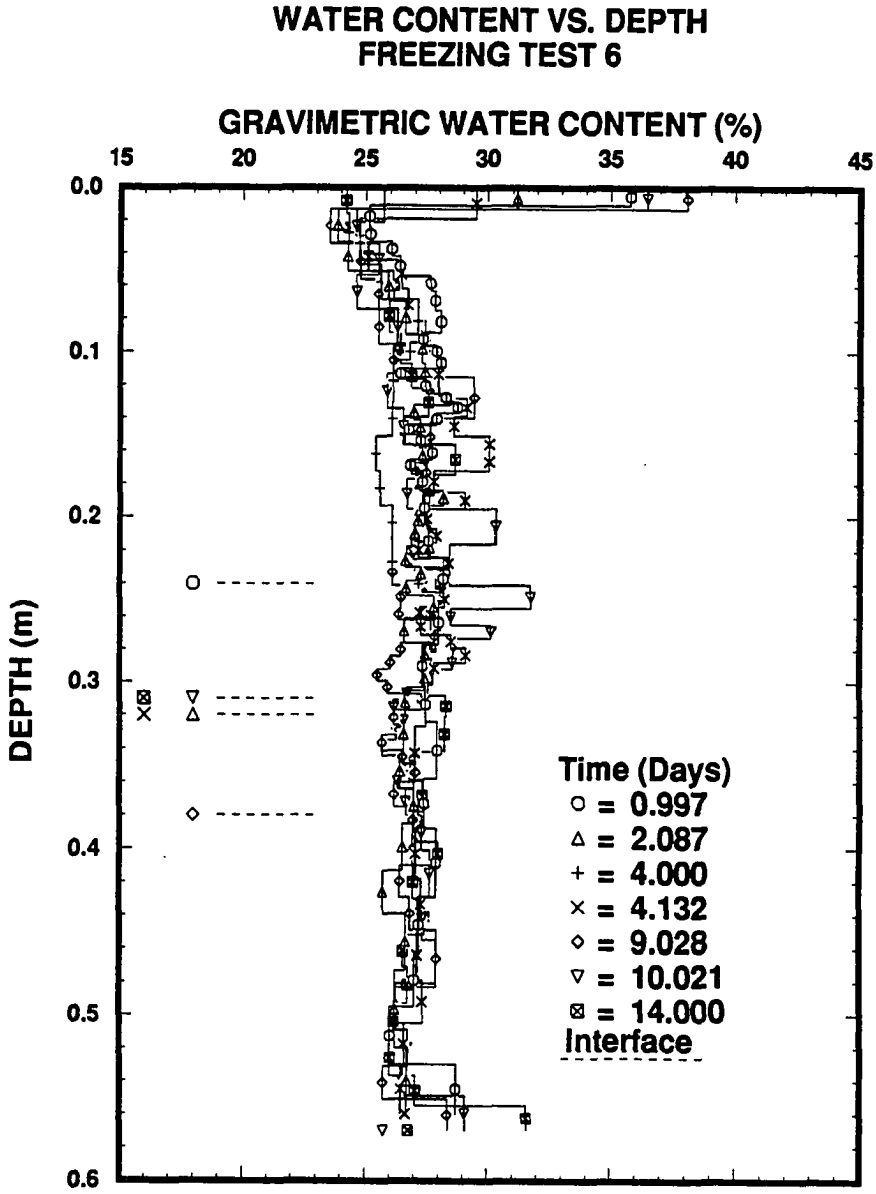

Figure 4.6: Water Content profiles measured in each column during Test 6.

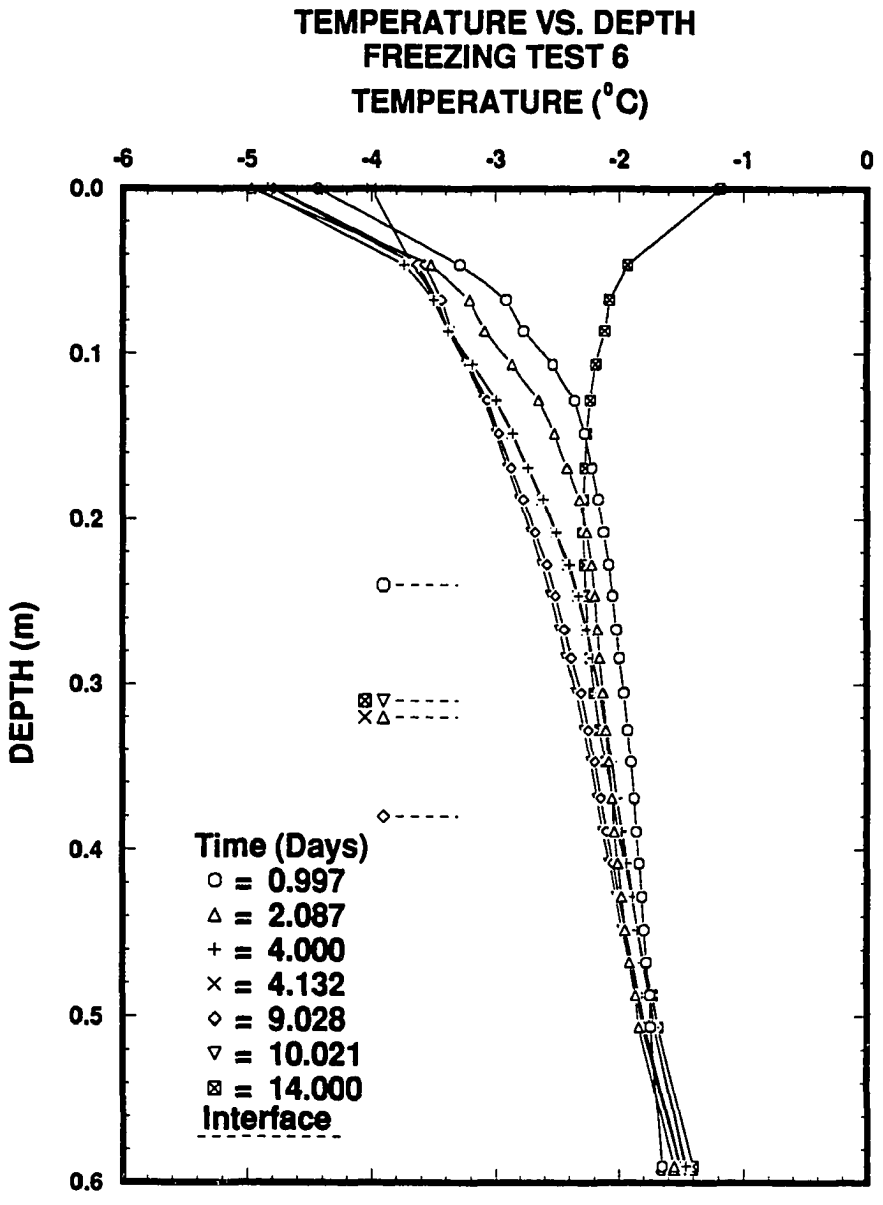

Figure 4.7: Temperature profiles measured during Test 6 at the time the columns were removed from the freezing apparatus. Temperature profiles were measured at the instrumented column.

Summary of Freezing Test 7

- Test Purpose
  1. This test was to confirm the results of Test 6 which suggested that a long time transient occurred before the onset of convection in the columns.
  2. Two columns were unsaturated over a portion of their length to determine if saturation affected the distribution of the solute during freezing.
  3. One column was frozen with the surface open to determine if capping the columns to reduce evaporation at the surface significantly affected the columns during freezing.
- Notes
  1. The column removed after 1.071 days of freezing was saturated with solution as usual. However, immediately prior to the start of freezing the top cap was removed and it was frozen uncovered.
  2. Columns removed after 6.125 and 8.132 days of freezing were saturated as usual. However, 2 hours prior to freezing each column was allowed to drain to field capacity at a level several centimeters above their base. The top was then closed and the column was frozen under a hydrostatic stress.
  3. The remaining four columns were frozen as usual.

Column	Date	Mass Fluid	Interface Location(m)		
Number	Removed	($kgx10^{-3}$)	Transition	Ice–Bonded	Thermodynamic
7	1.071	1.83	0.08	0.16	0.29
2	1.979	1.24	0.14	0.23	0.29
4	3.129	4.56	0.20	0.28	0.32
6	5.004	8.89	0.22	0.32	0.35
5	6.125	–	–	0.32	0.36
3	8.132	–	–	0.40	0.41
1	10.059	16.74	0.31	0.43	0.41

- Results
  1. Only the last column removed after $\approx$ 10 days of freezing appears to be affected by convection. The rate of change of bulk salinity is nearly constant through the ice–bearing interface in this profile.
  2. The two columns that were partially drained of solution prior to freezing appear to show a slight increase in bulk salinity near the surface. The last partially drained column removed exhibits a slight decrease in bulk salinity at the approximate half–way mark in the column.

3. An analog pressure gauge installed at the surface of the instrumented column did not measure any pressures in excess of atmospheric pressure during freezing.
4. While the first column was being sectioned with the bandsaw, the plug at the base of the column worked free and the column began to drain. This resulted in the anomalous water content values between 0.34 and 0.42 m.

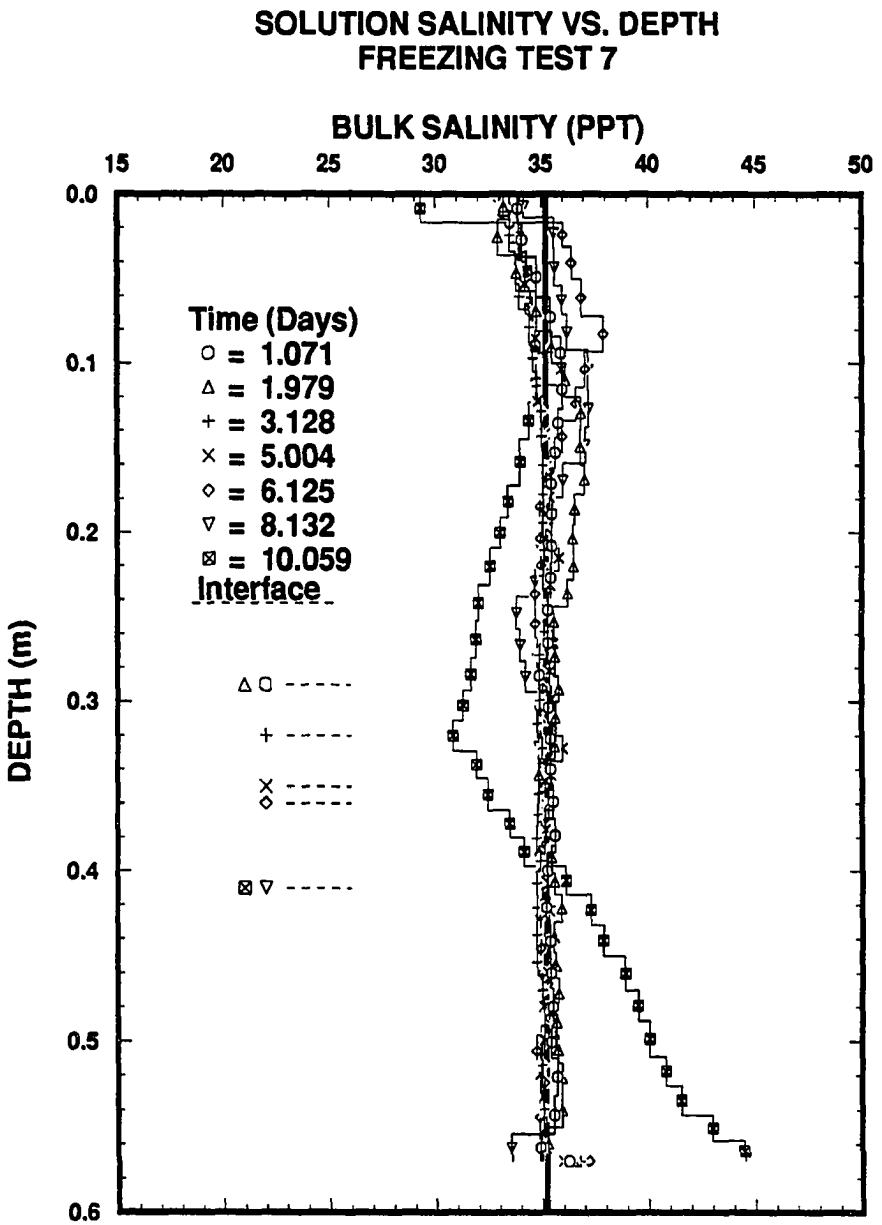

Figure 4.8: Bulk salinity profiles measured in each column during Test 7. The legend shows the time, in decimal days, when each column was removed from the freezing apparatus. The horizontal dashed line and symbol indicates the position of the ice–bearing interface at the time a column was removed from the freezing apparatus.

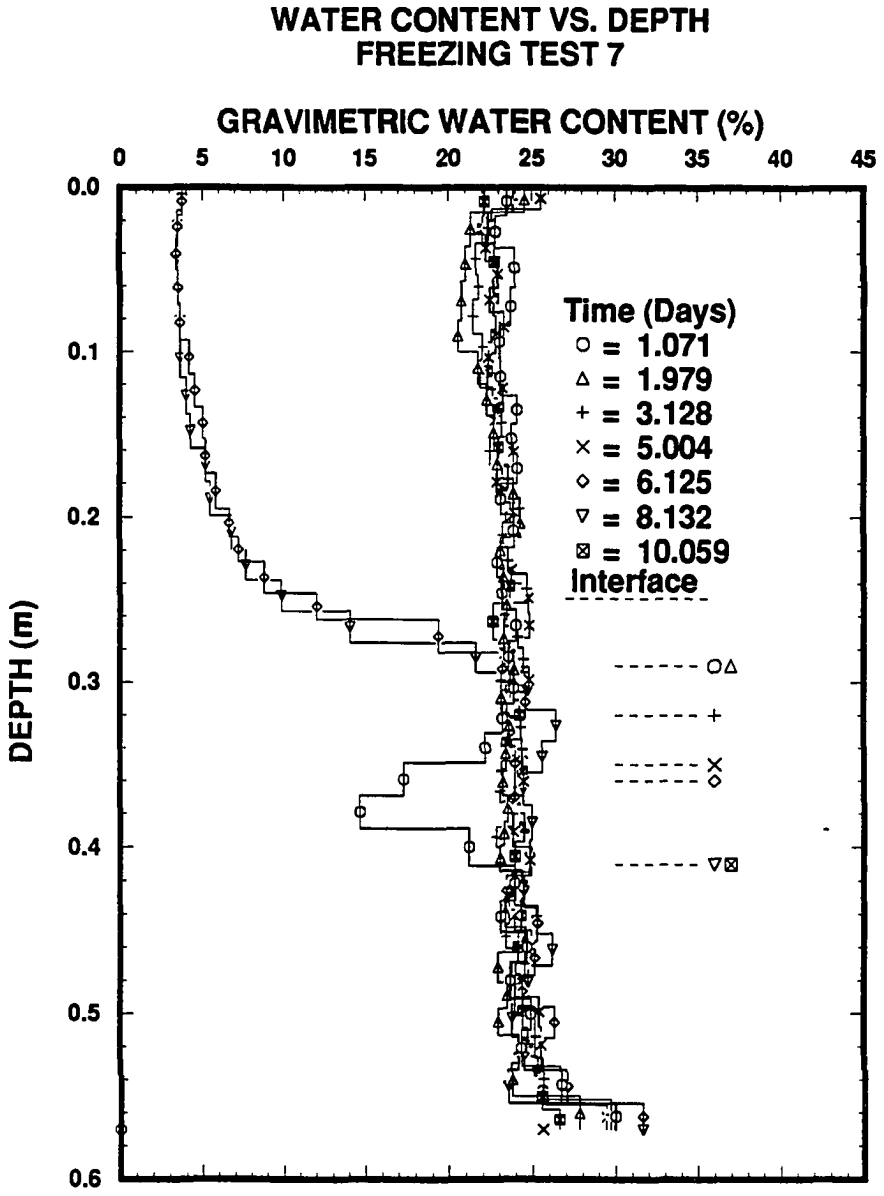

Figure 4.9: Water Content profiles measured in each column during Test 7.

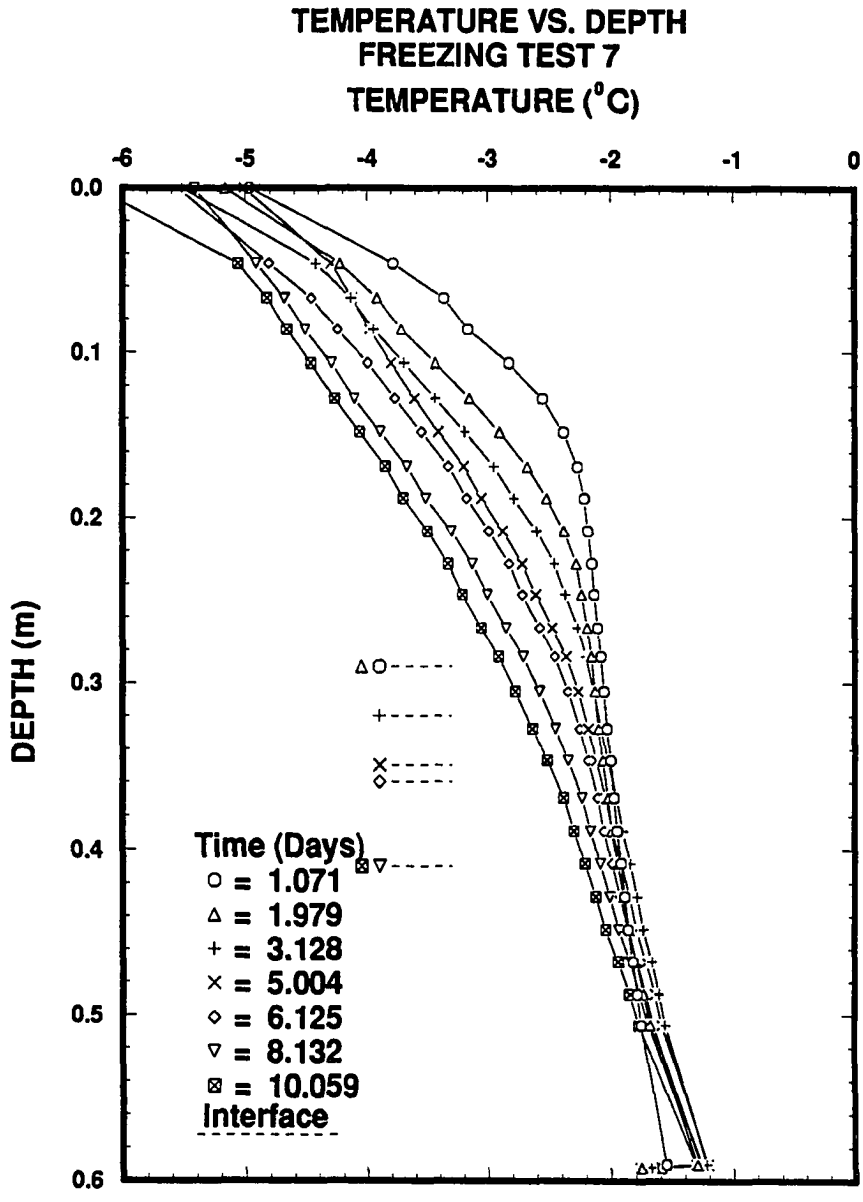

Figure 4.10: Temperature profiles measured during Test 7 at the time the columns were removed from the freezing apparatus. Temperature profiles were measured at the instrumented column.

Summary of Freezing Test 8

- Test Purpose
  1. This test was performed to further investigate the long time transient that preceded the onset of convection.
- Notes
  1. All seven columns were saturated with solution and frozen from the top down under a hydrostatic stress with the tops of the columns capped.
  2. The freezing data indicates that the columns in this test could have been either partially frozen or supercooled prior to the start of freezing.

Column Number	Date Removed	Mass Fluid ($kgx10^{-3}$)	Interface Location(m)		
			Transition	Ice–Bonded	Thermodynamic
4	1.000	8.78	0.07	0.15	0.21
3	2.000	12.96	0.16	0.23	0.32
7	5.000	19.45	0.18	0.29	0.35
2	6.093	22.18	0.19	0.31	0.37
5	7.015	22.11	0.20	0.34	0.39
6	8.969	25.19	0.22	0.38	0.43
1	10.245	33.31	0.23	0.39	0.44

- Results
  1. None of the columns in this test appear to be affected by convection of the pore fluid during freezing.
  2. This test shows well the decrease in bulk salinity between the surface and a depth of 0.1 m. It also shows well the increase in water content in the first section at the surface of the column and the decrease in these values below the first section and above 0.1 m.
  3. An analog vacuum gauge installed at the surface of the instrumented column did not measure pressures that were less than atmospheric pressure during freezing.

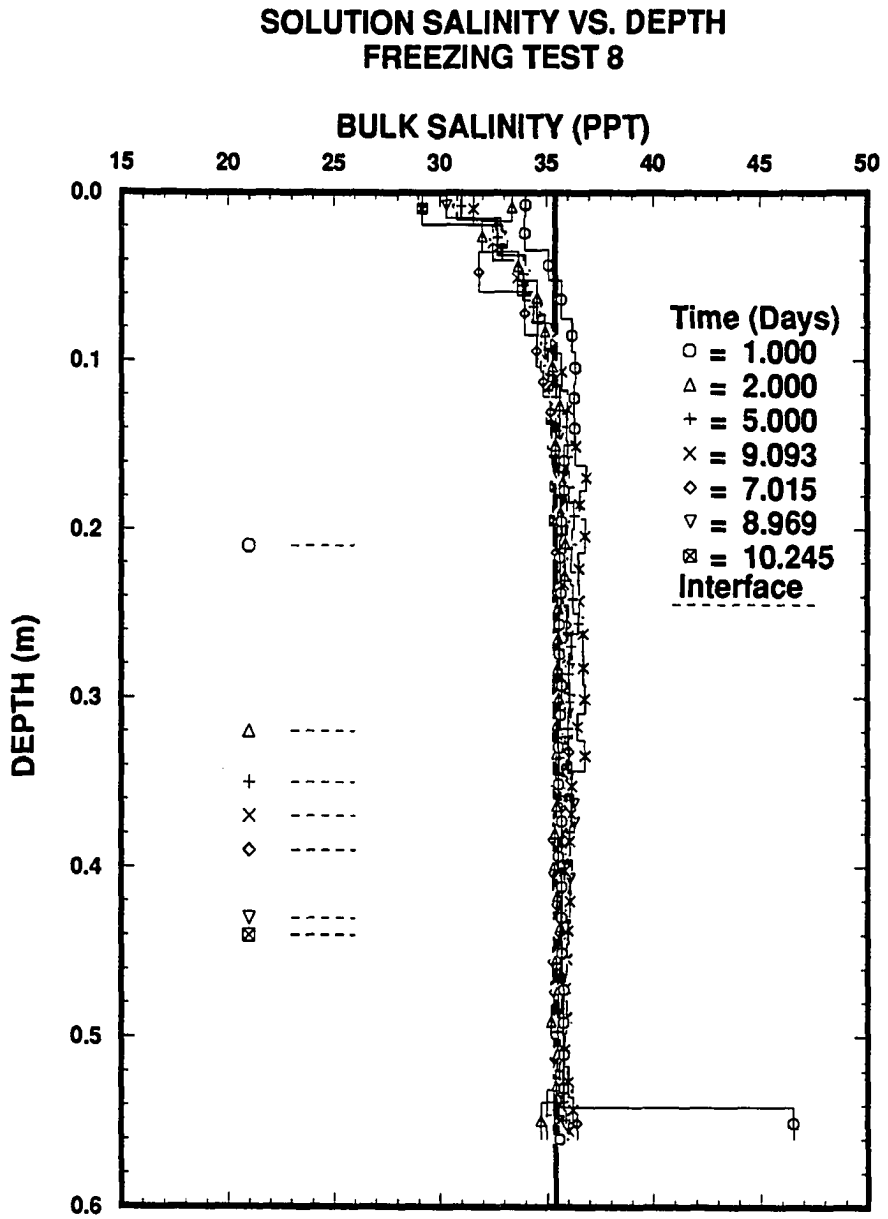

Figure 4.11: Bulk salinity profiles measured in each column during Test 8. The legend shows the time, in decimal days, when each column was removed from the freezing apparatus. The horizontal dashed line and symbol indicates the position of the ice-bearing interface at the time a column was removed from the freezing apparatus.

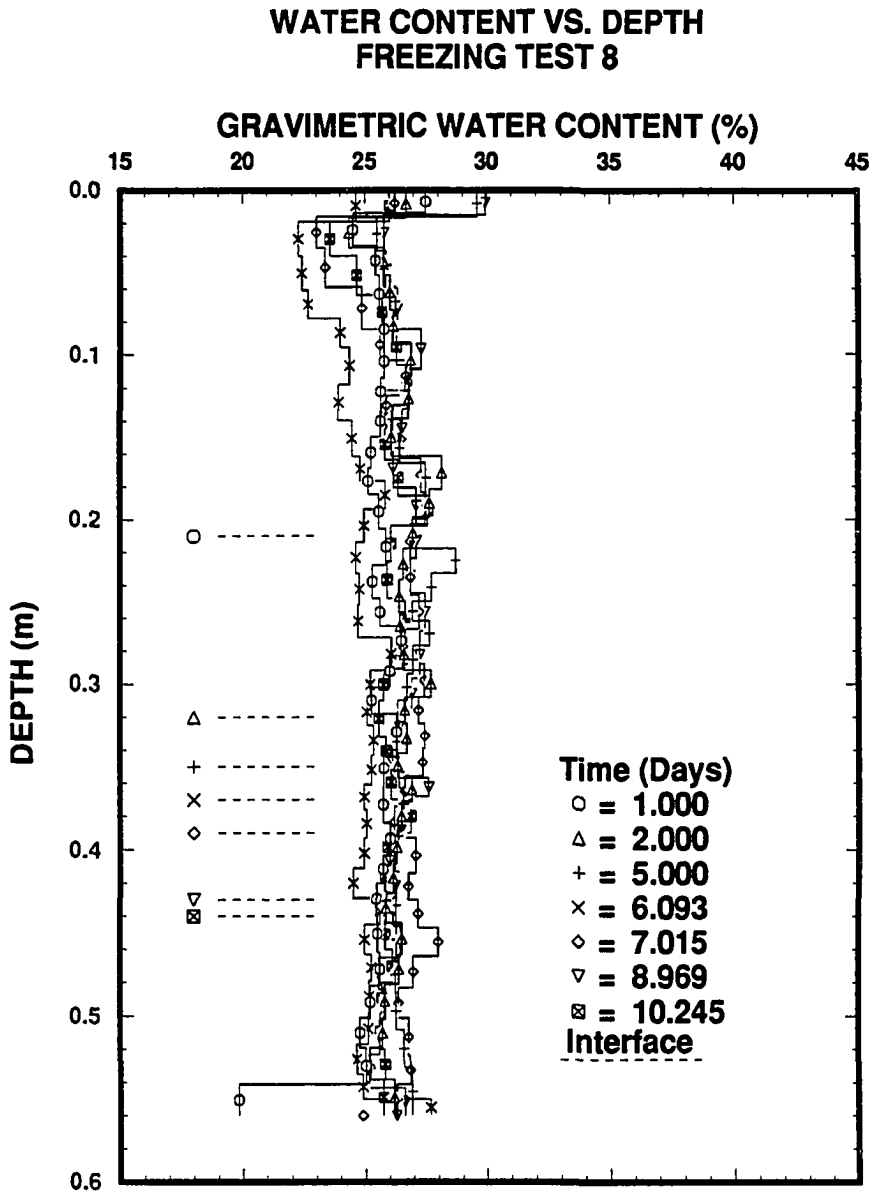

Figure 4.12: Water Content profiles measured in each column during Test 8.

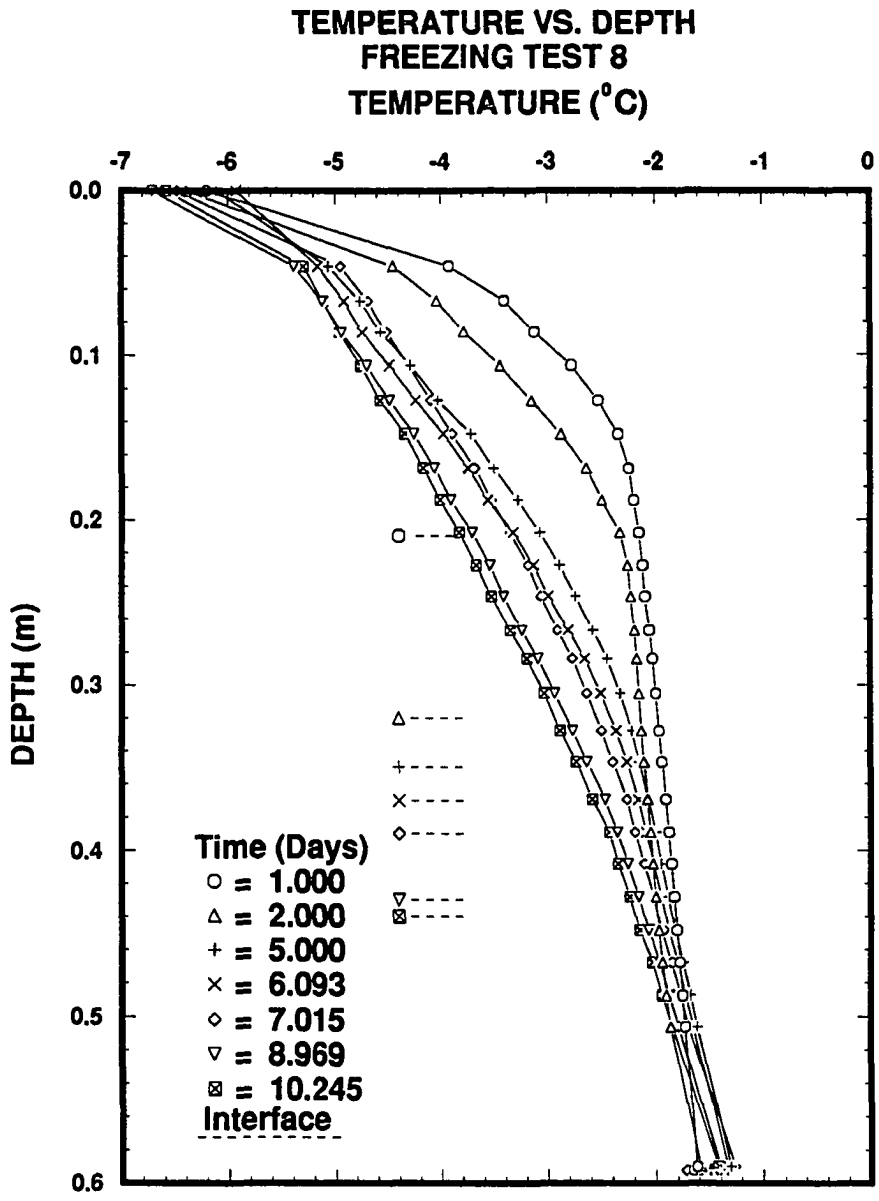

Figure 4.13: Temperature profiles measured during Test 8 at the time the columns were removed from the freezing apparatus. Temperature profiles were measured at the instrumented column.

Summary of Freezing Test 9

- Test Purpose

  1. This test was to determine the effects of a large surface temperature decrease on the distribution of the solute in the soil and the time transient that had been observed to precede the onset of convection in the previous tests.

- Notes

  1. All seven columns were saturated as usual and were frozen from the top down under a hydrostatic stress with the tops of the column capped and sealed.

Column	Date	Mass Fluid	Interface Location(m)		
Number	Removed	($kgx10^{-3}$)	Transition	Ice–Bonded	Thermodynamic
4	0.924	15.37	0.15	0.16	0.20
7	1.226	18.92	0.17	0.18	0.23
2	2.073	25.85	0.24	0.24	0.30
5	3.198	34.38	0.31	0.31	0.37
3	5.958	43.03	0.37	0.37	0.44
6	11.197	30.77	0.43	0.43	0.47
1	17.115	59.59	0.42	0.42	0.47

- Results

  1. The last two columns removed from the freezing apparatus appear to be affected by convection of the pore fluid.
  2. The second to last column removed exhibits a decreased water content profile over its entire length. Heat from the light in the heated chamber melted the tube which connects the base of the column with the expansion reservoir. Fluid from this column drained which led to erroneous water content measurements.
  3. Between the surface of the column and 0.1 m values of the bulk salinity exhibit a several ppt decrease. Values of the water content in this same region show an increase in the first section at the surface and a decrease to 0.1 m. These results are similar to experimental results from the other tests.

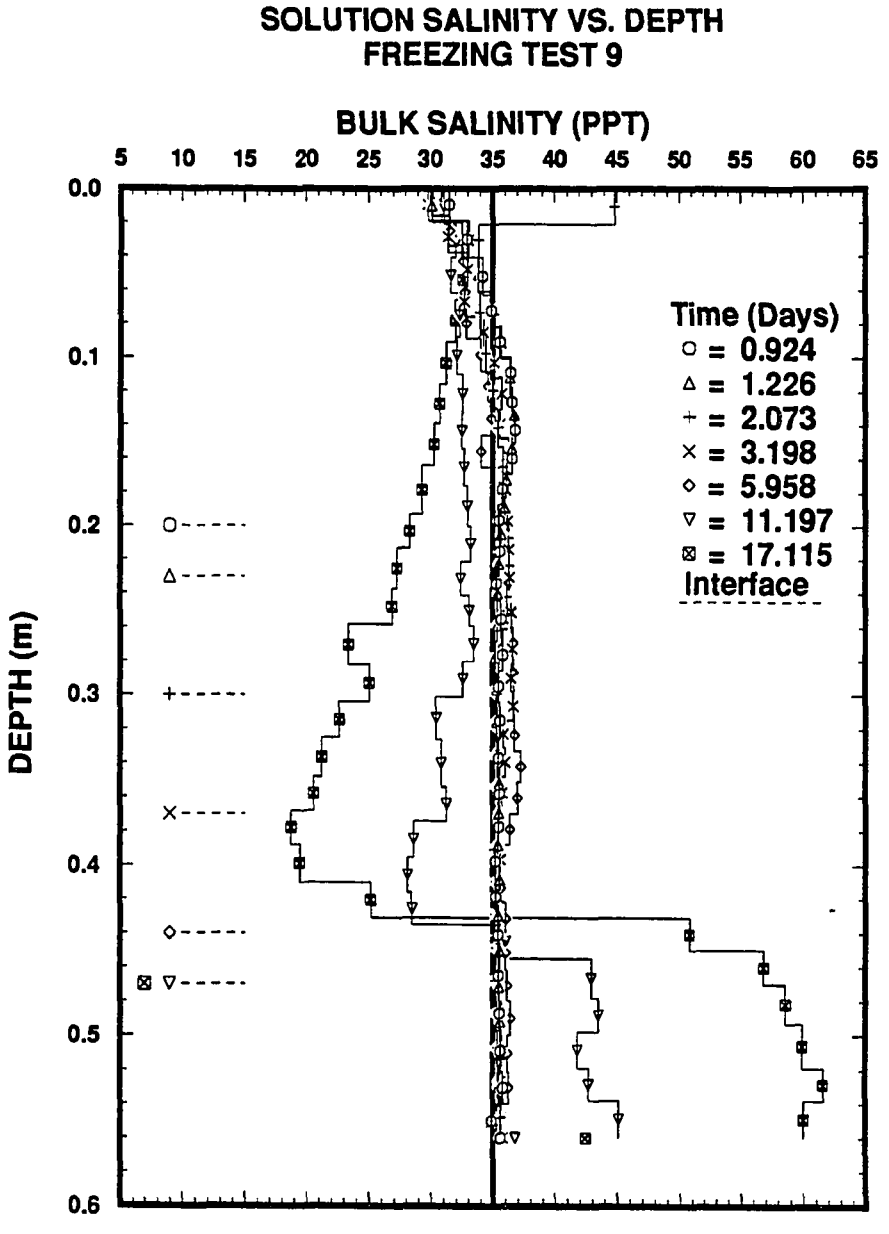

Figure 4.14: Bulk salinity profiles measured in each column during Test 9. The legend shows the time, in decimal days, when each column was removed from the freezing apparatus. The horizontal dashed line and symbol indicates the position of the ice–bearing interface at the time a column was removed from the freezing apparatus.

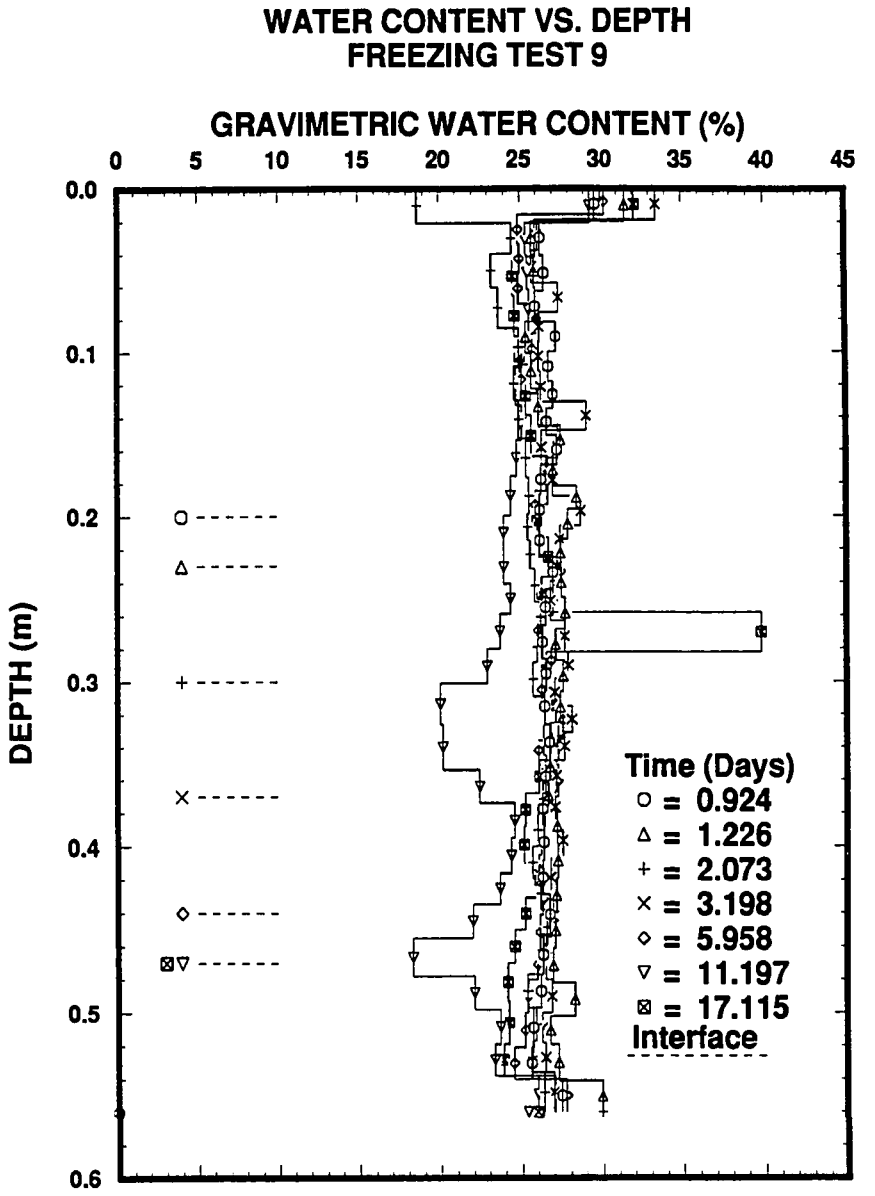

Figure 4.15: Water Content profiles measured in each column during Test 9. The first data point at the surface of one of the profiles extend beyond the scale of the figure. After 2.073 days of freezing, when this column was removed from the freezing apparatus, the surface water content value was 18.7%.

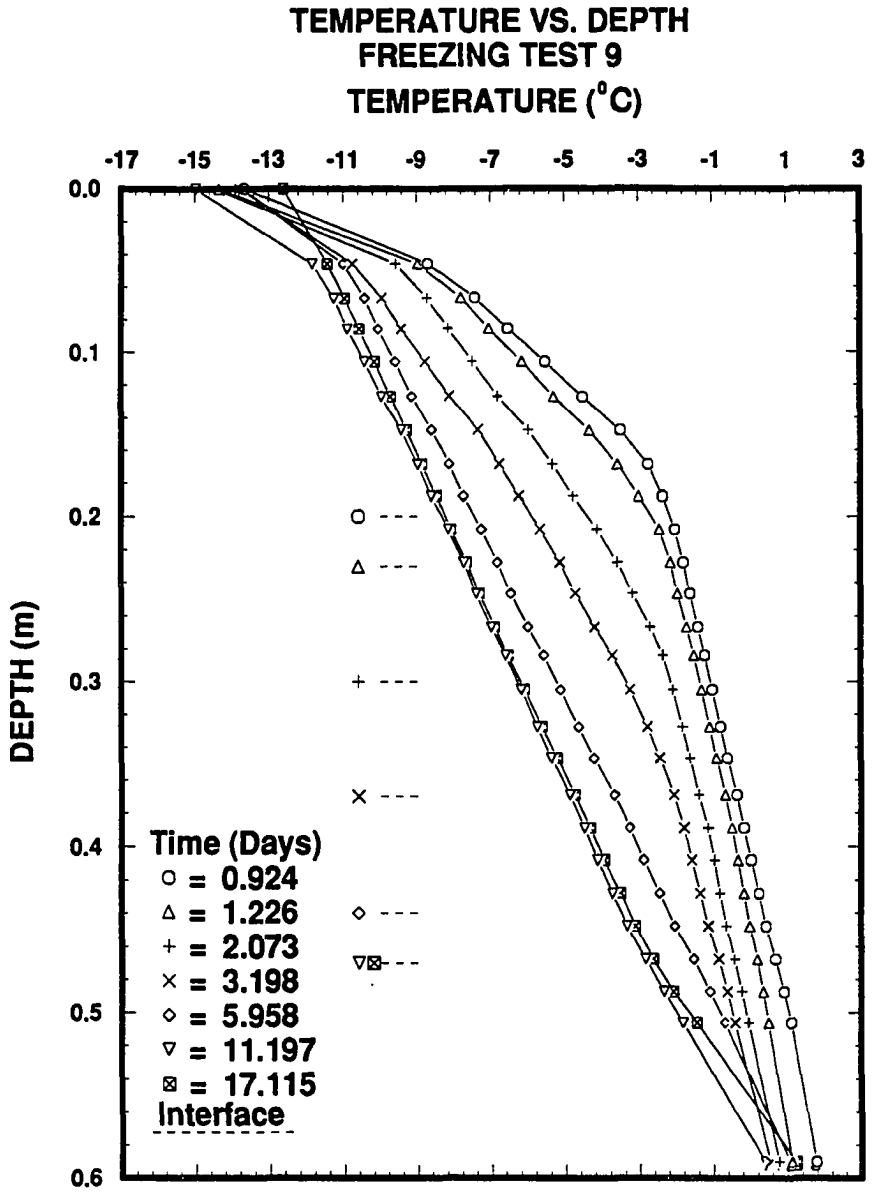

Figure 4.16: Temperature profiles measured during Test 9 at the time the columns were removed from the freezing apparatus. Temperature profiles were measured at the instrumented column.

Summary of Freezing Test 10

- Test Purpose

  1. This test was to determine the effects of rapid freezing on the distribution of the solute in the columns. The cold base temperature and relatively warm surface temperature insured that the ice–bearing interface quickly moved through the column.

- Notes

  1. All columns were saturated with solution in the usual manner, however, immediately prior to freezing, the tops were removed and the bases were plugged on columns removed after 0.925 and 7.153 days of freezing.

Column	Date	Mass Fluid	Interface Location(m)		
Number	Removed	(kgx10^{-3})	Transition	Ice–Bonded	Thermodynamic
7	0.876	–	0.10	0.14	0.31
4	0.925	7.12	0.12	0.16	0.29
2	3.167	14.46	0.17	0.29	0.43
3	5.158	15.72	0.26	0.32	0.46
5	7.119	19.30	0.29	0.38	0.51
6	7.153	–	0.31	0.37	0.40
1	17.036	28.39	0.24	0.50	0.57

- Results

  1. Only the column that was plugged at the base and open at the surface was affected by convection of the pore fluid.
  2. Inspection of the profile that was affected by convection shows that the bulk salinity minimum was within 0.1 m of the surface. Columns frozen under a hydrostatic stress have bulk salinity minimums just above the ice–bearing interface which is typically at a depth of 0.3 m.
  3. The location of the ice–bearing interface in each of the columns suggests that the columns that were plugged at the base and open at the surface froze quite differently than the other columns.
  4. Seven wires were installed in the instrumented column to act as conductivity cells within the sand and pore fluid. They were spaced at 5 centimeter intervals beginning at 5 centimeters below the surface. Each cell consisted of 10^{-2} m lengths of wire placed horizontally in the column separated by $\approx 10^{-2}$ m. Each cell was logged every half hour. D.C. excitation current was applied to each cell for 0.01 seconds before the reading was taken. Results showed that the resistivity of the cells could not be used to indicate the presence of ice or changes in the solute concentration in the sand.

5. In the column removed after 5.158 days of freezing, the tube connecting the base of column with the expansion reservoir was melted by heat from the light in the heated chamber sometime during freezing. Fluid from this column drained which led to erroneous water content measurements.
6. The entire column of sand contained ice by the time the last column was removed from the freezing apparatus.

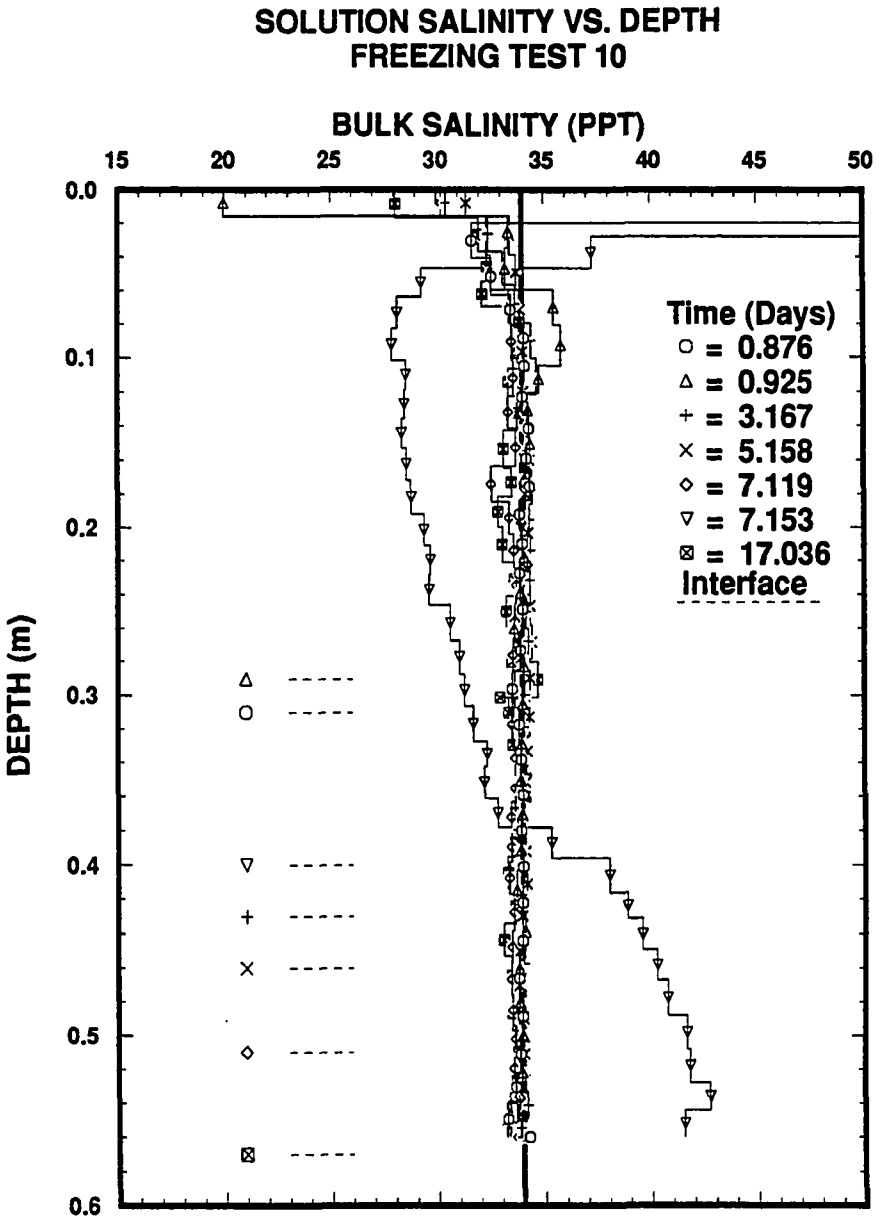

Figure 4.17: Bulk salinity profiles measured in each column during Test 10. The legend shows the time, in decimal days, when each column was removed from the freezing apparatus. The horizontal dashed line and symbol indicates the position of the ice–bearing interface at the time a column was removed from the freezing apparatus. The first data point at the surface of several profiles extended beyond the scale of the figure. At the time these columns were removed, the surface bulk salinity values were the following: 0.876 days 75.7 ppt, 7.153 days 51.9 ppt.

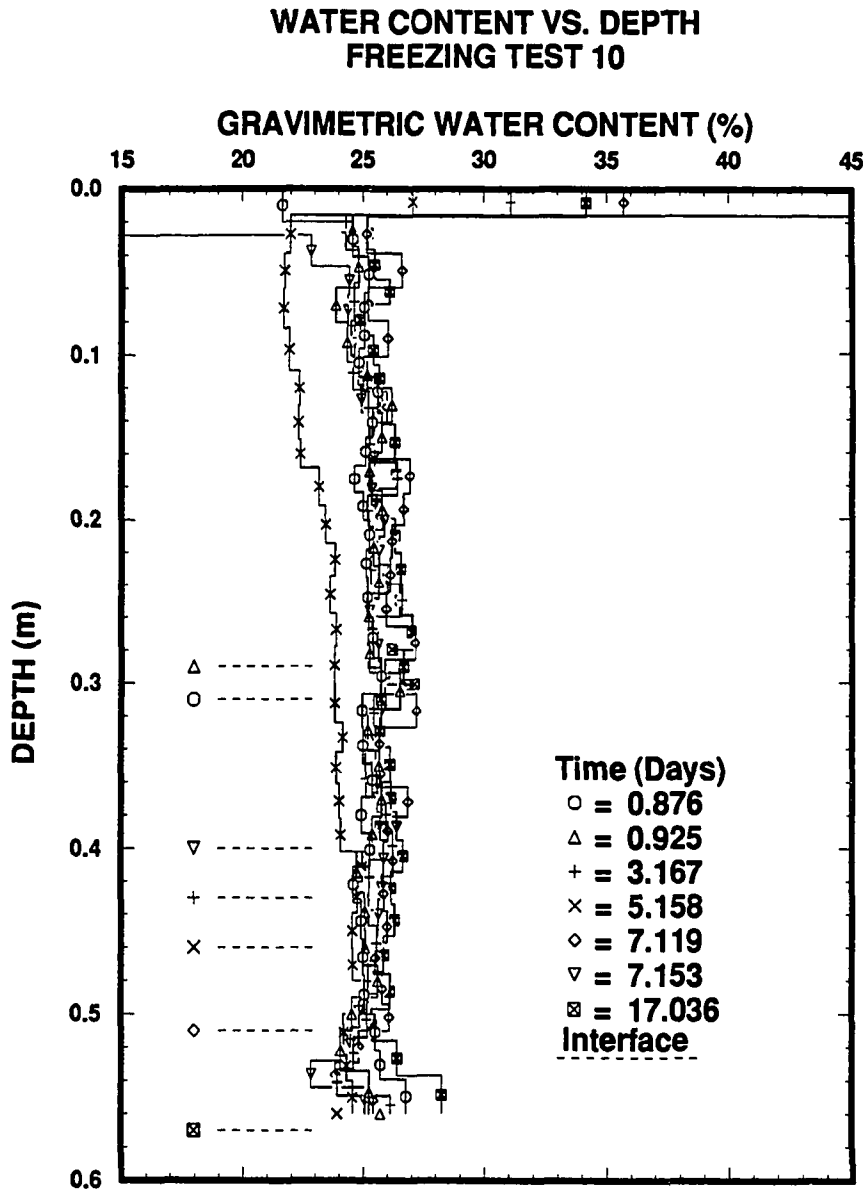

Figure 4.18: Water Content profiles measured in each column during Test 10. The first data point at the surface of two of the profiles extended beyond the scale of the figure. At the time these columns were removed, the surface water content values were the following: 0.925 days 52.7%, 7.153 days 14.2%.

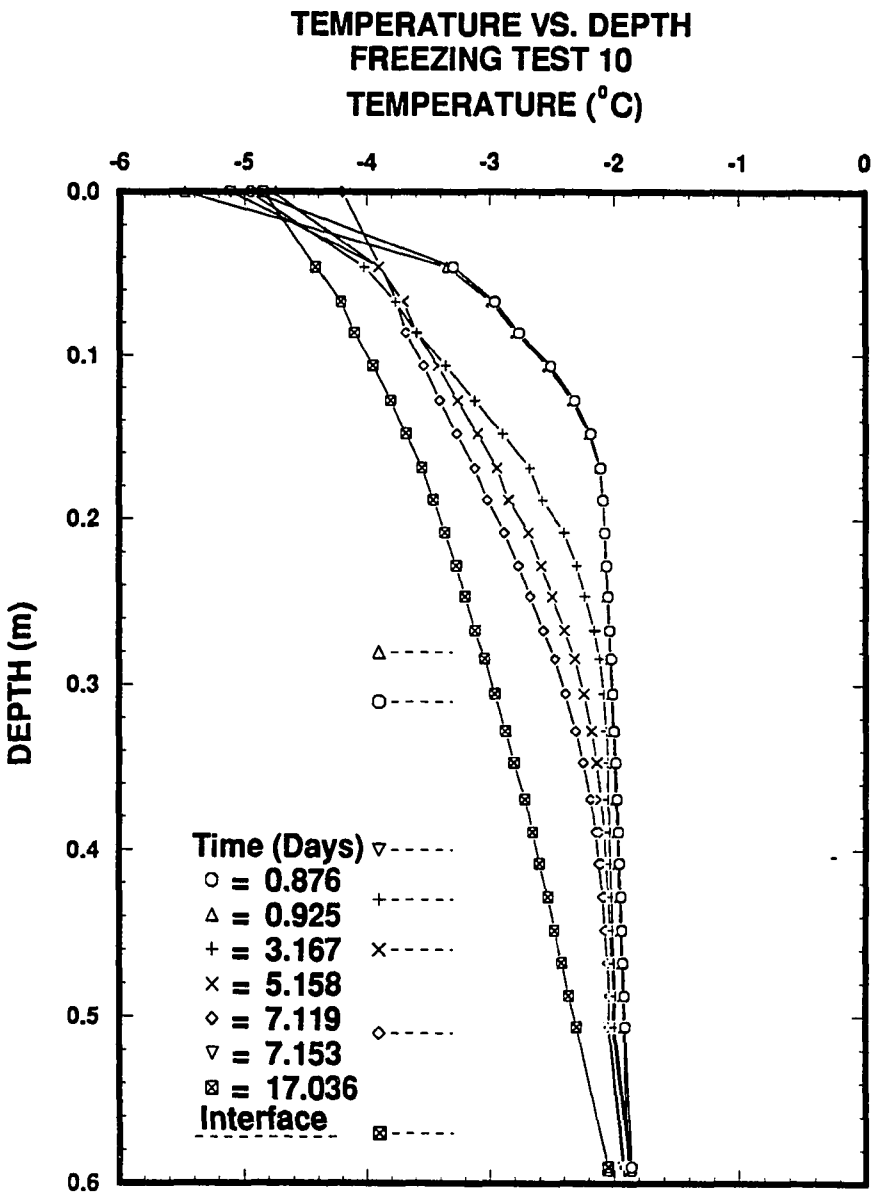

Figure 4.19: Temperature profiles measured during Test 10 at the time the columns were removed from the freezing apparatus. Temperature profiles were measured at the instrumented column.

Summary of Freezing Test 11

- Test Purpose
  1. Investigate the effects of a large vertical temperature gradient on the stability of the pore fluid.
  2. Trace the movement of the pore fluid by observing changes in position and form of horizontal layers of sand saturated with saline solution that had been dyed blue.
  3. Several columns were frozen with the base plugged and the tops open to determine if the direction of brine expulsion affected the pore fluid stability.
- Notes
  1. Sand in the columns for this test was saturated with saline solution and packed into the columns so that sand dyed with Rhodamine B indigo dye and sand containing no dye could be entered into the column without the two intermixing. The result were two alternating layers of saturated sand 5 to 10 centimeters thick separated by sand saturated with clear saline solution. These layers were placed near the surface of the columns.
  2. Columns removed after 3.990, 6.927 and 9.968 days of freezing were opened on the top and closed at the base immediately prior to freezing. The remaining four columns were frozen as usual.

Column	Date	Mass Fluid	Interface Location(m)		
Number	Removed	($kgx10^{-3}$)	Transition	Ice-Bonded	Thermodynamic
4	3.990	-	0.16	0.18	0.19
7	4.042	6.69	0.13	0.18	0.19
3	6.927	-	0.16	0.19	0.25
5	7.032	6.00	0.16	0.21	0.23
2	9.968	-	0.13	0.20	0.27
6	10.048	17.54	0.19	0.23	0.27
1	11.032	8.15	0.19	0.23	0.28

- Results
  1. Observations made while sectioning columns that were plugged at the base and open at the surface showed that brine was expelled towards the surface in isolated channels that decreased in width towards the surface. These channels indicated that freezing, and the pressure field associated with brine expulsion was three dimensional and not one dimensional as in the columns frozen under a hydrostatic stress.

2. In columns in which the pore fluid had convected, portions of each section were analyzed for bulk salinity and water content. For example, the portion of each section which contained downward moving pore fluid was always analyzed separately from the rest of the section. These results appear in each figure as multiple salinity and water content values at each level.

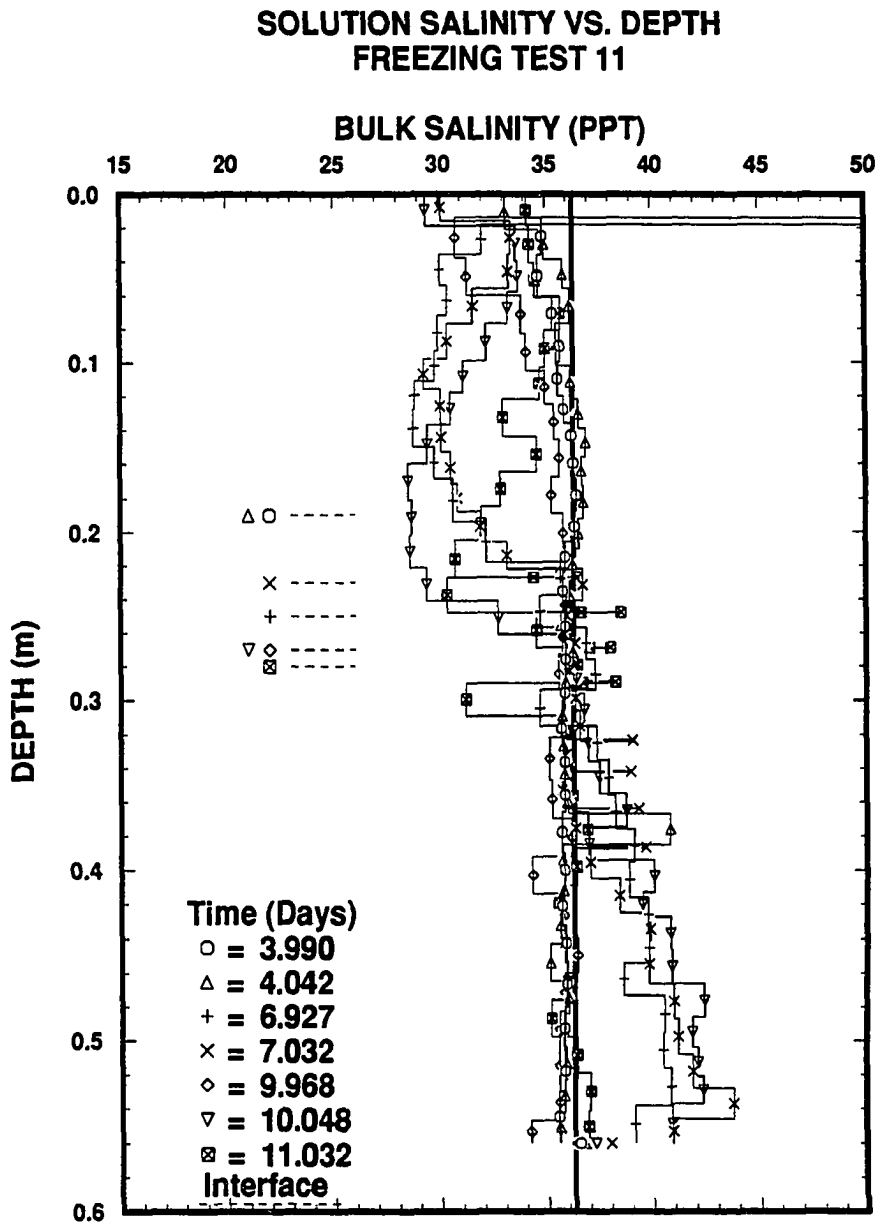

Figure 4.20: Bulk salinity profiles measured in each column during Test 11. The legend shows the time, in decimal days, when each column was removed from the freezing apparatus. The horizontal dashed line and symbol indicates the position of the ice–bearing interface at the time a column was removed from the freezing apparatus. The first data point at the surface of several profiles extended beyond the scale of the figure. At the time these columns were removed, the surface bulk salinity values were the following: 3.990 days 100.66 ppt, 6.927 days 102.53 ppt, 9.968 days 140.47 ppt.

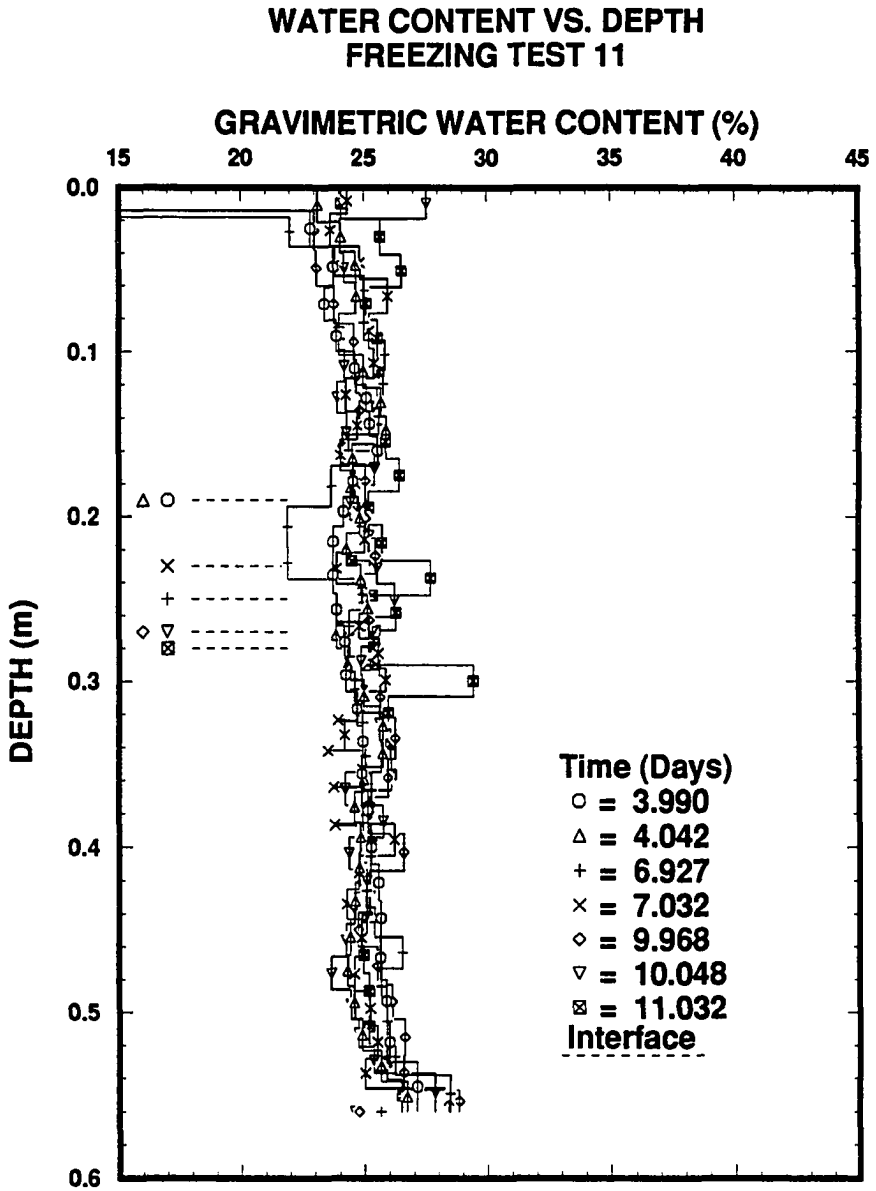

Figure 4.21: Water Content profiles measured in each column during Test 11. The first data point at the surface of several profiles extended beyond the scale of the figure. At the time these columns were removed, the surface water content values were the following: 3.990 days 10.7%, 6.927 days 12.2%, 9.968 days 12.3%.

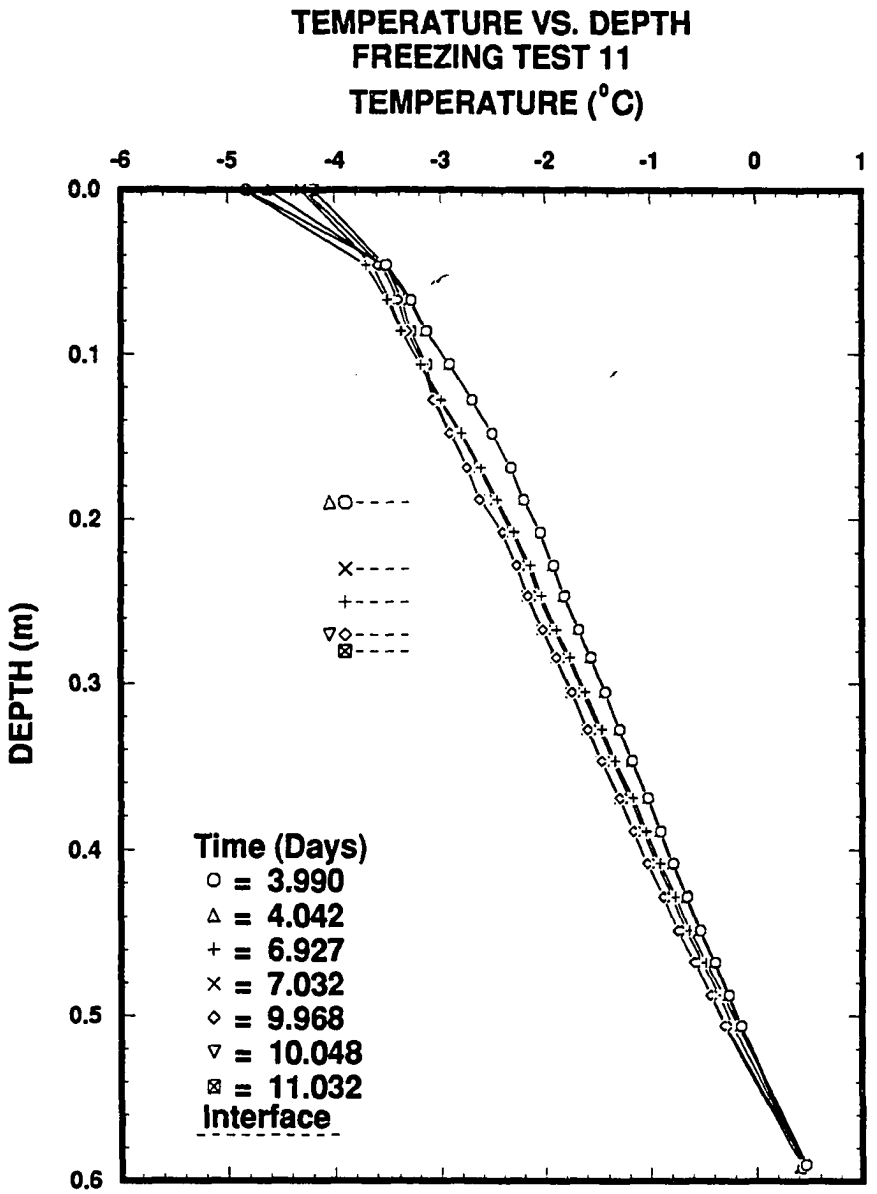

Figure 4.22: Temperature profiles measured during Test 11 at the time the columns were removed from the freezing apparatus. Temperature profiles were measured at the instrumented column.

Summary of Freezing Test 12

- Test Purpose
  1. This test was to determine the effects of a large initial salinity on the distribution of the solute in the freezing sand.
- Notes
  1. Each of the seven columns was saturated as usual, capped at the surface, open at the base and frozen under hydrostatic conditions.

Column Number	Date Removed	Mass Fluid ($kgx10^{-3}$)	Interface Location(m)		
			Transition	Ice-Bonded	Thermodynamic
7	2.017	4.39	0.18	0.23	-
4	3.931	8.32	0.12	0.41	-
3	3.957	-	0.13	0.29	-
6	6.969	13.31	0.20	0.47	-
2	7.063	11.43	0.57	0.57	-
5	9.896	12.11	0.57	0.57	-
1	10.001	13.97	0.57	0.57	-

- Results
  1. Problems with accurately determining the bulk salinity of the the solution made it difficult to reliably calculate the unfrozen parameters.
  2. The large brine volume throughout the partially frozen region made it difficult to determine the location of the transition and ice-bonded interfaces.
  3. Although it was difficult to obtain accurate bulk salinity measurements, none of the profiles in this test exhibited a decrease in bulk salinity in the partially frozen region or an increase in bulk salinity near the base. The lack of these two features suggest that convection of the pore fluid did not occur during freezing.
  4. Temperature profiles indicate that the entire column of sand contained ice after approximately four days of freezing assuming a pore fluid salinity of 109 ppt.

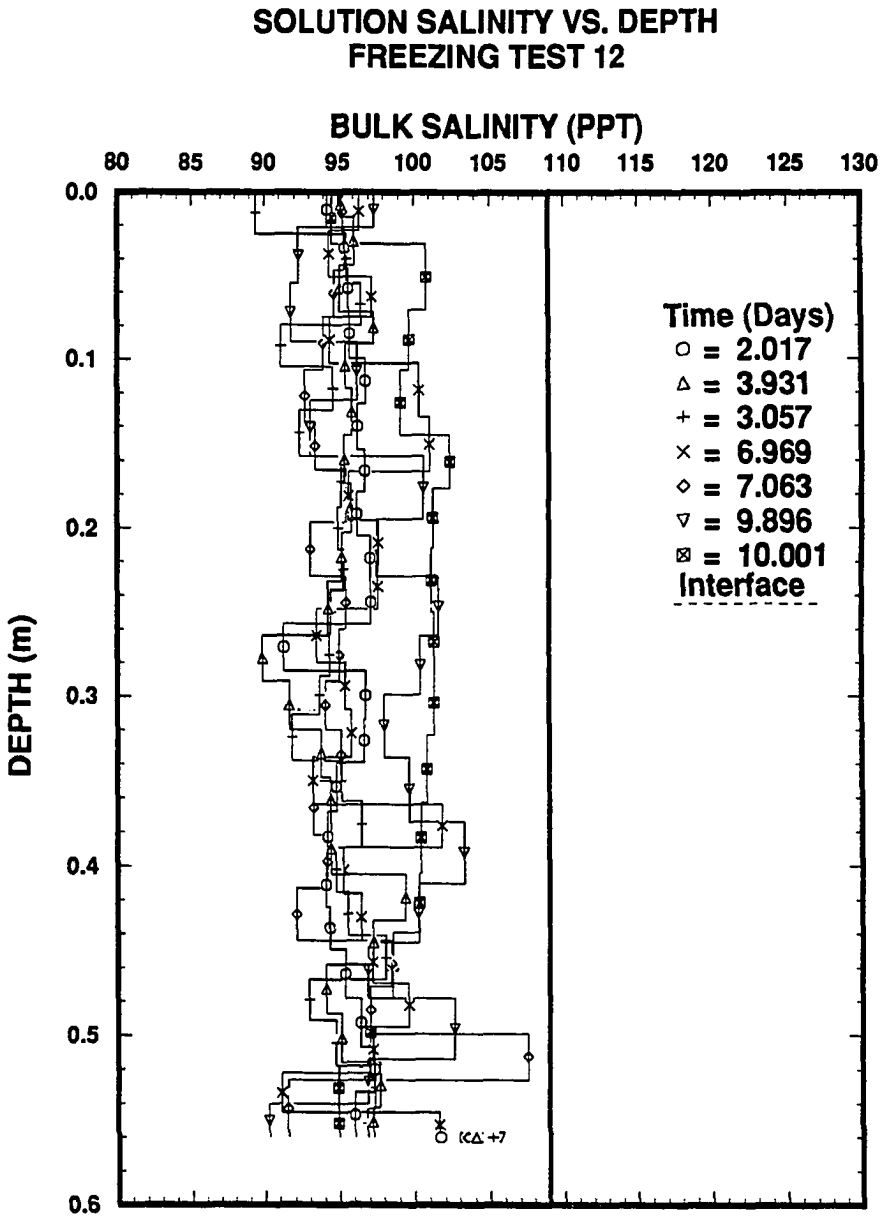

Figure 4.23: Bulk salinity profiles measured in each column during Test 12. The legend shows the time, in decimal days, when each column was removed from the freezing apparatus.

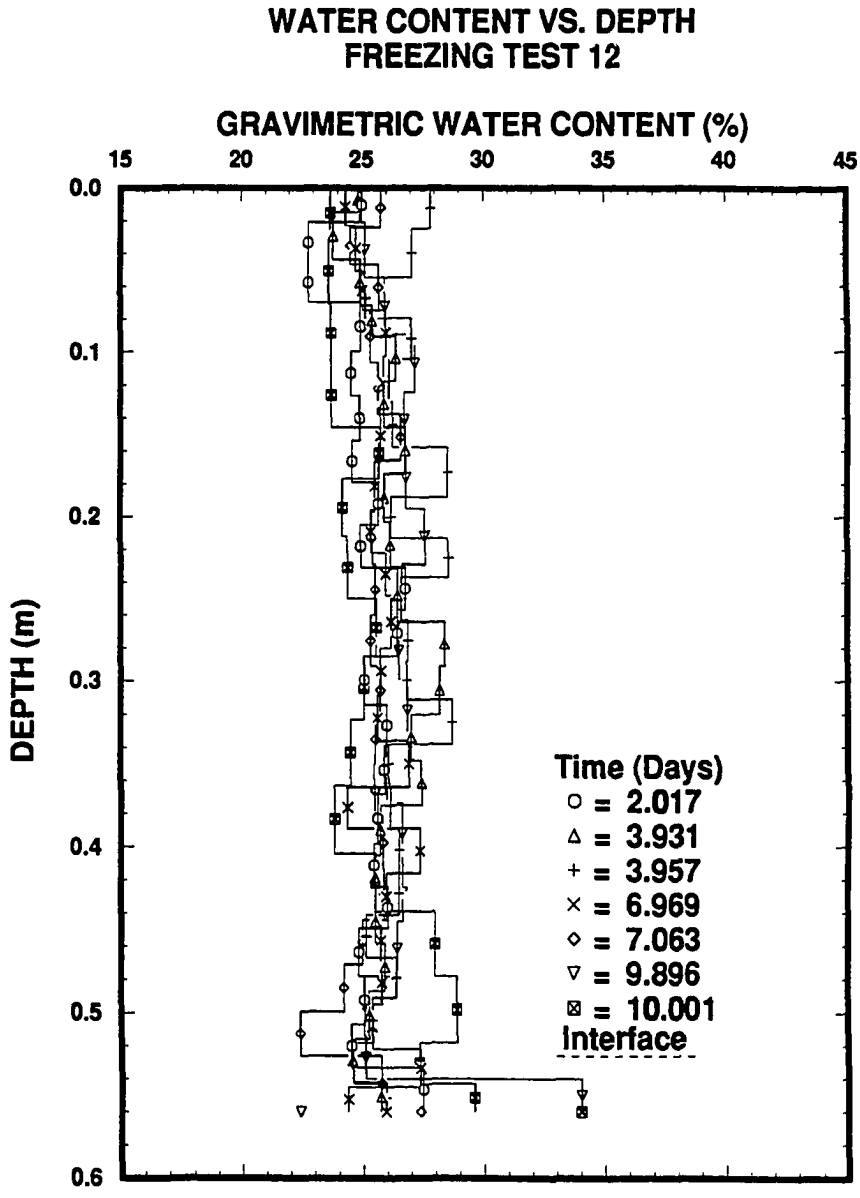

Figure 4.24: Water Content profiles measured in each column during Test 12.

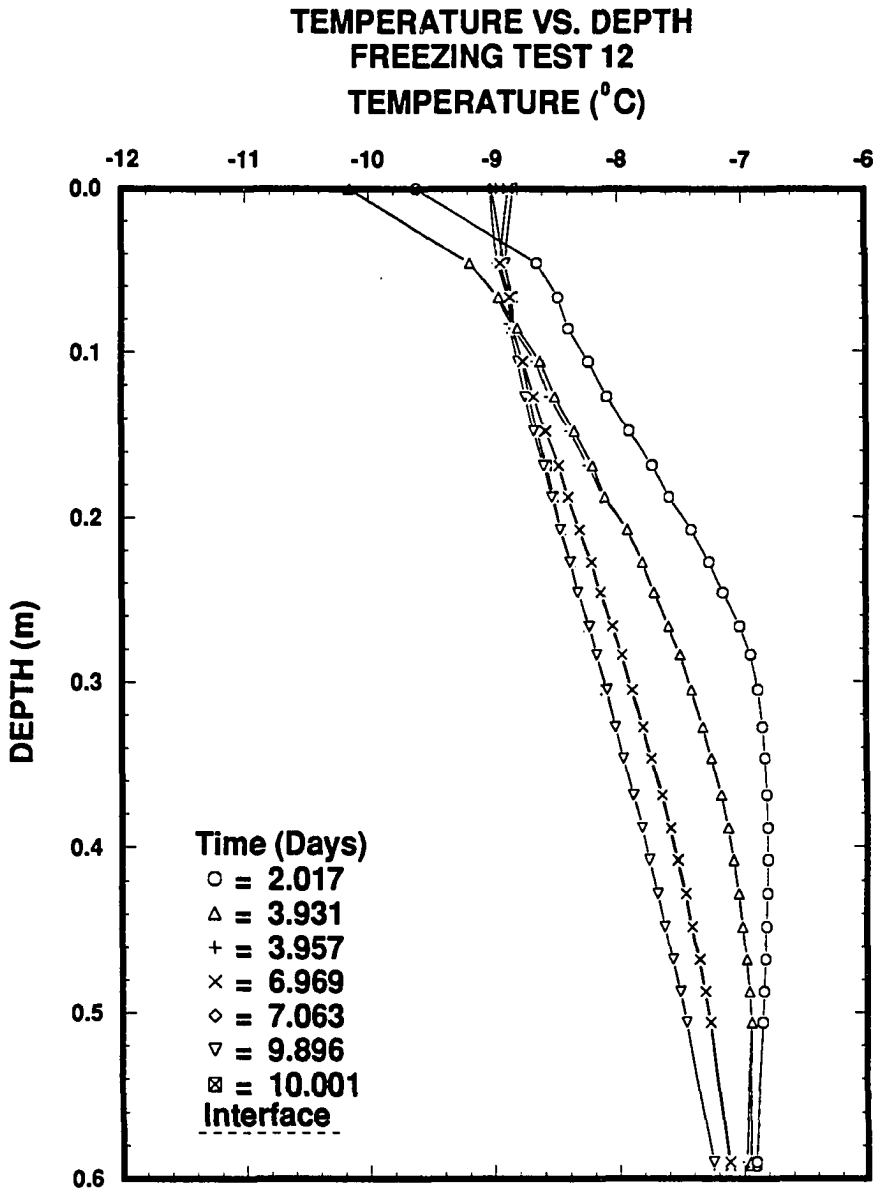

Figure 4.25: Temperature profiles measured during Test 12 at the time the columns were removed from the freezing apparatus. Temperature profiles were measured at the instrumented column.

Summary of Freezing Test 13

- Test Purpose
  1. This test was to determine the effects of a small initial salinity on the distribution of the solute during freezing.
- Notes
  1. Each of the seven columns was saturated as usual, capped at the surface, open at the base and frozen under hydrostatic conditions.
  2. A leak in the sand box was present during the initial equilibration stages of cooling. The leak was small and the pore fluid was recycled into the sand box. After $\approx$ 2 days of freezing the leak became large and the box drained to nearly the half way mark.
  3. Upon their removal from the freezing apparatus, columns were allowed to thaw at room temperature for up to 2 hours to facilitate sectioning them with a bandsaw. During this time the columns were kept in the vertical position.
  4. The position of the ice–bonded interface was determined by tapping the column until the thawed portion of the column settled enough that it decoupled from the bonded portion of the column. The location of the transition interface was not measured.

Column	Date	Mass Fluid	Interface Location(m)		
Number	Removed	(kgx10^{-3})	Transition	Ice–Bonded	Thermodynamic
4	0.958	8.53	–	0.14	0.12
7	3.003	23.50	–	0.17	0.24
2	4.919	20.50	–	0.25	0.30
3	6.906	41.39	–	0.30	0.32
5	9.113	41.33	–	0.27	0.35
6	11.169	46.25	–	0.30	0.36
1	12.969	41.77	–	0.30	0.38

- Results
  1. None of the columns appeared to have been affected by convection of the pore fluid.
  2. Essentially 100% of the solute was incorporated with the partially frozen sand.
  3. The ice–bonded interface was a sharp discontinuous interface in this test. A transition region was not observed.

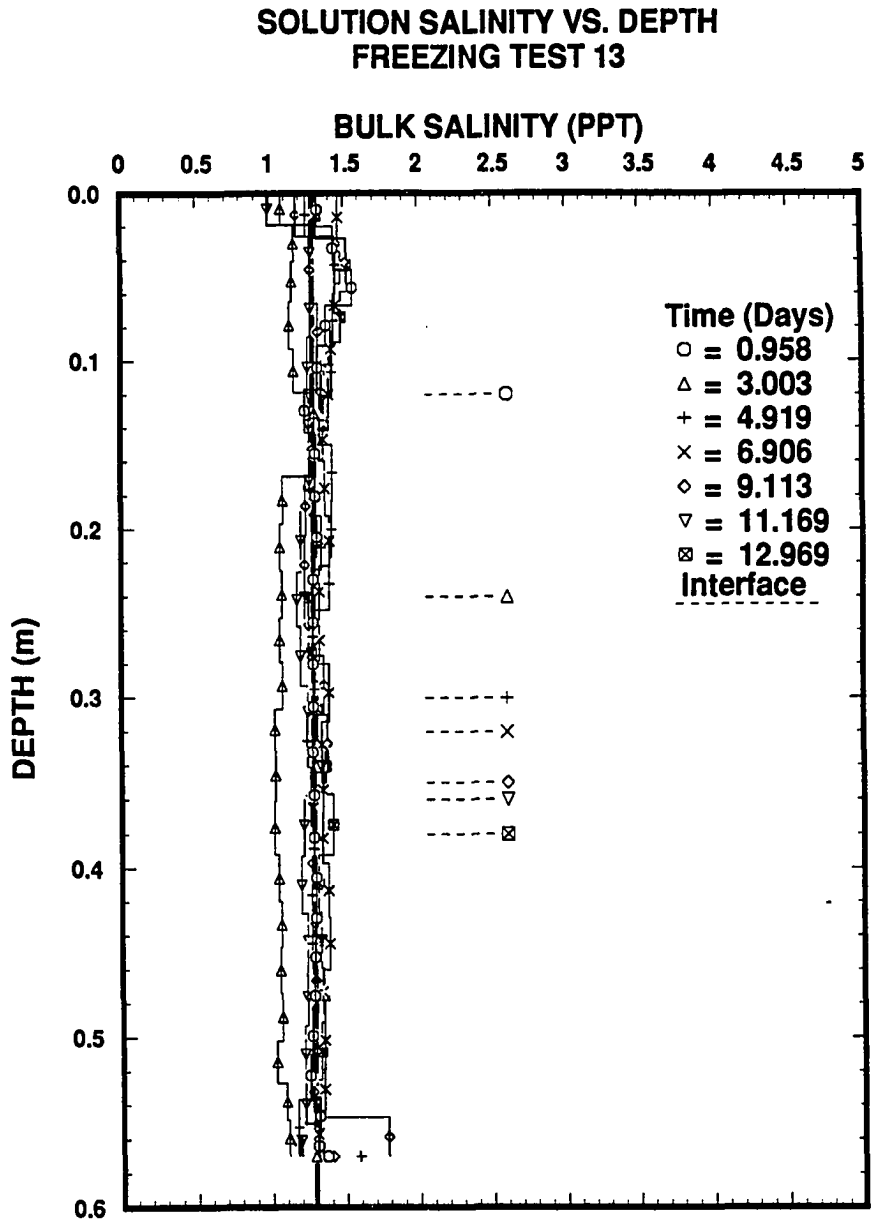

Figure 4.26: Bulk salinity profiles measured in each column during Test 13. The legend shows the time, in decimal days, when each column was removed from the freezing apparatus. The horizontal dashed line and symbol indicates the position of the ice–bearing interface at the time a column was removed from the freezing apparatus.

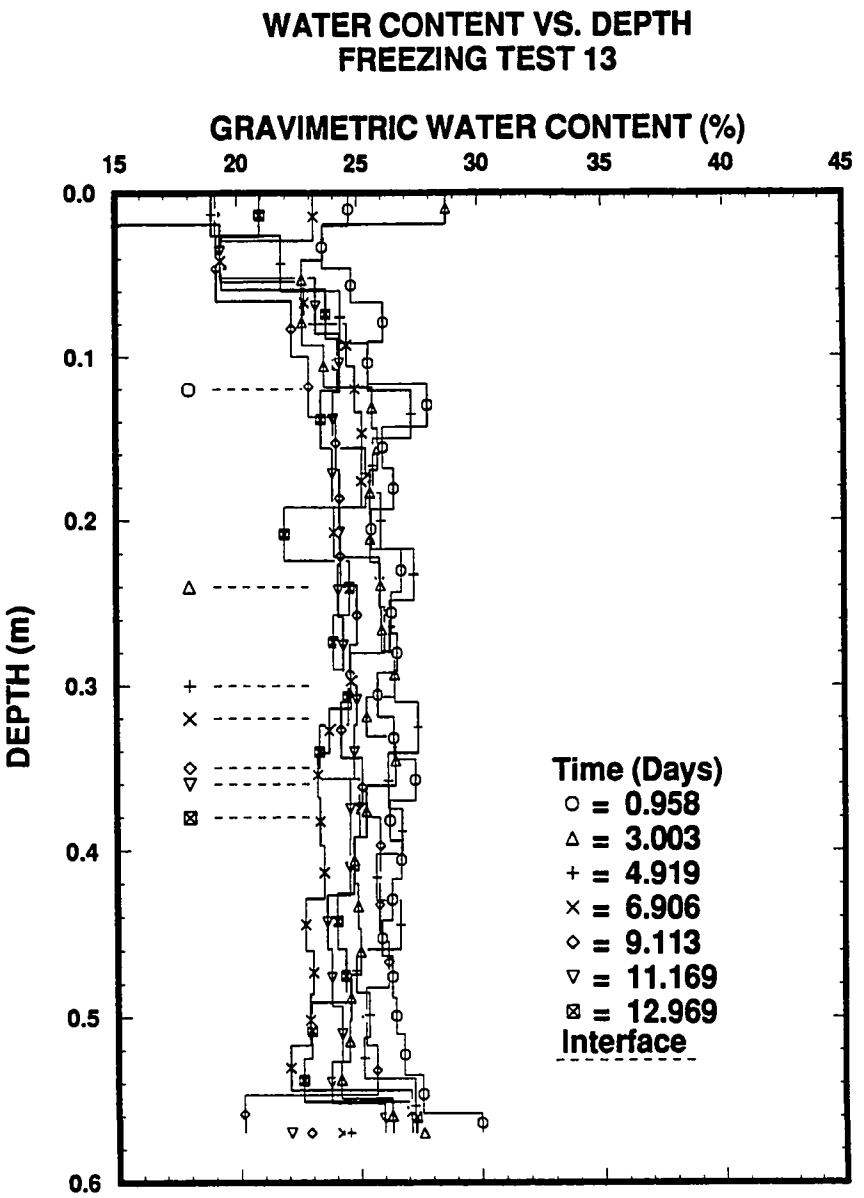

Figure 4.27: Water Content profiles measured in each column during Test 13. The surface water content value on the column removed after 11.169 days of freezing was 11.3%.

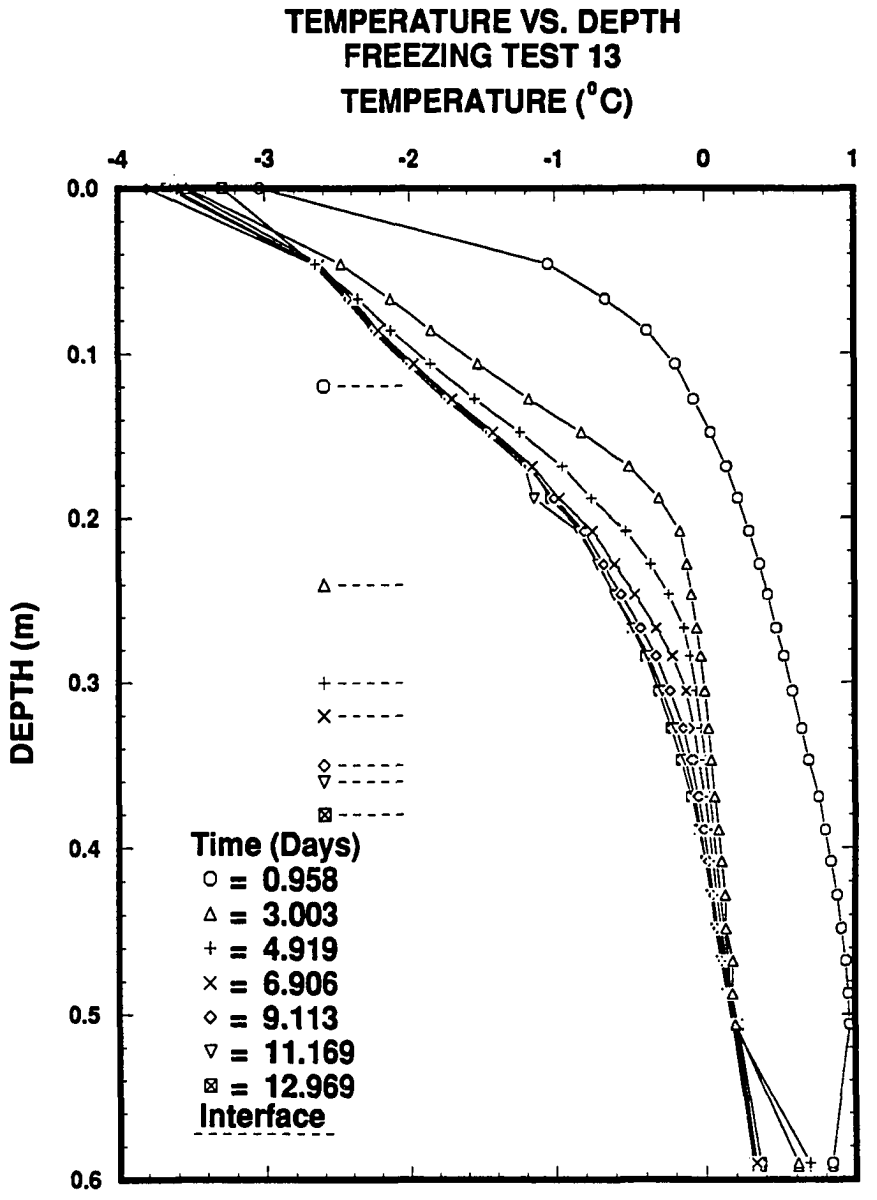

Figure 4.28: Temperature profiles measured during Test 13 at the time the columns were removed from the freezing apparatus. Temperature profiles were measured at the instrumented column.

In every column analyzed in this investigation, the interface was observed to be a diffuse interface in which the transition from the sand grains being firmly ice–bonded to thermodynamically thawed occurred over a vertical distance which was up to 0.19 m in length. General observations indicate that the greater the difference between the surface temperature and base temperature the smaller the vertical difference between the transition interface and ice–bearing interface (Test 9 for example). It was also observed that the greater the initial bulk salinity, the larger the vertical distance between these two interfaces (Test 13 for example).

It was generally observed that a several millimeter gap existed between the top of the sand surface and the base of the aluminum cap. This gap was filled with air and developed due to settling of the sand during saturation with the saline solution and while the columns equilibrated in the freezing apparatus. Bulk salinity measurements within the top 0.02 m of the column generally indicate a several percent decrease during freezing. Water content measurements generally indicate a several percent increase in the water content within the top 0.02 m of the column.

Bulk salinity measurements were used to determine when solute movement by convection of the pore fluid began in the columns. Characteristics of profiles which indicated the presence of convection were a decrease in the bulk salinity within the partially frozen portion of the column and a corresponding increase in the bulk salinity at the base of the thawed portion of the column. This criteria indicates that profiles of bulk salinity, Figure 4.5, were not affected by convection during the first 4 days of freezing. Changes in bulk salinity that can be associated with convection of the pore fluid began after the fourth day of freezing and continued in some of the columns until the last column was removed after 14 days of freezing. Throughout this investigation, it appears that the onset of convection occurred after a transient period of 4 to 10 days. The depth of minimum bulk salinity generally occurred at 25 to 80% of the maximum depth of freezing. Columns in Test 6 removed after 4 and 9 days of freezing did not exhibit profiles that could be associated with convection of the pore fluid. The column removed after 4.000 days of freezing was sectioned along the axis of the column so that the interface could be observed in section form. Only the ice–bonded sections of this column were analyzed. The column removed after 9 days of freezing did not exhibit features

associated with convection; it did, however have an ice–bearing interface which was 6 to 7 centimeters deeper than the other columns in this test.

Bulk salinity profiles exhibit features important to understanding the nature of solute movement in the columns. For example, in columns affected by convection, the highest rate of change in bulk salinity occurs immediately above the ice–bearing interface (Figure 4.5). Bulk salinity profiles after 10 and 14 days of freezing showed that the bulk salinity within the top 0.2 m of the column is greater after 14 days than after 10 days. However, above the ice–bearing interface, the bulk salinity in the bottom portion of the profile had decreased in the 4 day interval starting after 10 days of freezing. Figure 4.5 shows that once solute convection began, the downward flow of pore fluid penetrated the thawed length of the column and upward flow of pore fluid penetrated the complete length of the partially frozen portion of the column. However, convection in the upward direction did not affect the bulk salinity profiles in the partially frozen region as uniformly or to the extent that downward moving pore fluid affected bulk salinity profiles in the thawed length of the column. Profiles of bulk salinity from this test or any of the other tests do not appear to exhibit a build up of solute in front of any of the interfaces (transition, ice–bonded, thermodynamically thawed).

In an effort to understand the mode of convection within the columns once convection began, columns in Test 11 were frozen with sand saturated with solution containing horizontal layers of Rhodamine B indigo dye separated by layers of sand saturated with non–dyed solution. The purpose of placing layers of dye within the column was to trace the movement of the pore fluid during freezing. Columns in this test were filled with dyed and undyed sand saturated with saline solution rather than the dry sand which was later saturated. Filling the columns in this way did not allow the dry density of the sand prior to the start of freezing to be measured. Columns typically contained two 5 to 10 centimeter thick dyed layers in the upper half of the column. These layers were separated by a layer of saturated sand 5 to 10 centimeters thick. Observations from this test indicated that prior to the onset of convection, the dye moved uniformly down a few centimeters presumably due to brine rejection which was associated with the formation of ice and the density difference between brine and ice. When convection did occur, it was observed to consist of pore fluid containing dye which moved down one side of the column and up the opposite side. On the side of the column which consisted

of downward moving dye, the dye was observed along the side of the column in a several centimeter wide area and it extended the entire length of the thawed portion of the column. Figure 4.29 is a schematic graph of the brine movement during convection. The length that pore fluid moved up in the partially frozen region could not clearly be observed because of the slight affinity of the dye to the sand grains.

In the columns used in Test 11, the columns frozen under a hydrostatic stress (with the exception of the instrumented column) were momentarily removed from the freezing apparatus each day after the start of freezing to determine when convection of the pore fluid began. The instrumented column, the column frozen for the greatest length of time, could not be inspected to determine if convection had begun because it could have resulted in damage to the thermistor string. The first column was removed from the freezing apparatus and sectioned when pore fluid was observed to be convecting as indicated by the irregular dye pattern in the column which occurred after 4.042 days of freezing. Movement was observed by pore fluid near the ice–bearing interface in one half of the column moving down. The dye pattern indicated that convection had just begun in this column since the dye had extended only 4 centimeters down one side of the column. This was the only column of those checked that exhibited the effects of convection at this time. Periodic visual observations of the remaining columns were not made after 4.042 days. The columns removed after 7.032, 10.048 and 11.032 days of freezing exhibited the effects of convection in the dye pattern. Each column affected by convection exhibited a similar dye pattern.

The region between the transition interface and the ice–bearing interface exhibited radial asymmetries in the bondedness of the sand which were associated with the mode of convection. Where the pore fluid moved down, the sand was observed to be less well bonded than in the center of the column. Where the pore fluid moved up, the sand was observed to be less well bonded than in the center of the column but better bonded than on the side of the column where the pore fluid moved down. Bulk salinity and gravimetric water content measurements were made on portions of the sand within regions that were observed to contain pore fluid that moved up, moved down or did not appear to move. These measurements indicated that the pore fluid moving down had a bulk salinity that was

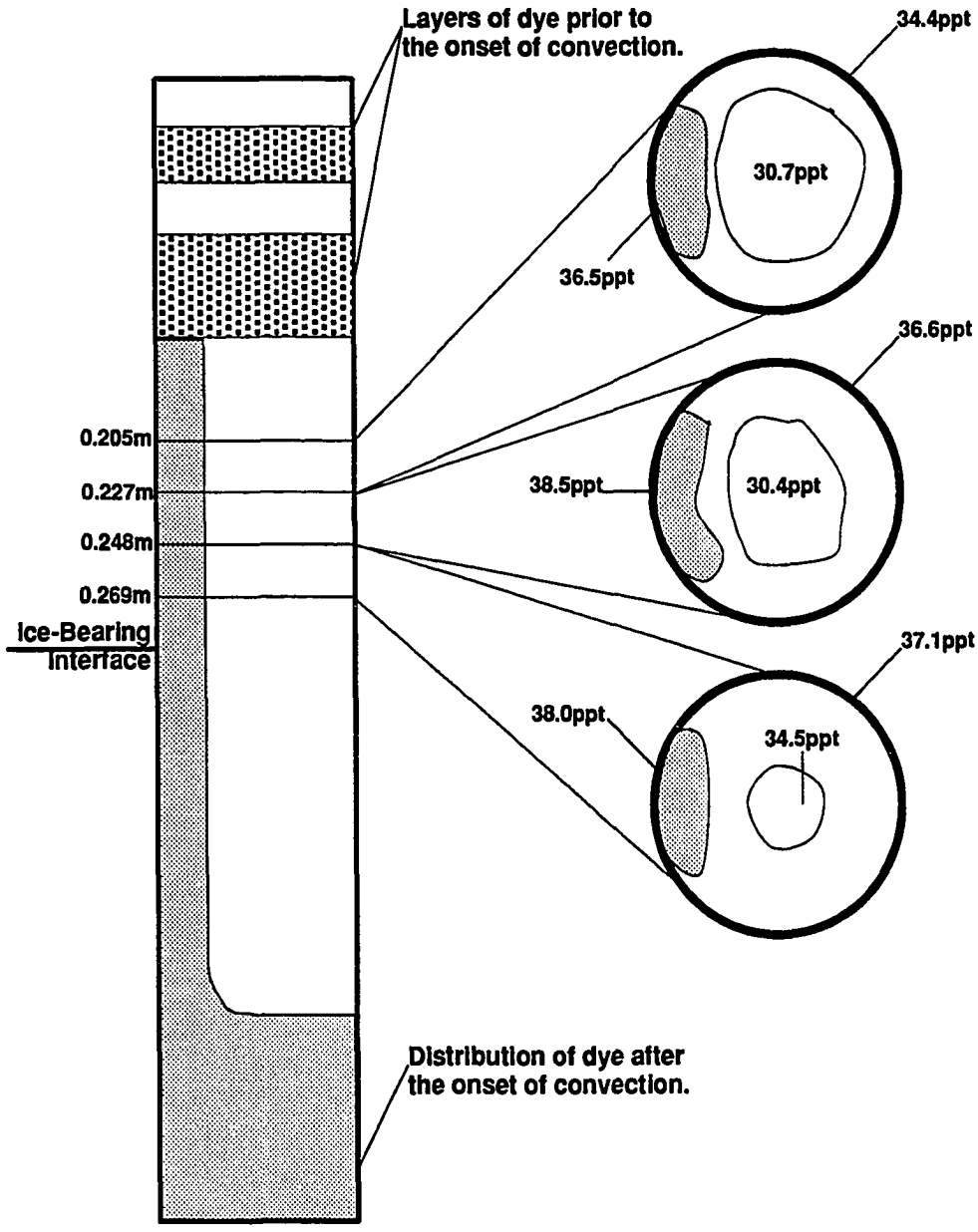

Figure 4.29: A schematic diagram of pore fluid motion during convection in the sand columns. The data presented in the figure was obtained from measurements made on Column 111 (Column 1, day 11.032 of Test 11) and is also presented in Table 4.4. The horizontal darkly stippled areas denote the initial configuration of the dyed solution. The lightly stippled areas denote the approximate dye distribution after the onset of convection. The initial pore fluid salinity was 36.3 ppt.

1 to 2 ppt greater than the pore fluid moving up, and the pore fluid moving up had a bulk salinity that was 1 to 8 ppt greater than the pore fluid in the middle of the section. The gravimetric water content appears to be slightly higher in the sand with upward moving pore fluid. The gravimetric water content appears to be approximately the same in the middle of the section and in the sand where pore fluid moves down. Table 4.4 is a summary of these measurements for Test 11. Figure 4.29 is a schematic graph of the bulk salinity and pore fluid motion during convection in the columns.

It was generally observed throughout this investigation that freezing would not lead to the redistribution of the solute if the location of the ice–bearing interface was at or near the base of the column. Tests 10 and 12 are examples of the case where the entire column contained ice early during freezing. During Test 10 the base temperature was relatively cold and was close to the freezing temperature of the solution and the surface temperature was relatively warm. These temperature conditions made it possible for the ice–bearing interface to move through the sand relatively quickly. By the seventh day of freezing the columns were frozen to within 5 centimeters of the base of the column. Another feature of this test is that the temperature gradient through the interface was smaller than the other freezing tests. During Test 12 the high initial solute concentration resulted in the interface moving quickly through the sand to freeze essentially the entire length of the column in 4 days. An exception to these results is Test 8. In this test, similar procedures were used to construct, pack and saturate the columns. Temperature data for this test indicate that the ice–bearing interface did not encounter the base of the column; however, pore fluid in the column did not convect during freezing.

Water content profiles were used to determine when differential movement of the solvent began. Figure 4.6 shows water content profiles from Test 6. Five of the 7 profiles show a several percent increase in water content within 0.02 m of the column surface. Inspection of the profiles of water content for all 9 of the tests generally shows that these results occurred throughout this investigation in columns capped at the surface and open at the base. Each of the profiles in Figure 4.6 show a slight systematic decrease in water content between 0.02 m and the top 0.1 m of the column surface. The water content profiles do not appear to exhibit features that are associated with the movement of the solute shown in

Figure 4.5. A slight differential movement of solvent should be expected to occur during freezing due to the density difference between brine and ice which results in brine expulsion from the partially frozen region during freezing. The effects of brine expulsion should be reflected in the gravimetric water content profiles and they are reflected in estimates of the systematic uncertainty of the measurements.

Further evidence for a decrease in gravimetric water content due to freezing is the loss of brine that was expelled from the base of the column during freezing. The contents of the expansion reservoir in the heated chamber were weighed and analyzed when a column was removed from the freezing apparatus so that the mass of fluid expelled from the column could be calculated and the salinity of the fluid could be measured. Table 4.5 presents the mass and salinity of the fluid in each expansion reservoir at the time a column was removed from the freezing apparatus. The salinity of this solution is presented in Figure 4.5 as the unconnected points at the base of the bulk salinity profile.

Temperature profiles were used to determine how the heat transfer and phase change was coupled to the distribution of the solute in the columns. Figure 4.7 shows profiles of temperature at the instrumented column at the time each column in Test 6 was removed from the freezing apparatus. The warming that occurred after the tenth day of freezing when the temperature in the environmental chamber was increased to -1 °C is also evident. Figure 4.7 also shows that the temperature profiles through the interface were smooth and did not exhibit a discontinuity that would occur at a sharp interface between a solid and liquid with appreciably different thermal diffusivities. Figure 4.7 also shows the temperature profiles in the freezing apparatus before and after the onset of convection in the sand columns. The temperature profiles through each of the interfaces after the onset of convection are nearly as smooth as those prior to the start of convection. It appears from Figure 4.7 that with the exception of the last column removed, the temperature gradient through the interface after the onset of convection is slightly increased over the gradient through the interface before the onset of convection.

Figure 4.30 is a three–dimensional time series of temperature profiles measured at the instrumented column during Test 6. This figure shows temperature profiles starting from the thermistor 0.05 m above the top of the column to the base of the column at 0.6 m. It also shows well the warming after the tenth day of freezing.

Fluctuations in temperature profiles near the surface are due to normal temperature fluctuations within the environmental chamber and have an amplitude of ≈ 0.3 °C except during defrost cycles where they may be up to 5 °C. Figure 4.30 shows that temperature fluctuations within the freezing apparatus that could be associated with the onset of convection of the solute within the sand columns were not observed. Similar results have been obtained from each of the 8 other tests.

4.3.2 Calculated Results

Bulk salinity and temperature profiles were used to calculate equilibrium profiles of brine salinity, brine density and volumetric unfrozen brine content in the column using the methods of Section 3.3. Brine salinity was calculated using equation 3.10. Brine density was calculated using equation 3.11. Volumetric brine content was calculated using equation 3.13. Profiles of brine salinity, brine density and volumetric unfrozen brine content from Test 6 are presented in Figures 4.31, 4.32, and 4.33.

Figures 4.31 and 4.32 show that freezing resulted in a decrease with depth of the salinity and density of brine in contact with the ice in the partially frozen region. In each of these figures, the changes are relatively continuous with depth except at the ice–bearing interface where a discontinuity exists due to the disappearance of ice from the pore space. of brine salinity, brine density and brine volume meet. Equilibrium profiles of brine salinity and density are dependent only on the temperature of the partially frozen solution since specification of temperature fixes the salinity of brine in contact with ice. Figures 4.31 and 4.32 do not appear to exhibit any features that could be associated with the convection that began after the fourth day of freezing. The brine volume, however, is a function of the bulk salinity. Figure 4.33 shows that the brine volume decreased in the region affected by convection of the solute and it appears that the curvature of the profiles of brine volume affected by convection are positive while those profiles not affected by convection are negative.

4.3.3 Salt Fingering Experiment

The salt fingering experiment consisted of placing Granusil 30 saturated with 5 ppt NaCl solution which contained Rhodamine B indigo dye over Granusil 30 saturated

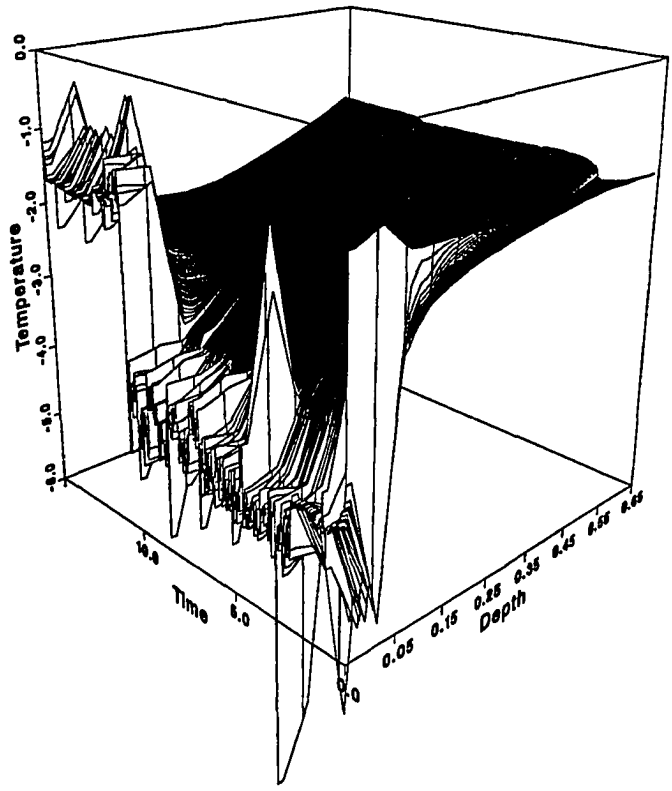

Figure 4.30: Three dimensional plot showing temperature data measured at the instrumented column. Time is measured in days since the start of freezing, temperature in °C and depth in meters.

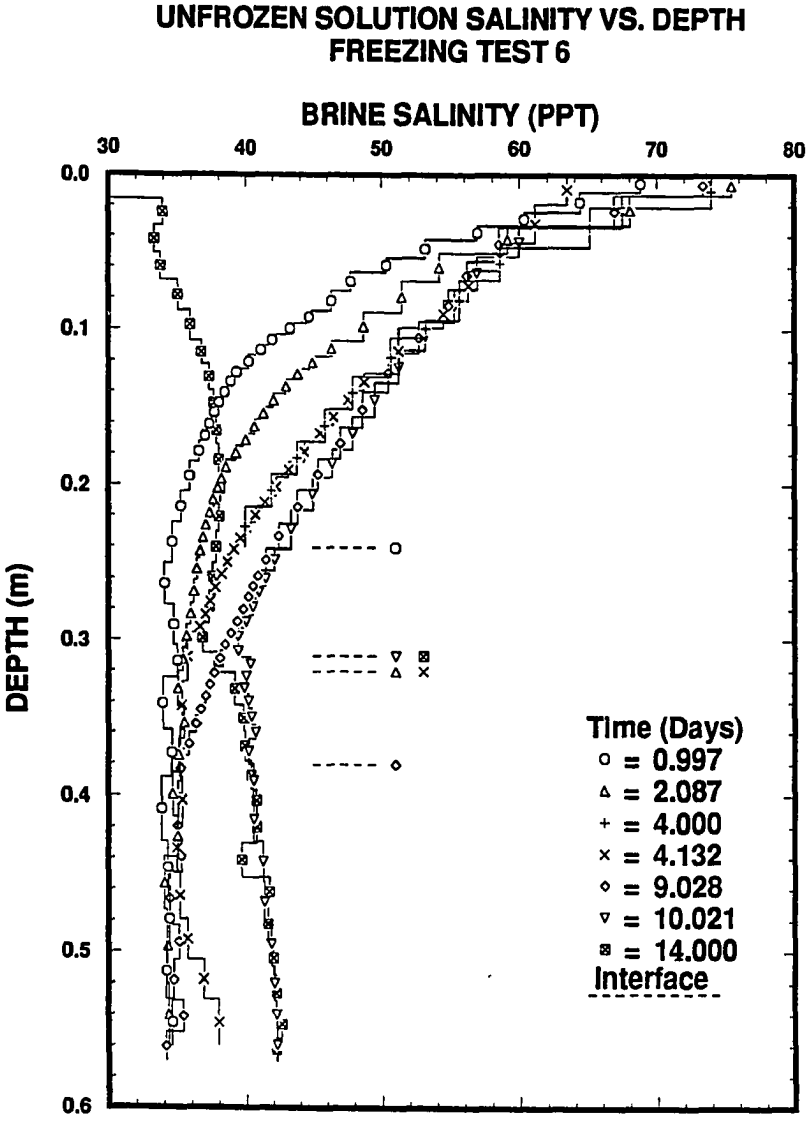

Figure 4.31: Equilibrium brine salinity in the columns of Test 6 at the time they were removed from the freezing apparatus.

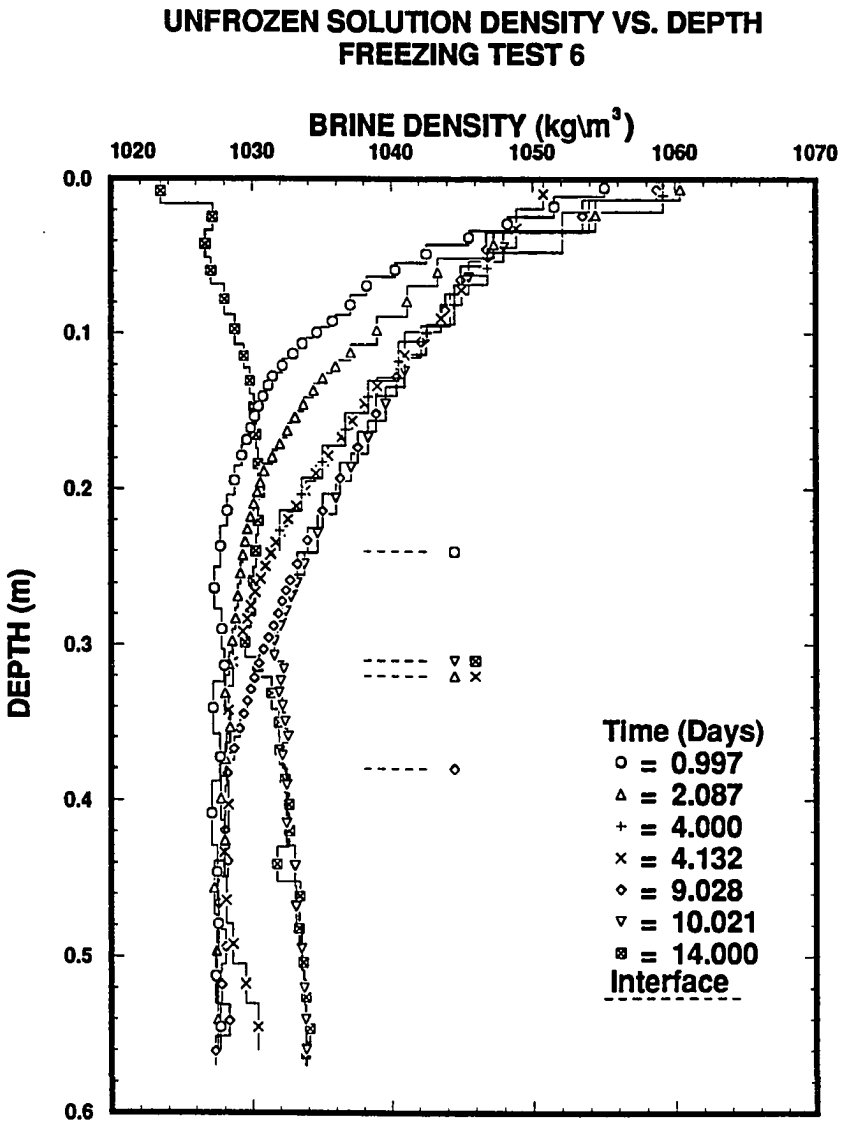

Figure 4.32: Equilibrium brine density in the columns of Test 6 at the time they were removed from the freezing apparatus.

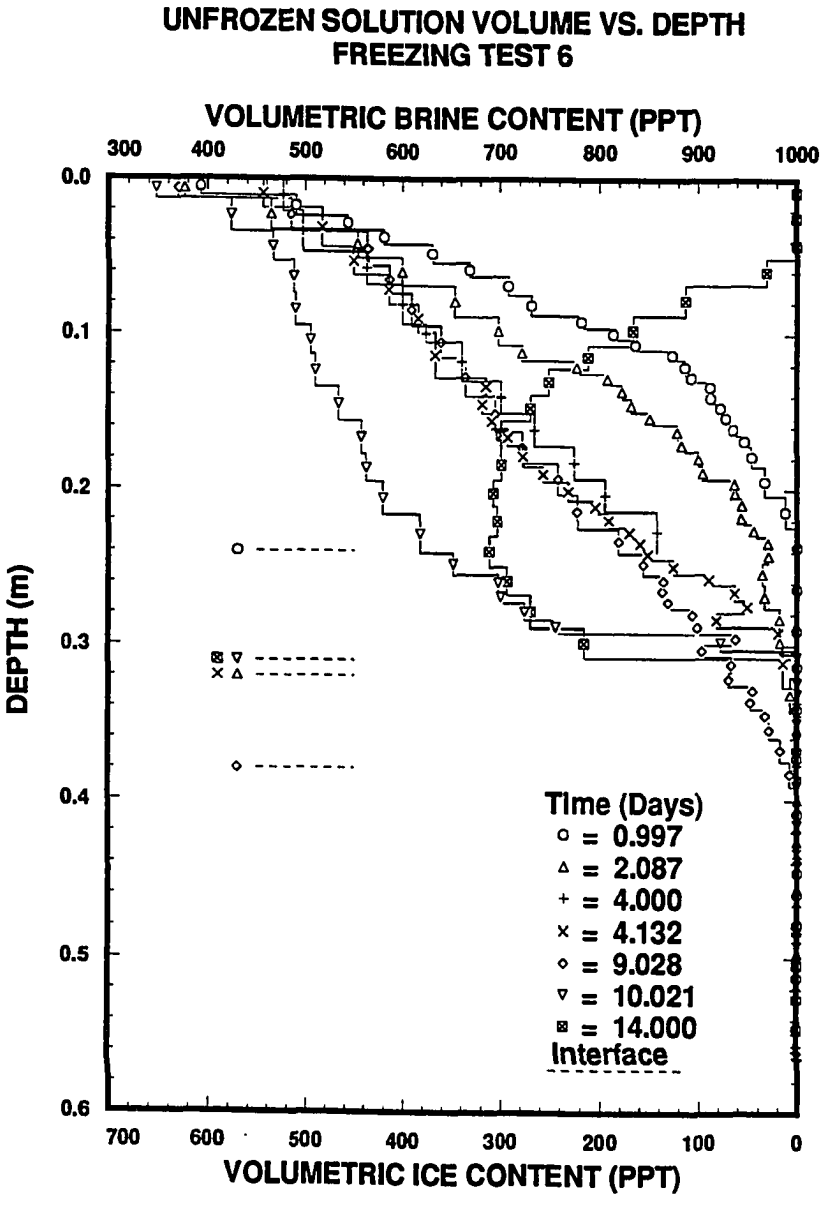

Figure 4.33: Equilibrium volumetric brine content in the columns of Test 6 at the time they were removed from the freezing apparatus.

with distilled water that did not contain dye. Section 2.5 contains the details of this experiment. The results of the salt fingering experiment were similar to the results presented by Baker (1987) and Baker and Osterkamp (1989) except the fingers did not form as quickly as they did in Baker's experiments and the maximum velocity of the fingers was slightly slower than were measured in his experiments. In Baker's experiment, salt fingers began to form several minutes after the cell was inverted. In this test, the fingers began to form approximately 1 hour after the cell was inverted. Velocities of the fingers in Baker's experiment ranged from $1x10^{-2}$ to 0.1 $\frac{m}{hr}$. The maximum velocity of the fingers in this experiment ranged from $1x10^{-2}$ to $3x10^{-2}$ $\frac{m}{hr}$. The growth rate appeared to increase with time in a manner similar to Baker's experiment. The length scale of the fingers was similar to the fingers observed in Baker's experiments.

4.4 Summary

In summary, results of the 9 freezing tests suggest that the effects of convection on the columns may be readily observed only in the bulk salinity profiles. Freezing of the pore fluid does not appear to affect the gravimetric water content profiles except within 0.1 m of the surface of the column. Profiles of water content do not appear to be affected by convection in a manner similar to the profiles of bulk salinity. Results from the bulk salinity measurements suggest that the mechanisms which lead to the redistribution of the solute during freezing are preceded by a transient period of between 4 to 10 days in length. Redistribution of the solvent (water) occurs at the top of the columns, but does not occur in the same location as the movement of the solute by convection. Profiles of temperature, brine salinity and density do not appear to be affected by the onset of convection. Profiles of bulk salinity and brine volume do exhibit the effects of solute redistribution through decreasing values in the area above the ice–bearing interface. Measurements of the rate that solution was expelled from the column base during freezing shows that the flux of brine from the column rapidly decreases after the start of freezing. Observations of the interface between the solid and liquid indicate that it is continuous in that the transition from a solid to a liquid occurs over a relatively large vertical distance instead of a short distance as would occur at a sharp solid–liquid interface. Associated with the continuous interface between the solid

and liquid are three interfaces which increase in depth: the transition interface in which the bondedness decreased significantly, the ice–bonded interface in which the grains were no longer bonded by ice, and the ice–bearing interface. Observations indicate that the bondedness of the sand grains, at a given depth in the column, increased radially inward although often asymmetrically. Asymmetries in the radial bonding of the sand grains were associated with brine movement. Results of the experiment in which horizontal layers of dye were placed in the columns to freeze showed the mode of convection consisted of pore fluid moving down one side of the column and up the opposite side of the column. Bulk salinity measurements indicate that the downward moving pore fluid had a bulk salinity that was 1 to 2 ppt greater than the upward moving pore fluid, and 1 to 8 ppt greater than the middle of the section. Radial asymmetries in the bonding of the sand were associated with the pore fluid movement. Results of the salt fingering experiment in the same cell as used by Baker (1987) suggest that fingers will form for salinity differences much less than those used by Baker (1987) and for density gradients which approach those encountered in the freezing tests of this study. The velocity of the fingers in this experiment were slower and the period between when the cell was inverted and when fingers were first observed was slightly longer than in Baker's experiment.

Table 4.4: A summary of measurements made of portions of sections which exhibited differential movement of the pore fluid during freezing. Direction of the pore fluid movement was determined by the movement of dye in the pore fluid. The column number refers to either the column number 1 of Test 11 which was removed after 11.032 days of freezing or column number 5 which was removed after 7.032 days of freezing. The initial salinity of the sand was 36.3 ppt.

Column Number	Depth (m)	Gravimetric Water Content(%)	Salinity (ppt)
111	0.205–0.227	25.7	30.7 [a]
111	0.205–0.227	25.4	36.5 [b]
111	0.205–0.227	24.5	34.4 [c]
111	0.227–0.248	27.7	30.4 [a]
111	0.227–0.248	25.3	38.5 [b]
111	0.227–0.248	25.1	36.6 [c]
111	0.248–0.269	26.3	34.5 [a]
111	0.248–0.269	25.5	38.0 [b]
111	0.248–0.269	24.4	37.1 [c]
111	0.269–0.290	25.4	36.5 [a]
111	0.269–0.290	25.4	38.3 [b]
111	0.269–0.290	25.1	36.7 [c]
115	0.324–0.342	24.2	35.9 [d]
115	0.324–0.342	23.9	39.1 [e]
115	0.342–0.364	24.9	35.7 [d]
115	0.342–0.364	23.5	39.0 [e]
115	0.364–0.387	24.9	36.4 [d]
115	0.364–0.387	23.8	39.3 [e]
115	0.387–0.405	26.2	37.1 [d]
115	0.387–0.405	23.8	39.7 [e]

[a] Approximate middle port of the section.
[b] Downward moving portion of the section.
[c] Upward moving portion of the section.
[d] Upward moving and middle portion of the section.
[e] Downward moving portion of the section.

Table 4.5: Mass of fluid contained in the expansion reservoir at the time it was removed from the heated chamber.

Column Number	Date Removed (Decimal Date)	Mass Fluid (x10^{-3} kg)	Flux (x$10^{-8}\frac{m}{s}$)	Salinity (ppt)
Column 67	0.997	3.17	0.85	37.0
Column 62	2.087	7.29	1.01	36.2
Column 63	4.000	8.43	0.16	–
Column 65	4.132	13.39	10.1	35.8
Column 64	9.028	16.63	0.18	35.6
Column 66	10.021	19.66	0.82	37.0
Column 61	14.000	17.64	-0.14	37.1

Chapter 5

Interpretation

5.1 Introduction

Observations and experimental results for the freezing conditions used in this investigation indicate that the interface between the solid and liquid in the saline porous material was a diffuse rather than a sharp, ice–bonded interface. A transient period of between 4 and 10 days in length after the start of freezing preceded the onset of convection and the redistribution of solutes. It has been shown that brine expulsion occurs throughout freezing (Baker 1987). However, the majority of expulsion in the columns occurred near the surface of the columns where the temperature changes were largest and was best observed before the onset of convection.

Observations and experimental results of a diffuse interface and the redistribution of the solute by convection are supported by the results of Wilson (1983) and Baker (1987) in which coarse–grained soils saturated with saline solution were frozen. Wilson (1983) showed that the interface between the solid and liquid existed over a vertical distance. He also showed that successful numerical modeling of the phase change heat transfer during freezing required the distribution of solutes through time to be known and the latent heat to be distributed over a range of temperatures. Baker's results (see Figures 3.5 and 3.7 in Baker 1987) shows that the ice–bearing interface was located 1 to 2 centimeters below the ice–bonded interface[1]. Baker (1987) interpreted his experimental results in terms of a gravity

[1]The location of the ice–bearing interface was calculated by comparing the bulk salinity data presented in Figure 3.5 with the temperature data presented in Figure 3.7 of Baker's thesis. The temperature data was used to calculate the brine salinity. The location at

drainage phenomenon and quantified the redistribution of a solute in terms of the steady rejection of the solute from the ice–bonded interface. Baker's results also show that variations in the amount of solute redistribution occur through time during the early stages of freezing.

The experimental results presented in the previous chapter clearly show that the physical processes that lead to convection are fundamentally dissimilar to the assumptions and boundary conditions which form the basis of the BPS theory (see sections 1.2.2 and 1.2.3). The purpose of this chapter is to present an interpretation of the results obtained during the experimental investigation. The second section of this chapter will present an interpretation of the experimental results in terms of the physical processes that occurred during freezing. The third section will present results of theory developed to determine the factors that lead to convection of the pore fluid. The fourth section will develop a method to estimate the maximum amount of solute redistribution due to freezing. The fifth and final section will present estimates of the pore fluid velocities during convection and the flux of the solute that may be expected during convection.

5.2 Interpretation of the Experimental Results

The purpose of this section is to present an interpretation of the experimental results of this investigation in terms of the physical processes that occurred in the sand columns during freezing. This discussion will first focus on the column surface and continue toward the base. Conditions within the column both prior to and after the onset of convection of the pore fluid will be considered. Throughout this section and the remainder of this chapter only the results involving columns frozen with the interface under hydrostatic pressure will be discussed. The majority of the freezing tests were conducted with the interface under a hydrostatic stress. Table 4.2 and the freezing test summaries presented along with the results of each of the freezing experiments in Chapter 4 distinguishes the columns in each test which were frozen under hydrostatic conditions from those that were not. The purpose of this laboratory investigation was to determine the effects of one-dimensional

which the brine salinity is less than the bulk salinity is the ice-bearing interface. Section 4.3.1 and equation 3.10 present methods used to calculate the location of the ice-bearing interface.

freezing under a hydrostatic stress on sands saturated with saline solution. In this investigation, columns which were open on the surface and closed at the base, similar to Baker (1987), were observed to freeze quite differently than one dimensionally and the hydrostatic stress at the interface of these columns was not measured and could not be estimated from the experimental results. Experimental results which were variations of the standard freezing experiments will not be discussed at this time.

5.2.1 Conditions Prior to the Onset of Convection

Conditions prior to the onset of convection in the columns consist of those conditions present after the third column and before the fourth column was removed in Test 6. The third column was removed after 4.000 days of the freezing and the fourth column was removed after 4.132 days of freezing.

Figures 4.5 and 4.6 generally show that freezing resulted in a change in the water content and bulk salinity in the top 0.1 m of the sand columns. Table 5.1 contains results from within the top 0.1 m of Column 65. It shows the increased water content, salt content, and the decreased bulk salinity in the top 0.02 m of the column. Table 5.1 also shows the decreased water content between 0.019 m and 0.081 m of the surface. The several millimeter air gap between the sand surface and the base of the aluminum cap and the low conductivity of the air could result in the larger temperature gradients that were observed at the surface of the columns. Section 4.3 discusses the reasons for the air gap at the sand surface.

Table 5.1: An example of the water content and bulk salinity profiles in the top 0.1 m of Column 65. The initial salinity of the pore fluid was 34.8 ppt.

Depth Range (m)	Water Content (%)	Salt Content[a] (%)	Bulk Salinity (ppt)
0.000 – 0.019	29.5	0.948	31.1
0.019 – 0.044	24.7	0.862	33.2
0.044 – 0.062	26.5	0.934	34.1
0.062 – 0.081	26.7	0.961	34.7
0.081 – 0.099	27.4	1.000	35.2

[a]The ratio of mass of the salt to the mass of the sand, $\frac{M_S}{M_{SL}}$, is defined as the salt content.

Assuming that the water and salt contents and bulk salinity were constant

during freezing, the amount of differential movement of water and salt may be estimated and compared with results presented in Table 5.1. The effect of a pure water layer of thickness δl at the surface of the column on the water content in the section of length l may be estimated with a modified form of equation B.3.

$$W_B(\%) = 100\frac{M_W}{M_{SL}} = 100\left(\frac{\rho_W}{\rho_{dry}} - \frac{1}{\gamma_{qtz}}\right) + 100\frac{\rho_W}{\rho_{dry}}\frac{\delta l}{l} \tag{5.1}$$

where ρ_W is the density of pure water, ρ_{dry} is the dry density of the sand, and γ is the specific gravity of quartz. Table 5.2 shows the effect of differential water movement at the surface of the column for various values of $\frac{\delta l}{l}$ using values of the soil parameters discussed in Appendix B. These values suggest that a pure water layer 3 to 4% of the section thickness could increase the water content at the surface of the column to the observed value in Table 5.1. Taking the thickness of the first section to be approximately 0.02 m suggests that an equivalent layer of pure water, $6\text{x}10^{-4}$ to $1\text{x}10^{-3}$ m in thickness, flows into the first section. Observations were not made of the location of this water layer in the section.

Table 5.2: Calculated changes in the water content and bulk salinity due to the transport of fluid to the surface of the column during freezing. The ratio $\frac{\delta l}{l}$ is the ratio of the thickness of the water layer to the thickness of the section.

$\frac{\delta l}{l}$	Water Content	Bulk Salinity
(%)	(%)	(ppt)
2	28.6	33.8
3	29.3	33.0
4	29.9	32.3
5	30.6	31.7
6	31.2	31.0
7	31.9	30.4
8	32.5	29.8
9	33.2	29.3

The decrease in bulk salinity at the surface of the column due to the transport of pure water into the first section may be estimated using equation 5.1 and the definition of salinity. The bulk salinity of a section of sand and solution can be

expressed as

$$S_B(\text{ppt}) = 1000\frac{\frac{M_S}{M_{SL}}}{\frac{M_W}{M_{SL}} + \frac{M_S}{M_{SL}}} \tag{5.2}$$

$$= 1000\frac{\frac{M_S}{M_{SL}}}{\left(\frac{\rho_W}{\rho_{dry}} - \frac{1}{\gamma_{qtz}}\right) + \frac{\rho_W}{\rho_{dry}}\frac{\delta l}{l} + \frac{M_S}{M_{SL}}} \tag{5.3}$$

Table 5.2 shows that the formation of a water layer 5 to 6% of the section thickness could result in the observed value of the bulk salinity at the surface of the column. In a section 0.02 m thick, this corresponds to a water layer $1\text{x}10^{-3}$ to $1.4\text{x}10^{-3}$ m thick.

Table 5.1 shows the decrease in both the gravimetric water content and bulk salinity within the top 0.1 m of Column 65. Between 0.02 m and $\approx$ 0.1 m of the sand surface, freezing generally resulted in up to a 1.6 ppt decrease in bulk salinity and a 1 to 2% decrease in the water content in the columns except for the region immediately below the top section where the water content decreases by as much as 3% from the initial values. The decrease in water content results from the flux of pure water to the surface of the column and the formation of ice in the fixed volume of the pore space.

The formation of ice in the pore space also results in a decrease in the water content and bulk salinity as both salt and brine are rejected from the pore space during freezing. The decrease in water content associated with partial freezing of the pore fluid may be estimated, neglecting the effects of salt transport, by

$$W_B(\%) = 100\frac{\eta(V_{AU}\rho_U + (1 - V_{AU})\rho_i)}{\rho_{dry}} \tag{5.4}$$

which is a ratio of the mass of brine and ice to the mass of soil. In equation 5.4, η is the porosity, and V_{AU} is the absolute brine volume which is the fractional equivalent of equation 3.12. Equation 5.4 provides only an estimate of the phase change effects on the water content because the mass of the brine is used instead of of the mass of the water. However, the error introduced by this approximation is negligible. Table 5.3 presents calculations for a 35 ppt solution which shows the decrease in gravimetric water content for various brine volumes. It shows that freezing results in a maximum decrease in the water content of 1.3%. The decrease in water content should be greatest in the region near the sand surface where the coldest temperatures are present.

Table 5.3: Decrease in gravimetric water content due to freezing sand saturated with a 35 ppt NaCl solution.

Temperature (°C)	Brine Volume (V_{AU})	Water Content (%)
$T_F = -2.1$	1.00	27.5
-2.2	0.95	27.4
-2.6	0.79	27.1
-3.0	0.68	26.8
-3.4	0.60	26.6
-3.8	0.54	26.5
-4.2	0.49	26.4
-4.6	0.44	26.3
-5.0	0.41	26.2

Since brine expulsion can result in only a 1.3% decrease in the gravimetric water content and the experimental results in Table 5.1 suggest that the water content decreases by up to 2%, flow of water out of the pore space between 0.02 and 0.1 m of the column surface must occur. The effect of this water transport will be most pronounced nearest to the surface of this region where the temperature gradient is large and may be estimated using an expression analogous to equation 5.1

$$W_B(\%) = 100\left(\frac{\rho_W}{\rho_{dry}} - \frac{1}{\gamma_{qtz}}\right) - 100\frac{\rho_W}{\rho_{dry}}\frac{\delta l}{l} \tag{5.5}$$

$$\Delta W(\%) = W_B(\%) - 100\left(\frac{\rho_W}{\rho_{dry}} - \frac{1}{\gamma_{qtz}}\right) = -100\frac{\rho_W}{\rho_{dry}}\frac{\delta l}{l} \tag{5.6}$$

Results of these calculations for the 0.08 m region of reduced water content are presented in Table 5.4. This table shows that a 1 millimeter thick layer of water must be transported to the surface of the column to produce a general 1% decrease in the water content between 0.02 m and 0.1 m of the surface. The thickness in the water layer at the of the column calculated in this manner is similar to the thickness necessary to produce bulk salinity and water content values at the surface of the column.

Results of a brine expulsion model presented by Cox and Weeks (1975) for laboratory grown NaCl ice and by Baker (1987) and Baker et. al (1990) for the frozen columns of saline solution suggests that a 1 ppt decrease in bulk salinity can be expected to occur during freezing. The decrease in the bulk salinity between

Table 5.4: Estimates of the reduction in water content between 0.02 m and 0.1 m due to water transport to the surface of the column. The reduction in water content is for a section 0.08 m in length. The equivalent thickness of the fluid layer, δl, is the amount of water transported from this region.

δl ($mx10^{-3}$)	Change in Water Content (%)
0.4	-0.33
0.8	-0.65
1.2	-0.99
1.6	-1.31
2.4	-1.96

0.02 m and 0.1 m appears to be on the order of 1 ppt which agrees well with the results presented by Cox and Weeks (1975) and Baker (1987).

Interpreting these results which suggest that pure water flowed towards the sand surface during freezing is difficult because it is not clear what physical process drives fluid flow in this region. The potentials which will be examined which could drive this flow include an osmotic potential due to concentration differences and a pressure potential due vertical vapor pressure differences in the brine.

Brine salinity concentration gradients near the surface of the column due to the large vertical temperature gradient results in a large osmotic potential within the brine. Flow in response to an osmotic potential occurs when the movement of ions are restricted relative to that of the water, at a semi–permeable membrane for example. Preferential flow of water has been conjectured to occur in the vicinity of negatively charged mineral surfaces (Hillel 1980) and has been termed a "salt sieving". When the thickness of the water layer approaches the thickness of the diffuse double layer that forms adjacent to charged soil particles, 10^{-10} to 10^{-9} m, then an appreciable degree of restriction of the charged ions can be expected (Hillel 1980) and preferential flow of pure water could occur. In practice, the effects of the diffuse double layer is observed in fine–grained soils where the specific surface area of the soil is large so that the accumulated effect of these double layers becomes great and where the permeability is low so that flow in response to other potentials does not occur. These conditions should also exist in the freezing sand for preferential flow of water to occur during freezing, however, they do not. In a fine–grained soil the specific surface area of the soil ranges from 10^5 to 10^6 $\frac{m^2}{kg}$ while

for Granusil 30 with an average radius of $2.5\text{x}10^{-4}$ m^2 suggests a specific surface area of 10 $\frac{m^2}{kg}$ which is 4 to 5 orders of magnitude smaller than in the fine–grained soil. For the same amount of fluid to flow along the mineral grains in a coarse–grained soil the flow velocities must be 4 to 5 orders of magnitude greater in the coarse–grained soil, or the thickness of the layers that the fluid flows must be 4 to 5 orders of magnitude greater in the coarse–grained soil than in the fine–grained soil. Further, the brine volume in these tests was generally greater than 30% of the pore space which suggests that the liquid layers next to the sand particles were fractions of the pore diameter which may be near 10^{-5} m and not the 10^{-9} m required for preferential water movement to occur in response to the osmotic potential. In short, although an osmotic potential exists in the coarse–grained soils during freezing, it is difficult to conclude that the experimental results, which show that pure water flows to the surface of the column during freezing, occur in response to the osmotic potential.

The transport of pure water in the freezing sand can also occur by vapor transport, however, for this to occur the soil must be unsaturated to allow the vapor phase to exist. It is very difficult to completely saturate a porous medium and evidence exists in Table 5.1 that the top 0.1 m of the column may not be completely saturated at the end of freezing, consequently, it is possible that vapor transport can occur near the surface of the columns during freezing. The diffusive flux of vapor due to a vapor density gradient has been expressed by Hillel (1980) as

$$q_v = -D_v \frac{\partial \rho_v}{\partial x} \tag{5.7}$$

where q_v is the vapor flux, D_v is the diffusion coefficient of water vapor in the soil and ρ_v is the density of the water vapor. Equation 5.7 may be rewritten with the chain rule to make explicit the temperature dependency of the vapor pressure

$$q_v = -D_v \frac{d\rho_v}{dT} \frac{\partial T}{\partial x}. \tag{5.8}$$

The vapor pressure of the brine in the partially frozen region may be determined from measurements of the vapor pressure of ice as a function of temperature since the equilibrium freezing temperature of a solution is the temperature that vapor pressure of the solid is equal to the vapor pressure of the liquid. Sturm (1990) formed a least squares fit to the vapor pressure of ice as a function of temperature

which was presented by List (1951) and found that

$$\rho_v(\frac{\text{kg}}{\text{m}^3}) = Ae^{BT} \tag{5.9}$$

where $A = 5.789\text{x}10^{-3}$ and $B = 9.658\text{x}10^{-3}$ and T is the temperature in degrees Celsius. Sturm (1990) also presented a value for the diffusion coefficient of water vapor in air, $D_o = 2.1\text{x}10^{-5}\ \frac{\text{m}^2}{\text{s}}$. Assuming that $D_v = D_o$, although it is probably much smaller and is a function of the soil saturation, and substituting equation 5.9 into equation 5.8 then differentiating gives

$$q_v(\frac{\text{kg}}{\text{m}^2 \cdot \text{s}}) = -1.2\text{x}10^{-8}e^{9.658\text{x}10^{-2}T}\frac{\partial T}{\partial x}. \tag{5.10}$$

Finally, dividing both sides of equation 5.10 by the density of pure water changes the mass flux of water vapor to the volume flux of water due to vapor transport

$$q_v(\frac{\text{m}^3}{\text{m}^2 \cdot \text{s}}) = -1.2\text{x}10^{-11}e^{9.658\text{x}10^{-2}T}\frac{\partial T}{\partial x}. \tag{5.11}$$

Figure 4.7 shows that prior to warming the surface temperature of the freezing apparatus, the average temperature within the top 0.04 m was -4.5 °C and the average temperature gradient was 25 $\frac{^\circ\text{C}}{\text{m}}$. Substituting these into equation 5.11 provides an estimate of the equivalent amount of water transported by vapor through the column and suggests that $q_v = 1.9\text{x}10^{-10}\ \frac{\text{m}}{\text{s}} = 1.64\text{x}10^{-5}\ \frac{\text{m}}{\text{day}}$. The experimental results suggest that approximately 1 millimeter of water must be transported in several days. These estimates suggest vapor transport cannot account for the observed water content and bulk salinity profiles within 0.1 m of the column surface even when a value of the vapor diffusivity in air is used.

In summary, the experimental results that show that the independent movement of pure water to the surface of the column during freezing cannot be interpreted using currently available hypotheses on the factors which cause fluid flow in soils during freezing. Fluid flow in response to an osmotic potential was considered as a mechanism for fluid flow, however, the present level of understanding of how this phenomenon occurs in a partially frozen soil suggests that it would not occur in the freezing sands. Vapor transport by diffusion near the surface of the column should occur because it is difficult to achieve 100% saturation in the sand columns. However, an analysis has shown that volume of pure water transported as a vapor is quite small and cannot account for the volume of pure water transported during freezing.

The region below 0.1 m and above the ice–bearing interface has a nearly constant salinity profile prior to the onset of convection. It appears from Figure 4.5 that some of the bulk salinity profiles show slight increases, between 0.5 and 1.0 ppt, in this region. A slight increase in bulk salinity in the column below the area affected by brine expulsion could be expected because brine expelled from a region due ice formation will be of relatively high salinity. In the sand columns, brine expulsion during freezing displaces fluid through the base of the column which may lead to a slight increase in the bulk salinity in the region below that affected by brine expulsion. Uncertainty in each bulk salinity measurement is 0.8 ppt. Consequently, the uncertainty in the bulk salinity measurements does not allow the slight increase in the bulk salinity profiles to be determined with certainty.

Between the ice–bearing interface and the base of the column the bulk salinity and gravimetric water content profiles are essentially constant. Slight variations in bulk salinity and gravimetric water content appear to be random and are due to limitations in the laboratory analysis. However, variations in the water content profiles could be due to differences in the packing of the sand within the column and the loss of water from the sections while they were cut with the bandsaw.

Relatively constant bulk salinity profiles through the ice–bearing interface indicate that the solute strongly affects the heat transfer within the columns (see Section 1.2.3.2 for a discussion). The high concentration of salt within the sand and uniform bulk salinity profiles means that the change in phase of brine to ice occurs over a large temperature range i.e., the solute strongly affects the heat transfer over a large temperature range. The high concentration of salt within the sand and initial temperatures that were generally within 0.6 °C of freezing means that temperature changes within the column associated with the surface temperature decrease moved through the sand more quickly than they would if the concentration of salt were low since only a fraction of the latent heat is evolved from a solute rich pore fluid. For example, the ice–bearing interface moved 0.24 m during the first 24 hours of Test 6 (initial salinity of 35 ppt), but only 0.12 m during the first 24 hours of Test 13 (initial salinity of 1 ppt) for approximately similar temperature boundary conditions.

In summary, the interpretation of the conditions and processes occurring within the sand columns prior to the onset of convection shows that redistribution of the solute during freezing was minimal. A small amount of flow to the column

surface supports a decrease in bulk salinity and an increase in the water content within the first section of the column, typically 0.02 m of the surface. Between 0.02 m and 0.1 m below the surface brine expulsion leads to a decrease in bulk salinity of approximately 1 ppt and a decrease in the gravimetric water content of approximately 1.3%. Fluid flow to the surface of the column leads to an additional slight, <1 ppt, decrease in the water content within this region, however this is mainly located near the surface of the column. These results have shown that the presence of the solute strongly affects heat transfer during freezing since the solute concentration is large. The large solute concentration and small difference between the initial temperature and freezing temperature of the solution at the start of freezing means that the ice–bearing interface propagated very quickly through the sand column with less latent heat evolved due to freezing than in the fresh water case.

5.2.2 Conditions After the Onset of Convection

Experimental results have shown that convection of the pore fluid leads to a progressive decrease in the bulk salinity within the partially frozen region, and a progressive increase in the bulk salinity within the thawed region. These results show that for a fixed initial salinity near 35 ppt and variable temperature boundary conditions, the onset of convection of the pore fluid generally occurs between 4 and 10 days after the start of freezing.

The main utility of the freezing apparatus was in the identification of the effects of freezing on the distribution of the solute in the columns and the timing for the onset of convection. Inconsistencies in the data trends in both of these areas suggest subtle changes in the initial or boundary conditions significantly altered the experimental results. For example, Test 6 showed that the first features that could be associated with convection were present in the columns removed after 4 and 10 days of freezing, but not in the column removed after 9 days of freezing. Also in this test, the position of the ice–bearing interface appears to have decreased by 0.07 m between the ninth and the tenth day of freezing. Test 8 showed that convection of the pore fluid does not always occur during freezing even though this test was quite similar in all known respects with Test 7 and the temperature profiles measured during freezing do not indicate inconsistencies that could lead

to the measured results. Results of Tests 6 and 8 suggest that care must be taken when comparing the results from columns that were part of the same freezing test.

After the onset of convection, it is principally the partially frozen region below the area affected by brine expulsion and above the ice–bearing interface that decreases in bulk salinity. This region is characterized by an overall decrease in bulk salinity from the column surface to the minimum bulk salinity which occurs from 40 to 80% of the length from the top of the column to the ice–bearing interface. Above the minimum in bulk salinity, the effects of convection appear to be minimized by a lower brine volume which results in a lowering of the permeability. Below the minimum in bulk salinity, the effects of convection appear to be reduced by similarities in brine salinity between the displaced and displacing fluids. The gravimetric water content does not appear to be affected by the movement of the solute within this region.

The diminished effects of convection in lowering the bulk salinity in the region between the bulk salinity minimum and the thermodynamic interface may be made by drawing an analogy to the dilution of a solution in a constant volume V which initially contains a solution of salinity S and density ρ. Dilution of this solution to a salinity S' with a solution of salinity S'' requires a fraction of the volume to be replaced which may be calculated from the change in the mass of salt in the control volume. The initial mass salt in the system is ρVS, the final mass salt is $\rho' VS'$, and the solution used to dilute the original solution is $\rho'' V'' S''$. The volume fraction that must be replaced to attain the final solution may be expressed as

$$\frac{\delta V}{V} = \frac{\rho' S' - \rho S}{\rho'' S'' - \rho S}. \tag{5.12}$$

Equation 5.1 shows that the fraction of the volume which must be replaced to obtain the final salinity becomes unbounded as the salinity of the displaced and displacing fluid approach each other. A reduction in bulk salinity in the partially frozen column due to convection occurs by a similar process except the process of dilution does not occur in a constant volume in the partially frozen sand.

In the partially frozen portion of the column, the brine salinity and density in equilibrium with ice are determined by the local temperature. During convection it has been observed that fluid from the thawed region displaces fluid from the partially frozen region. A warmer displacing fluid from below equilibrating with its colder surroundings leads to ice formation in the pore space which increases

the brine salinity to match the salinity specified by the local temperature. Return flow to the thawed region removes salt from the partially frozen region and leads to the progressive redistribution of the solute from the partially frozen region to the thawed region.

The analogy to the constant volume dilution experiment presented above may be drawn from the differences in brine salinity necessary to effectively reduce the bulk salinity. If the displacing and displaced brine are very close in salinity, i.e. have similar temperatures, then the amount of ice that must form as the fluid equilibrates with its new surroundings is minimal. As the temperature differences between displaced and displacing fluids increases, so does the diluting effect of convection. Such a result would suggest that the minimum in bulk salinity should occur where the temperature gradients are largest which is at the surface of the column. However, superimposed on this situation is the effect of changes in the permeability of the partially frozen soil. Darcy's law shows that, for a given flow, the pressure gradient necessary to maintain a constant discharge increases as the temperature decreases. Since permeability depends strongly on temperature (equation A.1) and the density gradient which drives the flow is proportional to the temperature gradient, as the permeability of the partially frozen sand decreases, the temperature gradient necessary to drive the flow must increase. It appears from these considerations that the minimum in bulk salinity occurs at a location where both the partially frozen permeability and temperature gradient are relatively large. Above the minimum in bulk salinity the lowered permeability implies that a larger temperature gradient is necessary than is available to drive convection and the flow of fluid by convection is diminished. Small temperature gradients in the region below the minimum in bulk salinity lead to similar temperatures in the brine which reduces the effectiveness of convection as a means for decreasing the solute concentration in the sand.

Figure 5.1 supports these arguments by showing that the largest rate of change in bulk salinity during Test 6 occurred where both the brine volume and temperature gradient were moderately large. Figure 5.1 shows that the decrease in bulk salinity occurs at a rate up to $1.5\text{x}10^{-4}$ $\frac{\text{ppt}}{\text{s}}$ for temperature gradients between 2 and 10 $\frac{^{\circ}\text{C}}{\text{m}}$. However, a large scatter exists in the data which makes it difficult to draw relationships between the rate of change in bulk salinity, brine volume and temperature gradient. Baker (1987) showed that decreases in the bulk salin-

ity within the sand columns occurred at rates of up to $2.5x10^{-5}$ $\frac{ppt}{s}$ for constant freezing rates of $5.8x10^{-8}$ $\frac{m}{s}$ and temperature gradients greater than 50 $\frac{°C}{m}$. His results show that for a given brine volume, the larger the temperature gradient, the greater the rate of bulk salinity decrease due to brine drainage. Cox and Weeks (1975) showed that decreases in the bulk salinity within salt ice occurred at rates which were less than $1x10^{-4}$ $\frac{ppt}{s}$ for temperature gradients that were less than 120 $\frac{°C}{m}$. In general, their results show that for a given brine volume, the greater the temperature gradient the greater the rate of decrease in bulk salinity. Both Cox and Weeks (1975) and Baker (1987) show that the bulk salinity did not change for brine volumes less than 50 ppt. In this investigation, the bulk salinity decreased at the lowest brine volume encountered (300 ppt), however, at a reduced rate.

The role of the temperature and temperature gradient on the amount of solute redistribution was investigated in Test 9, Figures 4.14 thru 4.16. In this test, 35 ppt solution was frozen under a cooler surface temperature and a warmer base temperature than the other tests conducted with an initial salinity of 35 ppt. Large differences between the surface and base temperatures resulted in temperature gradients that ranged 10 to 30 $\frac{°C}{m}$ during freezing. In this test, the region between the bulk salinity minimum and the ice–bearing interface was quite small due to the large temperature gradients and the minimum bulk salinity was lower than in the other freezing experiments. The interpretation of this test is that the larger gradients allowed more dilution of the brine to occur during convection due to the relatively large differences in brine salinity between the displaced and displacing fluids.

In all 9 of the freezing tests, the region below the ice–bearing interface was thawed extending to the base of the column. Prior to the onset of convection the bulk salinity profile in this portion of the column was constant. After the onset of convection the bulk salinity profile in the thawed section of the column increased with depth indicating that it was density stable. Bulk salinity gradients in the thawed layer after the onset of convection indicated that brine from the partially frozen region reaches the base of the column without mixing with fluid in the thawed region. This statement is supported by observations made during Test 11 that showed pore fluid containing dye extended down one side of the column, through the thawed layer, to the base of the column.

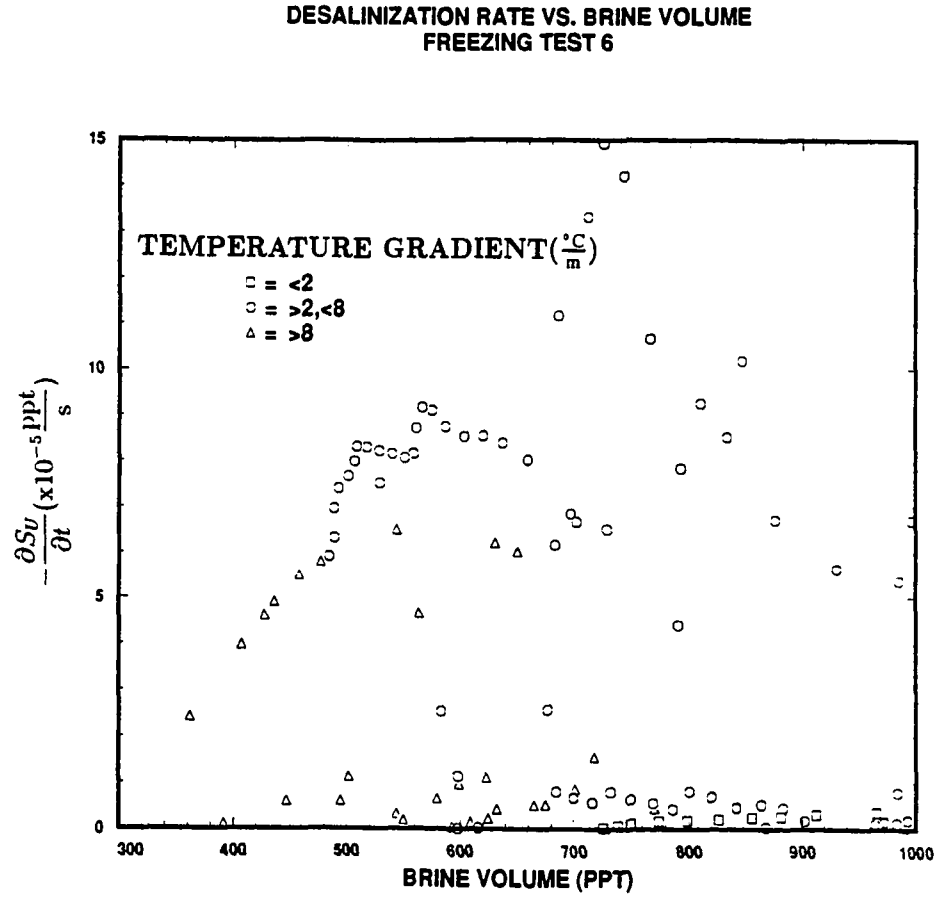

Figure 5.1: Rate of change in bulk salinity vs time for the gradients listed during Test 6. These data indicate that locations of a large temperature gradient and small brine volume or a small temperature gradient and large brine volume are where rapid desalinization in the sand column occurs. The highest rate of change in bulk salinity occurs where both the brine volume and temperature gradient are moderate.

In summary, transient convection of the pore fluid due to the unstable density gradient generated by freezing results in the redistribution of the solute from the partially frozen portion of the column to the base of the thawed portion of the column. Convection only redistributes the solute, the water content does not change significantly due to convection. Variations in brine volume and temperature gradient lead to a minimum in bulk salinity between 40 to 80% of the length from the top of the column to the ice–bearing interface. Below the ice–bearing interface, the pore fluid is density stable which suggests that it is modified by convection. Several inconsistencies in the experimental results obtained during this investigation bring into question the utility of this particular experimental apparatus as a means for monitoring the redistribution of a solute during freezing.

5.3 Stability of a Freezing Viscous Fluid in a Vertical Tube

The observations and measurements presented in Chapter 4 demonstrated that solute redistribution during freezing is a transient phenomena, and that the redistribution of the solute is due to convection of the pore fluid. This suggests that a steady state, diffusive, salt rejection model is not useful in describing the results obtained in this investigation. However, in sea ice research such a model can be used to describe the redistribution of a solute during freezing, although, in this case the physical processes also do not match the assumptions used in the mathematical model. The experimental results of this investigation have shown that for a model to successfully describe the processes leading to the redistribution of a solute in columns of sand during freezing, the effects of convection of the pore fluid in the partially frozen portion of the column must be included.

In the absence of potentials other than the gravitational potential during freezing, it is clear that the effect of gravity on the density gradient in the partially frozen region leads to convection of the pore fluid. However, the location of the instability is not known and the role of the thawed layer below the partially frozen region in determining the stability of the fluid in the column is not understood. The purpose of this section is to develop a stability criterion for the brine in the partially frozen portion of the column and to apply this criterion to the freezing experiments. Although the experimental results suggest that the presence of

the thawed layer below the partially frozen layer is important in determining the stability of the fluid in the column, the development presented here is for a system in which there is no coupling of the pore fluid in the partially frozen region with the pore fluid in the thawed region. Such a coupling is necessarily complex, two-dimensional and could not be developed analytically.

In the sand used in these freezing experiments, it will be assumed that the mineral grains do not affect the phase relations of the fluid (see Section 1.2.2 for a justification of this assumption). Phase relations for aqueous NaCl solutions show that the density gradient of the brine due to freezing a solution with a bulk salinity of 35 ppt (Weast 1976, Baker 1987) may be written as

$$\begin{aligned} \frac{\partial \rho_U}{\partial x} &= \frac{\partial \rho_U}{\partial T}\frac{\partial T}{\partial x} \\ &= \left(\frac{d\rho_U}{dS_U}\frac{dS_U}{dT} + \frac{d\rho_W^{pure}}{dT}\right)\frac{\partial T}{\partial x} \approx \frac{d\rho_U}{dS_U}\frac{dS_U}{dT}\frac{\partial T}{\partial x} \\ &\approx -13\ \frac{\mathrm{kg}}{\mathrm{m}^3 \cdot {}^\circ\mathrm{C}}\frac{\partial T}{\partial x}. \end{aligned} \tag{5.13}$$

The change in the density of pure water with temperature is approximately -3.3x10^{-2} $\frac{\mathrm{kg}}{\mathrm{m}^3 \cdot {}^\circ\mathrm{C}}$ (Weast 1976) which is two orders of magnitude smaller than the density of change of brine with temperature and will be neglected. The change in density of brine with temperature was calculated from the phase relations for sodium chloride presented in Section 3.3.3, equations 3.10 and 3.11.

In Chapter 4, it was shown that the mode of the instability leading to convection consists of pore fluid on one side of the column moving up and pore fluid on the opposite side moving down, which is similar to the instability quantitatively described by Wooding (1959) for a homogenous porous material in a vertical tube saturated with fluid. The similarity between the instability described by Wooding and the form of convection in the columns suggests that a similar stability analysis, suitably modified to include the effects of a variable permeability, could properly describe the system in partially frozen columns of sand. The stability analysis should also consider the effects of brine expulsion which results in a throughflow velocity flux which may be either stabilizing or destabilizing to the system depending on the flow direction[2]. Such a stability analysis would allow the role of

[2]In columns open at the surface and closed at the base brine expulsion occurs towards the surface of the column. In columns closed at the surface and open at the base brine expulsion occurs through the base of the column.

the density gradient in the partially frozen sand to be examined as well as to determine the effects, if any, of brine expulsion on the stability of the fluid in the column.

Appendix A presents a development of the stability criterion for the partially frozen sand with a variable permeability and a small throughflow velocity. The permeability of the partially frozen sand was calculated using an experimentally determined relationship for a solidifying metallic binary alloy. With the exception of the effects of a variable permeability and throughflow on the system, the development presented in Appendix A is analogous to the development presented by Wooding (1959). Neglecting, for now, the effect of a throughflow, the criterion for stability of fluid in a partially frozen column may be written as

$$3.390 \geq \frac{k_o(1+\gamma(T-T_F))b^2C_f}{\alpha_m \eta V_{AU}\mu}\frac{dT}{dx}\rho_o\beta g \qquad (5.14)$$

where k_o is a reference permeability, γ is the temperature coefficient for the permeability, T_F is the freezing temperature, b is the tube radius, C_f is the heat capacity of the fluid, ρ_o is a reference density, β is the temperature coefficient for the density, g is the gravitational acceleration, α_m is the thermal conductivity of the medium, η is the porosity, V_{AU} is the absolute brine volume, and μ is the viscosity. The left hand side of equation 5.3 is the Rayleigh number for stability of fluid in the vertical tube. The right hand side of equation 5.3 is the derived Rayleigh expression for the fluid in the partially frozen portion of the column. Although, the effect of temperature on permeability is non-linear, in this development it has been linearized throughout the temperature range to make the problem solvable over the entire length of the column. In general, the permeability must be linear only in the neighborhood of the point under consideration which leads to the generalization

$$3.390 \geq \frac{\bar{k}b^2C_f}{\alpha_m \eta V_{AU}\mu}\frac{dT}{dx}\rho_o\beta g \qquad (5.15)$$

where $\bar{k}$ is the average permeability.

Application of equation 5.4 to the results of the freezing experiments may be used to determine the utility of this theory as a means for predicting the stability of the pore fluid in the freezing columns. Without *a priori* knowledge of the location of the instability within the partially frozen region, it may only be assumed that it is located in the region with the largest Rayleigh number. Measured

values for the Rayleigh number, λ, may be obtained from the temperature profiles prior to the onset of convection to determine whether the interface is stable to small perturbations. Timing for the onset of convection was bracketed from data obtained in the bulk salinity analysis in each column since the presence of convection was not evident in the temperature profiles which were obtained on a continuous basis. In Test 6, convection started between day 4 and day 4.13, the temperature gradient at isotherms of -2.15, -3.1 and -3.5 °C were 2.4, 9.0 and 10 $\frac{°C}{m}$ respectively (Figure 5.2). Temperatures of -2.15, -3.1, -3.5 °C correspond to fractional brine volumes of 0.97, 0.7 and 0.6 respectively for an initial salinity of 35 ppt. The permeability of the partially frozen sand, $\bar{k}$, at these temperatures will be taken as $6.4\text{x}10^{-11}$, $6.6\text{x}10^{-12}$ and $2.2\text{x}10^{-12}$ m^2 as determined from equation A.1. The remaining parameters in equation 5.4 will be taken as: $\mu = 1.8\text{x}10^{-3}$ $\frac{kg}{m \cdot s}$ and $C_f = 4.1\text{x}10^6$ $\frac{J}{m^3 \cdot °C}$ (Cox and Weeks 1975), $\alpha_m = 1.4$ $\frac{W}{m \cdot °C}$ (Lunardini 1981), and measured values of $\eta = 0.4$, $b^2 = 1.33\text{x}10^{-3}$ m^2. Substitution of the measured temperature gradient and the above thermal parameters into equation 5.4 yields values for λ near the start of convection which are $1.1\text{x}10^{-1}, 3.3\text{x}10^{-2}, 1.1\text{x}10^{-2}$ for the three temperatures. These values range from 1 to 2 orders of magnitude less than the theoretical Rayleigh number of 3.390 presented in equation 5.4 with the largest value occurring in the partially frozen region near the ice–bearing interface.

The analysis performed on the temperature data in Test 6 was performed on each of the eight other freezing tests to calculate the Rayleigh number within the columns near the onset of convection for the thermal conditions presented above. The results of these calculations are presented in Table 5.5 and show that in general the Rayleigh number is at least an order of magnitude less than the theoretical value. These results also show that the largest value for the Rayleigh number consistently occurs near the ice–bearing interface.

Uncertainty in the thermal and physical parameters of the partially frozen soil needs to be considered because of the effect of parameter uncertainty on the measured value of the Rayleigh number. Possible sources of random uncertainty accounting for the order of magnitude difference between the measured and theoretical Rayleigh numbers include variations in the permeability and the thermal conductivity of the medium. The relationship between brine volume and permeability is not a consideration because results of the analysis suggest that the

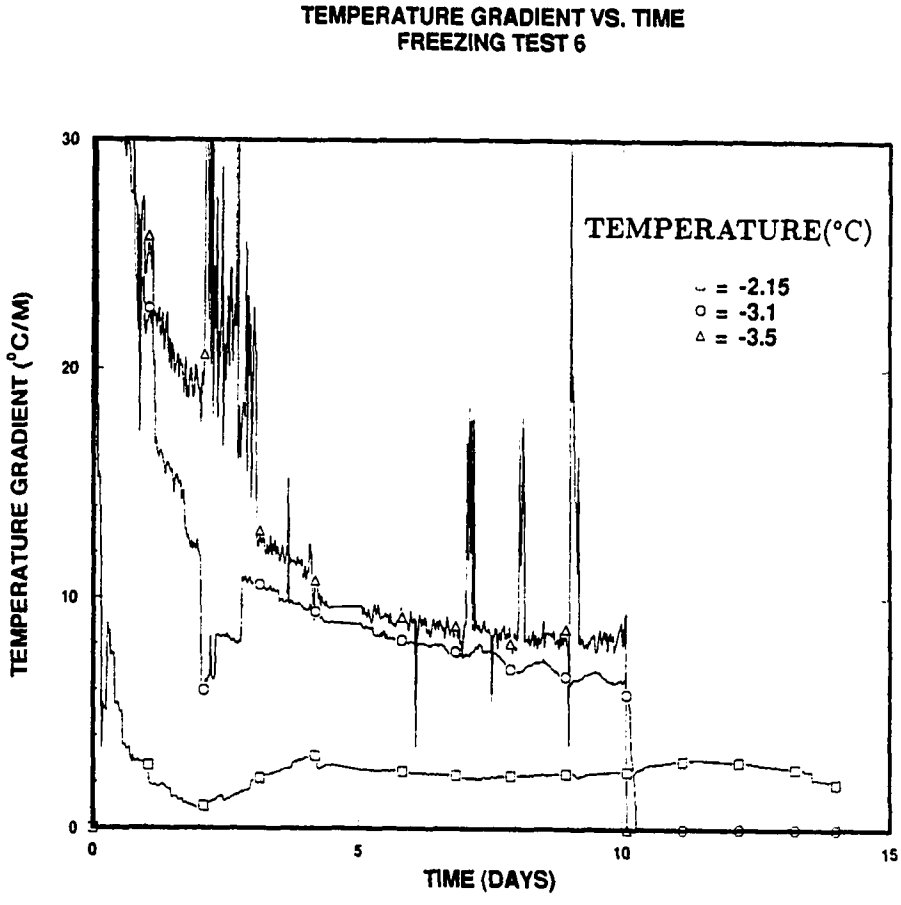

Figure 5.2: Temperature gradient as a function of time at isotherms of -2.15, -3.1 and -3.5 °C. These gradients were determined for Test 6 and were obtained at the instrumented column using the measured temperatures and thermistor spacings.

Table 5.5: Temperature gradient and Rayleigh number for each of the nine freezing tests near the onset of convection. Values for λ were calculated for the gradients measured at isotherms in the the column with temperatures of -3.5, -3.1 and -2.15 °C.

Test #	Time (days)	Gradient ($\frac{°C}{m}$)			Rayleigh Number (λ)			Convection (?)
		Temperature (°C)			Temperature (°C)			
		-3.5	-3.1	-2.15	-3.5	-3.1	-2.15	
5	7.96	4.8	4.1	4.2	$1.3x10^{-3}$	$2.8x10^{-2}$	$2.0x10^{-1}$	yes
6	4.13	10.	9.0	2.4	$1.7x10^{-2}$	$4.7x10^{-2}$	$1.1x10^{-1}$	yes
7	5.00	4.8	4.1	3.3	$1.3x10^{-2}$	$2.8x10^{-2}$	$1.6x10^{-1}$	yes
8	6.09	9.2	9.2	4.8	$2.4x10^{-2}$	$6.2x10^{-2}$	$2.2x10^{-1}$	no
9	5.96	23.	23.	23.	$6.1x10^{-2}$	$1.6x10^{-1}$	1.1	yes
10	7.12	6.5	5.8	.92	$1.7x10^{-2}$	$3.9x10^{-2}$	$4.4x10^{-2}$	no
11	4.04	21	7.5	5.5	$5.5x10^{-2}$	$5.1x10^{-2}$	$2.6x10^{-1}$	yes
12	3.96	–	–	7.0	–	–	$2.4x10^{-1}$	no
13	11.17	3.0	3.0	2.5	$1.4x10^{-2}$	$2.0x10^{-2}$	$1.2x10^{-1}$	no

measured Rayleigh number would be too small by at least a factor of 10 even if the thawed permeability were used in the calculations. Laboratory permeability measurements varied by only a maximum of 50% for maximum variations in dry density of 3%. Tabulated thermal conductivity values (Lunardini 1981) are typically accurate to better than 25% (Farouki 1982). However, the value for the thermal conductivity used in this analysis was the lower limit of the values presented by Lunardini (1981) in order to obtain slightly conservative values for the calculated Rayleigh number. Possible sources of systematic uncertainty include variations in the permeability between the sand in the columns and the sand in the permeameter. Differences in packing of the sand in each case would be the source of this uncertainty. However, the dry density of the sand in the permeameter deviated a maximum of 4% from the dry density of the sand in the columns. In short, even allowing for the maximum uncertainty in the Rayleigh number, which could be on the order of 100%, the measured Rayleigh number is still too small and cannot be used to predict the timing for the onset of convection.

Results from this analysis suggest that the Rayleigh number calculated near the onset of convection in the partially frozen columns cannot be used to time the onset of convection in the columns. The measured Rayleigh number appears to

be too small even when liberal estimates in the uncertainties in the thermal and physical parameters are taken into account. The result of the analysis presented in this section is that the density gradient in the partially frozen region does not directly lead to convection in the columns. However, it is still believed that the phase relations between brine and ice within the partially frozen region lead to convection of the pore fluid in the column. Although it is only speculative, the preliminary interpretation drawn from this analysis is that the instability which leads to convection in the columns is due to the unstable density gradient in the partially frozen region, but the location where the instability forms is in the thawed region below the ice–bearing interface.

For viscous fingers to form in a partially frozen soil the dissipating effects of viscosity and thermal diffusion must be overcome. However, for fingers to form in the thawed soil the dissipating effects of viscosity and molecular diffusion must be overcome. Molecular diffusion occurs at a rate 1 to 2 orders of magnitude less than the rate of thermal diffusion which implies that the density gradient necessary for the formation of viscous fingers in the thawed sand is much less than in the partially frozen sand. As oscillations in the growth rate of the instability within the partially frozen sand increase in both magnitude and frequency, which they will do as the temperature gradient increases (the imaginary part of the growth rate parameter, equation C.29, for example), perturbations will extend from the partially frozen region, through the ice–bearing interface, into the thawed region. Once in the thawed region, for fingers to grow they must overcome the much reduced damping forces of viscosity and molecular diffusion. The preliminary interpretation presented implies that the presence of both the partially frozen and thawed regions must be considered to calculate a theoretical Rayleigh number for the columns. This preliminary conclusion is consistent with the experimental observations that a thawed layer underneath the partially frozen layer is necessary for pore fluid in the column to convect.

A general observation which may be made from Table 5.5 is that a threshold temperature gradient exists above which convection occurs and below which it does not. Temperature gradient data for the tests involving 35 ppt solutions at the ice–bearing interface suggest that convection of the pore fluid generally occurred for temperature gradients greater than 5 $\frac{^{\circ}C}{m}$, and that convection did not occur for temperature gradients less than 1 to 2 $\frac{^{\circ}C}{m}$. If the results of Test 8 are excluded,

the threshold gradient appears to be 1 to 2 $\frac{°C}{m}$.

In summary, Wooding's stability criterion (Wooding 1959) can be used to determine the stability of pore fluid in a saturated porous medium contained within a vertical column. A density gradient within the column greater than the critical gradient is subject to convection of the pore fluid until the gradient in the column is less than a critical value. Experiments in a homogenous column have shown that the criterion developed by Wooding predicts well the stability condition within the column when the horizontal length scale of the convection cell approaches the horizontal length scale of the cylinder (taken to be the radius of the cylinder) (Wooding 1959). Wooding's criterion modified to develop a stability criterion based on the conditions in the partially frozen region of the sand column was presented in this part of the section. It was shown that the modified form of Wooding's criterion does not predict the onset of convection in the columns. This result and the experimental observation that a thawed layer below the partially frozen layer is important for convection to occur leads to the preliminary interpretation that the thawed layer is important in determining the stability of the pore fluid in the freezing columns.

5.3.1 Effect of Throughflow on the Fluid Stability

During the early stages of freezing, transient temperature gradients developed which were several times greater than the temperature gradients present at the onset of convection. Figure 5.2 shows that these large gradients last for 2 to 3 days and that they propagate from the surface towards the base of the column. In light of the previous part of this section, the large temperature gradients near the start of freezing suggest that the pore fluid should begin to convect near the start of freezing rather than later in the freezing experiment. However, this was not the case in these experiments and convection did not occur until after 4 to 10 days of freezing.

The large temperature gradients during the start of freezing are responsible for the rapid propagation of the ice–bearing interface. For example, the summary of Test 6 shows the location of the ice–bearing interface through time. In Test 6 the interface moved 0.24 m during the first 24 hours of freezing and 0.08 m in the next 26 hours. Results of the salt fingering tests, Section 4.3.3, showed that viscous

fingers began to form approximately 1 hour after the cell was inverted. Once the fingers began to form, they moved at a maximum velocity that ranged from 0.4 to $5.8\text{x}10^{-2}$ $\frac{m}{hr}$ with the finger velocity increasing through time during their initial growth. Several possible explanations exist for the lack of finger formation during the first several days of freezing when the temperature gradients were large: electrical potentials generated by freezing act to stabilize the gravitational potential that results from the density gradient; a stabilizing pressure force associated with brine expulsion during freezing that counteracts the large destabilizing pressure force due to the density gradient; and the dynamics of finger growth are such that the interface moves too quickly for the instability to form. The remainder of this section is devoted to exploring possible explanations for the lack of finger formation during the early stages of freezing.

Solutions containing electrolytes of low concentration develop electrical potentials, when frozen, due to preferential incorporation of ions within the crystal structure of the ice (Workman and Reynolds 1950). If these potentials are great enough they can lead to secondary fluid flow. Measurements have been made which suggest that these potentials may be static potentials and on the order of several tens of volts at low electrolytic concentration, but that they become diminished as the concentration increases (Workman and Reynolds 1950, Cobb and Gross 1969, Korkina 1975). Although interstitial voltage differences were not measured in this investigation, measurements on finer–grained soils than the sands used in this investigation and at much lower electrolytic concentrations suggest that these effects are negligible (Korkina 1975).

The flow of brine out of the partially frozen sand during freezing can result in a stabilizing pressure force on the fluid in the pore space due to the pressure gradient required to drive the flow. Appendix A addresses the physical reasons for this stabilizing force. Experiments on the formation of viscous fingers in a porous medium of uniform permeability have shown that the presence of throughflow and contrasts in viscosity can either stabilize or further destabilize an unstable density gradient (Saffmann and Taylor 1958, Wooding 1960, Homsy and Sherwood 1976, Park and Homsy 1984, Homsy 1987, Homsy 1989). Appendix A presents a development of theory which may be used to determine the effect of throughflow on a system of variable permeability. Results of this theory provide a stability criterion analogous to the criterion developed by Wooding (1959) to determine

the stability of a dense fluid overlying a less dense fluid in a porous media with constant physical properties, but with suitable modifications to account for the fact that the density gradient responds to changes in temperature rather than changes in species concentration. Based on the development presented in Appendix A, the stability condition for the brine in the partially frozen column may be expressed as

$$3.390 \geq \frac{\bar{k}b^2 C_f}{\alpha_m \mu \eta V_{AU}} \frac{dT}{dx}\left(\rho_o \beta g - \frac{\mu \gamma W}{\bar{k}}\right). \tag{5.16}$$

The relative importance of the velocity term in equation 5.5 may be determined by comparing it to the gravitational term. Since the gravitational term may be expressed as $\rho_o \beta g \approx O(10^2 \frac{\text{kg}}{\text{m}^2 \cdot \text{s}^2 \cdot ^\circ\text{C}})$, the velocity term in equation 5.5 should be of similar magnitude to affect the stability of the fluid in the column. Taking $\frac{\bar{k}}{k_o} \approx 1$ which is correct near the ice–bearing interface where the Rayleigh number is largest implies a velocity in the positive, downward, direction which must satisfy

$$(10^7 \frac{\text{kg}}{\text{m}^3 \cdot \text{s} \cdot ^\circ\text{C}})W = 10^2 \frac{\text{kg}}{\text{m}^2 \cdot \text{s}^2 \cdot ^\circ\text{C}}. \tag{5.17}$$

This implies that W must be on the order of $10^{-5} \frac{\text{m}}{\text{s}}$ which is approximately 2 to 3 orders of magnitude greater than the discharge velocity observed in Test 6, Table 4.5. Velocities required to make the velocity term comparable to the gravitational term in equation 5.4 are so large that they would invalidate the assumption that the throughflow not advect large quantities of heat and not appreciably affect the distribution of the solute in the soil. Lowering the permeability of the medium to that of a fine silt would increase the relative effect of the velocity term to the gravitational term in equation 5.4. However, it would be necessary for the the temperature gradient to become unrealistically large to drive convection. In short, throughflow due to brine changing phase to ice has a negligible effect on the stability of the system. The partially frozen permeability and the temperature gradient are the two critical parameters required to determine stability of the pore fluid.

In summary, an understanding of the mechanisms which control the dynamics of viscous finger growth in a porous medium is still far from complete. Interpretation of the stability conditions suggests that the small throughflow present during the initial stages of freezing has no effect on the overall stability of the fluid in the column. Since electrical potentials that develop during the freezing of solutions

of concentration used in this investigation are believed to be quite small, it may be concluded that the dynamics of associated with the onset of viscous fingers and the moving ice–bearing interface contribute to the overall stability of the fluid in the column during the early stages of freezing. It is not understood how the moving interface and the dynamics of finger growth promote stability of the fluid during the early stages of freezing.

5.4 Solute Redistribution During Freezing

The purpose of this section is to present a method which can be used to estimate salinity profiles in the partially frozen portion of the column. The first part of this section develops this method and then shows that it may be applicable for fitting bulk salinity profiles. The method is then used to fit the bulk salinity profiles in the partially frozen portions of the profiles affected by convection. The second part of this section uses the method developed in the first part of this section to predict the maximum amount of solute redistribution that can be expected due to freezing.

5.4.1 Development

Figure 4.5 and the other bulk salinity profiles affected by convection generally show a minimum bulk salinity at ≈40 to 80% of the length from the top of the column to the ice–bearing interface. The bulk salinity decreases nearly linearly from the surface of the column to the minimum. In Section 5.2.2 qualitative arguments were presented that suggest bulk salinity profiles in this region are a result of both the permeability of the partially frozen sand and the density gradient due to changes in brine salinity. Since the permeability and density depend on both the temperature and bulk salinity in the sand, simplified forms of the momentum equation and the energy equation will be used to parameterize the bulk salinity in terms of the temperature and temperature gradient.

The one dimensional momentum and energy equation for the partially frozen portion of the column may be written in terms of its average components

$$-\frac{\overline{\partial P}}{\partial x} - \frac{\mu}{\bar{k}}\bar{u} + \bar{\rho}g = 0 \qquad (5.18)$$

$$\left(C_m - L\eta\frac{dV_{AU}}{dT}\right)\overline{\frac{\partial T}{\partial t}} + \frac{C_f}{\eta V_{AU}}\bar{u}\overline{\frac{dT}{dx}} = \alpha_m\nabla^2\bar{T} \tag{5.19}$$

where each of the values are defined in Section 5.3, except for L which is the latent heat of fusion for the salt solution. The inertial term in the momentum equation has been neglected because of the short time constant, $\ll 1$ s, for the acceleration of the pore fluid (Gosink and Baker 1990). The equivalent terms in the energy equation cannot be neglected because pore fluid motion has only a negligible effect on the transport of heat. Curvature of the temperature profiles in the partially frozen region could be associated with either the diffusive heat flux or variations in the thermal parameters with ice content. However, both an order of magnitude analysis and a specific analysis of the the temperature data from Test 6 at day 9.028 of freezing[3] shows that curvature in the profiles is associated with the diffusive heat flux and not with the variations in the thermal parameters. Consequently, this term has been neglected in equation 5.19. The average density used in this analysis will be defined as

$$\bar{\rho} = \rho_o + \rho\beta(T - T_F) \tag{5.20}$$

which is similar to the form given in Appendix A. Utilizing the hydrostatic assumption in equation 5.7 with equation 5.9 removes the pressure term and $\rho_o g$ in equation 5.7. Equations 5.7 and 5.8 may then be used to eliminate the average velocity and the result rearranged in terms of the average permeability and brine volume as a function of the temperature to give

$$\frac{\bar{k}}{V_{AU}} = \frac{\alpha_m\mu\eta}{C_f\rho_o\beta g\overline{\frac{dT}{dx}}}\left(\nabla^2\bar{T} - \frac{1}{D}\overline{\frac{\partial T}{\partial t}}\right) \tag{5.21}$$

where D is an effective diffusivity and is defined as the ratio of the thermal conductivity of the medium divided to the apparent specific heat. Using equation A.1, the permeability may be written in terms of a power of the brine volume. The brine volume is a function of the brine salinity and bulk salinity the fractional brine volume may be expressed as

$$V_{AU} \approx \frac{S_B}{S_U} \tag{5.22}$$

[3]This temperature profile was obtained during the later stages of freezing when the curvature in the profiles was decreasing, see Figure 4.7.

which is analogous to equation 3.13. The temperature-dependency of the brine salinity may be made explicit by substituting into equation 5.11 an approximate expression for the brine salinity

$$S_U \approx \frac{\Delta S}{\Delta T} T = \frac{(0 - 35 \text{ ppt})}{(0 - 2.1°\text{C})} = -16.7\text{T} \tag{5.23}$$

which is valid in the 35 ppt range. Substituting these results into equation 5.10, the bulk salinity in the partially frozen region may be solved in terms of the temperature and the temperature gradient to give

$$S_B \approx \left(\frac{\alpha_m \mu \eta}{C_f \rho_o \beta g}\right)^{\frac{1}{n-1}} \left(\nabla^2 \bar{T} - \frac{1}{D}\frac{\overline{\partial T}}{\partial t}\right)^{\frac{1}{n-1}} \bar{T} \overline{\frac{dT}{dx}}^{\frac{1}{1-n}}. \tag{5.24}$$

The right hand side of equation 5.13 may be further simplified by showing that the heat conduction terms in brackets are relatively constant over the temperature range of interest. Figure 5.3 shows that the two components of heat conduction, the time rate of change of temperature divided by the effective diffusivity and the second derivative of spatial heat conduction, are essentially constant during the 5 day period after the onset of convection and before the temperature in the environmental chamber is increased at day 10. The assumption that both the thermal parameters and the conductive heat transfer terms are approximately constant is reinforced because they are taken to a fractional power in equation 5.24. Taking these values as constants over the temperature range normally encountered in each column leads to the final simplification of equation 5.12.

$$S_B \approx C \bar{T} \overline{\frac{dT}{dx}}^{\frac{1}{n-1}} \tag{5.25}$$

where C is approximately a constant which is the first two terms in brackets on the right hand side of equation 5.13. The unknown, n, has not been bracketed for partial freezing of components of water and NaCl.

The utility of the parameterization of bulk salinity by the temperature and a power of the temperature gradient presented in equation 5.13 may be observed in Figure 5.4 in which $n = 3$. Figure 5.4 shows that columns not affected by convection depend only slightly on the parameterization in the region near the surface of the column which is affected by brine expulsion. This figure also shows that for the two columns with bulk salinity profiles affected by convection the

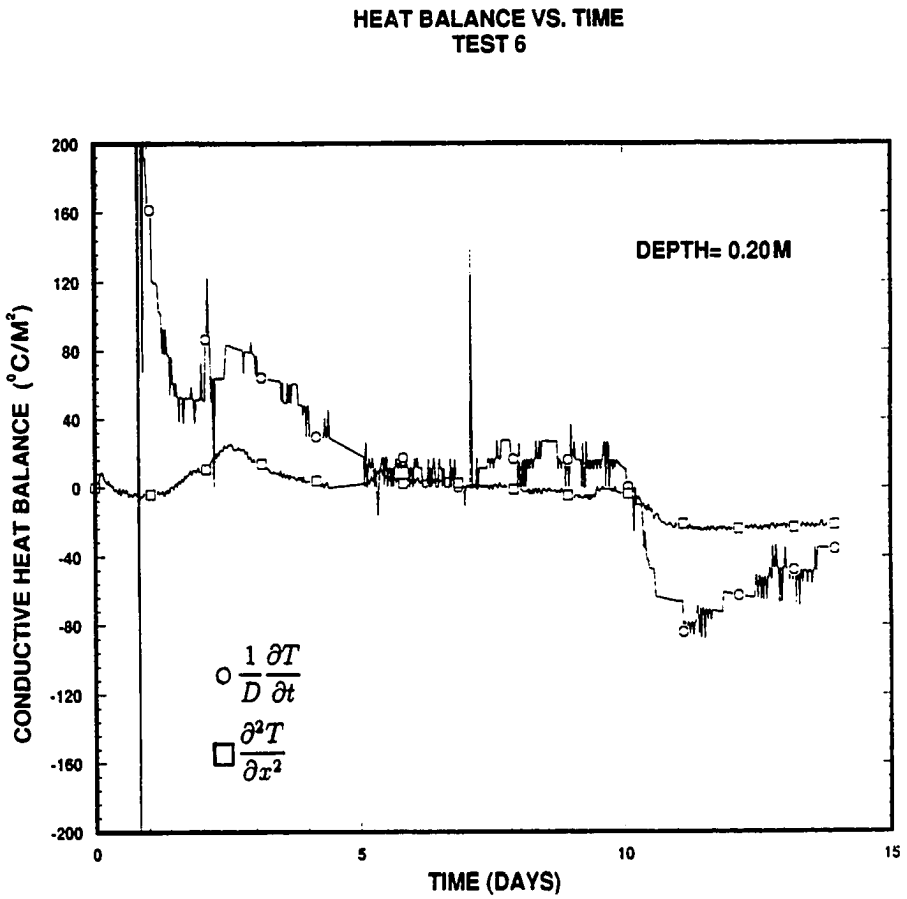

Figure 5.3: Time rate of change of temperature and the diffusion of heat vs. time for Test 6 at a depth 0.20 m below the surface of the column. The similarity between the two curves during convection suggest that they may be taken as constant in equation 5.12. The Thermal parameters used to calculate values for the distributed latent heat are given in Section 5.3.

bulk salinity is linearly related to the parameterization with each profile having similar slopes, or a constant C in equation 5.13. The parameterization does not appear to work well for the portion of the bulk salinity profiles between the bulk salinity minimum and the ice–bearing interface (low values of the temperature and temperature gradient). This region, as has been shown, is affected by the thawed layer.

The parameterization of bulk salinity with the temperature and a power of the temperature gradient, Figure 5.4, shows that changes in bulk salinity within the partially frozen portion of the column may be expressed through the temperature and temperature gradient within the column. Values for C, equation 5.13, which best fit the experimental data in columns affected by convection, were determined by the method of least squares for a given value of n. The best value for n was determined iteratively such that the sum of the squares of the deviation was minimized.

For each profile affected by convection two curves which had the form of equation 5.13 were fit to the data. The first curve was fit from the surface to a depth which was usually ≤ 0.1 m, the second curve was fit from the bottom of the first curve to the minimum in bulk salinity. Depth to the bottom of the first curve was determined by iteration such that the total sum of the squares of the deviation for both curves was minimized. Two curves were fit because they minimized the deviation and the results of Piwonka and Flemings (1966) permeability experiments suggest that at least two discrete values of n exist depending on the brine volume (see Appendix A)[4]. Results of the curve fit for the two profiles affected by convec-

[4]In fine–grained soils where unfrozen water content and freezing point depression are predominantly due to surface effects rather than the presence of a solute, a single value of n has been found to describe the partially frozen permeability reasonably well over a temperature range that is within 1 °C of the freezing point of the soil solution. In these tests the permeability of the soil decreases several orders of magnitude within this temperature range. For examples, see Kay and Perfect (1988). The presence of salt within the freezing solutions used in this study results in appreciable quantities of unfrozen solution to within 5 to 10 °C of the freezing point. Differences between the mechanisms which lead to the unfrozen water in the fine–grained solute free soils and the coarse–grained soils that contain solutes may mean that a single value of n may not adequately describe the permeability brine volume relation. Permeability measurements presented by Piwonka and Flemings (1966) made on a partially solidified binary melt of aluminum that contained 45 ppt copper suggest that at least 2 values of n are necessary to describe the permeability of the binary melt between the freezing temperature and eutectic temperature. Since the H_2O-NaCl system also solidifies as a binary mixture and has a concentration which is

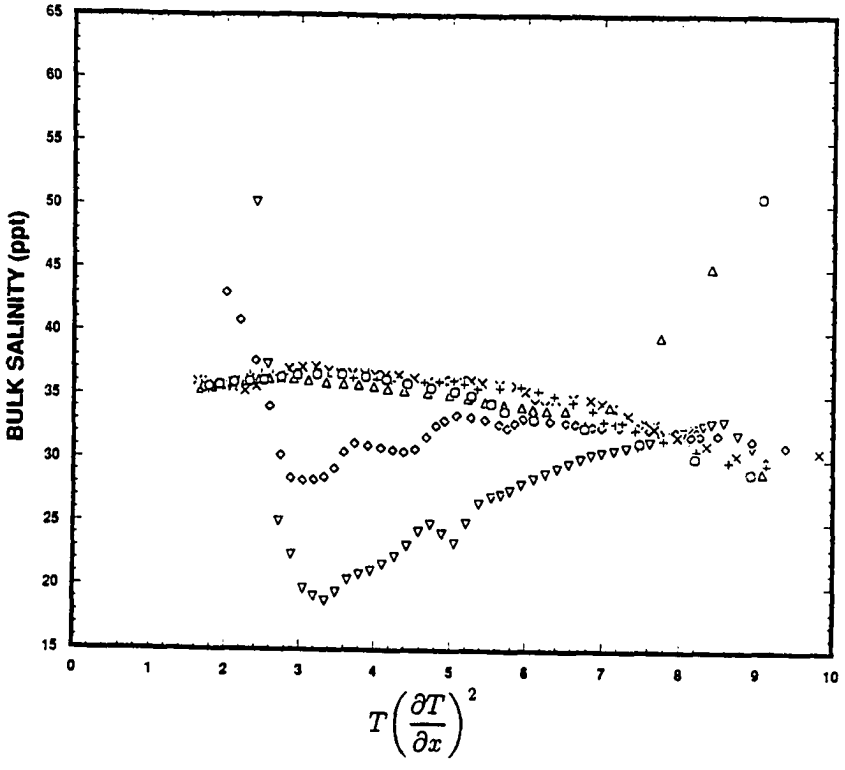

Figure 5.4: Parameterization of the bulk salinity measurements made in Test 9 with the temperature and temperature gradient. In this figure, data near the surface of the column corresponds to large values of the parameterization. The majority of the bulk salinity measurements show no dependence on the parameterization. However, the bulk salinity profiles affected by convection fit the parameterization well and appear to be linear. The slope of the line is equal to the constant C in equation 5.13.

tion in Test 6 are shown in Figures 5.5 and 5.6. Figure 5.7 shows a similar type of curve fit to the data from Test 11. Table 5.6 is a summary of the values of C and n obtained from this fitting procedure. In general, the curves seem to follow the data reasonably well except that they tend to be somewhat over sensitive to the parameterization suggesting that a power relationship exists for the temperature portion of the parameterization.

Table 5.6: Results of the curve fits of the bulk salinity data in the columns affected by convection to equation 5.13. Column 116 was fit with only one curve.

Column Number	Depth Range (m)	C	n
51	0.01–0.04	-54.2	2.01
51	0.05–0.28	-8.68	8.00
53	0.01–0.09	-25.9	2.34
53	0.10–0.20	-23.2	2.60
55	0.01–0.11	-13.0	3.05
55	0.12–0.22	-23.1	2.40
56	0.01–0.08	-8.85	4.40
56	0.09–0.20	-10.3	4.02
61	0.01–0.05	-21.1	4.17
61	0.06–0.24	-12.6	7.02
66	0.01–0.04	-35.1	3.01
66	0.05–0.20	-12.0	7.17
71	0.01–0.10	-13.0	4.99
71	0.11–0.30	-26.6	3.02
91	0.01–0.27	-63.0	2.02
91	0.28–0.40	-80.8	2.01
96	0.01–0.10	-5.51	5.83
96	0.11–0.40	-8.65	2.01
111	0.05–0.05	-20.0	4.56
111	0.06–0.25	-18.4	4.30
116	0.01–0.19	-13.7	6.72

To summarize, in Section 5.2 it was suggested that the bulk salinity profiles within the partially frozen region in columns affected by convection were due to

similar to the Al-Cu system, a generalization of the single value of n to multiple values of n may be necessary to describe the permeability of the partially frozen soil over the large temperature range encountered in this study.

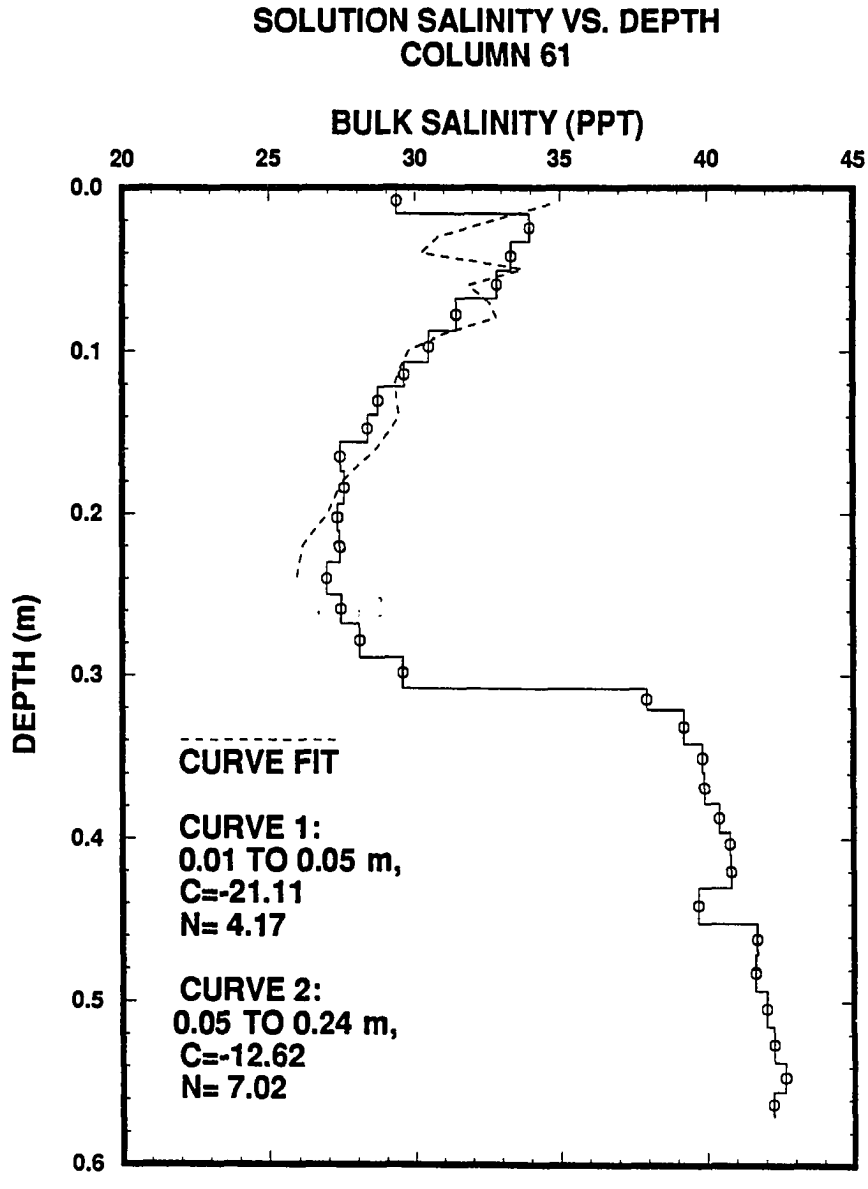

Figure 5.5: Results of a least squares fit to the bulk salinity data in the partially frozen portion of Column 61. The region in which each curve was fit is shown in the figure.

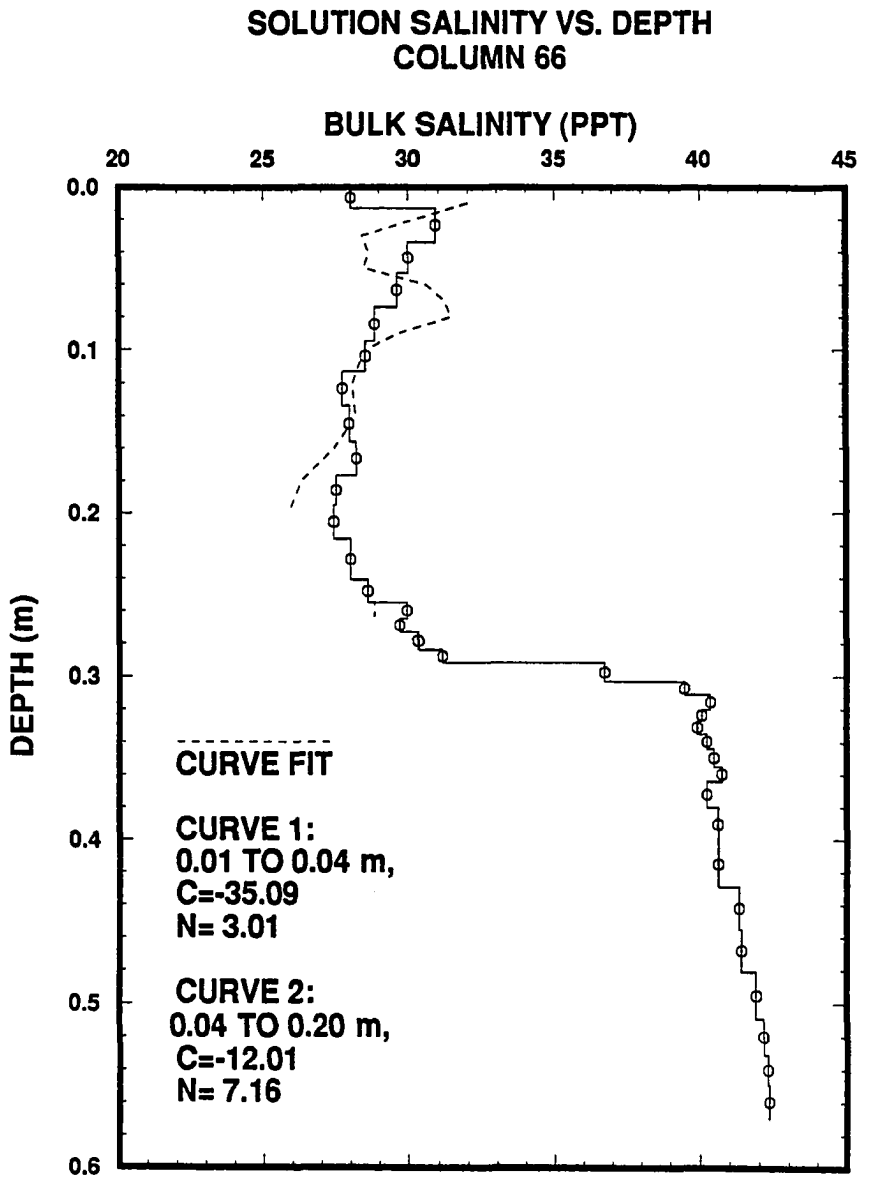

Figure 5.6: Results of a least squares fit to the bulk salinity data in the partially frozen portion of Column 66. The region in which each curve was fit is shown in the figure.

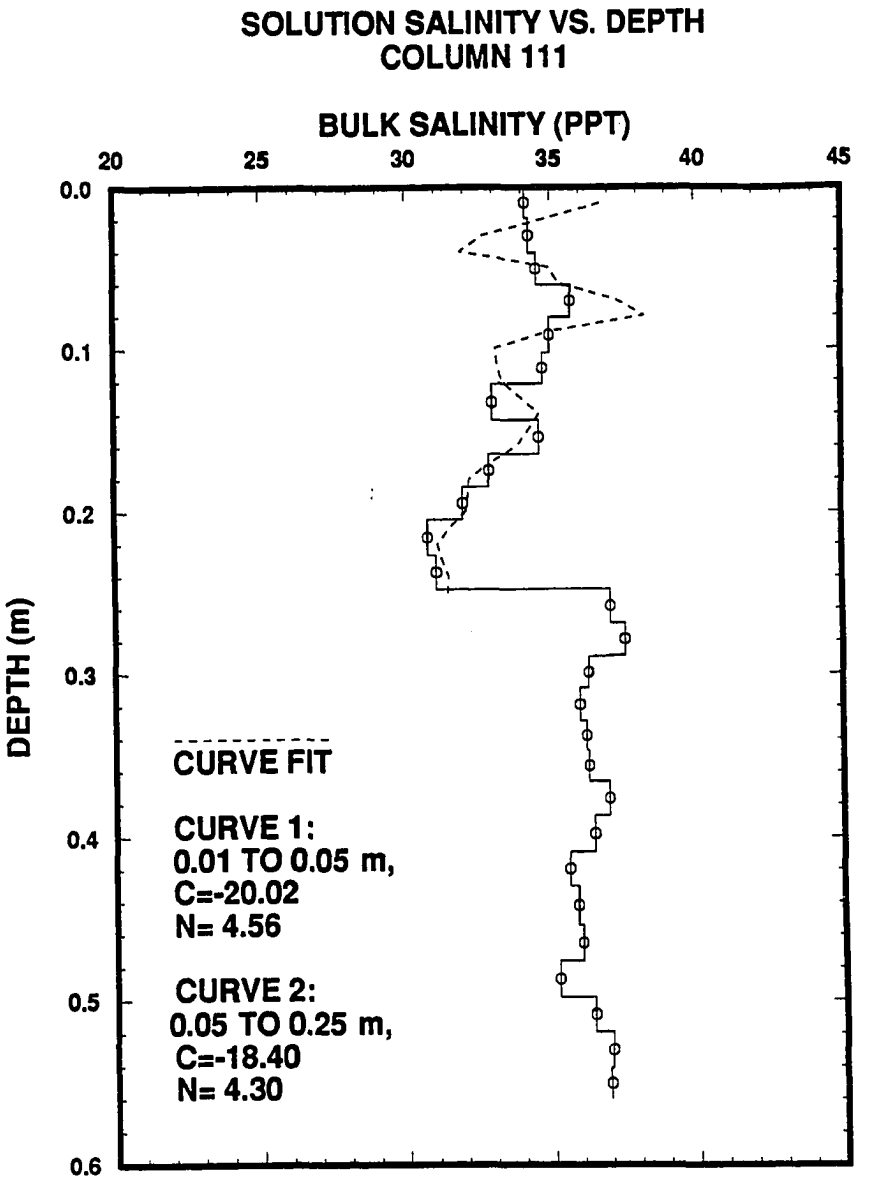

Figure 5.7: Results of a least squares fit to the bulk salinity data in the partially frozen portion of Column 111. The region in which each curve was fit is shown in the figure.

variations in both the permeability and the brine density. In this section, the momentum and energy equations were written in terms of the dependency of permeability on the bulk salinity and temperature, and the dependency of density on temperature. These two equations were then used to parameterize the bulk salinity to the temperature and a power of the temperature gradient. The utility of the parameterization as a method to represent the experimental results was shown in Figure 5.4. An iterative least squares fit was then used to determine the values of n and C in equation 5.13 which best fits the data. The least squares fit of the parameterization of the bulk salinity data appears to match the data reasonably well, however, the parameterization appears to be slightly oversensitive to changes in the temperature and temperature gradient. The remainder of this section will present a method to estimate the maximum amount of solute redistribution that can be expected to occur as a result of freezing.

5.4.2 Maximum Amount of Solute Redistribution During Freezing

Figures previously presented in this section showed that bulk salinity profiles affected by convection can be parameterized with the temperature and a power of the temperature gradient. Observations made during the freezing experiments have shown that convection appears to begin after an initial transient period when a threshold temperature gradient is reached and continues until the temperature profile within the column becomes steady. Values for C and n determined for the non-steady temperature profiles in the previous part of this section will be used with the steady temperature profiles to estimate the maximum amount of solute redistribution due to freezing.

Parameters C and n for equation 5.8 were calculated for each bulk salinity profile affected by convection in each of the freezing tests (Tests 5 through 13). The results of the curve fits are shown in Figure 5.8 which shows that C is related to n through a power function with general limits of $C \approx -90$ for $n = 2$ and $C = -11.9$ for $n = 7$. In general, n appears to be a function of temperature but this relationship is unclear for a freezing NaCl solution.

The maximum amount of redistribution during freezing may be estimated from bounds on C and n calculated from the non-steady temperature profiles in the

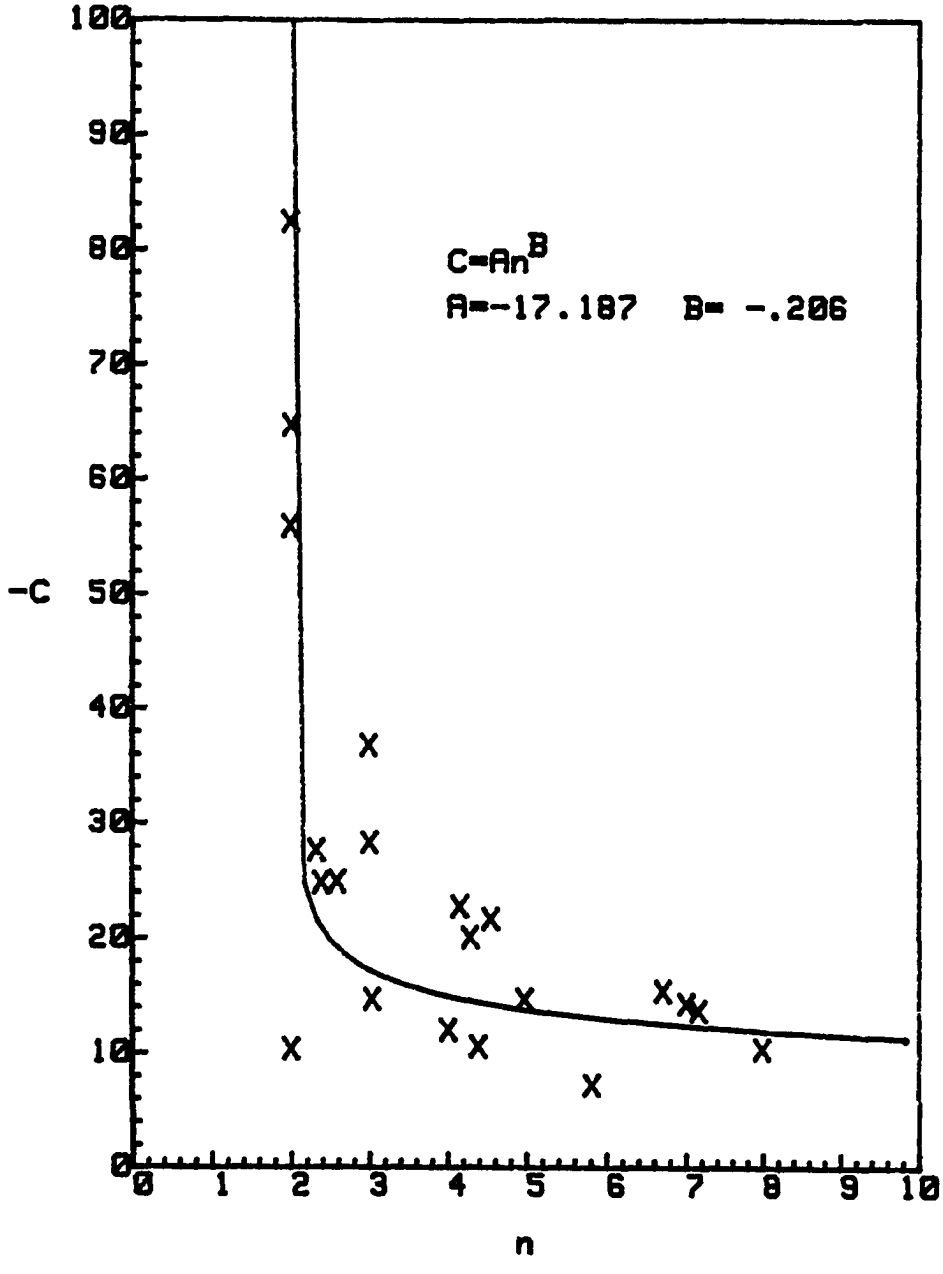

Figure 5.8: Summary of the curve of parameters resulting from the stability theory to the bulk salinity data in the sand columns affected by convection. Constants C and n were fit to the data using the method of least squares

previous part of this section. Bounds on C and n will be used with steady temperature profiles to estimate the maximum amount of redistribution during freezing. Since all of the discussion with regard to the maximum amount of redistribution due to freezing has concentrated on the partially frozen portion of the column, it will be necessary to estimate the amount of redistribution such that the bulk salinity profiles in the thawed portion of the column match the experimental results. These experimental results suggest that the difference between the initial bulk salinity and the minimum bulk salinity in the partially frozen portion of the column is approximately equal to the difference between the maximum bulk salinity in the thawed portion of the column and the initial bulk salinity.

Depth to the base of the ice–bearing interface is a function of profiles of both temperature and bulk salinity. For a steady temperature profile, the change in temperature with depth is constant. However, the bulk salinity profile in the partially frozen region depends both on the temperature and a power of the temperature gradient. The increase in bulk salinity in the thawed region depends on the bulk salinity minimum. Also, salt must be conserved throughout the column. Since the bulk salinity minimum determines the bulk salinity maximum, the location of the ice–bearing interface cannot be estimated, it must be determined through iteration. The iteration loop consists of the following steps:

- Choose the initial bulk salinity within the column.
- Choose the surface and base temperatures.
- Choose the values of C and n to be used. Only one set of values will be used between the surface of the column and the ice–bearing interface.
    1. Calculate the depth to the ice–bearing interface based on the initial, prior to freezing, bulk salinity profile and the steady state temperature profile using equation 3.10.
    2. Calculate the bulk salinity profile between the surface of the column and the ice–bearing interface which was calculated in step 1 using equation 5.25.

3. Calculate the bulk salinity at the base of the column using the criteria that the deviation between the maximum bulk salinity and the initial salinity is equal in amplitude to the deviation between the initial bulk salinity and the minimum bulk salinity. Or, $S_{initial} - S_{minimum} = S_{maximum} - S_{initial}$.
4. Determine the location of the new ice–bearing interface using equation 3.10 and the bulk salinity profile calculated in step 3.
5. Compare the location of the ice–bearing interface calculated in step 4 with previous estimates of the ice–bearing interface either from an earlier iteration or from step 1. If previous estimates of the location of the ice–bearing interface coincide with the updated estimates to within 0.01 m then go to step 6, else go to step 2.
6. Final bulk salinity within the sand column has been estimated.

Figure 5.9 presents the results of estimates of bulk salinity based on an initial bulk salinity of 35 ppt, surface temperature of -4.5 °C and a base temperature of -1.8 °C for limiting cases of C and n using the algorithm presented. In general, these results suggest a maximum amount of redistribution on the order of 35 to 42% of the initial salinity. These bulk salinity profiles indicate a somewhat smaller amount of redistribution than the results presented by Baker (1987) in which the columns were frozen under substantially cooler temperatures, but they agree well with the results presented by Wilson (1983) for similar surface temperatures.

Figure 5.9 compared to Figure 4.5, shows the importance of the coupling of the partially frozen layer with the thawed layer. It appears that the coupling between the two layers increases the bulk salinity in the partially frozen layer through the diffuse interface. Profiles of bulk salinity calculated from the parameterization, equation 5.7, underestimate the bulk salinity between the bulk salinity minimum and the ice–bearing interface.

The value for n is a result of the effect of brine volume on the partially frozen permeability of the sand. The brine volume is a function of both the bulk salinity and the brine salinity, therefore, values of n are temperature dependent which implies a series of n will best describe the bulk salinity profiles. An independent

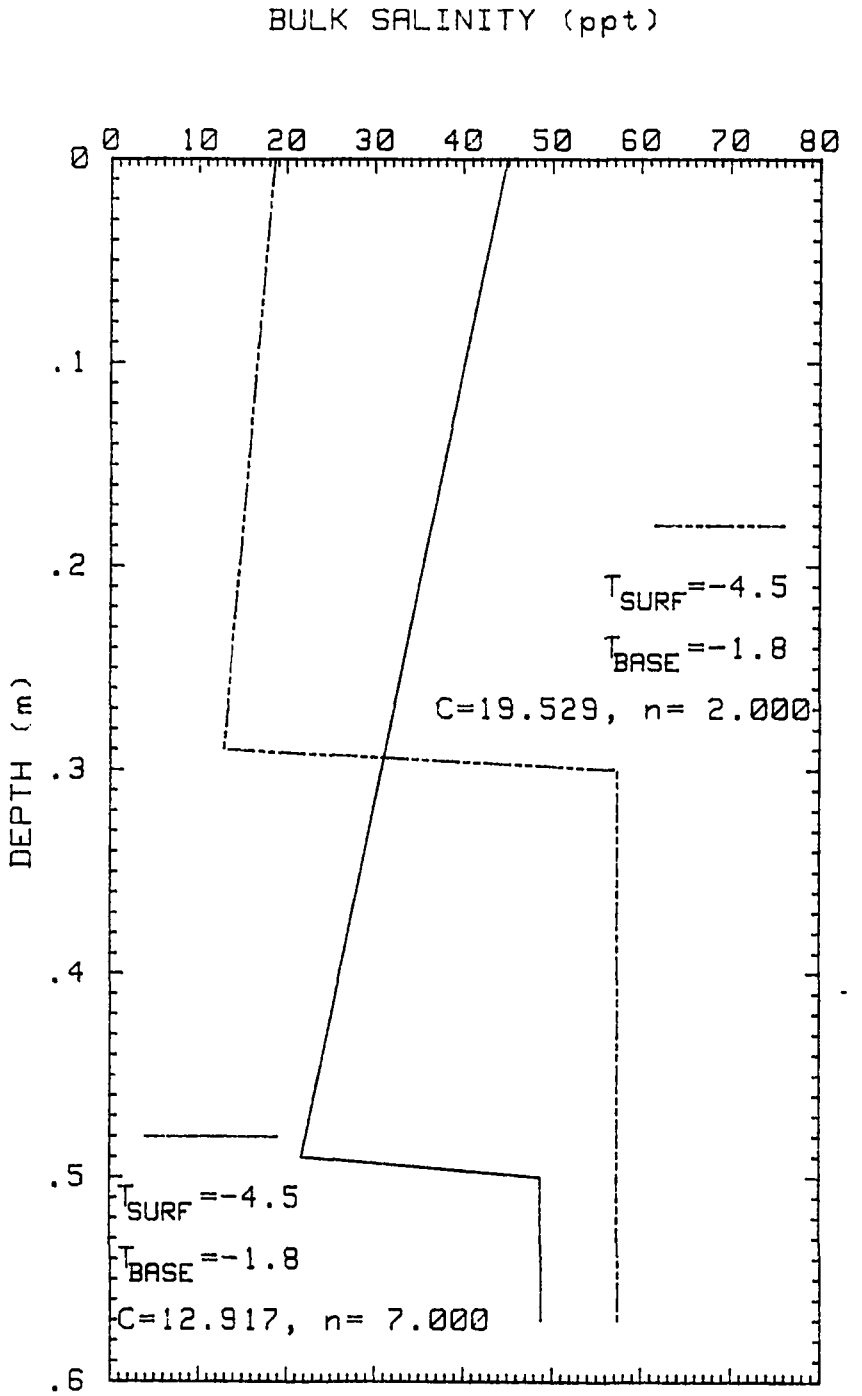

Figure 5.9: Maximum amount of solute redistribution that can be expected to occur as a result of freezing Granusil 30 sand for an initial salinity of 35 ppt, surface temperature of -4.5 °C and a base temperature of -1.8 °C. Values for C and n in each curve are shown in the figure.

measure of n can be obtained from measurements of the permeability as a function of temperature.

A check on the utility of applying the parameters C and n measured from the non-steady temperature profiles to the steady profiles to estimate the maximum amount of solute redistribution associated with freezing may be made by comparing these results with the results of Column 91 in which the temperature profile had constant slope. Figure 5.10 shows the results of this curve fit. In general, it appears that this bulk salinity profile would be better described by at least two values of n, however, one curve appears to fit the data qualitatively well in this case.

In summary, estimates of the maximum solute redistribution due to freezing may be made by using a parameterization of the form presented in equation 5.6. These estimates are relatively unrefined in that the temperature dependence of n is unknown, the mechanisms which affect the bulk salinity in the thawed section are not clear, and the coupling between the partially frozen and thawed regions has not been taken into account either in the theory or in the algorithm used to estimate the final bulk salinity in the partially frozen portion of the column.

5.5 Pore Fluid Velocity During Convection

Knowledge of the pore fluid velocity during convection is of interest since the flux of salts from the partially frozen to the thawed portion of the column depends on the pore fluid velocity. The purpose of this section is to bracket the pore fluid velocity that may be associated with gravitationally induced convection of the pore fluid. This section will present methods for determining bounds on the fluid velocity based on temperature measurements and an independent estimate of the pore fluid velocity based on the rate of change of bulk salinity.

5.5.1 Bounds on the Pore Fluid Velocities

Temperature measurements at either the instrumented column or the vertical tubes next to the columns did not exhibit features that could be associated with convection in the column even when it was known that convection of the pore fluid was occurring, Figure 4.30. These results suggest that in the energy equation the

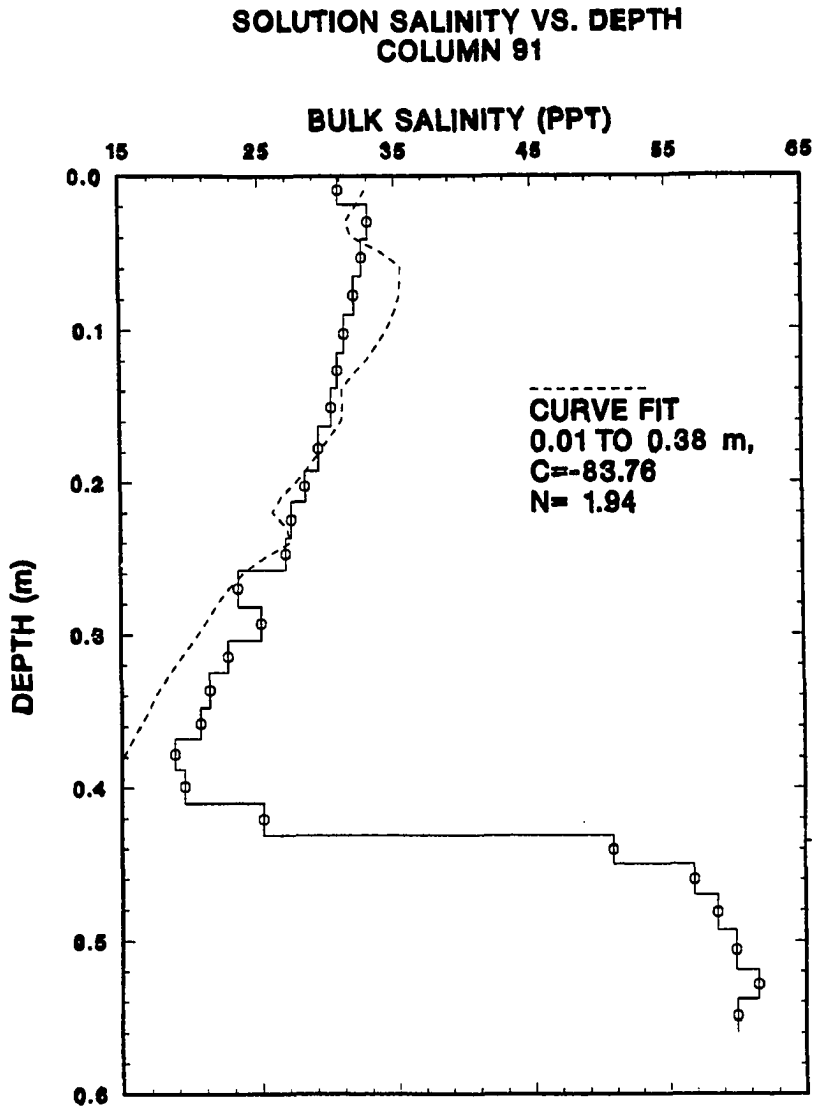

Figure 5.10: Bulk salinity profile in Column 91 at the time it was removed from the freezing apparatus. The solid line is the measured data and the dashed line is the estimated curve using the algorithm discussed in the text.

magnitude of the advective term relative to the conductive term is small. The ratio of the advective term to the conductive term is defined as the thermal Peclet number, Pe_t, which is expressed as

$$Pe_t = \frac{ub}{D} = \frac{ub\left(C_m - L\eta\frac{dV_{AU}}{dT}\right)}{\alpha_m}. \tag{5.26}$$

If $Pe_t \ll 1$ then the conductive term is much greater than the advective term in conducting heat. If $Pe_t \gg 1$ then the opposite is true. Since observations of the temperature at the instrumented column, Figure 4.30, do not indicate incoherent temperature events associated with convection, it may be assumed that that $Pe_t \leq 1$ and an estimate pore fluid velocity may be made. Taking $\left(C_m - L\eta\frac{dV_{AU}}{dT}\right) \approx 5\text{x}10^7 \frac{\text{J}}{\text{m}^3\cdot^\circ\text{C}}$ and using the same values for the remaining parameters as were used in section 5.3 suggests that

$$u \leq \frac{1.4 \frac{\text{W}}{\text{m}\cdot^\circ\text{C}}}{3\text{x}10^{-2}\ \text{m}\cdot 5\text{x}10^7 \frac{\text{J}}{\text{m}^3\cdot^\circ\text{C}}} \approx 10^{-6}\frac{\text{m}}{\text{s}} \approx 10^{-1}\frac{\text{m}}{\text{day}}. \tag{5.27}$$

A second estimate for the rate of brine movement in the partially frozen sand may be obtained from the rate that a temperature disturbance dissipates by conduction. For brine to convect in the partially frozen material, a density difference, and therefore a temperature difference, must exist between the displaced brine and the surrounding sand, pore fluid, and ice. Brine movement must occur quickly enough through the partially frozen region that the temperature disturbance associated with the movement does not dissipate or convection of the brine will cease. Assuming that the displacing brine takes the form of a sphere, the general solution to the energy equation for the sphere in terms of a similarity variable, ξ, may be expressed as

$$T(r,t) = \frac{C_1}{\xi^2}e^{-\xi^2} - C_2\int e^{-\xi^2}d\xi + C_3 \tag{5.28}$$

where $\xi = \frac{r}{2}\left(\frac{\left(C_m - L\eta\frac{dV_{AU}}{dT}\right)}{\alpha_m t}\right)^{\frac{1}{2}}$ and C_i are constants. The time constant, τ, for equilibration of a disturbance of radius $r = 1.8\text{x}10^{-2}$ m (half the tube radius to match experimental observations of pore fluid on one side of the column moving up and the opposite side down) may be expressed as

$$\tau = \frac{r^2}{4}\left(\frac{\left(C_m - L\eta\frac{dV_{AU}}{dT}\right)}{\alpha_m}\right) \approx \frac{3.3\text{x}10^{-4}\ \text{m}^2}{4}\frac{5\text{x}10^7 \frac{\text{J}}{\text{m}^3\cdot^\circ\text{C}}}{1.4 \frac{\text{W}}{\text{m}\cdot^\circ\text{C}}} = 3\text{x}10^3\ \text{s} = 0.9\ \text{hours}. \tag{5.29}$$

A time constant of 0.9 hours suggests that the disturbance should move 1.8x10^{-2} m in at least 3 time constants, this suggests a bound on the disturbance velocity which is on the order of 7x10^{-3} $\frac{\text{m}}{\text{hr}}$ or 1.6x10^{-1} $\frac{\text{m}}{\text{day}}$.

5.5.2 Pore Fluid Velocity Based on Solute Movement

A final estimate of the pore fluid velocity may be made from the rate of change in solute concentration within the partially frozen region. The relative contribution of the heat advection and conduction terms in the energy equation was expressed through the non-dimensional thermal Peclet number. For the equation which governs conservation of species, a similar number may be written but in this case it is referred to as the solute Peclet number. For solutes, Pe_s may be expressed as

$$Pe_s = \frac{ub}{\kappa} \tag{5.30}$$

where κ is defined as the diffusivity of the solute and is on the order of 10^{-11} $\frac{\text{m}^2}{\text{s}}$ Baker (1987). For pore fluid velocities on the order of 10^{-6} $\frac{\text{m}}{\text{s}}$, $Pe_s \gg 1$ which suggests that the advective term is important in describing the movement of the solute when even the smallest fluid motion is present in the columns. One dimensional conservation of a solute for NaCl dissolved in water may be written as

$$\frac{\partial M_{salt}}{\partial t} + u\frac{\partial M_{salt}}{\partial x} = \kappa \nabla^2 M_{salt} \approx 0. \tag{5.31}$$

The mass salt in the system may be expressed as $M_{salt} = \rho_T V_T S_B = \rho_U V_U S_U$ where the subscript U refers to the brine and subscripts T refer to the total volume and, as usual, S_B is the bulk salinity. Substitution of these parameters into the one dimensional advection equation, and using the relation $V_{AU} = \frac{V_U}{V_U + V_I}$ gives

$$u \approx -\frac{\frac{\partial S_B}{\partial t}}{\frac{\partial V_{AU} S_U}{\partial x}} \tag{5.32}$$

Figure 5.1 shows the rate of change in bulk salinity vs brine volume for several different temperature gradients. This figure shows that, for gradients in the range of 2 to 8 $\frac{^\circ\text{C}}{\text{m}}$, the flux of the solute from the partially frozen portion of the column is between 5 and 10x10^{-5} $\frac{\text{ppt}}{\text{s}}$. Data from day 4.13 of freezing in Test 6 suggests that $\frac{\partial S_U V_{AU}}{\partial x} = 28$ $\frac{\text{ppt}}{\text{m}}$. Substitution of the values presented above into the conservation

equation yields

$$u = \frac{5 \text{ to } 10\text{x}10^{-5} \frac{\text{ppt}}{\text{s}}}{28 \frac{\text{ppt}}{\text{m}}} = 1.8\text{x}10^{-6} \text{ to } 3.6\text{x}10^{-6}\frac{\text{ppt}}{\text{s}} = 1.5\text{x}10^{-1} \text{ to } 3.1\text{x}10^{-1}\frac{\text{m}}{\text{day}}. \tag{5.33}$$

In summary, three different techniques have been employed to bracket the magnitude of the fluid velocity occurring in the partially frozen columns during convection. These techniques have been used in a manner consistent with the experimental observations made during the freezing experiments. Results from this analysis suggest that the pore fluid velocity during convection ranges from 0.1 to 0.3 $\frac{\text{m}}{\text{day}}$. Measurements of the velocity of fingers in the salt finger cell built by Baker (1987), Baker and Osterkamp (1987) and in this study (Sections 2.5 and 4.4) showed that fingers had velocities that ranged from 0.1 to 1.4 $\frac{\text{m}}{\text{day}}$. These results in thawed Granusil 30 suggest an upper bound for the finger velocity in the partially frozen Granusil 30.

5.5.3 Interpretation of Pore Fluid Velocities

The pore fluid velocity estimated from the temperature data suggest that rates of 0.2 $\frac{\text{m}}{\text{day}}$ are present in the sand during convection. This result, along with the rate of change in bulk salinity with time may be used to obtain information about the nature of convection in the columns.

Figure 5.1 shows that the rate of change in bulk salinity with time is on the order of $1\text{x}10^{-4}$ $\frac{\text{ppt}}{\text{s}}$. Figure 4.5 shows that the average change in bulk salinity for the columns is on the order of 5 ppt over the 0.3 m length. Since the columns frozen in this test do not consistently show the presence of convection, it is difficult to believe the magnitude of the data presented in Figure 5.1 is representative of the true flux of salt from the partially frozen region. However, taking a somewhat low value of the bulk salinity change to be $2\text{x}10^{-5}$ $\frac{\text{ppt}}{\text{s}}$ suggests that once convection begins the pore fluid velocity must be fairly steady because the flux of the solute is so small. Further, if the pore fluid velocity were much greater than 0.2 $\frac{\text{m}}{\text{day}}$ and acted for shorter periods, then temperature fluctuations associated with convection could be measured with the thermistor string at the instrumented column.

Results from Test 6 show that the onset of convection is preceded by a transient period between 4 to 10 days in length. Baker (1987) presents data which

shows a similar transient period existed between the start of freezing and when the redistribution of the solute approached steady state, see Section 1.2.3.1 for a discussion. Once convection begins, it appears to progressively desalinate the partially frozen portion of the column. Results of Test 5 shows that, after the onset of convection, each column obtained after progressively longer periods of freezing exhibited a lower bulk salinity in the partially frozen region and an increased bulk salinity in the thawed region. These results are generally confirmed throughout the nine freezing tests with exceptions occurring only in tests in which the pore fluid did not convect.

5.6 Summary

In summary, the experimental results of this investigation have shown that the interface between the partially frozen sand and the thawed sand is a diffuse interface. These results have shown that the solute strongly affects the heat transfer that occurs in the columns. With the exception of the top 0.02 m of the column where a small amount of water, but not salt, moves into this region, freezing initially results in the incorporation of nearly 100% of the solute within the partially frozen sand. Several days later, after the ice–bearing interface has nearly reached its maximum depth, pore fluid in the column begins to convect and the solute is redistributed from the partially frozen region to the thawed region.

Attempts to understand the stability of pore fluid in the partially frozen region through the use of a stability criterion applied to the partially frozen layer only was not useful as a means for predicting the onset of convection. This analysis has shown that the Rayleigh number measured at the onset of convection is 1 to 2 orders of magnitude less than the theoretical value. It has also shown that the largest Rayleigh number is near the ice–bearing interface. This analysis and the experimental results have shown that a complete description of the mechanisms which leads to convection in the column must include the presence of the thawed region in the stability analysis. The several day long transient between the start of freezing and the onset of convection in which the temperature gradient was very large was addressed by considering the effect of the pore fluid velocity due to brine expulsion on the stability of the fluid in the column. It was concluded that the small component of velocity due to brine expulsion has a negligible effect on the

stability of the pore fluid in the column. The transient period between the start of freezing and the onset of convection was concluded to be due to dynamic effects associated with the formation of viscous fingers which are not understood.

Experimental results which suggest that the bulk salinity in the partially frozen portion of the column is affected by the permeability and the density gradient were used to parameterize the bulk salinity in the columns affected by convection with the temperature and a power of the temperature gradient. Results of this parameterization on the columns affected by convection of the pore fluid were then used to estimate the maximum amount of solute redistribution due to freezing the columns of sand saturated with saline solution. The analysis further highlighted the importance of the coupling between the partially frozen and thawed regions of the column in terms of their influence of the stability of the pore fluid and showed that the maximum amount of redistribution expected could be on the order of 28 to 42% of the initial salinity.

Finally, three different estimates were made to bracket the velocity of the pore fluid while the fluid in the columns was convecting. Two of these estimates were based on the conduction of heat and the thermal effects associated with convection and the third on the flux of brine from the partially frozen portion of the column. These three results bracketed the pore fluid velocity in the columns to be on the order of 0.1 to 0.3 $\frac{m}{day}$. Measurements of the velocity of fingers in the salt finger cell built by Baker (1987), Baker and Osterkamp (1987) and in this study (Sections 2.5 and 4.4) showed that fingers had maximum velocities that ranged from 0.1 to 1.4 $\frac{m}{day}$. These results from tests on thawed Granusil 30 suggest an upper bound for the finger velocity in the partially frozen Granusil 30.

Chapter 6

Conclusions, Potential Applications and Areas of Future Research Needs

6.1 Introduction

Solute movement in freezing soils is affected by the various potentials which may develop in the soil during freezing. These are thought to include: matric, osmotic, chemical, electrical and gravitational potentials. Prior investigations have suggested that the parameters important to determining which of these potentials develops during freezing include: grain size, degree of saturation, solute concentration, freezing rate and others. This thesis has presented the results of an investigation designed to understand the effects of the gravitational potential on the distribution of a solute in a saturated partially frozen coarse–grained soil. The purpose of this chapter is to summarize the interpretation of the experimental and theoretical results, apply these results to natural freezing processes and to suggest specific areas of additional research to address the shortcomings of this investigation.

6.2 Interpretation Summary

The purpose of this section is to summarize the results and interpretation of the experimental investigation of the processes leading to the redistribution of a solute in coarse–grained soils during freezing. The first part of this section presents a summary of the experimental observations. The second part presents a summary

of the experimental results and the third part summarizes the theoretical results.

6.2.1 Experimental Observations

Experimental observations made during this investigation were generally limited to the time while the column was being sectioned with a bandsaw. These observations indicate that the interface between the partially frozen and the thawed portion of the column was diffuse and occurred over several centimeters. It was observed that the vertical extent of the diffuse interface increased as the temperature gradient through the interface decreased.

Radial variations in the bonding of the soil grains by ice which varied from column to column were associated with the diffuse interface. Bonding always increased from the sides of the column towards the center. Often horizontal variations in bonding were radially symmetric. However, at other times it was asymmetric and one side of the column was appreciably less well bonded than the remainder of the column in the same section. Radial asymmetries in bonding were associated with convection of the pore fluid through the diffuse interface. In one test, dye was placed in the columns to trace the movement of the pore fluid during convection. The less well bonded regions were associated with downward moving pore fluid which was confined to a several centimeter wide area on one side of the column. On the opposite side of the column pore fluid was observed to move up from the thawed region to the partially frozen region. In the middle of the column, movement of the pore fluid during convection was not observed. The region containing downward moving pore fluid was observed to have a bulk salinity that was 1 to 2 ppt greater than the region containing upward moving pore fluid and 1 to 8 ppt greater than the middle region of the section. Measurements of the temperature difference between regions of sections exhibiting upward and downward movement of the pore fluid were not obtained.

6.2.2 Results

The results of this investigation consist of those results prior to and after the onset of convection in the columns as well as the theoretical results. Experimental results consist of measurements of profiles of bulk salinity, gravimetric water content and temperature. Theoretical results consist of the theory developed and applied to

the experimental results. This part of the section summarizes the experimental results both prior to and after the onset of convection, and the theoretical results of the investigation.

6.2.2.1 Results Prior to the Onset of Convection

Essentially 100% of the solute was incorporated within the partially frozen region prior to the onset of convection. Such high solute concentrations in the partially frozen region means that the quantity of latent heat released during freezing is distributed over a range of temperatures; a situation that leads to large freezing rates in the column. For example, after 24 hours of freezing under similar temperature boundary conditions, the ice–bearing interface moved 0.24 m during freezing in a 35 ppt and only 0.12 m during freezing in a 1 ppt solution. These results suggest that the presence of the solute strongly affects the heat transfer within the columns by increasing the freezing rate of the sand.

The physical processes occurring within the column prior to the onset of convection include a small amount of fluid flow within 0.02 m of the column surface, and brine expulsion between 0.02 m and 0.1 m of the surface of the column. These results showed that water flowed to the surface of the column, however, the solute did not. Fluid flow led to an approximately 3% increase in the water content and an approximately 3 ppt decrease in the bulk salinity within 0.02 m of the column surface. It appears that the water content of the region immediately below 0.02 m of the surface was depleted several percent by flow to the surface. Brine expulsion in the region between 0.02 and 0.1 m of the column surface could produce an approximately 1 ppt decrease in the bulk salinity and an approximately 1% decrease in the gravimetric water content. The mechanism which drove the fluid flow from the region between 0.02 m and 0.1 m below the column surface to the region within 0.02 m of the column surface could not be determined. Calculations of the amount of fluid flow due vapor transport suggest that the flux of vapor is much smaller than the amount necessary to match the experimental observations. Calculations have also shown that a salt sieving phenomena in which water but not salt flows along the sand grain surfaces could not occur because of the low surface area of the mineral grains and the large brine volume in the sand. At locations between 0.1 m and the ice–bearing interface the bulk salinity appears to increase less than

1 ppt. This increase could be due to the effects of brine expulsion occurring near the surface of the column. However, the increase is smaller than the estimated uncertainty in the measurements.

Results from these tests indicate that if the ice–bearing interface reached the base of the column, convection of the pore fluid did not occur. Test 10 is such an example showing that the ice–bearing interface was within 5 centimeters of the base of the column after approximately 7 days of freezing and the entire column was partially frozen after 17 days of freezing. Test 6 is an example which shows that after a transient period of 4 to 10 days in length pore fluid in the column began to convect. A preliminary interpretion of these results is that a thawed layer underneath a partially frozen layer is important in determining the stability of the pore fluid.

6.2.2.2 Conditions After the Onset of Convection

The effects of convection of the pore fluid during freezing were observed only in the bulk salinity profiles. Convection resulted in a lowering of the bulk salinity in the partially frozen region and an increase in the bulk salinity in the thawed region. The effects of convection were not observed in the profiles of gravimetric water content, or temperature. Profiles of gravimetric water content exhibit a slight decrease in water content in the top 0.1 m of the column, however, they do not exhibit features that can be associated with convection of the pore fluid. Profiles of temperature also do not exhibit features that can be associated with convection of the pore fluid. Unlike bulk salinity profiles which clearly exhibit the differences between the diffusive and convective regimes of the solute, the temperature profiles show that the heat transport in the columns is conductive.

Experimental results have shown that convection began after the temperature gradient at the ice–bearing interface began to increase and after the velocity of the ice–bearing interface reached a nearly steady value. The increase in the temperature gradient at the ice–bearing interface was associated with the fixed base temperature of the column. A decrease in the velocity of the ice–bearing interface is associated with heat conduction, and the increase in the temperature gradient at this interface. Since the instability generated by freezing is proportional to the temperature gradient, the increasing temperature gradient near the ice–bearing

interface promoted the instability of the pore fluid.

Bulk salinity profiles in the thawed portion of the column are density stable in that less saline, thus less dense, solutions overly more dense solutions. This result is interpreted to show that brine movement from the partially frozen region to the thawed region occurs without appreciable mixing of the brine in the thawed region. This interpretation is supported by observations of pore fluid movement when layers of dye were placed in the columns and frozen. Observations indicated that pore fluid containing dye moved down one side of the column to the base where it spread out over the entire cross-sectional area of the column.

Pore fluid velocities during convection were estimated based on the experimental results of the laboratory investigation. Velocity estimates were based on a small thermal Peclet number, time transients associated with convection and a large solute Peclet number. A small thermal Peclet number results from the heat transfer occurring by diffusion. The time transient of convection results from the thermal disequilibrium that is necessary for convection to occur, the length scale of the convective cells and the apparent diffusivity of the soil matrix. A large solute Peclet number results from the transport of the solute occurring mainly by convection instead of by diffusion. These three methods for estimating pore fluid velocities during convection suggest that these velocities ranged from 0.1 to 0.3 $\frac{m}{day}$.

6.2.2.3 Theoretical Results

The observations which indicate that pore fluid motion during convection consisted of pore fluid on one side of the column moving down and pore fluid on the opposite side moving up are consistent with the pattern of convection that occurs in a stability criterion presented by Wooding (1959). Wooding (1959) developed a stability criterion for pore fluid motion in a column filled with a homogenous material and saturated such that a dense pore fluid overlies less dense pore fluid. Wooding's stability criterion was modified to take into account the presence of a variable permeability due to the variable ice content in the porous matrix and a small amount of throughflow that is associated with brine expulsion during freezing. The modified form of Wooding's criterion takes into account only the partially frozen region and not the thawed region which is under the partially

frozen region.

The modified form of Wooding's stability criterion in the partially frozen region was then used to compare the theoretical Rayleigh number with the measured Rayleigh numbers at the onset of convection. Results of this analysis at the start of convection showed that the measured Rayleigh number was consistently 1 to 2 orders of magnitude less than the critical theoretical value. The largest measured Rayleigh number was consistently located near the ice–bearing interface. The parameter with the greatest effect on the measured Rayleigh number is the partially frozen permeability. However, when permeability values which were measured in the thawed sand were substituted into the Rayleigh expression, the calculated Rayleigh number was still and order of magnitude less than the critical theoretical value. Finally, the effect of brine expulsion during freezing was shown to have a negligible effect on the stability of the pore fluid. A preliminary interpretation of these results shows that the presence of the thawed layer underneath the partially frozen region is important in determining the stability of the pore fluid. The 4 to 10 day period between the start of freezing and the onset of convection is not understood, however, downward movement of the interface could suppress the formation of fingers of convecting pore fluid.

6.2.3 Summary

In summary, the major effect of convection that results from freezing the sand columns was the redistribution of the solute from the partially frozen region to the thawed region of the column. Observations indicate that the mode of convection consists of pore fluid on one side of the column moving down and pore fluid on the opposite side of the column moving up. The bulk salinity in the regions containing downward moving pore fluid was 1 to 2 ppt greater than regions where the pore fluid was moving up, and 1 to 8 ppt greater than in the middle of the column where pore fluid was not observed moving.

Convection began after a 4 to 10 day transient period and was associated with both an increase in the temperature gradient at the ice–bearing interface, and a slowing of the rate of change in the position of the ice–bearing interface. Theory developed to characterize the stability of fluid in a column filled with a homogenous porous material was modified to take into account the variable permeability due to

variations in the ice content and the throughflow due to brine expulsion. Results of this theory applied to the freezing experiments showed that the measured Rayleigh number is one to two orders of magnitude less than the theoretical value. The largest measured Rayleigh number was at the ice–bearing interface. It was also shown that brine expulsion has a negligible effect on stability of the pore fluid. Observations that a thawed layer, below the partially frozen layer, was important in determining the stability of pore fluid were preliminarily interpreted as the reason for the disparity between the measured and theoretical Rayleigh numbers. Pore fluid velocities associated with convection have been estimated to be on the order of 0.1 to 0.3 $\frac{m}{day}$.

Additionally, freezing affected the bulk salinity and water content near the surface of the column. These effects were mainly observed in columns not affected by convection since the magnitude of their effect was smaller than the effects of convection on the bulk salinity and water content. Within the top 0.02 m of the column, the first section of the column, freezing resulted in an approximately 3% increase in the water content and an approximately 4 ppt decrease in the bulk salinity over the initial values. Below 0.02 m and above 0.1 m the water content is decreased below its initial value by up to 2% and bulk salinity is decreased by up to 1 to 2 ppt. The increased water content and the lowered bulk salinity within 0.02 m of the column surface has been interpreted in terms of the flow of pure water, independent of the salt, to the surface. It was shown that a water equivalent of approximately 5% of the section thickness flowing into the section can produce the observed bulk salinity and water content values. Presumably the water flowed to the surface from the region between 0.02 and 0.1 m of the surface because these parameters are also shown to be affected by a decrease in the water content. However, it is difficult to distinguish between the effects of pure water flow and brine expulsion due to freezing in this region. The driving mechanism for the flow of water but not salt in this region is unknown but an analysis has shown that it is probably not a result of vapor transport nor is it likely a result of salt sieving.

6.3 Potential Applications to Natural Freezing

The purpose of this laboratory investigation was to develop an interpretation of the experimental results that is consistent with the processes that occurred during freezing. It was also the purpose of this study to express the interpretation in a form so that the maximum amount of solute redistribution during freezing could be estimated. Since it was not possible to develop a theory consistent with the experimental observations and it was not possible to apply the results of the BPS theory to these results, [1] the application of these results to natural freezing situations in which soils saturated with saline solutions are frozen is quite limited. The purpose of this section is to discuss the potential applications of these experimental results to natural freezing situations. The first part of this section will discuss the limitations imposed by the finite size of experimental apparatus. The second part of this section will discuss the application of this work to natural freezing situations.

6.3.1 Limitations of the Experimental Apparatus

Features of this experimental apparatus which must be considered before applying these results to natural freezing situations are the fixed length and diameter of the columns, and the constant surface and base temperatures imposed by the environmental chamber and the radiator.

Temperature measurements during freezing suggest that the onset of convection occurred near the time when the temperature gradient at the ice–bearing interface began to increase. The temperature gradient at the ice–bearing interface increased because the interface was nearing the base of the column which had a fixed temperature. The heat flux from the base of the column also decreased the velocity that the interface moved through the column.

The surface temperature of the columns was fixed and was relatively constant except for short periods when the environmental chamber went through a defrost cycle. During the initial stages of freeze-up the ground surface is not covered with

[1] A plot of $\ln(\frac{1}{k} - 1)$ versus freezing rate, where k is the ratio of bulk salinities on the thawed and partially frozen sides of the ice–bonded interface, for the results of Test 5 is not as linear as the data presented by Baker (1987) and the line fit to the data has a slope which has the opposite sign of the results presented by Baker (1987).

an appreciable thickness of snow so that temperature fluctuations in the soil may be as large as 10 °C (Johnson and Hartman 1971). Diurnal temperature fluctuations as well as fluctuations associated with changing weather patterns can result in temperature gradients near the surface of the soil which were not encountered nor investigated in this research. Fluctuations in the weather have been observed to result in convection within the snowpack (Sturm 1990) and colder ground surface temperatures than would be expected based on temperature diffusion through the snowpack.

Experimental observations indicated that the horizontal dimensions of the convection cells were constrained by the diameter of the sand column. Theory used to describe the stability of the fluid in the column used boundary conditions imposed by the rigid boundary encountered along the side of the column. Natural freezing situations do not have such horizontal boundary conditions and would not be expected to have the horizontal length scales constrained as in the columns.

6.3.2 Application of the Experimental Results to Natural Freezing Situations

The results of this investigation showed that for the freezing conditions imposed on the columns. and for the sand permeability used in the tests, fluid in the column was marginally stable. The density gradient near the most unstable location in the column was approximately -65 $\frac{kg}{m^4}$ (equation 5.2 with a temperature gradient of 5 $\frac{°C}{m}$). Baker (1987) showed that for a similar sand with similar initial salinity, convection always occurred for a density gradient at the ice–bonded interface that was approximately -1300 $\frac{kg}{m^4}$. Baker also showed that the redistribution of a solute during freezing could be modeled with a steady state diffusive theory, BPS theory. The results presented in this thesis suggest that convection will not occur if the initial pore fluid salinity is near 35 ppt and if the temperature gradients are significantly smaller than 5 $\frac{°C}{m}$.

Experiments conducted using solutions with initial salinities that were 1 and 100 ppt rather than 35 ppt showed that convection of the pore fluid did not occur. However, like the 35 ppt solutions, essentially 100% of the solute was incorporated within the partially frozen sand. The differences between these two solutions and the 35 ppt solution are the density gradient due to freezing and

the brine volume in the partially frozen region. The density gradient is shown to be related to the temperature gradient in equation 5.2. However, the change in brine salinity with temperature, used in equation 5.2, is not constant with temperature; at -1 °C, $\frac{dS_U}{dT} = -16.80 \frac{\text{ppt}}{\text{°C}}$; at -2 °C, $\frac{dS_U}{dT} = -16.43 \frac{\text{ppt}}{\text{°C}}$; and at -10 °C, $\frac{dS_U}{dT} = -11.00 \frac{\text{ppt}}{\text{°C}}$. At the freezing temperature of a 100 ppt solution, the density gradient is 33% less for a given temperature gradient than it is at the freezing temperature of a 35 ppt solution. This implies that the brine volume is large, or that only a small amount of latent heat is released during freezing in very concentrated solutions. The result is that the ice–bearing interface moves much more quickly during freezing in a 100 ppt solution, than it does in a 35 ppt solution. Also, the density gradient in a 100 ppt solution, the driving force for convection, is 33% smaller than in a 35 ppt solution. In the test with a 100 ppt solution, the entire column contained ice before the pore fluid could convect. In the test involving the 1 ppt solution, just the opposite occurred; freezing resulted in the removal of $\approx$ 95% of the latent heat at the ice–bearing interface and convection did not occur. For convection to occur during the freezing of concentrated solutions, solutions with concentration of 100 ppt, the temperature gradient at the ice–bearing interface must be increased significantly. For convection to occur in dilute solutions, solutions with concentration of 1ppt, the temperature gradient at the ice–bearing interface must be decreased to the point that a significant volume of brine is present in the partially frozen region. These results are non-intuitive and warrant further investigation. However, they suggest very critical and restrictive bounds on the occurrence of convection in saline porous soils when they are frozen.

In natural freezing situations, soils are not constrained by the boundaries that were imposed on the columns by the freezing apparatus. Consequently, the application of the results of the laboratory investigation to field situations is not clear. The experimental results indicated that convection of the pore fluid was dependent on the presence of a thawed layer underneath a partially frozen layer, an increase in the temperature gradient at the ice–bearing interface and a slowly moving ice–bearing interface. An active layer underlain by permafrost could freeze over a period of months without a substantial increase in the temperature gradient near the ice–bearing interface. In this case, convection of the pore fluid is not likely to occur unless the active layer is thick enough for the temperature gradient through the ice–bearing interface to increase before the active layer is completely

frozen. During the annual freezing of soil that is not underlain by permafrost, the soil is likely to have the largest temperature gradient through the ice–bearing interface during winter, disregarding the initial freezing when a snow cover might be absent. Since the temperature gradient increases as the freezing rate slows and the soil is underlain by thawed ground, it would appear that the conditions necessary for convection to take place are present. The effects of temperature variations during freezing, however, could complicate this simple interpretation. For example, multiple freeze–thaw events associated with freezeup could lead to convection because large temperature gradients are associated with rapid freezing and thawing. Variations in the distribution of solutes with depth could also complicate this interpretation because of changes in the freezing rate as the ice–bearing interface passes horizons of different solute concentration. However, the effects of these variations in salinity on the stability of the pore fluid are largely unknown.

An initial attempt to determine the effects of natural temperature variations during freezeup on the distribution of the solute in Granusil 30 were made by freezing 3 columns under a hydrostatic stress during the fall of 1988 at the University of Alaska Experimental Farm. These columns were frozen in tight fitting PVC sleeves similar to those used in the laboratory investigation. However, the method used to maintain the hydrostatic stress during freezing was different from method used in the laboratory investigation. The diameter of these tubes was 4.45×10^{-2} m. Figure 6.1 shows the bulk salinity profiles in two of these columns. These bulk salinity profiles show that the effects of natural freezing complicates the interpretation of the profiles. However, the general effects of convection and pore fluid motion may be observed to affect the distribution of the solute in one of the columns in a manner similar to the laboratory experiments. These profiles also show that similar columns frozen under approximately similar conditions were not affected by freezing as uniformly as the columns obtained in the laboratory experiments. Finally, these profiles show that natural freezing, which includes the effects of diurnal temperature changes, complicates the interpretation of the bulk salinity profiles.

Based on the results of this study, the maximum amount of solute redistribution during freezing is more difficult to calculate than previously hypothesized.

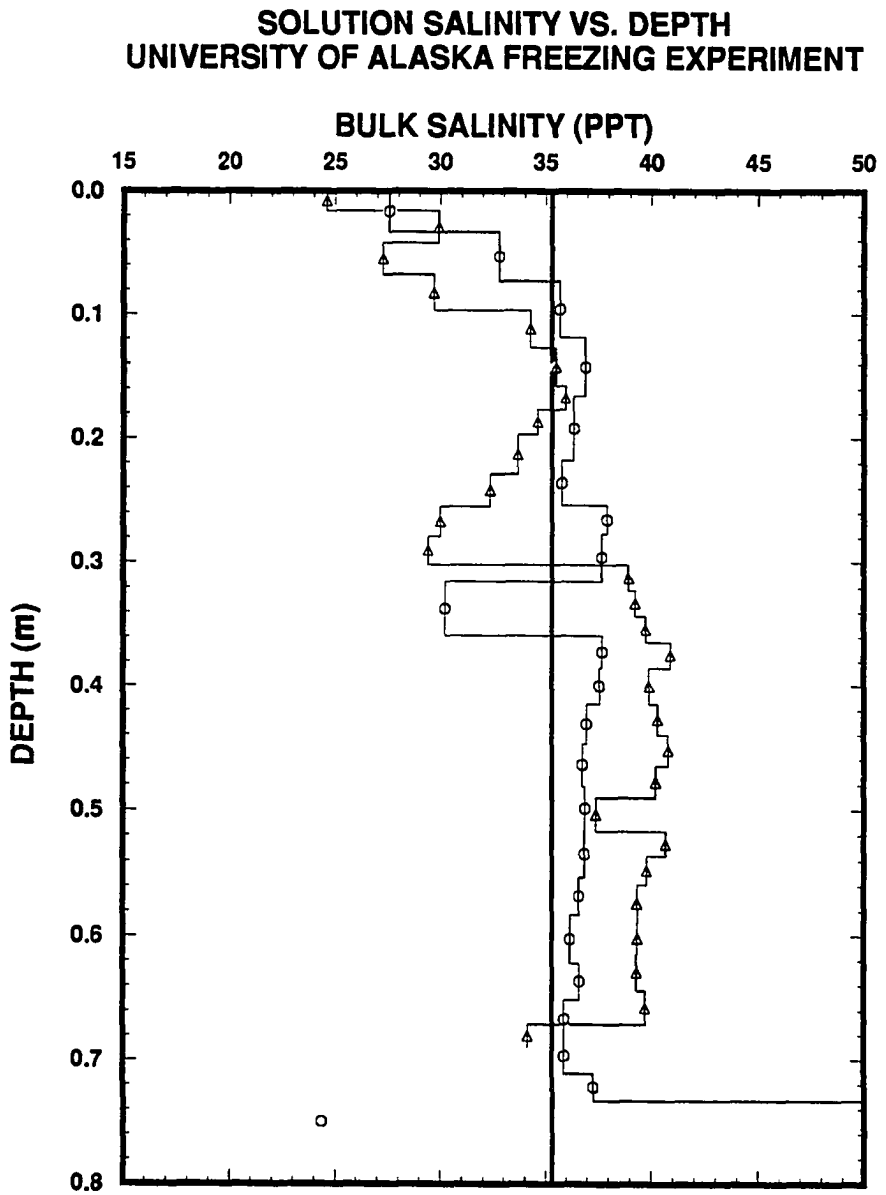

Figure 6.1: Bulk Salinity profiles from two columns frozen under natural freezing conditions in the field of the University of Alaska Experimental Farm. The columns were completely frozen when they were sectioned.

Baker (1987) froze columns saturated with 35 ppt solution at constant rates and with interfacial temperature gradients that were approximately 1 to 2 orders of magnitude greater than those that occur in natural freezing conditions and was able to fit his results with a steady state diffusive theory. This study has shown that when freezing rates and temperature gradients through the ice–bearing interface are imposed to approximate those that occur during freezeup, it is very difficult to predict whether convection of the pore fluid will occur. Further, it has been shown that the methods and techniques available to estimate the maximum amount of solute redistribution during freezing are quite limited.

A useful method to estimate the amount of solute redistribution during freezing may be to simply summarize the results of the freezing experiments performed in this study and the results presented by Wilson (1983), Chamberlain (1983), and Baker (1987). Wilson's results showed that freezing resulted in the lowering of the bulk salinity in the partially frozen region of the soil by between 26 to 43% of the initial solute concentration of a sandy gravel. Wilson's results also showed that the lower the initial solute concentration, the greater the percentage change in salinity. Chamberlain's one test in a sandy silt showed that freezing resulted in a maximum change in bulk salinity of 19%. Baker's freezing tests showed that freezing resulted in an approximately 50 to 75% reduction in salinity in the partially frozen region. In general, Baker's results show a greater amount of solute redistribution at the lower freezing rates. This investigation has shown freezing results in an approximately 30% reduction in bulk salinity when convection occurs. Results from these four studies may be generalized as follows: (1) the higher the freezing rate, the less salt redistribution (Baker 1987); (2) the greater the difference between the freezing temperature of the initial solution and the temperature which leads to freezing in the column, the greater the amount of salt redistribution (Baker's results compared with the results of this study); (3) the coarser the soil, the greater the permeability, and the more salt redistribution during freezing (Chamberlain's (1983) results compared to results from this study); and (4) the smaller the initial concentration the greater the salt redistribution (Wilson 1983).

6.3.3 Summary

In summary, several limitations associated with the finite size of the freezing experiment make it difficult to apply the results of this investigation to natural freezing situations. These limitations are the column length and radius, and the fixed temperature boundary conditions. This study has shown that the thawed layer underneath the partially frozen layer was important in determining the stability of the pore fluid. In natural freezing situations constant temperature boundary conditions are not present during freezing. Variable temperature boundary conditions may lead to the active layer completely freezing before convection of the pore fluid begins. When the freezing soil is not underlain by permafrost, the temperature gradient at the interface will not increase during freezing as it did in this study and the interface velocity may not decrease as quickly as it did in the soil columns. Since, the onset of convection requires a relatively stationary ice–bearing interface, natural freezing could lead to significantly greater transient periods between the start of freezing and the onset of convection. When determining the stability of the pore fluid, it is necessary to have a density gradient sufficiently unstable to overcome the dissipating effects of thermal diffusion. For Granusil 30 saturated with 35 ppt solution and surface temperatures between 2 to 7 °C below the freezing temperature of the solution, this density gradient appears to be on the order of -65 $\frac{kg}{m^4}$. A method for calculating the amount of solute redistribution during freezing that is consistent with the experimental observations does not exist. However, freezing generally led to a 30 to 70% decrease in solute concentration within the partially frozen region.

6.4 Recommendation for Areas of Additional Research

Conclusions drawn from this research suggest several areas which additional research should lead to significant insight into the mechanisms which lead to convection and solute redistribution in freezing sands. Additional research in these areas is important because they play a key role in understanding the processes that lead to convection and also because they are not understood well. Factors shown to be important in determining the stability of the fluid in the freezing of saturated

porous media include: the density gradient; the interaction between the thawed and partially frozen regions in the column; the permeability of the partially frozen region to fluid flow; and the dynamics of finger growth during the initial stages of freezing when the freezing rate is large. Of these, only the density gradient is sufficiently well known and this is the case only if the soil is coarse–grained enough that the mineral grains do not affect the freezing relationships. The purpose of this section is to discuss the additional research needed in these areas.

6.4.1 The Influence of the Thawed Region on the Stability of the Pore Fluid

This research suggests that the stability of the pore fluid in the column is dependent on the presence of a thawed layer underneath the partially frozen layer. The processes by which this thawed layer affects the stability of the pore fluid is unclear and must be investigated before a stability criterion that properly addresses the physical processes leading to convection can be developed. To understand the nature of this instability, laboratory experiments should be performed to determine the pertinent length scales and growth rates of the instability at the ice–bearing interface during the onset of convection. Numerical solutions, in at least two and possibly three directions, of the coupled equations on either side of the ice–bearing interface should be developed so that the critical temperature gradient may be determined. At this point there appears to be little hope of obtaining an analytical solution for the Rayleigh number of a form similar to the result presented by Wooding (1959).

The interaction between a partially solidified porous media and a fluid has only been recently addressed in the literature for the case of solidification of metals (Chen and Chen 1988). Results of this research suggests that the stability conditions are affected to a large degree by the presence of a fluid layer next to the porous medium. A similar coupling could be performed for a partially frozen porous medium above a thawed porous medium to determine the stability conditions. Such a method could be used to determine the critical Rayleigh number in the columns. Numerical modelling of the conditions during convection could be used to determine the flux of pore fluid associated with convection.

6.4.2 Dynamics of Finger Growth in Freezing Sand

The dynamics of finger growth in the partially frozen sand could be significantly different from the processes occurring at a miscible front of variable density and viscosity but constant permeability (Park and Homsy 1984, Homsy 1988). Displacement of the ice–bearing interface in the freezing columns is not a pressure displacement as in the case of most miscible displacements which have been studied. Rather, the interface displacement is due to the heat conduction and the instability is due to a phase transformation. In short, it is clear that the phase relations between brine and ice lead to the fluid instability, but it is not clear why the pore fluid did not convect when both the temperature gradient and freezing rate were large at the start of freezing. It would seem that large freezing rates somehow suppresses the onset of convection, however, it is not clear how this occurs in the freezing soil.

6.4.3 Permeability of Partially Frozen Sand

Knowledge of the permeability of the partially frozen region to fluid flow is an essential parameter for virtually any analysis involving fluid flow during convection in a porous medium. Metallurgists investigating phenomena associated with macrosegregation in metals have developed techniques to measure the permeability in a structured medium in each of the 3 different directions. Complications with such measurements are associated with temperature control of the medium and making certain that the hydraulic gradients are such that local remelting of the sample does not occur (Nasser–Rafi, et al. 1985).

Permeability measurements of the partially frozen region as a function of brine volume will determine the temperature dependance of the power relationship between brine volume and permeability. Knowledge of the dependence of permeability on temperature will allow the pressure gradient at the onset of convection to be determined.

6.4.4 Summary

In summary, three main research topics are required to further address the processes that lead to convection in columns of sand saturated with saline solution

and then frozen. These topics include: the effects of the thawed layer underneath the partially frozen layer on the stability of the pore fluid; the dynamics of growth of the instability in a partially frozen media and the effects of a moving phase boundary on the growth of the instability; and the partially frozen permeability of a porous material containing saline solution. Addressing these three topics will lead to further questions, the directionality of permeability in the partially frozen region for example. However, they should also lead to new insights into the nature of the instabilities that occur during freezing of a partially frozen porous material containing saline solution.

Bibliography

[1] Aguirre-Puente, J., Fremond, M., 1976. Frost and Water Propagation in Porous Media. Proceedings of the Second Conference on Soil–Water Problems in Cold Regions. National Research Council, Canada, pages 137–154.

[2] Alcoa Structural Handbook, 1960. Aluminum Company of America, Pittsburgh. Pennsylvania, 353 pages.

[3] Assur, A., 1958. Composition of Sea Ice and Its Tensile Strength. Arctic Sea Ice. National Academy of Science–National Research Council, Division of Earth Sciences, pages 106–138.

[4] Baird, D.C., 1962. Experimentation: An Introduction to Measurement Theory and Experiment Design. Prentice-Hall, 198 pages.

[5] Baker, G.C., 1987. Salt Redistribution During Freezing of Saline Sand Columns With Applications to Subsea Permafrost. Ph.D. Thesis, 232 pages. University of Alaska Fairbanks. Fairbanks. Alaska.

[6] Baker. G.C., 1987a. Electrical Conductivity. Freezing Temperature, and Salinity Relationships for Seawater and Sodium Chloride Solutions for the Salinity Range from 0 to Over 200 ppt. Geophysical Institute Report UAG R–309. University of Alaska Fairbanks, Fairbanks, Alaska. 99775–0800. 87 pages.

[7] Baker. G.C., Osterkamp, T.E., 1988. Implications of Salt Fingering For Salt Movement in Thawed Coarse-Grained Permafrost. Cold Regions Science and Technology, Vol. 15, pages 45–52.

[8] Baker, G.C., Osterkamp, T.E., 1989. Salt Redistribution During Freezing of Saline Sand Columns at Constant Rates. Water Resources Research. Vol. 25, No. 8, pages 1825–1831.

[9] Baker. G.C., Osterkamp, T.E., Matava, T., 1990. Brine Movement During Freezing of Saline Sand Columns. Proceedings of the Fifth Canadian Permafrost Conference, National Research Council of Canada. pages 69–75.

[10] Bear, J., 1972. Dynamics of Fluids in Porous Media. American Elsevier Publishing Co. Inc., New York. 764 pages.

[11] Black, P.B., 1990. Three Functions that Model Emperically Measured Unfrozen Water Content Data and Predict Relative Hydraulic Conductivity. USA-CRREL, Report 90-5, 7 pages.

[12] Burton, J.A., Prim, C.S., Schlichter, J.S., 1953. The Distribution of Solutes in Crystals Grown from the Melt, Part I, Theoretical. Journal of Chemical Physics, Vol. 21, No. 11, pages 1987–1991.

[13] Burton, J.A., Prim, C.S., Schlichter, J.S., 1953a. Distribution of Solutes in Crystals Grown from the Melt, Part II, Experimental. Journal of Chemical Physics, Vol. 21, No. 11, pages 1991–1996.

[14] Carslaw, H.S., Jaeger, J.C., 1959. Conduction of Heat in Solids. Clarendon Press, 510 pages.

[15] Cary, J.W., Mayland, H.F., 1972. Salt and Water Movement in Unsaturated Frozen Soil. Soil Science Society of America Proceedings, Vol. 36, pages 549–555.

[16] Chamberlain, E.J., 1983. Frost Heave of Saline Soils. Proceedings of The Fourth International Permafrost Conference, National Academy Press, pages 121–126.

[17] Chen, F., Chen, C.F., 1988. Onset of Finger Convection in a Horizontal Porous Layer Underlying a Fluid Layer. Journal of Heat Transfer, Vol. 110, pages 403-409.

[18] Cho, S.H.. Sunderland, J.E., 1969. Heat Conduction Problems with Melting or Freezing. Journal of Heat Transfer, Vol. 91, pages 421–426.

[19] Cobb, A.,W.. Gross, G.,W., 1969. Interfacial Electrical Effects Observed During the Freezing of Dilute Electrolytes in Water. Journal of Electrochemical Science, Vol. 116, No. 6, pages 796–804.

[20] Cox, G.F.N.. Weeks, W.F., 1975. Brine Drainage and Initial Salt Entrapment in Sodium Chloride Ice. USA–CRREL, Research Report 354, 85 pages.

[21] Eide, L.. Martin, S.. 1975. The Formation of Brine Drainage Features in Young Sea Ice. Journal of Glaciology, Vol. 14, No. 70, pages 137–154.

[22] Farouki, O.. 1982. Evaluation of Methods for Calculating Soil Thermal Conductivity. USA–CRREL Res. Report 82-8. Hanover, New Hampshire. 90 pages.

[23] Flemings, M.C.. 1974. Solidification Processing, McGraw–Hill, 364 pages.

[24] Glicksman, M.E.. Copley, R.A.. Coriel, P.J.. 1986. Interaction of Flows with the Crystal–Melt Interface. Annual Reviews of Fluid Mechanics, Vol. 18, pages 307–335.

[25] Gosink, J.P.. Baker, G.C., 1990. Salt Fingering in Subsea Permafrost: Some Stability Energy Considerations. Journal of Geophysical, Vol. 95, No. C5, pages 9575–9584.

[26] Hallet, B.. 1978. Solute Redistribution in Freezing Ground. Proceedings of The Third International Permafrost Conference, Canadian National Research Council, pages 86–91.

[27] Heiss, J.F.. Kuhajek, E.J.. 1983. Sodium Compounds. Encyclopedia of Chemical Technology, Third Edition. Vol. 21, pages 205–223.

[28] Hillel, D.. 1980. An Introduction to Soil Physics. Academic Press, 364 pages.

[29] Hoekstra, P., 1966. Moisture Movement in Soils Under Temperature Gradients with the Cold-Side Temperature Below Freezing. Water Resources Research, Vol. 2, pages 241–250.

[30] Homsy, G.M., Sherwood, A.E., 1976. Convective Instabilities in Porous Media with Through Flow. American Institute of Chemical Engineers, Vol. 22. No. 1. pages 168–174.

[31] Homsy, G.M., 1987. Viscous Fingering in Porous Media. Annual Review of Fluid Mechanics, Vol. 19. pages 271–311.

[32] Homsy, G.M., 1989. The Effect of Dispersion on Fingering in Miscible Displacements. In Disorder and Mixing, Nato Advanced Studies Institute. E. Guyon. et al. ed., pages 237–251.

[33] Horiguchi. K., Miller. R.D., 1983. Hydraulic Conductivity Functions of Frozen Materials. Proceedings of The Fourth International Permafrost Conference. National Academy Press. pages 504–508.

[34] Johnson, P.R., Hartman, C.W., 1971. Environmental Atlas of Alaska. University of Alaska. College, Alaska. 111 pages.

[35] Kay and Groenevelt, P.H., 1983. The Redistribution of Solutes in Freezing Soil: Exclusion of Solutes. Proceedings of The Fourth International Permafrost Conference. National Academy Press, pages 584–588.

[36] Kay, B.D., Perfect. E., 1988. State of the Art: Heat and Mass Transfer in Freezing Soils. Proceedings of The Fifth International symposium on Ground Freezing. Jones and Holden ed., pages 3–21.

[37] Konrad. J.M., 1989. Ice Formation in Saline Soils. Volumes 1 thru 3. Geological Survey of Canada. Open File 2117.

[38] Korkina, R.I., 1975. Electrical Potentials in Freezing Solutions and their Effect on Migration. USA-CRREL. Draft Translation 490, 15 pages.

[39] List, R.J.. 1951. Smithsonian Meteorological Tables, 6th Edition. Smithsonian Institution, Washington D.C.

[40] Loon, W.K.P. van, Perfect, E.. Groenevelt, P.H., 1990. Application of Time Domain Reflectometry to Measure Solute Redistribution During Soil Freezing. Proceedings of Frozen Soil Impacts on Agricultural, Range and Forest Lands, K.R. Cooley ed.. USA-CRREL, Special Report 90-1, pages 186-194.

[41] Lunardini. V.J.. 1981. Heat Transfer in Cold Climates. Van Nostrand Reinhold. 731 pages.

[42] Lunardini. V.J.. 1988. Heat Conduction with Freezing or Thawing. USA-CRREL. Monograph 88-1. 329 pages.

[43] Mahar. L.J.. Wilson. R.M.. Vinson. T.S.. 1983. Physical and Numerical Modeling of Uniaxial Freezing of a Saline Gravel. Proceedings of The Fourth International Permafrost Conference. National Academy Press. pages 773-778.

[44] Maples. A.L.. Poirer. D.R.. 1984. Convection in the Two Phase Zone of Solidifying Alloys. Metallurgical Transactions B, Vol. 15B, pages 163-172.

[45] Miller. R.D.. Lock. J.P.G., Bresler. E.. 1975. Transport of Water and Heat in a Frozen Permeameter. Journal of the Soil Science Society of America. Vol. 39. pages 1029-1036.

[46] Nakawo. M.. Sinha. N.K., 1981. Growth Rate and Salinity Profile of First Year Sea Ice. Journal of Glaciology. Vol. 27. No. 96, pages 315-330.

[47] Nasser-Rafi. R.. Deshmukh. R.. Poirer. D.R., 1985. Flow of Interdendritic Liquid and Permeability in Pb-20 Wt Pct Sn Alloys. Metallurgical Transactions A. Vol. 16A. pages 2263-2271.

[48] Niedrauer. T.M., Martin, S., 1979. An Experimental Study of Brine Drainage and Convection in Young Sea Ice. Journal of Geophysical Research. Vol. 84, no. C3, pages 1176–1186.

[49] Oliphant, J.L., Tice, A.R., Nakano, Y., 1983. Water Migration Due to a Temperature Gradient in Frozen Soil. Proceedings of The Fourth International Permafrost Conference. National Academy Press, pages 951–956.

[50] Ono. N., 1975. Thermal Properties of Sea Ice. Part 4: Thermal Constants of Sea Ice. USA–CRREL. Draft Translation 467.

[51] Osterkamp. T.E., 1984. Temperature Measurements in Permafrost. State of Alaska. Department of Transportation and Public Facilities, Fairbanks. Alaska. Report No. FHWA-AK-RD-85-11, 87 pages.

[52] Osterkamp. T.E., 1987. Freezing and Thawing of Soils and Permafrost Containing Unfrozen Water and Brine. Water Resources Research, Vol. 12. No. 12. pages 2279–2285.

[53] Osterkamp. T.E., Walker. G.G., 1987. Temperature Variation of the Thermal Properties of Ice. University of Alaska. Geophysical Institute Report. UAGR-309. University of Alaska Fairbanks. 99775-0800, 16 pages.

[54] Page. A.L., Jackson. R.A., Chamberlain. R., 1982. Methods of Soil Analysis–Part II. Second Edition. Soil Science Society of America Inc., 1159 pages.

[55] Park. C.W., Homsy. G.M., 1984. Two Phase Displacement in Hele–Shaw Cells: Theory. Journal of Fluid Mechanics. Vol. 139. pages 291–308.

[56] Perfect. E., Williams. P.J., 1980. Thermally Induced Water Migration in Frozen Soils. Cold Regions Science and Technology. Vol. 3, pages 101–109.

[57] Piwonka, T.S., Flemings, M.C., 1966. Pore Formation in Solidification. Transactions of the Metallurgical Society, Vol. 236, pages 1157–1165.

[58] Rutter, J.W., Chalmers, J.B., 1953. A Prismatic Substructure Formed During the Solidification of Metals. Canadian Journal of Physics, Vol. 1, pages 15–39.

[59] Saffman, P.G., Taylor, G. 1958. The Penetration of a Fluid into a Porous Medium or Hele–Shaw Cell Containing a more Viscous Liquid. Proceedings of the Royal Society A. Vol. 245, pages 312–329.

[60] Skoog, D.A., 1985. Principles of Instrumental Analysis. CBS College Publishing, 851 pages.

[61] Standard Practice for Description and Identification of Soils (Visual and Manual Procedure), Test D2488–84. American Society for Testing and Materials, Philadelphia, Pa., 15 pages.

[62] Standard Test Methods for Electrical Conductivity and Resistivity of Water, Test S1125–82. American Society for Testing and Materials, Philadelphia, Pa., 8 pages.

[63] Standard Test Method for Particle Size Analysis of Soils, Test D422–63. American Society for Testing and Materials, Philadelphia, Pa., 10 pages.

[64] Standard Test Method for Permeability of Granular Soils (Constant Head), Test D2434–66. American Society for Testing and Materials, Philadelphia, Pa., 7 pages.

[65] Steinhart, T.S., Hart, S.R., 1968. Calibration Curves for Thermistors. Deep-Sea Research, Vol. 15, pages 497-503.

[66] Sturm, M., 1990. The Role of Thermal Convection in Heat and Mass Transport in The Subarctic Snow Cover. Ph.D. Thesis, 189 pages, University of Alaska Fairbanks, Fairbanks, Alaska.

[69] Viskanta, R., 1988. Heat Transfer During Melting and Solidification of Metals. Journal of Heat Transfer, Vol. 110, pages 1205–1219.

[70] Voller, V.R., Cross, M., 1981. Accurate Solutions of Moving Boundary Problems Using the Enthalpy Method. Internation Journal of Heat and Mass Transfer, Vol 24, No. 6, pages 545–536.

[71] Voller, V.R., et al. 1989. The Modelling of Heat, Mass and Solute Transport in Solidification Systems. International Journal of Heat and Mass Transfer, Vol. 32, No. 9, pages 1719–1731.

[72] Weast, R.C., 1976. CRC Handbook of Chemistry and Physics. CRC Press Inc., West Palm Beach, Florida.

[73] Weeks, W.F., 1962. Tensile Strength of NaCl ice. Journal of Glaciology, Vol. 4, No. 31, pages 25–52.

[74] Weeks, W.F., Lofgren, G., 1967. The Effective Solute Distribution Coefficient During the Freezing of NaCl Solutions. In Physics of Snow and Ice, H. Oura ed., Institute of Low Temperature Science, Hokkaido, Japan, Vol. 1, No. 1, pages 579–597.

[75] Weeks, W.F., Ackely, S.F., 1982. The Growth, Properties and Structure of Sea Ice. USA–CRREL, Monograph 82-1, 130 pages.

[76] Wilson, R.C., 1983. Solute Redistribution and Freezing Rates in a Coarse–Grained Soil Saturated With Saline Porewater, M.S. Project Report, 212 pages, Oregon State University, Corvallis, Oregon.

[77] Wooding, R.A., 1959. The stability of a Viscous Liquid in a Vertical Tube Containing Porous Material. Proceedings of The Royal Society A, Vol. 252, pages 120–134.

[78] Wooding, R.A., 1960. Rayleigh Instability of a Thermal Boundary Layer in Flow Through a Porous Medium. Journal of Fluid Mechanics, Vol. 9, pages 183–192.

[79] Workman, E.J., Reynolds, S.E., 1950. Electrical Phenomena Occurring During the Freezing of Dilute Aqueous Solutions and their Possible Relationship to Thunderstorm Activity. Physical Reviews, Vol. 258, No.3, pages 254–260.

[80] Wuttig, F.J., 1988. Occurrence, Distribution and Movement of Salts and Moisture in Permafrost Near Fairbanks, Alaka. M.S. Thesis, 120 pages, University of Alaska Fairbanks, Fairbanks, Alaska.

[81] Yoneyama, K., et al. 1983. Water Redistribution Measurements in Partially Frozen Soil By X–Ray Technique. Proceedings of The Fourth International Permafrost Conference, National Academy Press, pages 1445–1450.

[82] Yong, R.N., et al. 1978. Prediction of Salt Influence on Unfrozen Water Content in Frozen Soils. Proceedings of The First International Symposium on Ground Freezing, H.L. Jessberger ed., pages 137–156.

[83] Zegelin, S.J., et al. 1989. Improved Field Probes for Soil Water Content and Electrical Conductivity Measurements Using Time Domain Reflectrometry. Water Resources Research, Vol. 11, pages 2367–2376.

[84] Zubov, N.N., 1963. Arctic Ice. Translated from Russian by U.S. Naval Electronics Laboratory, San Diego, California, 360 pages.

Appendix A

Stability Theory

A.1 Introduction

Phase relationships between brine and ice show that freezing a saline solution from the top down results in an instability in the pore fluid due to dense brine overlying less dense brine. During the growth of sea ice, it is this instability and the resulting convection that leads to the progressive desalinization of the ice. During the growth of ice in a coarse–grained porous material saturated with saline solution the same phase relationships apply which result in desalinization of the partially frozen portion of the porous material. However, because the porous material has a much lower permeability than sea ice, transients in the movement of solutes have longer time scales and can be more readily observed than in sea ice (see Baker 1987, Table 3.10 and Chapter 4 of this text). The purpose of this appendix is to develop the theoretical concepts which may be applied to determine the stability of dense fluid overlying less dense fluid in a porous medium of variable permeability. This theory will be developed for the conditions present in a long (with respect to diameter) vertical tube in which the permeability is small on the top and large on the bottom and in which the density is large on top and small on the bottom (the development will not consider the partially frozen layer to be underlain by a thawed layer). Both density and permeability will be considered continuous along the length of the tube and the pore fluid is taken to be completely miscible throughout the column. The development presented here is similar to that presented by Wooding (1 who considered constanpermeability and no throughflow velocity through aniform porous column. In this development, the permeability will vary and a constant throughflow velocity will be imposed on the system. This

appendix consists of three sections. In the first section the relationship between brine volume and permeability will be presented. This is followed by a section in which the base state, or zero order state of the problem is defined. The appendix is concluded with a section on the appropriate form of the linear stability analysis for the scaled field equations. A discussion of the application of this theory to the experimental results of the laboratory investigation is presented in Chapter 5 of the main body of this work.

A.2 Permeability of Partially Frozen Sand

Unfrozen water in a porous material occurs when the change in phase from solid to liquid or liquid to solid occurs over a range of temperatures instead of at a single temperature. The partially frozen material, therefore, may have a significant, but reduced, permeability. In fine–grained soils that do not contain solutes, mineral grain surface effects lead to the presence of unfrozen water at temperatures below the freezing point of the fluid. Solutes in the pore fluid result in the change in phase occurring over a range in temperatures, similar to the surface effects, but the temperature range over which a solute can affect the volume of unfrozen solution is much greater. For example, unfrozen water in a soil due to surface effects occurs within only several 0.1 °C of the freezing point, but a soil saturated with a 35 ppt NaCl solution will contain significant amounts of unfrozen water at temperatures 7 to 10 °C below the freezing point of the solution. Hydraulic conductivity measurements on fine–grained soils show that the conductivity drops 4 orders of magnitude within 0.3 °C of the freezing point (Perfect and Williams, 1980). These results have been fit with a single power of temperature over the temperature range. Hydraulic conductivity measurements in a coarse–grained soil saturated with a solute have not been made; however, it is not clear, nor is it realistic to expect that the permeability could be fit with one single curve over such a large temperature range.

Metallurgists interested in understanding the physical processes associated with macrosegregation between the solidus and liquidus in solidifying melts have performed measurements to determine the permeability of this partially solidified region. An early study of the permeability of partially solidified binary melts was performed by Piwonka and Flemings (1966) who measured the permeability of

a copper aluminum alloy. Results of their research showed that permeability is related to brine volume according to

$$k = k_o V_{AU}{}^n \tag{A.1}$$

where k_o is the reference permeability, V_{AU} is the absolute brine volume and n is an integer which depends on the brine volume. For $V_{AU} < 0.3$, it was found that $n = 2$. For $V_{AU} \geq 0.3$, $n = 7$. Subsequent research on solidifying metals indicated that the permeability of the partially frozen medium is a tensor, and that flow direction affected values of the permeability (Nasser–Rafi, et al. 1985). Equation A.1 will be used as a measure of the permeability of the partially frozen medium. The reference permeability, k_o, will be taken as the thawed permeability of Granusil 30. Equation A.1 and the dependence of n on the brine volume is a generalization of the single value of n that has been used by Perfect and Williams (1980) to describe the relationship between permeability and brine volume in a partially frozen fine–grained soil.

A.3 Base State Conditions

Base state conditions in the partially frozen soil are the steady, non-convecting, conditions on which convection will be superposed. In this case, the freezing conditions and distribution of the solute in the sand prior to the onset of convection will be regarded as the base state. The purpose of this section is to present these base state conditions for the instability which will be discussed in the next section.

Consider a fluid in a vertical column which consists of contrasting densities and permeabilities as discussed in the introduction. The vertical column is assumed to be contained between two plates with the bottom plate temperature at the freezing temperature of the pore fluid (T_F) and the top plate at some colder temperature which is warmer than the eutectic temperature of the solution. The plates of the column are assumed to be located far enough from the point of interest that boundary conditions imposed at the end of the column are unimportant. It is assumed that (1) meeting the thermal conditions discussed above have not resulted in any initial redistribution of the solute and that (2) the bulk salinity profile is constant throughout the column. Superposed upon these conditions, assume the presence of a steady weak throughflow on the system in the negative, downward,

direction[1]. Superposition of a very weak, but constant, throughflow on this system does not appreciably affect the thermal field of the system because the flow velocity is assumed to be small enough that the thermal Peclet number for the soil is small. Consequently, fluid flows through the system at a rate small enough that the heat conduction isotherms are not significantly affected by movement of the fluid. Vertical changes in brine volume are assumed to be small within the neighborhood of the region considered which makes it possible to obtain a spatially constant velocity in the vertical direction. It is assumed that the throughflow velocity is small enough that the distribution of the solute is not affected by this flow [2]. Since the system as it has been described is steady and one dimensional, the momentum equation may be written as

$$0 = -\frac{\partial P}{\partial x} + \frac{\mu}{k}u - \rho g \tag{A.2}$$

where P is pressure, μ is the viscosity, u is velocity, ρ is the density, and g is gravity. The pressure gradient in equation A.2 is due to the combined effects of brine density and flow velocity. The sign on the Darcy and gravitational terms reflect the choice of the positive x direction being directed vertically upward.

The location where the instability will occur is assumed to be the position where the contrast in the destabilizing pressure force is greatest. The pressure gradient across the interface may be written as

$$\delta P = [\mu u(\frac{1}{k_2} - \frac{1}{k_1}) - (\rho_2 - \rho_1)g]\delta x. \tag{A.3}$$

Where subscripts 1 and 2 refer to the top and bottom layers, respectively. The velocity, u, is considered constant across the layers since only small variations in brine content, or porosity of the partially frozen soil, can result in large permeability changes according to equation A.1. For freezing saline soils, the viscosity is only slightly temperature dependant compared to the permeability contrasts and is also taken as constant. The density, ρ, is temperature dependant and contributes

[1]In this development throughflow is superimposed on the system so that it may be treated as steady. In practice throughflow is due to brine expulsion during ice formation and is not steady, nor spatially constant throughout the column, however, it is to be considered constant in the neighborhood of the point to be considered.

[2]Although the assumption that throughflow associated with brine expulsion does not affect the bulk salinity is not strictly valid, experimental observations have shown that the amount of the solute advected by this throughflow to be quite small.

to the instability of the fluid. There are two limiting cases in which $\delta P < 0$ that demonstrate the applicability of equation 1.3. The first case occurs when $k_1 = k_2$ (constant permeability), $\rho_2 < \rho_1$ which implies more dense fluid overlies less dense fluid. The second limiting case occurs when $\rho_1 = \rho_2$ and $k_2 < k_1$, which implies a more permeable material overlies a less permeable one. These two cases match the intuitive expectation for the occurrence of the instability.

If the pressure gradient on the upper surface is greater than the pressure gradient on the lower surface, then δP is < 0 and the interface is unstable to perturbations. If the pressure gradient on the lower surface is greater than the pressure gradient on the upper surface, then δP is > 0 and the interface is stable. It is clear that given the permeability and density contrasts discussed earlier, dense fluid overlying less dense fluid, a downward velocity of sufficient magnitude will stabilize the otherwise unstable density gradient generated by freezing. A similar analysis has been used in porous media of constant permeability but with a variable viscosity to show that fluid flow in a porous media can either stabilize or further destabilize the fluid (Saffmann and Taylor 1958, Wooding 1960, Homsy and Sherwood 1976, Park and Homsy 1984, Homsy 1989). However, in this analysis only the permeability is allowed to vary since freezing is likely to lead to large permeability changes, but the viscosity will change by only 50% between -4 and -10 °C (Cox and Weeks 1975).

Through the simple analysis presented here the destabilizing pressure force as well as a stabilizing pressure force may be identified. The presence of a stabilizing pressure force depends on the flow direction and permeability contrast. The destabilizing pressure force is due to the density contrast. The right hand side of equation A.3 must be negative for an instability to grow. However, the equation offers no insight into the timing for the onset of the instability or the wavenumber it will have once it begins. Consequently, $\delta P < 0$ in equation A.3 may be thought of as a necessary condition for the onset of an instability. The necessary and sufficient conditions for an instability to grow will be discussed in the next section.

A.4 Linear Stability Analysis

Establishing necessary and sufficient conditions for the onset of a gravitational instability in either a pure fluid or a fluid contained in a porous medium usually involves determining a critical Rayleigh number for the fluid where the Rayleigh number is a ratio of the destabilizing forces to stabilizing forces. Derivation of the Rayleigh number for the onset of an instability results from linearization of equations which describe the incompressibility of the fluid, conservation of momentum, and either conservation of species (concentration for example) or energy (through the temperature of the system for example). The purpose of this section is to derive a Rayleigh number for the fluid in a partially frozen porous medium using a linear stability analysis and to apply the analysis to the conditions present in the columns frozen in the freezing apparatus. Throughout this section the formulation of Wooding (1959) will be used, however, with the modifications discussed above.

The stabilizing forces in the fluid are viscosity, and molecular and thermal diffusivity. However, since the unknowns are pressure, velocity and concentration, only three equations are necessary to describe the system. Since the concentration of brine is specified by the temperature and since the thermal diffusivity of the brine is orders of magnitude greater than the molecular diffusivity, the appropriate expression to describe the conservation of brine is the energy equation. The three field equations applied to this problem are

$$0 = \vec{\nabla} \cdot \vec{u} \tag{A.4}$$

$$\rho \frac{\partial \vec{u}}{\partial t} = -\vec{\nabla} P - \frac{\mu}{k} \vec{u} + \rho \vec{\mathrm{g}} \tag{A.5}$$

$$\left(C_m - L\eta \frac{dV_{AU}}{dT} \right) \frac{\partial T}{\partial t} + \frac{C_f}{\eta V_{AU}} \vec{u} \cdot \vec{\nabla} T = \vec{\nabla} \cdot \alpha_m \vec{\nabla} T \tag{A.6}$$

where C_f is the heat capacity of the fluid, C_m is the heat capacity of the medium, α_m is the thermal conductivity of the medium, L is the latent heat of the pore fluid, η porosity and V_{AU} is the brine volume. Together ηV_{AU} form the porosity of the partially frozen material. The velocity is defined as $\vec{u}$ and is the Darcy velocity of the pore fluid. The advective term in equation A.6 has the partially frozen porosity included to scale the Darcy velocity to the velocity of the fluid through the pore space.

Boundary conditions for this problem are applied only to the wall of the tube

since it is considered long compared to the diameter. At the wall of the tube no material enter or leaves the tube so the horizontal velocity is zero. Also, observations indicate that it is not necessary to apply the no-slip velocity boundary condition at the wall of the tube since fluid flow is concentrated along this boundary. A non-zero velocity is assumed rather than the physically correct no-slip boundary condition to match the observations. The boundary condition for vertical velocity is that the horizontal gradient in the vertical velocity is zero at the wall of the tube. These two boundary conditions may be expressed as

$$v = w = 0 \tag{A.7}$$

$$\frac{\partial \vec{u}}{\partial \hat{n}} = 0 \tag{A.8}$$

$$\tag{A.9}$$

where u is the vertical component of velocity, and v and w are the two horizontal components of velocity.

Two elements important in this derivation are the change in density and permeability associated with changes in temperature. These two relations may be expressed as

$$\rho = \rho_o(1 + \beta(T - T_F)) \tag{A.10}$$

$$k = k_o(1 + \gamma(T - T_F)) \tag{A.11}$$

where the relations between temperature and density and permeability have been linearized. The variation in density with temperature is expressed as β

$$\beta = \frac{1}{\rho_o}\frac{\partial \rho}{\partial T} \tag{A.12}$$

$$= \frac{1}{\rho_o}\left(\frac{d\rho_b}{dS_b}\frac{dS_b}{dT} + \frac{d\rho_{water}^{pure}}{dT}\right) \approx \frac{1}{\rho_o}\frac{d\rho_b}{dS_b}\frac{dS_b}{dT} = \frac{-.013}{^\circ\mathrm{C}}. \tag{A.13}$$

Where ρ_b and S_b are the density and salinity of the brine. Similarly, the variation in permeability with temperature is expressed through γ which is defined as

$$\gamma = \frac{1}{k_o}\frac{\partial k}{\partial T} \tag{A.14}$$

$$= nV_{AU}^{n-1}\frac{dV_{AU}}{dT} \approx -n\frac{S_i^n}{S_b^{n+1}}\frac{dS_b}{dT} = \frac{2.2}{^\circ\mathrm{C}}. \tag{A.15}$$

Both γ and β have been calculated for T_F near the freezing temperature of a 35 ppt solution.

Perturb the system of equations, A.4 through A.6, by letting $\theta = T - T_F$, and let each of the variables of interest consist of average and fluctuating terms according to

$$\begin{aligned}
\vec{u} &= \bar{\vec{u}} + \vec{u}' \\
\theta &= \bar{\theta} + \theta' \\
P &= \bar{P} + p' \\
\rho &= \bar{\rho} + \rho' = \rho_o(1 + \beta\bar{\theta}) + \rho_o\beta\theta' \\
k &= \bar{k} + k' = k_o(1 + \gamma\bar{\theta}) + k_o\gamma\theta'
\end{aligned}$$

Since 0^{th} order quantities are properties of the base state and 2^{nd} order and higher quantities are assumed to be small, they and higher order terms may be subtracted from the field equations to give three equations which contain only first order terms. These three field equations may be expressed as

$$\vec{\nabla} \cdot \vec{u}' = 0 \qquad \text{(A.16)}$$

$$-\vec{\nabla}p' - \mu\left(\frac{\vec{u}'}{\bar{k}} - \frac{k'\bar{\vec{u}}}{\bar{k}^2}\right) + \rho'\vec{g} = \bar{\rho}\frac{\partial \vec{u}'}{\partial t} \qquad \text{(A.17)}$$

$$\left(C_m - L\eta\frac{dV_{AU}}{dT}\right)\frac{\partial\theta'}{\partial t} + \frac{C_f}{\eta V_{AU}}(\vec{u}' \cdot \vec{\nabla}\bar{\theta} + \bar{\vec{u}} \cdot \vec{\nabla}\theta') = \vec{\nabla} \cdot \alpha_m \vec{\nabla}\theta' \qquad \text{(A.18)}$$

The Boussinesq approximation will be used to perturb the density term. The term $\left(C_m - L\eta\frac{dV_{AU}}{dT}\right)$ is considered to be relatively constant over small temperature ranges as will the partially frozen porosity term. The velocity and permeability perturbation terms in the momentum equation were solved by writing the Taylor series expansion to the permeability term. This may be expressed as

$$\frac{\bar{\vec{u}} + \vec{u}'}{\bar{k} + k'} = \frac{\bar{\vec{u}} + \vec{u}'}{\bar{k}}\left(1 - \frac{k'}{\bar{k}} + \left(\frac{k'}{\bar{k}}\right)^2 + \ldots\right) \qquad \text{(A.19)}$$

Prior to the onset of convection the gradient in the average temperature is one dimensional in the vertical direction. Similarly, throughflow which occurs in the base state, expressed as $\bar{\vec{u}} = W$, acts only in the vertical direction and is constant. Scaling the field equations with these assumptions and definitions, and substituting in the temperature dependence for the average and fluctuating

permeability terms, the three scaled field equations may be written in terms of three variables: velocity, pressure and temperature.

$$\vec{\nabla} \cdot \vec{u}' = 0 \tag{A.20}$$

$$-\vec{\nabla} p' - \mu\left(\frac{\vec{u}'}{k_o(1+\gamma\bar{\theta})} - \frac{\gamma\theta' W}{k_o(1+\gamma\bar{\theta})^2}\right) + \rho_o\beta\vec{g}\theta' = \bar{\rho}\frac{\partial\vec{u}'}{\partial t} \tag{A.21}$$

$$\frac{\eta V_{AU}}{C_f}\left(C_m - L\eta\frac{dV_{AU}}{dT}\right)\frac{\partial\theta'}{\partial t} + W\frac{\partial\theta'}{\partial x} + u'\frac{dT}{dx} = D\nabla^2\theta' \tag{A.22}$$

where $D = \frac{\alpha_m \eta V_{AU}}{C_f}$ is an effective diffusivity which will be taken as a constant in the neighborhood of the instability.

As usual, the pressure term is eliminated from the momentum equation with the use of the continuity equation which reduces the three field equations to two scalar equations containing only perturbed vertical velocity and pressure terms. Following the formulation of Wooding (1959), each of the three spatial directions are scaled to a characteristic length, b, with the exception of the term in the average temperature gradient with distance, to give

$$\rho\frac{\partial\nabla^2 u'}{\partial t} + \frac{\mu}{k_o(1+\gamma\bar{\theta})}\nabla^2 u' - \frac{\mu\gamma b}{k_o(1+\gamma\bar{\theta})^2}\frac{\partial u'}{\partial X}\frac{dT}{dx} = -(\rho_o\beta g - \frac{\mu\gamma W}{k_o(1+\gamma\bar{\theta})^2})\nabla_H^2\theta' \tag{A.23}$$

$$b^2\frac{\eta V_{AU}}{C_f}\left(C_m - L\eta\frac{dV_{AU}}{dT}\right)\frac{\partial\theta'}{\partial t} + bW\frac{\partial\theta'}{\partial X} + b^2 u'\frac{dT}{dx} = D\nabla^2\theta'. \tag{A.24}$$

The horizontal Laplacian is denoted as ∇_H^2. The third term on the left in equation A.21 is due to the variation in $\bar{\theta}$ with x.

A solution to these two equations involves seeking a separable solution of the form

$$u' = U(X)\Phi(r,\phi)\exp\omega t \tag{A.25}$$

$$\theta' = \Theta(X)\Phi(r,\phi)\exp\omega t \tag{A.26}$$

with limits of $0 < r < 1$ and $0 < X < \frac{x}{b}$. A property of Φ is that it satisfies $\nabla_H^2\Phi = -\zeta^2\Phi$ which is Helmholtz' equation on a circle. Expressions of u' and θ' substituted into the two equations above reduce the two partial differential equations into ordinary differential equations in terms of U and Θ with the result

$$\frac{\mu}{\bar{k}}(1+\frac{\bar{k}\bar{\rho}\omega}{\mu})(U'' - \zeta^2 U) - \frac{\mu\gamma b k_o}{\bar{k}^2}U'\frac{dT}{dx} = \zeta^2(\rho_o\beta g - \frac{\mu\gamma k_o W}{\bar{k}^2})\Theta \tag{A.27}$$

$$b^2\frac{\eta V_{AU}}{C_f}\left(C_m - L\eta\frac{dV_{AU}}{dT}\right)\omega\Theta + bW\Theta' + b^2U\frac{dT}{dx} = D(\Theta'' - \zeta^2\Theta) \qquad \text{(A.28)}$$

Substitution of a functional form of the disturbance of U and Θ which is assumed to be of the form $U = A\exp iSX$ and $\Theta = B\exp iSX$ gives

$$-A(1+\frac{\bar{k}\bar{\rho}\omega}{\mu})(S^2+\zeta^2) - iA\frac{\gamma k_o Sb}{\bar{k}}\frac{dT}{dx} = \frac{\bar{k}\zeta^2}{\mu}(\rho_o\beta g - \frac{\mu\gamma k_o W}{\bar{k}^2})B \qquad \text{(A.29)}$$

$$B\frac{b^2}{\alpha_m}\left(C_m - L\eta\frac{dV_{AU}}{dT}\right)\omega + iB\frac{bSW}{D} + B(S^2+\zeta^2) = -A\frac{b^2}{D}\frac{dT}{dx} \qquad \text{(A.30)}$$

A phase lag between the temperature and velocity is not considered since it is reasonable that the two disturbances occur together.

The growth rate, ω, is a quadratic expression, however, since the term $\frac{\bar{k}\bar{\rho}\omega}{\mu}$ is small compared to $\frac{b^2}{\alpha_m}\left(C_m - L\eta\frac{dV_{AU}}{dT}\right)$, the expression for ω may be written as

$$\omega = \frac{\alpha_m}{\left(C_m - L\eta\frac{dV_{AU}}{dT}\right)b^2}\left(-(S^2+\zeta^2) - i\frac{WSb}{D} + \frac{S^2+\zeta^2 - i\frac{\gamma k_o Sb}{\bar{k}}\frac{dT}{dx}}{(S^2+\zeta^2)^2 + (\frac{\mu\gamma k_o Sb}{\bar{k}^2}\frac{dT}{dx})^2}\zeta^2\lambda\right) \qquad \text{(A.31)}$$

where λ is defined as the Rayleigh number of the instability

$$\lambda = \frac{\bar{k}b^2C_f}{\mu\alpha_m\eta V_{AU}}\frac{dT}{dx}(\rho_o\beta g - \frac{\mu\gamma k_o W}{\bar{k}^2}) \qquad \text{(A.32)}$$

Neutral stability occurs when $\omega = 0$ and a minimum in λ occurs when $S \approx 0$ which corresponds to pore fluid on one side of the column moving up and moving down on the other side. This suggests that $\lambda_{min} = \zeta^2$ where ζ is a root of Bessel's equation which is used to solve $\nabla^2\Phi = -\zeta^2\Phi$ subject to the boundary condition that the flow perpendicular to the wall of the tube is zero at the wall of the tube where r=1 (in non-dimensional units). This solution suggests that the initial disturbance occurs much like the vibrations of a thin membrane subject to the boundary condition given and the continuity condition that the average of the oscillation across the interface must be zero. For this solution $\zeta^2 = 3.390$.

Prior to the onset of convection, when $\omega \leq 0$, perturbations decay. However, according to equation A.29, perturbations may have both real and imaginary components. This implies that the possible solutions include oscillatory perturbations. Oscillations in these perturbations scale with the temperature gradient. As the temperature gradient increases both the magnitude and frequency of the oscillations increase.

This completes the derivation of the Rayleigh number for a dense fluid overlying a less dense fluid in a porous material of variable permeability with a small throughflow in the vertical direction. Note that in this derivation the throughflow term can have either a stabilizing or destabilizing effect on the system. In either case the effect is symmetric with respect to the direction of the velocity. The stability condition for the tube may be stated as follows: the fluid in the column may be stable as long as the following condition is satisfied

$$3.390 \geq \frac{k_o(1+\gamma(T-T_F))b^2C_f}{\alpha_m\mu\eta V_{AU}}\frac{dT}{dx}(\rho_o\beta g - \frac{\mu\gamma W}{k_o(1+\gamma(T-T_F))^2}) \qquad \text{(A.33)}$$

Appendix B

Estimation of Parameter Uncertainty

B.1 Introduction

In each of the measured and calculated profiles presented in chapter 4 there is a degree of uncertainty which must be considered when interpreting the results of the freezing experiments. The uncertainty associated with each profile consists of the uncertainty associated with each point in the profile and the uncertainty associated with entire profile. The uncertainty that is associated with measurements made on each section of a column is the random uncertainty. The uncertainty that is associated with the entire set of measurements on each profile is the systematic uncertainty. For example, analysis of each section of a column determined the bulk salinity of the section which was used to compile a profile of bulk salinity within the column. Uncertainty exists in each bulk salinity measurement which is the random uncertainty. Since the columns in a freezing test all had the same initial salinity, the differences between the mean uncertainty in each of the seven salinity profiles in a test were used to derive the systematic uncertainty for the bulk salinity profiles.

The standard method for estimating the random uncertainty in measurements is often referred to as *Propagation of Uncertainties* (Baird 1962) which involves determining how sensitive a calculated parameter is to each of the components used in its calculation. The sensitivity of the parameter to its components and estimates of the uncertainty of the components is used to estimate the parameter uncertainty. The uncertainty of a parameter is estimated as a finite difference

form of the total differential of the parameter,

$$\delta f(x,y,z,\ldots) = \frac{\partial f}{\partial x}\delta x + \frac{\partial f}{\partial y}\delta y + \frac{\partial f}{\partial z}\delta z + \ldots \qquad \text{(B.1)}$$

Where $\delta x, \delta y, \delta z, \ldots$ are the uncertainties associated with each component of the parameter $x, y, z, \ldots$ and δf is the uncertainty associated with the parameter f. Equation B.1 shows that uncertainty estimates of a parameter depend on the sensitivity of the parameter to its components and the uncertainty of each component. A limitation of this technique is that as the number of components to a parameter increases, the uncertainty estimate obtained through equation B.1 becomes less accurate since the final uncertainty estimate is a result of each of the estimates of the components. Another limitation of this technique is that it linearizes the sensitivity of the parameter to the components. Highly non–linear relations may over or underestimate the uncertainty of the parameter.

Estimating the systematic uncertainty of each profile is not as straightforward as estimating the random uncertainty. Accurate estimates of the systematic uncertainty requires more innovative techniques which involve comparing the results from the seven columns in each test. In this research, systematic uncertainty will be estimated by comparing profiles of the same parameter from all seven columns to determine how average values compare in a manner similar to the example presented in the first paragraph of this section.

The purpose of this Appendix is to estimate the random and systematic uncertainty associated with each of the profiles presented in Chapter 4. Estimates of uncertainty pertain to Freezing Test 6, however, the results are applicable to any of the eight remaining freezing tests. The first section of this appendix will present the uncertainties associated with the measured parameters: bulk salinity, water content, and temperature. The second section will utilize the uncertainties in the measured quantities (bulk salinity and temperature) measurements to estimate the uncertainties associated with the calculated parameters: brine salinity, density, and volumetric brine content.

B.2 Uncertainty of the Measured Parameters

Bulk salinity and water content are two fundamental quantities for monitoring the effects of freezing of sand columns, consequently, accurate estimates of the

uncertainty in each of these parameters was necessary in order to properly interpret the experimental results. Accurate estimates of the uncertainty in bulk salinity measurements are particularly important since changes in bulk salinity was the principal indicator of convection. Uncertainty estimates for water content measurements are also important since changes in water content was the principal indicator of differential solvent movement.

Calculation of the bulk salinity in each section is a nine–step procedure in which the electrical conductivity, salinity relation is non–linear, consequently, the limitations of propagation of uncertainties applies to the procedure for determining the bulk salinity. To avoid the limitations of equation B.1, an alternate method of estimating the random uncertainty of the bulk salinity measurements was used. This method involved saturating two columns with salt solution and then, without first freezing them, sectioning the columns to determine the bulk salinity of the column. Methods used to determine the bulk salinity of each section were the same as those outlined in Section 3.3. Results from these measurements are presented in tables B.1 and B.2 and were used to calculate the average salinity and standard deviation of salinity in the sections of each column. The uncertainty of each measurement may be estimated by

$$\delta S_B = 1.65\sigma \tag{B.2}$$

where σ is the standard deviation of the measurements in tables B.1 and B.2 and the coefficient corresponds to estimating the uncertainty at the 90% confidence interval. The 90% confidence interval implies that the uncertainty associated with each bulk salinity measurement is estimated to be large enough that only 1 data point in 10 exceeds the uncertainty estimate. When this technique was applied to the two standard columns that were sectioned without being frozen, δS_B was estimated to be 0.5 ppt for each salinity measurement in each section.

Systematic uncertainty estimates were determined by measuring how well the average salinity in each column compared with the average salinity in the other six columns in the same freezing test. In each freezing test all seven columns were saturated with a portion of $\approx 15l$ of NaCl solution which had been made at least 24 hours prior to saturating the columns. The average bulk salinity in each column was calculated using a difference form of the Mean Value Theorem which

Table B.1: Results from analyzing each section of a partially saturated column of silica sand drained to field capacity. The standard deviation for the salinity data was .239 ppt

Sample No.	Depth Range (m)	Water Content (%)	Salinity (ppt)
1	0.000–0.015	3.0	35.2
2	0.015–0.029	3.0	35.8
3	0.029–0.047	3.2	35.4
4	0.047–0.080	3.2	35.5
6	0.080–0.096	3.3	35.5
7	0.096–0.111	3.4	35.5
8	0.111–0.127	3.4	35.2
9	0.127–0.147	3.5	35.2
10	0.147–0.165	3.4	35.6
11	0.165–0.181	3.6	35.5
12	0.181–0.197	3.5	35.6
13	0.197–0.215	3.5	35.6
14	0.215–0.234	3.7	35.2
15	0.234–0.255	3.6	35.6
16	0.255–0.272	3.9	35.7
17	0.272–0.289	4.0	35.6
18	0.289–0.307	5.3	35.6
19	0.307–0.327	5.9	35.5
20	0.327–0.346	9.5	35.5
21	0.346–0.364	15.4	35.5
22	0.364–0.380	25.4	35.5
23	0.380–0.396	27.0	35.5
24	0.396–0.409	26.5	35.5
25	0.409–0.424	26.1	35.5
26	0.424–0.441	27.4	35.2
27	0.441–0.458	27.0	35.5
28	0.458–0.476	26.3	35.3
29	0.476–0.496	27.0	35.6
30	0.496–0.514	25.8	35.9
31	0.514–0.532	26.2	36.7
32	0.532–0.548	26.1	35.5
33	0.548–0.570	26.6	34.7

Table B.2: Results from sectioning and analyzing a saturated soil column without first freezing it. The standard deviation in the salinity measurements was 0.305 ppt.

Sample No.	Depth Range (m)	Water Content (%)	Salinity (ppt)
1	0.000–0.017	32.1	35.6
2	0.017–0.032	27.3	35.9
3	0.032–0.050	27.4	35.5
4	0.050–0.065	26.0	35.6
5	0.065–0.083	27.3	35.5
6	0.083–0.100	26.8	35.5
7	0.100–0.118	27.0	35.5
8	0.118–0.136	27.5	35.6
9	0.136–0.153	25.4	35.7
10	0.153–0.172	26.3	35.7
11	0.172–0.193	26.0	35.8
12	0.193–0.207	26.7	35.9
13	0.207–0.227	26.9	35.6
14	0.227–0.243	26.5	35.6
15	0.243–0.263	26.8	35.6
16	0.263–0.279	26.1	35.8
17	0.279–0.296	27.6	35.7
18	0.296–0.315	27.2	35.6
19	0.315–0.332	26.0	35.4
20	0.332–0.350	26.1	35.6
21	0.350–0.364	26.2	35.6
22	0.364–0.376	25.3	35.6
23	0.376–0.389	26.3	35.7
24	0.389–0.405	26.5	35.7
25	0.405–0.420	26.0	35.7
26	0.420–0.429	27.1	35.7
27	0.429–0.436	27.1	36.1
28	0.436–0.443	26.4	36.0
29	0.443–0.452	25.5	36.0
30	0.452–0.460	26.4	36.0
31	0.460–0.471	27.0	35.8
32	0.471–0.488	26.3	35.6
33	0.488–0.507	26.4	35.7
34	0.507–0.529	26.0	35.5
35	0.529–0.550	27.2	35.5
36	0.550–0.570	29.4	34.6

weighted the sample length in the calculation of the average salinity. Results of such a comparison for Freezing Test 6 indicates that a systematic uncertainty of 0.3 ppt exists between each column.

Systematic uncertainty in the bulk salinity measurement was thought to be a result of the drying the samples after they were sectioned (D. Hawkins pers. comm. 1990). Since the samples were quite large, typically 0.1 kg, it was difficult to redissolve all the salt into solution after the samples were dried. It should be noted that the systematic uncertainty only applies to the comparison of salinity values between columns, in which case the uncertainty in salinity is 0.8 ppt, otherwise the salinity values within each column have an uncertainty of 0.5 ppt.

Water content, the ratio of mass water to mass dried soil, was determined using a scale that was accurate and repeatable to 10^{-5} kg. This would suggest that water content measurements were very accurate and only slight changes in water content could be associated with differential movement of the solvent during freezing. However, variations in dry density must be taken into account to determine minimum changes in water content that could be associated with differential movement of the solvent. In a soil saturated with pure water it is possible to show that

$$W_B(\%) = 100\left(\frac{\rho_W}{\rho_{dry}} - \frac{1}{\gamma_{qtz}}\right) \tag{B.3}$$

where ρ is the density of water and dry density of the sand and γ is the specific gravity of quartz. In this investigation, the silica sand was packed to a dry density of 1530 ± 20 $\frac{\text{kg}}{\text{m}^3}$. The density of water will be taken as 1000 $\frac{\text{kg}}{\text{m}^3}$, and the specific gravity of quartz as 2.63 ± 0.03 (Lunardini 1983). These values substituted into equation B.3 yield a water content of 27.5%. Propagating the uncertainty associated with each measurement in B.3 suggests that water content values are accurate to 0.6%.

Systematic uncertainty in water content measurements result from systematic variations in ice content within each column. The formation of ice from solution results in an $\approx$ 10% expulsion of brine from the pore space. When the column is sectioned and each section analyzed to determine its water content, the water content will reflect the mass of ice within the section. Since the porosity of the sand is 40% and the volume change of solution to water is 10%, up to 4% of the solution

mass is expelled upon complete freezing of the pore fluid. However, complete freezing of the pore fluid occurs only at temperatures lower than the eutectic temperature. In this research, the ice content in the pore fluid continuously ranged from 0 to < 500 ppt by volume of the pore fluid. Systematic changes in water content in the partially frozen portion of the columns reduced the water content continuously from 0 to $\approx$ 2%. If the systematic uncertainty in the water content measurements were removed, then the uncertainty could be estimated to be less than 0.6%. If the volume of ice is not taken into account in the water content measurements, then the overall uncertainty would be estimated at 2.6%.

Temperature measurements were used to determine brine salinity, density in the partially frozen portion of the columns. Uncertainty in the measurement of temperature consists of random uncertainty associated with routine temperature measurements and systematic uncertainty associated with temperature variations throughout the freezing apparatus.

Thermistors used in this research were calibrated using a three point technique (see Section 2.4) with the calibration results fit to the Steinhart equation to produce an accuracy of 0.01°C (Osterkamp 1984). Sensitivity of the thermistors was 0.001°C. Therefore, the random uncertainty of the temperature measurements is mainly associated with calibration uncertainty and is on the order of 0.01°C.

Systematic uncertainties of the temperature measurements were due to variations in temperature across the freezing apparatus and self heating of the thermistors. Temperature variations across the freezing apparatus were measured by logging the fluid filled stainless steel tubes distributed throughout the apparatus. Figures B.1, B.2, B.3 show typical temperature profiles measured with the both the thermistor string and measured by lowering a thermistor into a liquid filled stainless steel tube. These profiles indicate a maximum variation of 0.1°C near the top of the profile where the temperatures were coldest, and near 0.05 °C at the base. The brine volume in the region where the temperature variations were largest was $<\approx$ 600 ppt. Temperature variations throughout the freezing apparatus and near the surface are thought to be associated with the contact between the sand and steel plate covering the freezing apparatus.

Thermistor self heating occurs when too much power is applied to the thermistors during temperature measurements and results in an elevation of the thermistor

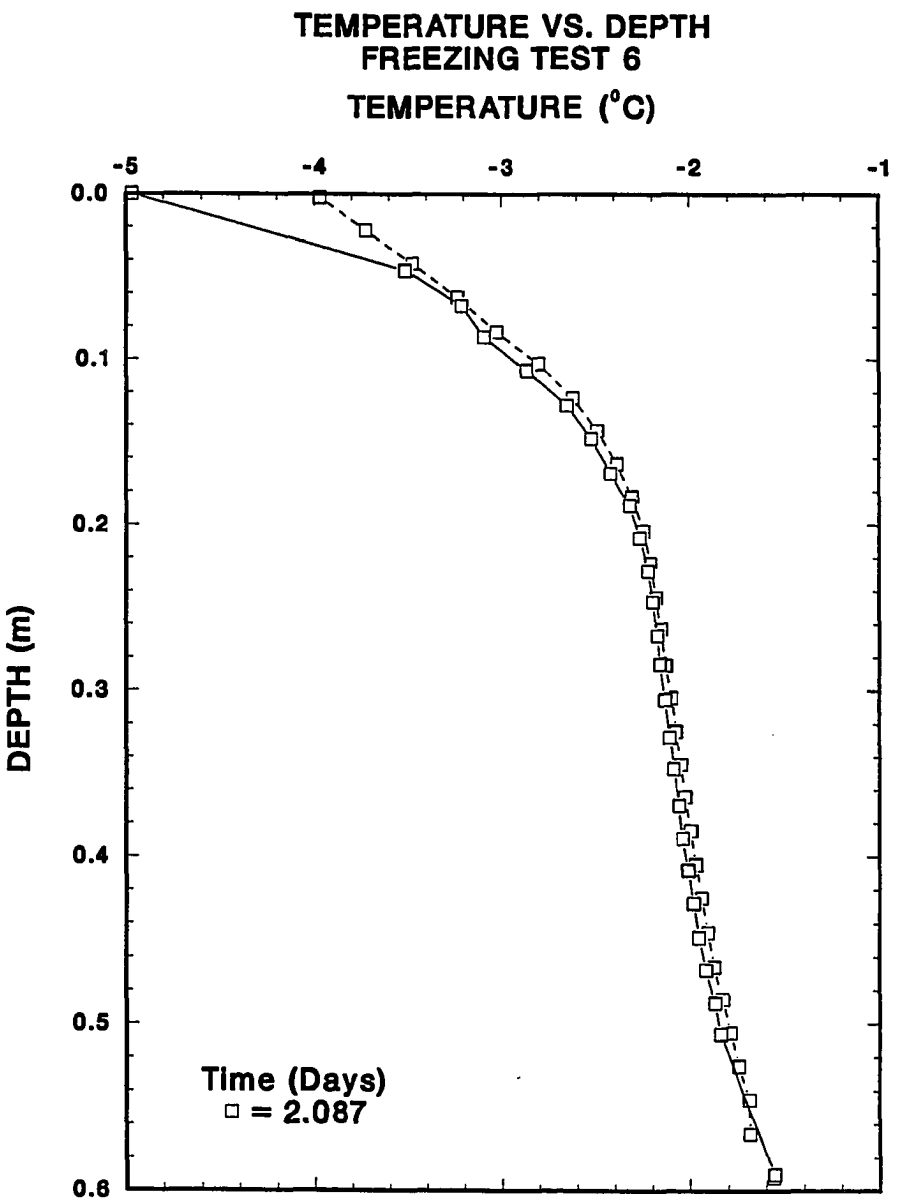

Figure B.1: Temperature profiles in the freezing apparatus measured with both the fixed thermistor string (solid line) adjacent to the instrumented column and in the liquid filled stainless steel tubes (dashed line). The decimal date since the start of the experiment is shown in the legend. These profiles indicate variations in the temperature field of less than 0.1°C across the apparatus except at the surface of the column.

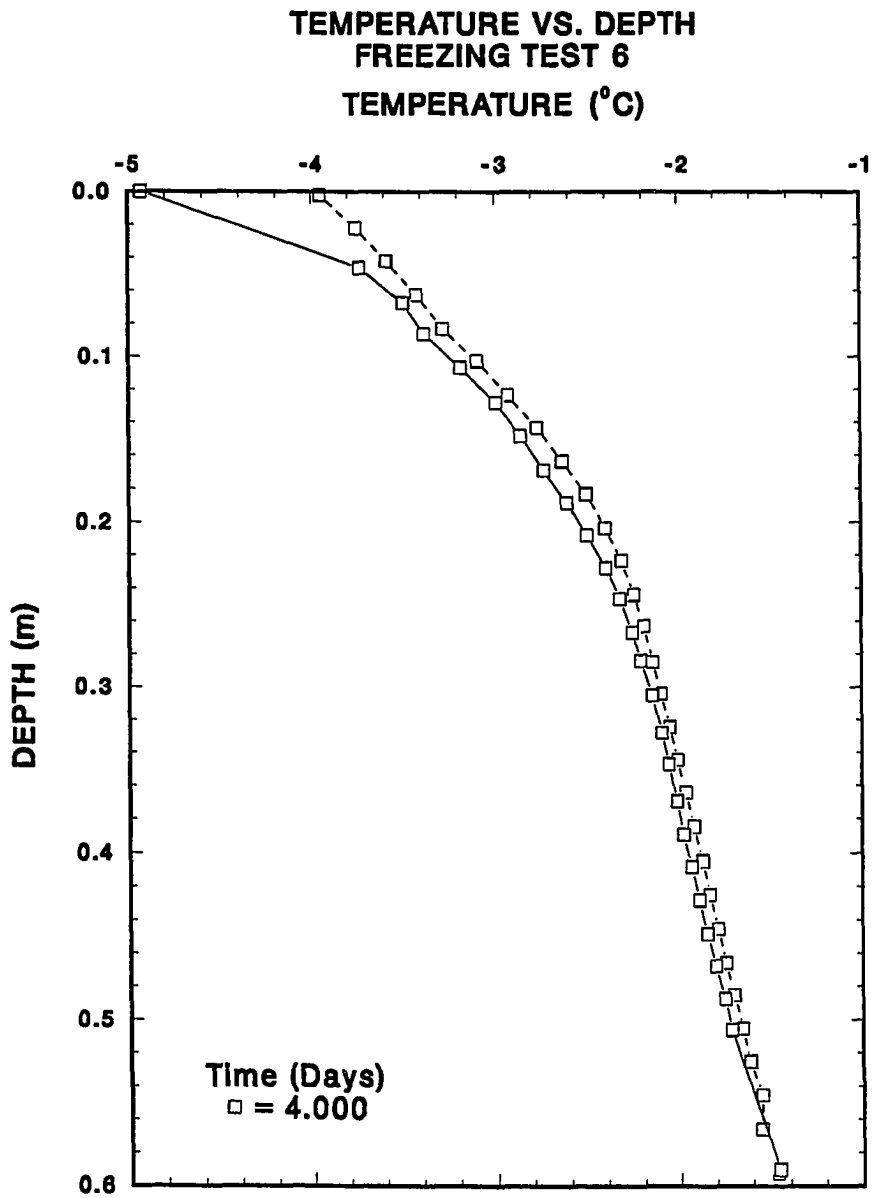

Figure B.2: Temperature profiles in the freezing apparatus measured with both a fixed thermistor string (solid line) and by lowering a probe into a liquid filled stainless steel tube (dashed line).

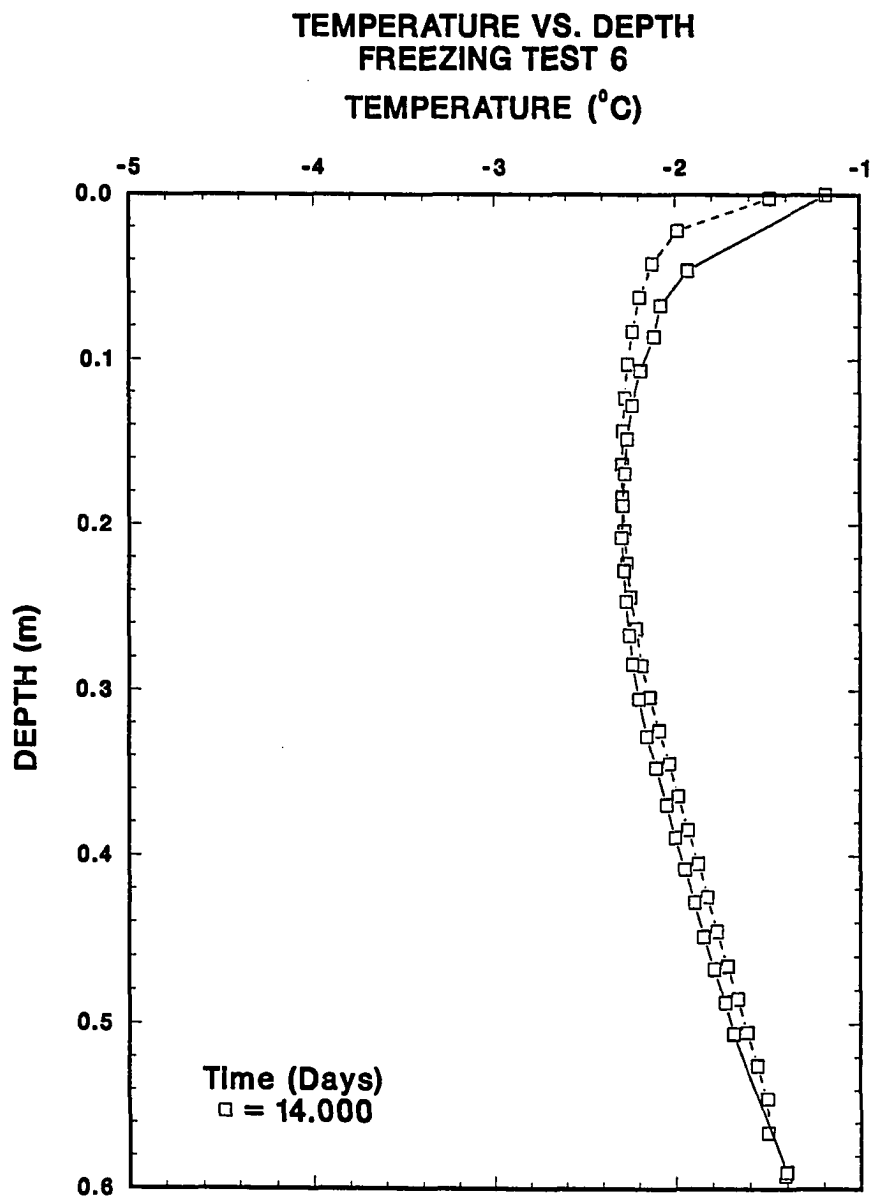

Figure B.3: Temperature profiles in the freezing apparatus measured with both a fixed thermistor string (dashed line) and by lowering a probe into a liquid filled stainless steel tube (dashed line).

temperature above the ambient temperature. Self heating was estimated from the power dissipation factor for these thermistors, the excitation current used in the temperature measurements and the thermistor resistances used in this research. The power dissipation factor for these thermistors was $\approx 10^{-3}\ \frac{W}{°C}$. The excitation current was 10^{-5} amperes. Typical resistance values were on the order of 10^4 ohms. This information implies that self heating affected temperature measurements on the order of 0.001°C.

Systematic uncertainty associated with the temperature measurements is associated with variations in the temperature field across the freezing apparatus and has been measured to be on the order of 0.1°C. Overall uncertainty associated with the temperature measurements may be estimated to be $\approx$ 0.1°C when profiles are compared and 0.01°C between each thermistor in a profile.

B.3 Uncertainty of the Calculated Parameters

Calculated parameters are those that describe the phase relations between the brine and ice and they are determined from the measured parameters. Brine salinity and density depend only on the temperature of the system and the brine volume depends on the temperature and the bulk salinity. The purpose of this section is to estimate the random and systematic uncertainty associated with the calculated parameters.

Brine salinity, the salinity of brine in contact with ice in the partially frozen portion of the column, depends only on temperature. Equation 3.10 is a polynomial expression used to calculate the salinity of brine in the partially frozen section of the column. The effect of random and systematic temperature uncertainties of 0.01 and a 0.1°C respectively on the uncertainty in brine salinity can be estimated by propagating the uncertainty associated with temperature through equation 3.10 and noting that only the first term in the expression is important for the temperatures used in this research. This calculation indicates that the random and systematic uncertainties in brine salinity are estimated to be approximately 0.17 and 1.7 ppt.

Brine density, the density of the brine in contact with ice in the partially

frozen portion of the column is a function of both temperature and salinity, but since the temperature specifies the salinity, the brine density may be expressed as either a function of temperature or brine salinity. Equation 3.11 is a relation between brine salinity and density. Propagating the uncertainty in brine salinity through equation 3.11 using random and systematic uncertainties of 0.17 and 1.7 ppt suggests that the uncertainty in brine density is approximately 0.14 and 1.4 $\frac{kg}{m^3}$ respectively.

Estimates of the bulk salinity, brine salinity and brine density may be used to determine the uncertainty in brine volume. Equation B.1 was applied to the simplified form of equation 3.12 to estimate the uncertainty in brine volume using S_B=35 ppt, δS_B=0.5 and 0.8 ppt, and S_U=50 ppt, δS_U=0.17 and 1.7 ppt. These values suggest estimates of the random and systematic uncertainty to be approximately δV_U=14 and 56 ppt.

B.4 Summary

In summary, this section has presented the methods used to determine the random and systematic uncertainty in both measured and calculated parameters used in this investigation. These calculations have been presented for the results of Freezing Test 6, however, they are generally valid for the 8 remaining freezing tests. Table B.3 summarizes the results of the analysis to calculate the random and systematic uncertainty for each of the parameters used in this investigation.

Table B.3: Summary of the estimates of the random and systematic uncertainty associated with the measured and calculated parameters in Freezing Test 6. These results are generally applicable to the remaining 8 freezing tests.

Parameter		Uncertainty	
		Random	Systematic
Bulk Salinity	S_B(ppt)	0.5	0.3
Water Content	W_B(%)	0.6	2.
Temperature	T(°C)	0.01	0.1
Brine Salinity	S_U(ppt)	0.17	1.7
Brine Density	$\rho_U \left(\frac{\text{kg}}{\text{m}^3}\right)$	0.14	1.4
Volumetric Brine Content	V_U(ppt)	14	56

Appendix C

Measurement of Permeability

Permeability measurements were made on the sand used in the freezing experiments with the constant head method. These measurements were conducted with a Soil Test Combination Permeameter, Model K–605. Tests were conducted by closely following procedures outlined in ASTM (American Society For Testing and Materials) D2434–68, Standard Test Method For Permeability Of Granular Soils (Constant Head). Tests were conducted at 100% relative density of the dried sand. The sand was compacted using the falling weight method outlined in the ASTM test.

Five separate samples were tested for permeability. The samples were drawn at random from twelve, 45 kg bags of Granusil 30 that had been intermixed. Permeability tests were performed at a variety of hydraulic heads with values of permeability calculated from the slope of the line fitted by the method of least squares. All tests were conducted using de–aired distilled water. Figure C.1 is an example of the results from measurements made to determine the permeability of the sand. Results of permeability tests on Granusil 30 with dry densities of 1530, 1570, 1530, 1550 $\frac{kg}{m^3}$ indicate an average hydraulic conductivity of the sand was 7.9×10^{-4} $\frac{m}{sec}$ at 25 °C. The average permeability of the sand was 8.1×10^{-11} m^2.

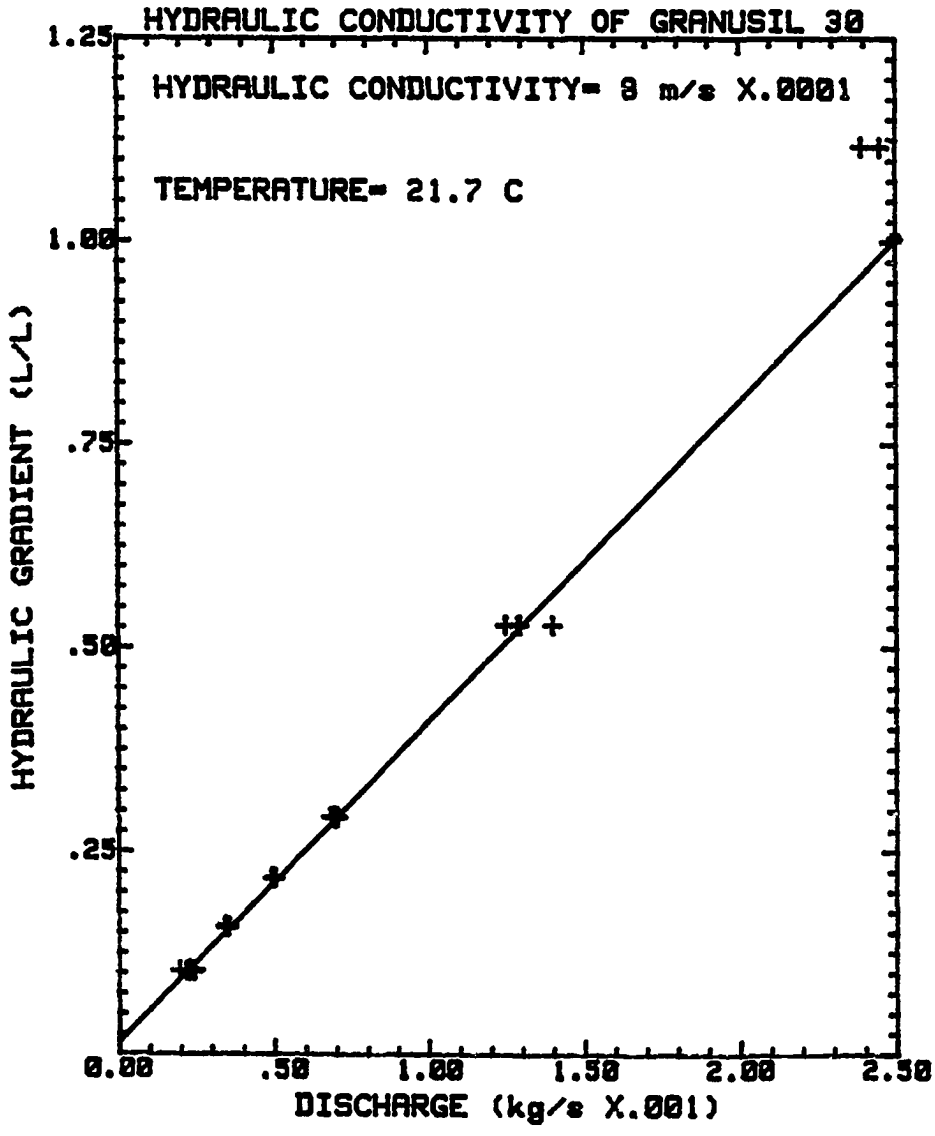

Figure C.1: An example of the results of measurements of the permeability of Granusil 30. The two data points at the large head have not been included in the curve fit because they indicate turbulent flow in the sand.

Appendix D

Sensor Spacing and Probe Spacing

The purpose of this section is to present the spacing of the 28 thermistors relative to the top of the column and the spacing of the probe depths on the thermistor probe. Because the probe spacing depths are marked on the side of the probe, they are relative to the top of the stainless steel tube, consequently, a correction of 0.0435 m must be subtracted from each spacing measurement to obtain the depth below the sand surface.

Table D.1: Spacing of temperature sensors for each of the nine freezing tests. The first column is the spacing for Freezing Test 5, the second column is the sensor spacing for the eight remaining freezing tests. Negative values correspond to distances above the top of the column. The origin is taken to be the top of the sand surface or the bottom of the top aluminum cap.

Sensor Spacing (m)	
Freezing Test 5	Freezing Tests 6–13
-.05	-.05
-.0001	-.0001
.0461	.0461
.0685	.0673
.0871	.0863
.1066	.1065
.1285	.1279
.1487	.1481
.1697	.1689
.1889	.1882
.2085	.2079
.2284	.2277
.2468	.2462
.2674	.2667
.2853	.2838
.3071	.3051
.3279	.3278
.3481	.3469
.3690	.3692
.3811	.3890
.4077	.4080
.4291	.4280
.4489	.4480
.4692	.4676
.4887	.4874
.5071	.5060
.5900	.5900
.5920	.5920

Table D.2: Spacing of the temperature probe for the thermistor lowered into the stainless steel tubes adjacent to the sand columns. Distances are relative to the probe. To obtain the distance below the sand surface 0.0435 m must be subtracted from each of the values given in this table.

Probe Spacing (m)
.0407
.0605
.0806
.1010
.1217
.1411
.1618
.1816
.2019
.2215
.2421
.2617
.2822
.3014
.3233
.3425
.3627
.3829
.4026
.4228
.4431
.4632
.4837
.5043
.5237
.5437
.5635
.5837
.6044
.6242

Appendix E

Data Acquisition

Temperature data were acquired with a Hewlett Packard data acquisition system. This system consisted of an HP 85 controller, an HP 9836 voltmeter, and multiplexer and an HP 82901, $5\frac{1}{4}$ inch dual disk drive. The purpose of this appendix is to present the data acquisition program and to discuss features of the program. The program presented in this appendix is a direct copy of the working program and should work without alteration on an HP 8000 series computer supported with an HP82901 disk drive at address 700 and a multiplexer at address 709.

The main purpose of this program was to acquire data from the 28 thermistors located at the instrumented column twice each hour. The program was written so that the seven vertical tubes could be logged between loggings of the instrumented columns. Printouts and graphical displays of the loggings could be obtained with the use of the 8 softkeys. An auto start feature has been included which enables the program to restart and initialize itself in the event of an interruption of power to the computer. The auto start feature is such that the first temperature logging after a power interruption is placed one record after the last record prior to the interruption. The keyboard has been disabled to avoid crashing the program by inadvertently pressing the keys on the keyboard.

```
   5 ! STORE "Autost:TAPE"
10 ! This program is to log
15 ! temp sensors as part of
20 ! the sandbox freezing exp.
25 ! The program will allow
30 ! holes in the sand
35 ! box to be logged using an
40 ! external thermistor.
45 !
50 ! The main features of this
55 ! program will be the
60 ! to log any of 7 holes at will and
65 ! to display the results.
70 ! Hardcopy printouts of the
75 ! sensor temps and logging
80 ! temps both in graphical
85 ! and printout form will be
90 ! available.
95 !
100 ! As usual I will back this
105 ! software with my uncon-
110 ! ditional guarantee.
115 ! Since you didn't write it
120 ! and your paying nothing for
125 ! it, if your are in any
130 ! way dissatisfied with
135 ! the results or the logic
140 ! you can just go back to
145 ! where you came from.
155 !
160 ! Tim Matava-881214
165 !
170 ! Set up the initial prgm
175 ! parameters.
180 !
185 OPTION BASE 1
190 DIM A(28),C(28,3),B(30),D(24
),R(30),E(8)
195 L=.6138 ! cm 25-26 spcng
200 K=.4 ! cal/cm-s-c
205 ! 6061-T651-QQ-A-225/8 Al.
210 !
215 FOR I=1 TO 30
220 R(I)=I*500
225 NEXT I
230 !
235 MASS STORAGE IS ":TAPE"
240 ASSIGN# 1 TO "T_COEF"
245 FOR I=1 TO 28
250 READ# 1,I ; C(I,1),C(I,2),C(
I,3)
255 NEXT I
260 ASSIGN# 1 TO *
265 !
270 ! Read in the sensor spacing
275 !
280 ASSIGN# 1 TO "T_SPCNG"
285 FOR I=1 TO 24
290 READ# 1,I ; D(I)
295 NEXT I
300 ASSIGN# 1 TO *
305 !
310 MASS STORAGE IS ":D700"
315 !
320 CRT IS 1 ! dflt is display
325 !
330 G=709 ! Datalogger address
335 OUTPUT G ;"ARVC1AC33"
340 !
345 ! **********************
350 !
355 ! Begin main body of prgm.
360 !
365 ON TIMER# 1,1800000 GOSUB
1070
370 !
375 GOSUB 715
380 ! GOSUB 2060
385 !
390 ON KEY# 1," GRAPH" GO-
SUB 1430
395 ON KEY# 2," PRINT" GOSUB
440
400 ON KEY# 3," LGGNG" GO-
SUB 795
405 ON KEY# 4," END " GOSUB
430
410 !
415 GOTO 415 ! SPIN#1
420 !
425 ! End of the main body
430 STOP
435 ! **************************
440 !  SUBROUTINE TO PRINT
DATA
450 CRT ON
455 !
460 ON TIMER# 2,5000 GOTO 495
465 OFF KEY# 2
470 OFF KEY# 3
475 ON KEY# 1,"HRD COPY" GOTO
490
480 GOTO 480 ! SPIN #2
485 !
490 CRT IS 703
495 OFF TIMER# 2
500 !
505 ON KEY# 1,"SENSORS" GOTO
525
510 ON KEY# 4,"LOGGINGS" GOTO
620
```

```
515 GOTO 515 ! SPIN #3
520 !
525 ! Print out of sensors
530 DISP "Time=";INT(T5/3600);IN
T(FP(T5/3600)*60);"Hrs-min"
535 DISP "Julian Date=";T6
540 DISP "Record #";N0
545 !
550 FOR I=1 TO 26
555 DISP USING 585 ; I,A(I)
560 NEXT I
565 !
570 DISP USING 590 ; K*(A(25)-A(
26))*4.184*10000/L
575 !
580 DISP USING 595 ; A(28),A(27)
585 IMAGE XX,DD,XXX,MDD.DD
590 IMAGE "heat flux through bas
e=",MDDD.D,"Watts/m 2"
595 IMAGE "top temp=",MDD.DD,"
a
ir temp=",MDD.DD
600 DISP " " @ DISP " "
605 !
610 GOTO 695 ! Return to main
615 !
620 ! PRINT OUT OF LOGGINGS
625 !
630 DISP "Time=";INT(T7/3600);IN
T(FP(T7/3600)*60);"hrs-min"
635 DISP "Julian Date=";T8
640 DISP "Record #";N1
645 !
650 IMAGE XX,DD,XX,MDD.DD
655 !
660 DISP "SPCNG# TEMP"
665 !
670 FOR I=1 TO 30
675 DISP USING 650 ; I,B(I)
680 NEXT I
685 DISP " " @ DISP " "
690 !
695 CRT IS 1
700 GOTO 385
705 RETURN
710 ! ************************
715 ! SUBROUTINE KEYBRD
720 ! Purpose is to disable
725 ! the keyboard so hoseheads
730 ! won't be able to mess up
735 ! logging. Pause key still alive.
740 !
745 ON KYBD Z,"1234567890-=
QWERTYUIOP()ASDFGHJKL;'ZX
CVBNM,./" GOSUB 785
750 ON KYBD Z,"!@#$% &*()-+—
qwertyuiop()asdfghjkl;'zx
cvbnm¡¿?" GOSUB 785
755 ON KYBD Z,CHR$(136)&
CHR$(137)&CHR$(140)&
CHR$(141)&CHR$(144) GOSUB 785
760 ON KYBD Z,CHR$(145)&
CHR$(147)&CHR$(148)&
CHR$(149) GOSUB 785
765 ON KYBD Z,CHR$(153)&
CHR$(154)&CHR$(155)&
CHR$(156)&CHR$(157) GOSUB 785
770 ON KYBD Z,CHR$(158)&
CHR$(159)&CHR$(160)&
CHR$(161)&CHR$(162) GOSUB 785
775 ON KYBD Z,CHR$(163)&
CHR$(165)&CHR$(166)&
CHR$(168)&CHR$(169) GOSUB 785
780 ON KYBD Z,CHR$(170)&
CHR$(172)&CHR$(173)&
CHR$(32)&CHR$(164) GOSUB 785
785 RETURN
790 ! ************************
795 ! SUBROUTINE LOG
800 ! Purpose is to log the separate
805 ! holes in the sandbox
810 !
815 ! Thermistor Coefficients
820 C1=9.72687889265E-4
825 C2=2.72988410808E-4
830 C3=1.05159739735E-7
835 !
840 ON KEY# 1," LOG " GOTO
875
845 OFF KEY# 2
850 OFF KEY# 3
855 ON KEY# 4," RETURN " GOTO
1055
860 !
865 GOTO 865 ! SPIN
870 !
875 T7=TIME
880 T8=DATE
885 ON KEY# 1,"STORE PT" GOTO
950
890 !
895 OUTPUT G ;"AC32VC1"
```

```
900 !
905 R1=0
910 N3=0
915 FOR M=1 TO 30
920 WAIT 7000
925 N3=N3+1
930 ENTER G ; R(M)@ R(M)=
R(M)/.00001
935 IF ABS(R1-R(M))<1.2 THEN
GOTO 950
940 R1=R(M)
945 GOTO 920
950 B(M)=1/(C1+C2*LOG(R(M))+
C3*LOG(R(M)) 3)-273.15
955 BEEP 20,1000
960 DISP M;N3;R(M);B(M)
965 N3=0
970 NEXT M
975 !
980 BEEP 20,1000
985 !
990 BEEP 50,3000
995 !
1000 OUTPUT G ;"AC33"
1005 ASSIGN# 2 TO "CNTR"
1010 READ# 2,2 ; N1
1015 N1=N1+1
1020 PRINT# 2,2 ; N1
1025 ASSIGN# 2 TO *
1030 !
1035 ASSIGN# 1 TO "LOGGINGS"
1040 PRINT# 1,N1 ; T7,T8,B()
1045 ASSIGN# 1 TO *
1050 !
1055 GOTO 385
1060 RETURN
1065 ! ************************
1070 ! SUBROUTINE T_SENSOR
1075 ! Purpose is to log the
1080 ! sensors fixed adjacent to
1085 ! column #1
1090 !
1095 ! ON TIMER# 2,5000 GOTO
1125
1100 !
1105 ! FF KEY# 1
1110 !  ON KEY# 4," RETURN"
GOTO
1380
1115 ! GOTO 1115 ! SPIN #4
1120 !
1125 ! OFF TIMER# 2
1130 !
1135 ASSIGN# 2 TO "CNTR"
1140 READ# 2,1 ; N0
1145 N0=N0+1
1150 PRINT# 2,1 ; N0
1155 ASSIGN# 2 TO *
1160 !
1165 T5=TIME
1170 T6=DATE
1175 !
1180 FOR I=1 TO 3
1185 IF I=1 THEN OUTPUT G ;
"AF00AL07AC00"
1190 IF I=2 THEN OUTPUT G ;
"AF08AL15AC08"
1195 IF I=3 THEN OUTPUT G ;
"AF20AL27AC20"
1200 FOR J=1 TO 8
1205 WAIT 15000
1210 ENTER G ; R
1215 A(J+8*(I-1))=R/.00001
1220 OUTPUT G ;"AS"
1225 NEXT J
1230 NEXT I
1235 !
1240 OUTPUT G ;"AF28AL31AC28"
1245 FOR I=1 TO 4
1250 WAIT 15000
1255 ENTER G ; R
1260 A(I+24)=R/.00001
1265 OUTPUT G ;"AS"
1270 NEXT I
1275 !
1280 OUTPUT G ;"AC39"
1285 !
1290 ! ***************
1295 ! chnls 25 & 26 reversed
1300 ! P=A(25)
1305 ! A(25)=A(26)
1310 ! A(26)=P
1315 ! ***************
1320 !
1325 FOR I=1 TO 28
1330 A(I)=1/(C(I,1)+C(I,2)*LOG(A
(I))+C(I,3)*LOG(A(I)) 3)-273.15
1335 NEXT I
1340 !
1345 ASSIGN# 1 TO "T_SENSOR"
1350 PRINT# 1,N0 ; T5,T6,A()
1355 ASSIGN# 1 TO *
1360 !
1365 ! FOR I=1 TO 8
1370 ! OUTPUT G ;"AS"
1375 ! ENTER G ; E(I)
```

```
1380 ! NEXT I
1381 !
1382 OUTPUT G ;"AC33"
1385 !
1390 ! ASSIGN# 1 TO "CNDTVTY"
1395 ! INT# 1,N0 ; T5,T6,E()
1396 ! ASSIGN# 1 TO *
1397 !
1400 IF N0¿720 THEN GOSUB 1680
1405 !
1410 BEEP 20,2000
1415 ! GOTO 385
1420 RETURN
1425 ! **********************
1430 ! SUBROUTINE GRAPH
1435 ! Purpose is to graph the
1440 ! T-sensor & logging data
1445 !
1450 CRT ON
1455 CRT IS 1
1460 !
1465 X1=60
1470 X0=-5
1475 Y1=5
1480 Y0=-10
1485 !
1490 SCALE X0,X1,Y0,Y1
1495 !
1500 XAXIS Y0,5,X0,X1
1505 YAXIS X0,1,Y0,Y1
1510 !
1515 XAXIS Y1,5,X0,X1
1520 YAXIS X1,1,Y0,Y1
1525 !
1530 OFF KEY# 2
1535 OFF KEY# 3
1540 ON KEY# 1,"SENSORS"
GOSUB 1565
1545 ON KEY# 4,"LOGGINGS"
GOSUB 1630
1550 !
1555 GOTO 1555
1560 !
1565 ! Plot sensors
1570 PENUP
1575 MOVE -5,A(27)
1580 PLOT -.9,A(28)
1585 !
1590 FOR I=1 TO 24
1595 PLOT D(I),A(I)
1600 NEXT I
1605 !
1610 PLOT 64.1,A(25)
1615 PLOT 64.1+L,A(26)
1620 !
1625 GOTO 1670
1630 ! Plot loggings
1635 MOVE 0,B(1)
1640 FOR J=1 TO 30
1645 N3=N3+2
1650 PLOT N3,B(J)
1655 NEXT J
1660 PENUP
1665 !
1670 GOTO 385
1675 RETURN
1680 ! ************************
1685 ! SUBROUTINE DISK CHANGE
1690 !
1695 N2=N2+1
1700 IF N2=1 THEN GOTO 1710
1705 IF N2=2 THEN GOTO 1720
1710 MASS STORAGE IS ":D701"
1715 GOTO 1730
1720 MASS STORAGE IS ":D700"
1725 !
1730 ! Reset counters
1735 N0=0
1740 N1=0
1745 !
1750 GOTO 385
1755 RETURN
```

Appendix F

Definition of Terms and List of Notation

The purpose of this appendix is to present the notation used throughout the text. Recently, a second set of notation was introduced into the literature beginning with Baker (1987) to describe the properties of partially frozen solutions in a coarse–grained porous material. This notation is different from the notation previously used to describe the properties of partially frozen solutions of salt and water which was first introduced by Weeks (1962). However, the two sets of notation are completely equivalent, are based on similar principles, and rely on the same phase diagram. Throughout the text of this thesis the notation introduced by Baker (1987) has been used. In this appendix both sets of notation are presented to avoid the ambiguity that could occur for the reader who has approached this topic from the sea ice point of view rather than the soils viewpoint. When two symbols are used to describe a parameter, the first symbol denotes the notation used in the thesis and the second, but equivalent, symbol denotes the older, more longstanding, notation. In the case where only one symbol is presented, only one symbol has been presented in the literature or a variety of symbols have been presented and a standard notation does not exist.

Definition of Terms

Ice–Bearing Interface A term used to describe the location within the column where the last ice is present in the soil matrix. Here, the presence of the ice is considered in the thermodynamic sense.

Ice–Bonded Interface A term used to describe the location within the column where the ice was no longer bonded by ice. Bonding was determined by probing the sand with a knife while the column was sectioned.

Transition Interface A term used to describe the location within the column where the sand was bonded by ice but not firmly bonded uniformly across a horizontal section of the column.

Approximate Nuemann Conditions A term used to describe the temperature boundary conditions during freezing. Classical Nuemann conditions are applied to a half-space, while Approximate Nuemann conditions are applied to over a fixed length. These conditions consist of a constant initial temperature, and constant top and base temperatures during freezing.

List of Notation

A Constant.

B Constant.

b(m) Diameter of the sand columns, and length scale used in the stability analysis.

C Constant.

$C(\frac{\mathrm{S}}{\mathrm{m}})$ The electrical conductivity of a solution.

$CF(\frac{\%}{^{\circ}\mathrm{C}})$ A temperature correction factor applied to the conductivity of a solution of unknown salinity, but known temperature to determine the equivalent conductivity of the solution at 25°C is defined as CF.

$C_f(\frac{\mathrm{J}}{\mathrm{m}^3.^\circ\mathrm{C}})$ Heat capacity of the fluid.

$C_m(\frac{\mathrm{J}}{\mathrm{m}^3.^\circ\mathrm{C}})$ Heat capacity of the medium.

$D(\frac{\mathrm{m}^2}{\mathrm{s}})$ Effective thermal diffusivity.

$D_v(\frac{\mathrm{m}^2}{\mathrm{s}})$ The diffusivity of water vapor in a soil.

$D_o(\frac{\mathrm{m}^2}{\mathrm{s}})$ The diffusivity of water vapor in air.

$g(\frac{\mathrm{m}}{\mathrm{s}^2})$ Gravitational acceleration.

$k(\mathrm{m}^2)$ Permeability.

$L(\frac{\mathrm{J}}{\mathrm{m}^3})$ Latent heat of fusion of brine.

$M_S(\mathrm{kg})$ Mass of salt.

$M_{SL}(\mathrm{kg})$ Mass of the soil with the effects of the salt removed.

$M_{SW}(\mathrm{kg})$ Mass of the distilled water added to the dried section.

$M_W(\mathrm{Kg})$ Mass of pure water.

n A coefficient used to relate brine volume to the permeability of the partially frozen sand.

$\hat{n}$ A unit vector normal to a surface.

$P(\mathrm{Pascals})$ Pressure.

R_{25} The ratio of the conductivity of a solution of unknown concentration at 25°C to the conductivity of a solution with a concentration at 34.33 ppt and temperature at 25°C is defined as R_m. Dimensionless

R_m The ratio between the measured conductivity at a know temperature to the conductivity of a solution of salinity at 35 ppt and 20°C is defined as R_m. Dimensionless

$q_v(\frac{\mathrm{kg}}{\mathrm{m}^2.\mathrm{s}})$ The vapor flux of water in a soil.

S_B(ppt) = S_i Bulk salinity. The salinity of a thawed sample of soil that contains both salt and water is defined as the bulk salinity.

S_D(ppt) Salinity of the diluted solution.

S_U(ppt) = S_b Brine salinity. The salinity of brine in contact with ice is defined as the brine salinity.

T(°C) Temperature.

T_F(°C) Equilibrium freezing temperature of a solution.

$u(\frac{\mathrm{m}}{\mathrm{s}})$ Velocity. The Darcy velocity of the pore fluid.

V_{AU} The absolute ratio of brine volume to the volume of ice and brine in the porous matrix.

$V_I(\mathrm{m}^3) = V_i$ The absolute volume of ice in the porous matrix.

V_U(ppt) = ν_b The Brine volume in the soil. The ratio of the absolute brine volume to the absolute volume of ice and brine is defined as the brine volume.

$W(\frac{\mathrm{m}}{\mathrm{s}})$ Throughflow velocity, this is also expressed as a Darcy velocity.

$W_B(\%)$ Bulk gravimetric water content. The ratio of the mass of pure water to mass of salt free water is defined as the gravimetric water content.

$\alpha_m(\frac{\mathrm{J}}{\mathrm{m \cdot s \cdot ^\circ C}})$ The thermal conductivity of the medium.

$\beta(\frac{1}{^\circ\mathrm{C}})$ Temperature coefficient of brine density.

$\gamma(\frac{1}{^\circ\mathrm{C}})$ Temperature coefficient of the permeability in the partially frozen soil.

γ_{qtz} Specific gravity of quartz. Dimensionless.

ΔC A temperature correction applied to the conductivity readings to obtain an equivalent conductivity at 25°C.

δ A symbol used to denote a small thickness (Chapter 5) or the uncertainty of a parameter (Appendix B).

η The porosity of the sand. Dimensionless.

$\theta(°C)$ A temperature difference used in the stability analysis.

$\kappa(\frac{m^2}{s})$ Molecular diffusivity of the solutes.

λ Rayleigh number. Dimensionless.

$\mu(\frac{kg}{m \cdot s})$ Viscosity of the brine.

ξ A dimensionless similarity variable used to describe the conduction of heat on a sphere.

$\rho_{dry}(\frac{kg}{m^3})$ Dry density of the sand.

$\rho_i(\frac{kg}{m^3})$ Density of pure, salt free ice.

$\rho_U(\frac{kg}{m^3}) = \rho_b$ Brine density. The density of brine in contact with ice is defined as the brine density.

σ Standard deviation.

$\tau(s)$ Time constant.

$\omega(\frac{1}{s})$ Growth rate parameter.